DOCTOR OF PHILOSOPHY

Exploring the Role of PKD Enzymes in the Innate and Adaptive cells of the Mammalian Immune System

Robertson, Lyndsey

Award date:
2015

DOCTOR OF PHILOSOPHY

Exploring the Role of PKD Enzymes in the Innate and Adaptive cells of the Mammalian Immune System

Lyndsey Robertson

BSc. (Hons) Immunology

February 2015

This thesis is submitted

for the degree of

Doctor of Philosophy (Ph.D.)

to the University of Dundee

February 2015

Tables of contents

List of figures

List of tables

Abbreviations

Ab	Antibody
Ag	Antigen
ACK	Ammonium Chloride Potassium solution
APC	Antigen presenting cell
APC	Allophycocyanin
APC-Cy7	Allophycocyanin - Alexa Fluor 750
BCR	B Cell Receptor
β -Me	β-Mercaptoethanol
BMDM	Bone Marrow Derived Macrophages
BMDC	Bone Marrow Derived Dendritic Cells
BSA	Bovine Serum Albumin
CaMK	Ca^{2+} - Calmodulin-dependent kinase
CD	Cluster of Differentiation
cDC	Conventional Dendritic Cell
cDNA	Complementary DNA
CDSs	Cytosolic DNA sensors
COX	Cyclooxygenase
CST	Cell Signaling Technology
CTL	Cytotoxic T cell
CTLA-4	Cytotoxic T lymphocyte antigen 4
DAG	Diacylglycerol
DAPI	4', 6-diamidino-2-phenylindole
DC	Dendritic cell
DMEM	Dulbecco's Modified Eagles Media
DMSO	Dimethyl Sulpoxide
DNA	Deoxyribonucleic acid
DSTT	Division of Signaling Transduction Therapy
ECL	Enhanced Chemiluminescense Reagent
EDTA	Ethylenediaminetetraacetic Acid
EGTA	Ethyleneglycotetraacetic Acid

ELISA	Enzyme Linked Immunosorbent Assay
ERK	Extracellular Regulated Kinase
FACS	Fluorescence activated cell sorting
FC	Crystallisable fragment (antibody)
FBS	Fetal Bovine Serum
FITC	Fluorescein isothiocyanate
FSC	Forward light scatter
FoxO	Forkhead box O
FoxP3	Forkhead box P3
g	Gram
GM-CSF	Granuocyte Macrophage Colony Stimulating Factor
Grb2	Growth factor receptor bound protein 2
h	Hour
HEPES	N-2-hydroxyethylpiperazine-N'-2-ethane sulphonic acid
HBSS	Hanks Balanced Salt Solution
HRP	Horseradish Peroxidase
HSC	Hematopoietic Stem Cell
IBD	Inflammatory Bowel Disease
ICAM	Intracellular Adhesion Molecule
IELs	Intraepithelial Lymphocytes
IFN	Interferon
Ig	Immunoglobulin
IL	Interleukin
IP3	Inositol-1, 4,5-triphosphate
IMDM	Iscoves Modified Dulbecco's Medium
Treg	Induced Regulatory T cell
IRAK	IL-1 Receptor Association Protein Kinase
JAK	Janus Kinase
kDA	Kilo-Dalton
KI	Knock In
KO	Knock out
LN	Lymph nodes
LP	Lamia Propria

LPS	Lipopolysaccharide
m	Milli
M	Molar
µ	Micro
MAPK	Mitogen Activated Protein Kinase
M-CSF	Macrophage- Colony Stimulating Factor
MEK	MAP Kinase or ERK Kinase
MES	2-(N-morpholino)ethanesulfonic acid
Min	Minute
MHC	Major histocompatibility complex
Mol/M	Molar
mRNA	Messenger RNA
MyD88	Myeloid Differentiation Factor 88
n	Nano
nTreg	Natural Regulatory T cell
NFAT	Nuclear Factor of Activated T cells
NF-κB	Nuclear Factor κB
p-	Phospho
PAGE	Polyacrylamide Gel Electrophoresis
PAMP	Pathogen Associated Molecular Pattern
PBS	Phosphate Buffered Saline
PBST	PBS Tween
PCR	Polymerase Chain Reaction
PE	Phycoerythrin
PFA	Paraformaldehyde
PH	Pleckstrin homology
PI3K	Phosphoinositide 3-Kinase
PIP2	Phosphatidylinositol Biphosphate
PKC	Protein Kinase C
PKD	Protein Kinase D
pDC	Plasmacytoid Dendritic Cell
PLC-γ	Phospholipase C –γ
Poly (I: C)	Polyinosine-Polycytidylic Acid

PRR	Pattern Recognition Receptor
PdBu/PMA	Phorbol 12,13 Myristate Acetate
qPCR	Quantitative PCR
RNA	Ribonucleic Acid
Rpm	Revolutions per Minute
RORγT	Retinoic acid receptor-related orphan receptor gamma T
ROS	Reactive oxygen species
RMPI	Roswell Park Memorial Institute media
RT	Reverse Transcription
SD	Standard Deviation
SDS	Sodium Dodecyl Sulphate
S/Ser	Serine
SEM	Standard Error of the Mean
SOCS	Suppressor of Cytokine Signalling
STAT	Signal Transducer and Activator of Transcription
T/Thr	Threonine
TAK	Transforming Growth Factor-Beta-Activated Kinase
T-bet	T-box expressed in T cells
TCR	T Cell Receptor
TGF-β	Transforming Growth Factor Beta
TLR	Toll-Like Receptor
TNF	Tumour Necrosis Factor
TRAF	TNF-Receptor-Associated Factor
TRAM	TRIF-Related Adaptor Molecule
Treg	Regulatory T cell
TRIF	TIR-Related Adaptor Protein Inducing Interferon
Tris	Tris (hydroxymethyl) aminoethane
V	volts
v/v	Volume/Volume
WT	Wild Type
w/v	Weight/Volume
Z	Zymosan

Abstract

Protein kinase D (PKD) enzymes are a family of serine/threonine kinases that belong to the calcium/calmodulin-dependent kinase superfamily. Recently, a role for PKD enzymes has been established in the adaptive immune system where murine PKD2 was shown to be essential for normal peripheral CD4+ and CD8+ cytotoxic T lymphocyte function *in vivo*. PKD enzymes are known to be involved in adaptive immunity but it is not known if this is true for PKD in cells of the myeloid lineage, including dendritic cells (DCs) and macrophages or in myeloid malignancies such as chronic myeloid leukaemia (CML). Moreover, the literature on the role of PKD is complicated by the use of dual and non-specific pharmacological inhibitors.

Accordingly, one objective of this thesis was to characterise new generation small molecule inhibitors of PKD to verify their specificity. A second aim was to define PKD isoform expression and their role in the development and effector functions of myeloid cells. Thirdly, the requirement for PKD2 in the homeostasis of T lymphocytes within the small intestine was explored. The final objective was to determine if the development of regulatory T cells (Tregs) and if their effector functions *in vivo* from $PKD2^{KI/KI}$ mice were normal.

Three novel inhibitors of PKD were shown to be specific and target PKD catalytic activity effectively in a CML cell line, although some off-target effects were observed. *In vitro* experiments revealed that PKD2 is the dominant isoform expressed in both primary DCs and macrophages but is not required for the development of these subsets *in vivo*. Analysis of DC effector function implicated a role for PKD in the negative regulation of TLR4 stimulation. *In vivo* studies of Tregs lacking PKD2 catalytic activity revealed normal Treg development within the thymus. However, analysis of the periphery including the spleen and mesenteric lymph nodes revealed significantly increased Treg populations. Finally, investigation of an *in vivo* colitis model suggested that PKD2 is required for normal Treg effector function in the suppression of colitis. Collectively, the data in this thesis reveal novel roles for PKD enzymes in both the innate and adaptive mammalian immune systems.

Declaration

Candidate:

The candidate is the author of the thesis: that, unless otherwise stated, all references cited have been consulted by the candidate; that the work of which the thesis is a record, has been done by the candidate and that it has not been previously submitted for a higher degree. Provided that if the thesis is based upon joint research, the nature and the extent of the candidates individual contribution shall be defined.

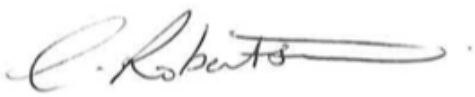

Lyndsey Robertson

Supervisor:

I certify that the conditions of the relevant Ordinance and Regulations have been fulfilled.

Dr. Sharon Matthews
University of Dundee

Acknowledgements

I would like to take the time to thank everyone who has helped and supported me throughout my PhD. Firstly, thank you to my supervisors: Dr Sharon Matthews for the opportunity to complete my PhD within her laboratory and to Professor Simon Herrington for fulfilling the role of second supervisor. Secondly, I would like acknowledging and thank the MRC for providing the financial funding that allowed me to complete my PhD.

I have been extremely lucky to work with truly talented and lovely people. Especially, I am thankful to Matt and to Mark who provided me with a source of constant assistance, support, advice, instruction and who made my PhD the experience a great journey with room for hilarious coffee chat and for this I feel very lucky. I am also thankful to Vicky who took the time to teach me multiple techniques and who was an absolute pleasure to work alongside during our time at Ninewells. I would also like to especially thank George Ramsay for our collaborative work, George, I learnt a lot from you during our gut experiments and thank you for your time, help and advice putting everything together (I imagine you will be glad to see the back of my boots).

I would also like to express my gratitude to work with great and truly lovely people within the DAC lab past and present including Professor Doreen Cantrell, Arlene, Rosie, Liz, George, Marcos, Kasia, Maria, Christina, Linda, Sarah, Mahima, David, and Jens who all essentially adopted me into their lab since when I became the last member of the Matthews lab. You made my last year fun and I never felt lonely – so thank you and I will miss you all and wish you all the very best for the future.

Rosie and Arlene also deserve a second mention to express my gratitude for all of the invaluable advice, instruction and work within anything and everything flow cytometry.

I am also very grateful to Don Tennant and colleagues within the animal unit for their hard work, assistance and advice during the entirety of my PhD.

I am truly grateful for my dad, Andrew, Katelyn and to my Aunty Jane and her family who have always supported me throughout my whole life but ever more so within my PhD. I am thankful for my dearest friends Laura, Benjamin and Helen who are essentially my extended family (Laura you of course are family!) – thank you for simply always being there and for never failing to make me laugh and or dance.

I am significantly grateful to Lauren and Susan (Miss Juicy Athena Swan) who have been a constant source of support through our payday dinners that have kept me sane and socialised especially during my write up. Lauren, a tremendous thank you for constantly shaking some perspective into me yet never judging, you also deserve a massive thank you for relentlessly reading my thesis and for helping me with countless issues - thank you for being such a dear friend and for making my write up significantly smoother.

I am also thankful to the immunology gang for simply being there for moral support including Carly, Lauren, Joanne (especially for providing me with countless papers during my write up, maybe I should also thank the University of Edinburgh's outstanding journal subscription) and A.J.Hutton for your magnificent science chat.

Last but absolutely not least, I would like to thank Stuart, who I am forever grateful and indebted to for providing me with the support, encouragement and for your patience that truly allowed me to complete my PhD, I couldn't have done it without you thank you for everything and most especially thank you for making me laugh when I needed to the most.

1 Introduction

1.1 The mammlian immune system - an overview

The immune system exists to recognise non-self in order to protect the body from disease. To be effective in doing this the mammalian immune system is capable of two types of immune response: the innate and the adaptive responses. The innate (*or natural*) immune system relies on the immediate recognition of evolutionary conserved invariant patterns on invading pathogens. The innate immune system includes macrophages, dendritic cells, neutrophils, basophils and eosinophil's.

The adaptive (*or acquired*) immune response in contrast is slower but highly specific and ultimately results in the generation of immunological memory and establishment of immunity to eliminate pathogens in future encounters. Not only is immunological memory established but also the immune response to the re-encountered pathogen is faster and with an increased magnitude. The adaptive immune system is compromised of multiple subsets of T- and B-lymphocytes that express receptors that are specific for particular antigens upon a pathogen. Both branches of the immune system work towards the same goal to clear the pathogen from the body. However, the immune system must also have intricate mechanisms in place to prevent a normal immune response becoming out of control by promoting immune homeostasis. This process is required to ultimately avoid reactivity or harm towards self, otherwise known as auto-immunity, or indeed to harmless particles such as pollen that will led to the development of allergies. The importance of a functional immune system is frequently highlighted in individuals in whom the immune system is compromised, often leading to serious and potentially fatal infections by pathogens that are regularly cleared on a daily basis by a healthy individuals.

1.2 Innate immune system

The front line of the innate immune system is barrier protection whereby anatomical and physiological barriers effectively prevent infection, such as the epithelial barrier provided by intact skin or the low pH of the stomach. When pathogens successfully breach these barriers the innate immune cells must rapidly respond to provide initial defense by engulfing pathogens as well as infected or dying cells, in a process known as phagocytosis. In addition to providing the early immune response the innate immune system also has the ability to communicate with and drive the adaptive immune response towards a pathogen, thereby linking the two branches of the immune system together (extensively reviewed (Basset et al. 2003) (Janeway & Medzhitov 2002)).

1.2.1 Innate immune cell subsets: cells of the myeloid lineage

1.2.1.1 Myeloid cell development and function

The mammalian immune system consists of cells that have differentiated from hematopoietic stem cells (HSCs) that reside within the bone marrow. Differentiating from HSCs both the myeloid and lymphoid lineages arise that go on to generate the innate and adaptive immune system respectively (extensively reviewed (H. Iwasaki & Akashi 2007)).

The myeloid lineage develops from common myeloid progenitor cells (CMPs) and includes a number of morphologically similar but functionally distinct cells (reviewed (Geissmann et al. 2010)). These include subsets of granulocytes (neutrophils, basophils and eosinophil's) monocytes, macrophages, mast cells, erythrocytes, megakaryocytes and dendritic cells (DCs) (Akashi et al. 2000). Myeloid and lymphoid cell differentiation from HSCs is depicted in Figure 1.1. The differentiation pathways that govern monocyte and DC development have been elegantly delineated using fate-mapping studies. However, the differentiation pathways determining tissue macrophages is less defined.

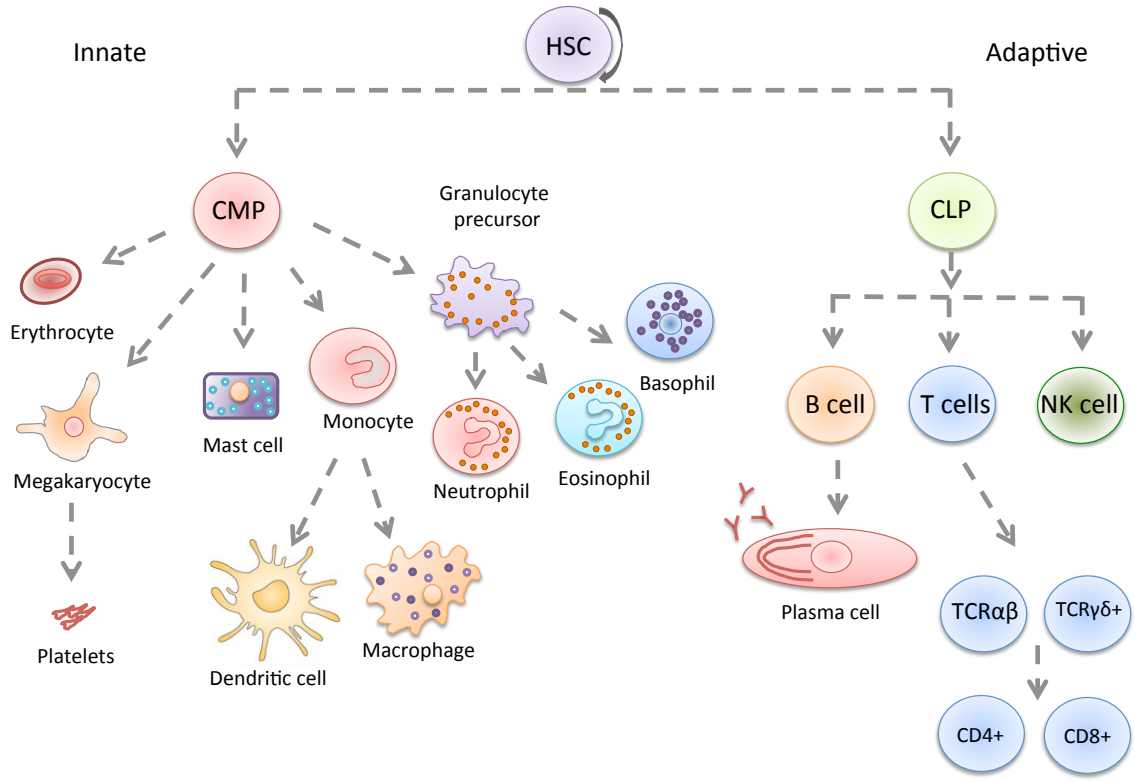

Figure 1.1 Development of innate and adaptive immune cells from hematopoietic stem cells

Hematopoietic stem cells (HSCs) give rise to common progenitors including common myeloid progenitor cells (CMPs) and common lymphoid progenitor cells (CLPs) which make up the innate and adaptive immune systems respectively. CMPs give rise to erythrocytes, megakaryocytes, mast cells, granulocyte precursors and monocytes. Granulocyte precursors go onto to give rise to neutrophils, eosinophils and basophils. Monocytes further differentiate into dendritic cells and macrophages. CLPs give rise to B and T lymphocytes as well as natural killer (NK) cells. B lymphocytes upon activation differentiate into plasma cells that secrete antibodies. T lymphocytes under go further development within the thymus to generate multiple subsets including TCRαβ+ and TCRγδ+ cells as well as CD4+ and CD8+ positive subsets. *Adapted from (Imhof & Aurrand-Lions 2004) and (Geissmann et al. 2010).*

1.2.1.2 Neutrophils

Neutrophils are the most common white blood cell within the body and are one of the first cells to sense and respond to an infection. Neutrophils are present in the blood, but are also attracted to sites of inflammation upon infection by local soluble mediators, such as cytokines and chemokines,

produced by epithelial cells upon damage, stress or infection. The role of neutrophils is two-fold, they are able to phagocytose pathogens and undergo a process called degranulation whereby anti-microbial granules are released, both of which strongly promote pathogen clearance (reviewed (Kolaczkowska & Kubes 2013)).

1.2.1.3 Monocytes and dendritic cells

Monocytes primarily reside within the bone marrow and can give rise to a variety of innate immune cell subsets within peripheral tissues via migration in the blood. Monocytes routinely differentiate into macrophages under normal circumstances to promote immune homeostasis, this is known to occur within the steady state (Auffray et al. 2009; Swirski et al. 2009). Upon inflammation, circulating monocytes can proliferate and give rise to specialised macrophage populations upon extravasation from the blood via the epithelium into peripheral tissues (Serbina et al. 2008). Dendritic cells within the innate immune system are derived from the common myeloid progenitor within the bone marrow and migrate into peripheral tissues to carry out distinct functions (Ginhoux & S. Jung 2014).

Importantly, neutrophils, macrophages and DCs are characterised by the ability sense, respond and phagocytose pathogens and dying or infected cells (Savina & Amigorena 2007). DCs are highly efficient at this and process acquired antigen for presentation upon the cell surface via major histocompatibility complex (MHC) class II along with soluble mediators, including cytokines and chemokines, to the instruct adaptive immune system and generate immunological memory (Hespel & Moser 2012).

1.2.1.4 Basophils and mast cells

Other innate cells such as basophils and eosinophils primarily function through their ability to perform degranulation, which is the release of cytoplasmic granules that contain proteins and enzymes that are highly effective in clearing parasites from the body.

Finally, mast cells are are characterised by immunity against parasitic infections but have a well documented role within allergic responses predominantly through the release of large amounts of histamine upon activation (Wernersson & Pejler 2014).

1.2.1.5 Macrophages

Macrophages are highly heterogeneous cells that are able to perform different functions depending on the subset and anatomical location (Wynn et al. 2013). The main function performed by macrophages is phagocytosis of pathogens such as bacteria after activation of PPRs, which also induces the production of pro-inflammatory cytokines such as IFNγ and TNFα, both of which alert and recruit other immune cells of an existing infection. Macrophages also play an important role in phagocytosing apoptotic cells promoting tissue homeostasis (Henson & Hume 2006) (Muñoz et al. 2010). This is largely achieved by scavenger receptors expressed on macrophages which are now recognised as a subclass of PPR (Canton et al. 2013). Macrophages differentiate from circulating monocytes within the blood. In contrast to DCs, macrophages are not migratory cells and instead reside in peripheral tissues. Tissue specific subsets of macrophages include; kupffer cells (liver), Langerhans cells (skin), microglia (central nervous system) and osteoclasts (bone) (Davies et al. 2013).

Recent studies have developed the idea of macrophage polarisation into two distinct subsets, to mimic the nomenclature used for Th subsets (Martinez & Gordon 2014).

Classically activated macrophages are described as pro-inflammatory 'M1' macrophage that are characterised by the induction by IFNγ and TNFα (Dale et al. 2008) and known to play a major role in the immune response to invading pathogens including bacteria and viruses. Due to the pro-inflammatory nature of classically activated macrophages they have also been implicated in multiple chronic inflammatory diseases such as rheumatoid arthritis, systemic lupus erythematous (SLE) and irritable bowel diseases (Mosser & Edwards 2008) (Hamilton & Tak 2009).

Alternatively activated macrophages, also know as ‘M2’, which are characterised as anti-inflammatory phenotype with high production of IL-10. More recently, alternatively activated macrophages have been renamed wound healing or regulatory macrophages (Gordon & Martinez 2010). Wound healing macrophages are activated in response to IL-4 and although the exact source of IL-4 remains to be elucidated it is thought to be highly likely that it is produced by basophils or eosinophils in response to tissue damage or stress (Loke et al. 2007).

It should be highlighted however that in regard to both of these distinct macrophages subsets it still remains to be elucidated if these subsets are stable and do not simply convert depending on context.

1.2.1.6 Dendritic cells

Ralph Steinman and Zanvil Cohn discovered the existence of dendritic cells in the 1970's and their importance within the immune system was met with skepticism (Steinman & Cohn 1973). DCs are classed as professional antigen processing and presenting cells within the innate immune system with the unique ability to not only induce T cell activation but also subsequently shape the differentiation of specific T cell subsets (Steinman & Witmer 1978) (Steinman 2012). DCs can also be further categorised depending on expression of distinct cell surface markers, anatomical location and more appropriately the function they perform within the immune system and immune response (reviewed(Mildner & S. Jung 2014)). Research into therapeutically harnessing DCs ranges from studies into wealth of diseases including improving vaccination to infectious disease, cancer prevention and within autoimmune disease (Palucka & Banchereau 2012) (Ganguly et al. 2013).

Following activation by infection of inflammatory stimuli, DCs undergo maturation, which results in dramatic changes in their antigen uptake, processing and presentation capabilities. This maturation process involves three consecutive processes; upregulation of MHC class II for presentation of processed antigen, costimulatory molecules (including CD40, CD80, CD86, ICOSL) which act as a secondary confirmation promoting T cell activation, and CCR7 upregulation which promotes migration to T cell rich zones within

lymphoid tissue that express high levels of CCL19/21, the ligand for CCR7 (Dieu et al. 1998; Yanagihara et al. 1998) (Sozzani et al. 1998). Mature DCs also upregulate the production of context dependent cytokines, which in turn instructs T cell differentiation into specific cell subsets (Sallusto et al. 1999; Tan & H. C. O'Neill 2005).

As well as from detecting infection, DC subsets also have an essential role in establishing tolerance whereby multiple studies have shown depletion of key regulators within DC subsets or indeed constitutive deletion of DCs themselves can lead to autoimmunity (Travis et al. 2007) (Melillo et al. 2010) (S. J. Kim et al. 2011) (Ohnmacht et al. 2009).

However, the involvement of DCs in the generation of tolerance is also complex and bidirectional whereby DCs can also participate in the development of autoimmunity towards self by promoting the differentiation of Th17 cells, which are frequently the basis of autoimmune inflammation (Bettelli et al. 2007). Contrasting roles of the promotion or inhibition of the immune response is shown in Figure 1.2.

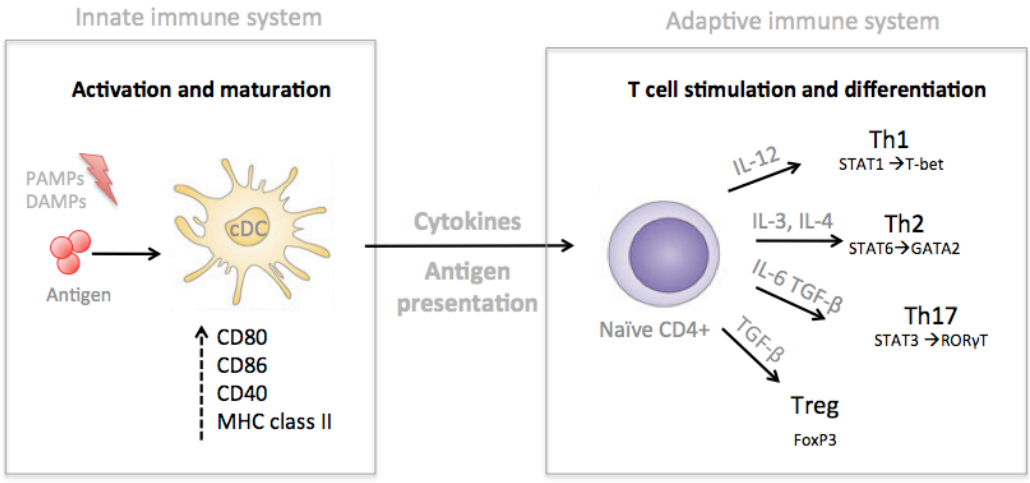

Figure 1.2 Activation and maturation of dendritic cells within the innate immune system orchestrates the adaptive immune response

Depending on the inflammatory context, DCs can undergo activation and maturation and subsequently drive the activation, proliferation and differentiation into various subsets of CD4+ T helper cells. Adapted from (Ganguly et al. 2013).

As mentioned, DCs are a heterogeneous population and exist in two major populations including conventional DCs (cDCs) and plasmacytoid DCs (pDCs). Both of these subsets are phenotypically and functionally distinct in the role they perform within the immune system and in a resulting immune response (Satpathy et al. 2012).

1.2.1.6.1 Conventional DCs

cDCs are characterised by multiple key attributes. cDCs are highly migratory cells that are also present in non-lymphoid tissues within the steady state, constantly surveying the body for antigen whether pathogen or self (Merad et al. 2013). cDCs also have superior antigen processing and presenting abilities (Segura & Villadangos 2009) (Joffre et al. 2012). Finally, cDCs have a superior ability to prime naïve T cells responses (Banchereau & Steinman 1998).

cDCs can be divided in two major subgroups based upon localisation within tissues or their migratory pathways through the body (Figure 1.3).

Migratory cDC subset is most frequently identified by CD11b+ cDCs and CD11b- CD103+ cDCs subsets. CD11b+ cDCs are found in the lymph node that act as sentinels to sense antigen throughout the body. This subset is frequently attributed to being in the steady state and for their role in the maintenance of peripheral tolerance (Jakubzick et al. 2008). However upon inflammation and infection CD11b+ cDCs are key in the initiation of the adaptive immune response. The migratory CD11b- CD103+ cDC subsets are more commonly found in mucosal linings such as the small intestine where they perform distinct functions and are discussed later in this chapter (Helft et al. 2010) (del Rio et al. 2010).

The second major group of cDCs is the lymphoid resident DCs, found in major lymphoid tissues including the spleen, lymph nodes and the thymus. Lymphoid resident cDCs are divided into 3 distinct groups by expression of distinct surface markers including CD4+ cDCs, CD8α+ cDCs and double negative CD4-CD8α- cDCs (Vremec et al. 1992) (Vremec et al. 2000).

CD8α+ cDCs are specialised DCs with the ability to perform cross presentation, a process in which exogenous antigen is phagocytosed and displayed on MHC class I to CD8+ CTLs (Haan et al. 2000) (Schliehe et al. 2011).

CD4+ cDCs and DN CD4-CD8α- cDCs have also been shown to present antigen MHC class I antigens (T. S. Kim & Braciale 2009) (Smith et al. 2003) but are more efficient at MHC class II antigen presentation and therefore are considered specialised for CD4+ naïve T cell activation (Allenspach et al. 2008) (Mount et al. 2008).

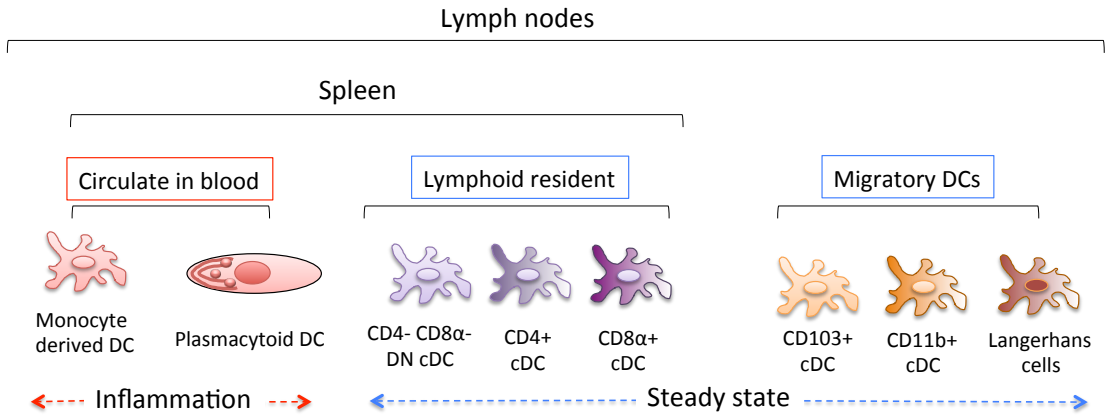

Figure 1.3 DC subsets: differentiation and trafficking

Monocyte derived DCs and pDCs circulate within the blood populating the lymph nodes and the spleen during the inflammatory response. cDC subsets are broadly divided into two subsets including lymphoid resident and migratory and maintain homeostasis within the steady state. CD4- CD8α- DN cDCs, CD4+ cDCs and CD8α+cDCs are lymphoid resident whereas CD103+ cDCs, CD11b+ cDCs and Langerhans cells migrate throughout the body and travel to secondary lymphoid organs. Adapted from (Belz & Nutt 2012).

1.2.1.6.2 Plasmacytoid DCs

pDCs are morphologically, phenotypically and functionally distinct from cDCs and exist as a small population that primarily reside in the blood and circulate to lymphoid tissues throughout the body (Sozzani et al. 2010) (Randolph et al. 2008). The key differences between cDCs and pDC subsets are depicted in Figure 1.4. Although the exact identity of a distinct and committed pre- pDC precursor has not yet been elucidated it is known that the upregulation of the basic helix-loop-helix transcription factor (E protein) E2-2 is to be crucial for pDC development (Cisse et al. 2008) (Reizis 2010). Functionally, pDCs are specifically important against viral infection as they specialise in the production

of large amounts of type I interferon (IFN), particularly IFNα but also IFNβ (Reizis et al. 2011) (Takeuchi & Akira 2009). Human pDCs have been reported to produce 1–2 units per cell or 3–10 pg per cell) within 24 hours, which is 200 to 1,000 times more than the amount produced by any other blood cell type (Siegal et al. 1999). The production of type I IFN follows the detection of foreign nucleic acids produced during viral replication by preferential expression of endocytic TLRs including TLR7 and TLR9. Type I IFN promotes an anti-viral response by promoting cell apoptosis in infected cells, stimulating hematopoiesis, promoting the maturation of cDCs, and activating the adaptive immune response including the activation of CD8+ CTLs, NK cells and stimulating B cell proliferation (Ivashkiv & Donlin 2014) (Gilliet et al. 2008).

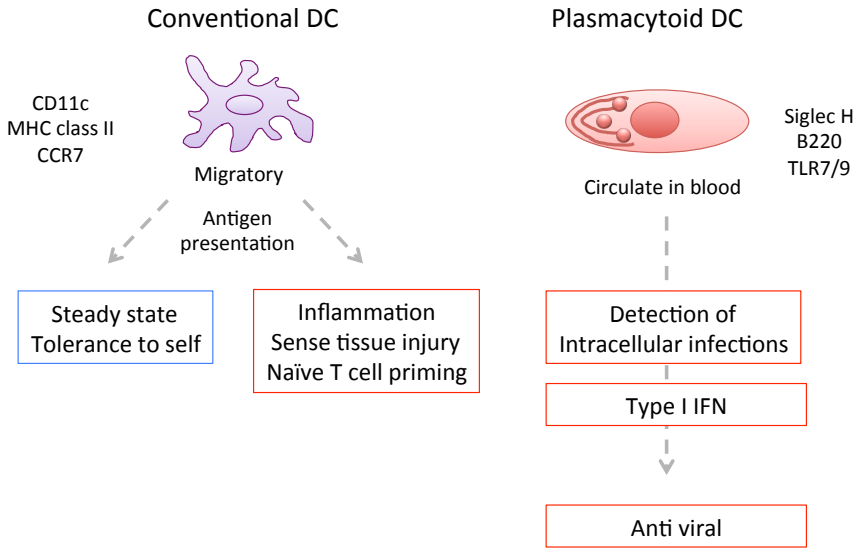

Figure 1.4 Key differences between cDCs and pDC subsets

cDCs are highly migratory cells with superior antigen presentation skills yet are involved in both tolerance towards self during the steady state but also during the immune response and therefore naïve T cell activation. pDCs in contrast circulate within the blood and are key mediators during an anti-viral immune response due to their superior type I IFN production. Adapted from (Takeuchi & Akira 2009).

1.2.2 Pathogen recognition receptors

The first step towards an immune response is the sensing of an invading pathogen. This is achieved by the use of germline encoded multiple pattern recognition receptors (PRRs) by innate immune cells. The four main classes of PPRs used by the innate immune system include: Toll-like receptors (TLRs), NOD-like receptors (NLRs), Retinoic acid- inducible gene (RIG)-I -like receptors (RLRs) and C-type lectin receptors (CLRs) and more recently identified cytosolic DNA sensors (CDSs) (extensively reviewed (Akira et al. 2006)).

PRRs are germline-encoded receptors that recognise highly conserved pathogen associated molecular patterns (PAMPs). PRRs also have the ability to recognise markers of cellular stress that are released by damaged or infected cells, these signals are collectively termed danger associated molecular patterns (DAMPs). Activation of these receptors promotes the transcription of multiple genes involved in the inflammatory response; this response is specific depending on the activated PRRs.

1.2.2.1 Toll like receptors

Toll-like receptors (TLRs) are a family of PRRs expressed on the cell surface and within the cell found in endosomal and lysomal compartments of multiple cells, including macrophages and DCs (reviewed (L. A. J. O'Neill et al. 2013)).

TLRs are a type I transmembrane proteins that are conserved between humans and insects. TLRs comprise of an ectodomain, which contains leucine-rich repeats allowing the recognition of PAMPs, a transmembrane region and a cytosolic toll-1R-receptor (TIR) (that resembles the IL-1R) domain that facilitate downstream signalling cascades after TLR ligation.

To date, 13 TLR receptors have been discovered including 10 (TLR1-10), which are expressed in humans, and 12 TLRs in (TLR1-9 and TLR11-13) are expressed in mice (Akira & Takeda 2004). Importantly, TLR family members are expressed differently among subsets of immune cells. TLRs are also expressed on non-immune cells including epithelial cells in the intestine and within the skin to maximise environmental sensing at vulnerable areas of the body. The various receptors, their specific ligands and their location are described in Table 1.1.

TLR2 resides on the plasma membrane and recognises lipid-containing PAMPS including lipoteichoic acid and di and tri-acylated lipopeptides. TLR2 achieves this by forming a dimeric complexes with another chain of TLR2 former a homodimer or by dimerising with TLR1 or TLR6 to form heterodimers (M. S. Jin et al. 2007) (J. Y. Kang et al. 2009). TLR4 does this in combination with MD2 and CD14 (H. M. Kim et al. 2007) (B. S. Park et al. 2009a). TLR4 was the first TLR to be discovered binds lipopolysaccharide (LPS), a major component of Gram-negative bacteria cell wall that causes endotoxin shock largely mediated by the release of TNFα and IFNγ by activated macrophages (Sparwasser et al. 1997). Mice deficient in TLR4 are hyposensitive to LPS (Hoshino et al. 1999). TLR5 recognises flagellin found on flagellated bacteria (F. Hayashi et al. 2001) and is highly expressed within the gut including DCs within the lamina propria of the small intestine (Uematsu & Akira 2009).

TLR3, 7,8 and 9 recognise viral nucleic acids and are expressed within endosomal membrane. The intracellular localisation of these TLRs allows the immune system to sense non-self nucleic acids that are produced during viral replication after a virus infects a cell. The activation of TLR3, 7,8 and 9 leads to the induction of signalling pathways to produce type I IFN, that mediates antiviral responses (Uematsu & Akira 2007) (González-Navajas et al. 2012). TLR3 is located within cell endosomes and recognises double stranded RNA (dsRNA) produced by viruses during replication (Alexopoulou et al. 2001) (Weber et al. 2006) (Leonard et al. 2008). TLR7 and TLR8 recognise ssRNA and have been shown to recognise multiple viruses including Influenza, Sendai and Coxsackie B viruses (Lund et al. 2004) (Heil et al. 2004) (Diebold et al. 2004) but also recognise bacteria including Group B Streptococcus (Mancuso et al. 2009). TLR9 recognises unmethylated CpG DNA motifs found in bacterial and viruses, and induces pleiotropic immune responses that are cell type specific (Hemmi et al. 2000) (Kumagai et al. 2008).

TLR	Specific ligands	Location
TLR1:2 heterodimer	Multiple triacylated lipoproteins (Gram- bacteria)	Plasma membrane
TLR2	Lipopeptides Lipoproteins Gram+ bacteria Lipomannans (Fungi and mycobacteria)	Plasma membrane
TLR2: TLR6 heterodimer	Bacterial diacylated lipoproteins (Gram+ bacteria)	Plasma membrane
TLR3	Double stranded RNA (Viruses)	Endosome
TLR4	LPS, heat shock proteins fibrinogen	Plasma membrane
TLR5	Flagellin	Plasma membrane
TLR6	Multiple diacylated lipopeptides	Plasma membrane
TLR7	Single stranded RNA (Viruses)	Endosome
TLR8	Single stranded RNA Poly T oligonucleotides (Viruses)	Endosome
TLR9	Unmethylated CPG DNA (Bacteria and herpes viruses)	Endosome

TLR10 (Human only)	Unknown	Plasma membrane
TLR11 (Mouse only)	Profilin (Uropathogenic bacteria)	Plasma membrane
TLR12 (Mouse only)	Profilin (Uropathogenic bacteria)	Plasma membrane
TLR13 (Mouse only)	23S ribosomal RNA sequence	Endosome

Table 1.1 Toll like receptor family, their ligands and expression location *Adapted from* (Takeda et al. 2003) (Botos et al. 2011) (Akira & Takeda 2004)

1.3 Adaptive immune system: cells of the lymphoid lineage

The adaptive immune system includes B cells, T cells and natural killer (NK) cells. The adaptive immune system arises from the lymphoid committed lineage within the bone marrow. B lymphocytes develop in the bone marrow from common lymphoid progenitor cells (CLPs) that are derived from HSCs (Kondo et al. 1997) (Figure 1.1). In contrast to cells of the myeloid lineage, T lymphocytes undergo development in the thymus after CLPs that have differentiated from HSCs have populated the thymus. During the development of B and T lymphocytes within the bone marrow and thymus respectively, both subsets undergo gene rearrangement to successfully generate a unique B cell receptor (BCR) and T cell receptor (TCR) respectively. After development, B and T lymphocytes migrate into the periphery, circulate the blood and enter peripheral lymphoid tissues including the lymph nodes, spleen and mucosal lymphoid tissues of the respiratory tract and the gastrointestinal tract.. It should also be noted that natural killer cells (NK cells) also arise from the lymphoid

lineage, another type of cytotoxic lymphocyte that are required during microbial infection and the control of several types of tumors (Vivier et al. 2008).

Importantly, the adaptive immune system is heavily dependent upon innate immune cell instruction to orchestrate and regulate responses. Upon successful activation of the adaptive immune system, activated adaptive lymphocytes will feedback to amplify and regulate innate immune responses creating a very effective and elegant system.

1.3.1 B lymphocytes

B lymphocytes have three principle functions which are: to produce specific antibodies to antigens that are present on pathogens, to perform the role of antigen presentation and to form immunological memory in the form of long lived memory B lymphocytes.

Within development within the bone marrow, B lymphocytes undergo a complex progression of differentiation and maturation to generate a functional and specific BCR that is specific to one antigen. This process is tightly regulated and failure to produce a functional BCR will result in a form of programmed cell death known as apoptosis (reviewed (Cooper 2015)). It is also essential that the BCR does not recognise self-antigens or is auto-reactive.

After successful maturation B cells leave the bone marrow and populate various lymphoid tissues throughout the body. Upon recognition of a B cells cognate antigen they become activated and undergo proliferation. The activation of B cell results in processes such as somatic hyper-mutation (SHM) and antibody class switching whereby B cells can heighten their specificity or avidity for their specific antigen. Activated B cells can also become plasma cells, which are able to release large amounts of antibodies during an immune response; this typically takes place in germinal centers within lymphoid tissues (De Silva & Klein 2015). Follicular helper T cells assist this process by providing specific cytokines that can also shape the immune response depending on the invading pathogen (Breitfeld et al. 2000) (reviewed(Crotty 2011)). Within germinal centers, B cells typically undergo multiple rounds of proliferation and antigen-affinity driven selection (Shlomchik & Weisel 2012). Activated B cells release

antibodies, which are secretory form of the BCR. These antibodies are therefore antigen-specific, although isotypes may be different if the B cell has undergone class switching. A mature naïve B cell expresses immunoglobulin M (IgM) as the BCR, but four additional isotypes of antibody exist which include: IgG, IgA, IgD, and IgE, all of which have distinct functions.

After an infection is eliminated a subset of B cells can become long-lived memory B cells that provide humoural immunity to pathogens in the future. These memory B cells require less help to instigate the initial response to a known infection, and for this reason are extremely efficient at clearing a pathogen before it can establish an active infection (reviewed (Tarlinton & Good-Jacobson 2013)).

1.3.2 T lymphocyte subsets and differentiation

T lymphocytes undergo development within the thymus where T cells will generate a functional TCR ((Koch & Radtke 2011)). The TCR is composed of a heterodimers, approximately 95% of T cells express the αβ chains and 5% express a γδ chain, however this percentage is highly disposed to change depending on anatomical location, infection and indeed during disease. Expression of these two distinct TCR defines the two divergent lineages of T cells that perform distinct roles within the immune system and within homeostasis. The TCRαβ+ subsets primarily reside in peripheral lymphoid organs such as the spleen and lymph nodes. In contrast, the TCRγδ+ T cells are most prominent within the epithelial layers such as the skin, lung and intestinal epithelium (Girardi 2006). TCRγδ T cells display a much more limited diversity of TCR when compared to TCRαβ+ T cells, this is thought to account for the ability of TCRγδ+ T cells to respond to conserved ligands expressed by pathogens and stressed cells in sites within the body that are highly susceptible to infection, such as mucosal linings (Xiong & Raulet 2007).

Additionally, T lymphocytes will also express one of the MHC co-receptors CD4 or CD8 thereby creating two functionally distinct groups termed CD4+ T

cells and CD8+ T cells (Koch & Radtke 2011). CD4+ T cells and CD8+ T cells are restricted to antigen recognition via MHC class II and MHC class I respectively.

T cells that develop successfully migrate from the thymus to populate secondary lymphoid tissues and perform distinct roles within the immune system.

Resting naïve CD8+ T cells, also known as cytotoxic T lymphocytes (CTLs) are characterised by their ability to sense and react to pathogens by substantial expansion and differentiation into cytotoxic effector cells ((N. Zhang & Bevan 2011)). CTLs recognise antigen displayed on MHC class I molecules, most cells within the body express MHC class I to display intracellular contents. This allows CTLs to scan cells for the presence of foreign peptides on the cell surface indicating that a cell is infected, particularly in the case of viral infection. Activated CTLs can kill target cells through enzymatic means by the release of perforin, a cytolytic protein that forms pores in the target cell membrane (Russell & T. J. Ley 2002) (Catalfamo & Henkart 2003).

Naïve CD4+ T cells that experience their cognate antigen and become activated and instructed by cytokines from APCs include subsets called T helper cells (Th) which includes multiple subgroups including; Th1, Th2, Th17, and T regulatory T cells (Treg) (Zhu et al. 2010). The specific cytokines that instruct the differentiation of each subset and the identification of distinct CD4+ Th subsets by transcription factors are detailed in Figure 1.5.

Th1 cells are particular effective in cell-mediated immune response against intracellular pathogens, the most characterised of which is the requirement for Th1 cells for protection against *Mycobacterium tuberculosis* (Flynn et al. 1993). Naïve CD4+ T cells are promoted to differentiate into Th1 cells by the production of interleukin (IL)-12 (Hsieh et al. 1997) and express the transcription factor T-bet (Szabo et al. 2000). Characteristically, Th1 cells produce high levels of interferon-gamma (IFNγ) (Wenner et al. 1996) which is known to activate macrophages during an immune response (Mosser 2003).

IL-4 promotes the differentiation of Th2 cells from naïve CD4+ T cells (Swain et al. 1990). The Th2 subset is defined by the presence of the GATA3 transcription factor (W. Zheng & Flavell 1997) and characteristically produce IL-4, IL-3 and IL-15 Th2 cells have been well documented to be extremely effective

at clearing parasitic pathogens, mainly through the ability of IL-3 and IL-15 cytokines to activate mast cells and promote degranulation (Shelburne & Ryan 2001).

Th17 cells are defined by the production of IL-17 and presence of the retinoic-acid receptor-related orphan receptor gamma T (RORγT) transcription factor (Korn et al. 2009). Th17 cells have been implicated in a variety of inflammatory diseases due to their ability to cause tissue damage by pro-inflammatory nature of IL-17 (Langrish et al. 2005).

Naïve CD4+ T cells under instruction of anti-inflammatory cytokines such as TGF-β can differentiate into a regulatory T cell (Treg) subset; this subset is discussed in depth in the following section.

Finally, naïve CD4+ T cells under the instruction of IL-21 and IL-6 can differentiate into a follicular helper T cell subset (Tfh) (Vogelzang et al. 2008), which as mentioned function to provide B cell help within germinal centers during an immune response and facilitate the development of memory B cell populations.

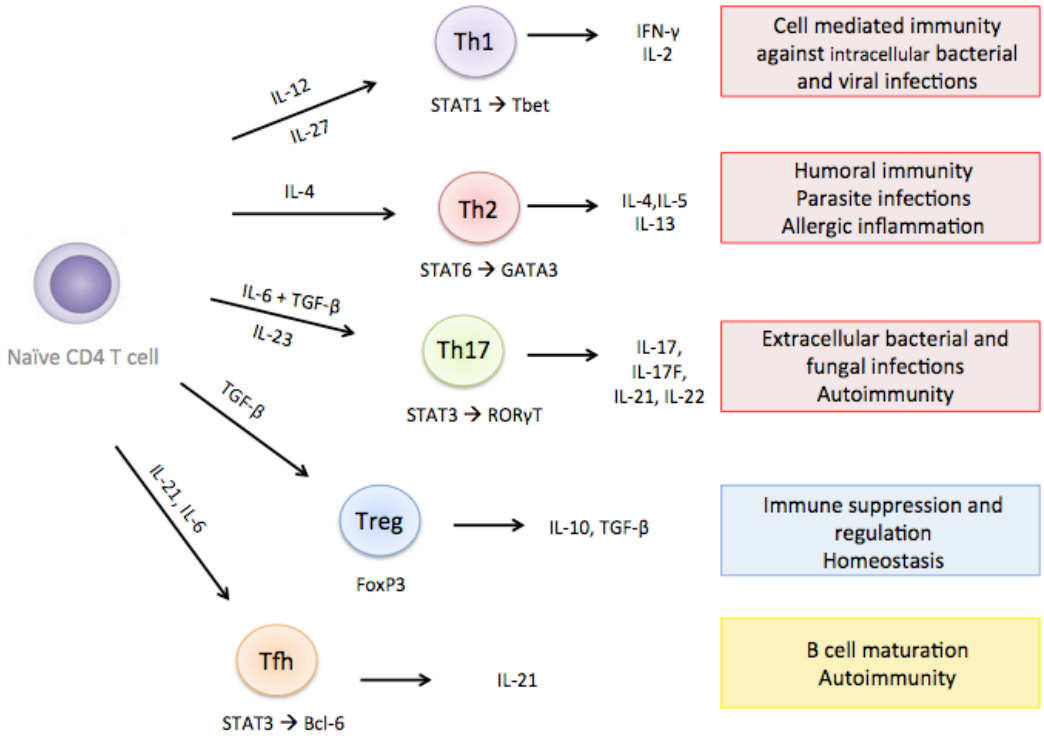

Figure 1.5 CD4 T cell differentiation into distinct T helper subsets

Naïve CD4+ T cells undergo proliferation and differentiation following a resulting immune response to pathogens or during normal immune cell homeostasis in the case of Treg subsets. Subset differentiation is dependent on specific cytokines received during T cell activation by APCs. Th subsets are defined by present of specific transcription factors and production of characteristic cytokines and ultimately their specific function within the immune system and within an immune response. *Adapted from* (Wan 2010)

The existence of multiple helper T cell subsets allows the immune system the flexibility to tailor an immune response according to the type of pathogen that encountered or indeed during normal immune homeostasis.

1.3.2.1 Regulatory T cells (Tregs)

This thesis has a particular focus on Treg cells and therefore a more detailed description of this CD4+ regulatory T cell subset is required.

An immune response involving the adaptive immune system is very potent and within a healthy individual these responses must be tightly regulated. In order to provide balance suppressive regulatory CD4+CD25+ Tregs exist (reviewed extensively (Rudensky 2011) (Josefowicz et al. 2012)). The presence of a regulatory T cell subset capable of suppression was first noted in studies observing protection from inflammatory lesions in mice receiving CD4+CD25 (IL-2Rα) + T cells after thymectomy (Asano et al. 1996). These findings promoted further exploration to define the development and function of Tregs, leading to the discovery of the transcription factor forkhead box P3 (FoxP3), as a master regulator of both the development and function of Tregs (Fontenot et al. 2003). The significance of the Foxp3 transcription factor is highlighted in studies whereby loss of function mutations within FoxP3 result in severe multi-organ autoimmune and inflammatory disorder (IPEX) and a similar disease in the transgenic mouse strain *scurfy* (Brunkow et al. 2001) (Bennett et al. 2001) (Wildin et al. 2001). Additional studies have also shown that loss of FoxP3 and resulting pathologies are caused by the lack of regulation of CD4+ T cells within *scurfy* mice (Blair et al. 1994), further emphasising the indispensible requirement for Tregs in the normal regulation and homeostasis of the immune system.

Tregs exist in two main groups: natural Tregs (nTreg) and induced iTregs (iTregs). nTregs arise in the thymus during T cell development whereby CD4+ T cells with a self-reactive TCR recognise self-peptide (Hsieh et al. 2012). iTregs in contrast differentiate from naïve CD4+ T cells within the periphery in response to cytokines such as TGF-β and IL-10 (Bilate & Lafaille 2012). nTreg and iTreg development is depicted in Figure 1.6. By definition, nTregs and iTregs both express high levels the transcription factor FoxP3 as well high surface expression of CD4 and constitutively high levels of CD25.

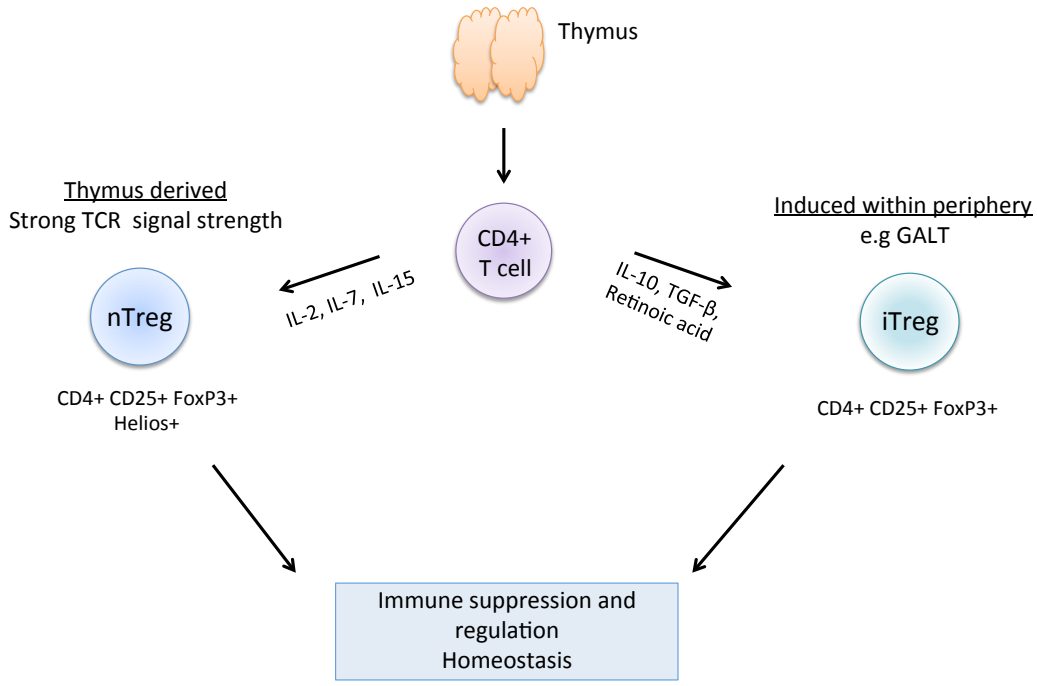

Figure 1.6 Generation of natural and inducible Tregs

Tregs can be divided into two distinct subsets characterised by their site of development however both subsets arise from CD4+ T cells. nTreg arise within the thymus upon generation of a self-reactive TCR and response towards self antigen whereas iTreg are converted within the periphery in response to environmental cues such as TGF-β, IL-10 and retinoic acid, commonly found in GALTs. Adapted from (Josefowicz et al. 2012).

Despite the accumulating knowledge defining molecular mechanisms of Tregs development and their obvious role within immune regulation, the understanding of molecular mechanism of suppression by Tregs is still limited. Evidence largely from *in vitro* studies have indicated multiple mechanism of

suppression including; inhibition of T cell proliferation by sequestering available IL-2 (Pandiyan et al. 2007), cytotoxic T-lymphocyte-associated protein 4 (CTLA-4) which can provide a inhibitor signal to T cells via CD28 ligation but CTLA-4 has also been shown to promote the removal of costimulatory molecules CD80 and CD86 on the cell surface of APCs (Qureshi et al. 2011) (Read et al. 2006), suppression through secretion of potent anti-inflammatory cytokines including IL-10 and TGFβ (Rubtsov et al. 2008) and finally cell contact dependent mechanisms of target cell killing by release of granzyme B (Gondek et al. 2005) (Cao et al. 2007). These suppressive functions are illustrate in detailed mechanisms of Treg suppressive abilities are extensively reviewed (Josefowicz et al. 2012).

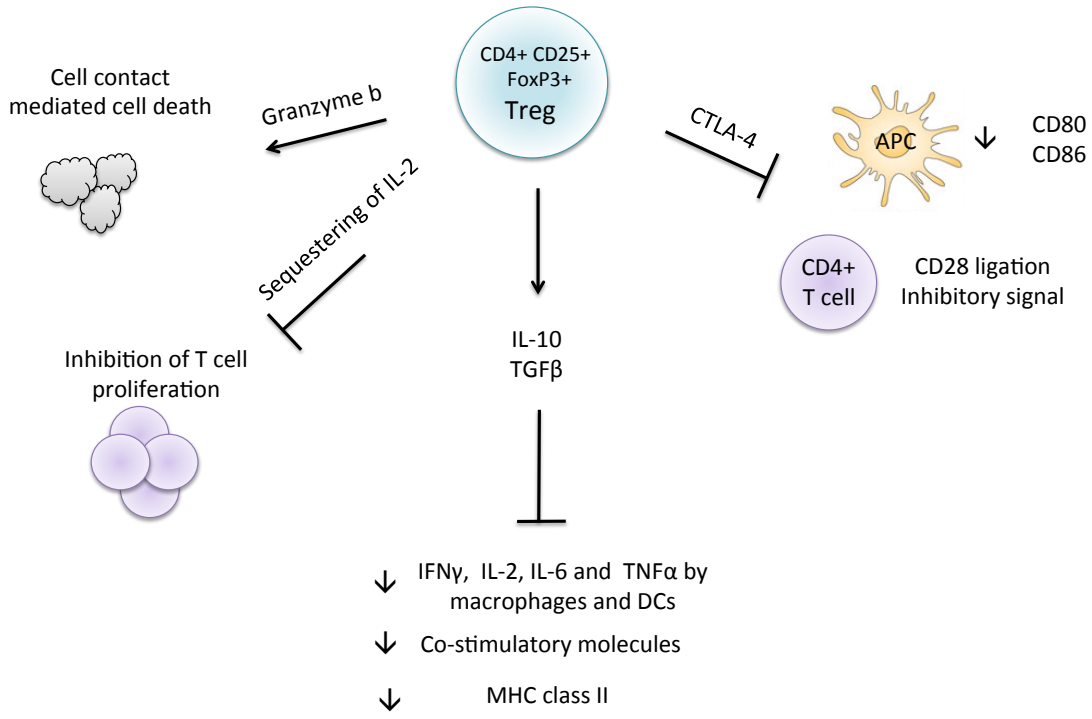

Figure 1.7 Mechanisms of suppressive functions by Tregs

CD4+ FoxP3+ Tregs regulate the immune response and maintain homeostasis via multiple mechanisms. Including; cell contact mediated cell death performed by the release of granzyme B, out competing other T lymphocytes via sequestering available IL-2, CTLA-4 mediated down-regulation of co-stimulatory molecules on APCs but also by delivering an inhibitory signal via CD28 expressed on CD4+ T lymphocytes and finally the production of potent anti-inflammatory mediators such as IL-10 and TGF-β.

Memory Treg subsets have also been shown to exists in mice with their identification largely based on the expression of the $\alpha_E\beta_7$ integrin (CD103) on CD4+ FoxP3+ populations (Huehn et al. 2004). CD103 is most commonly found on intraepithelial lymphocytes within mucosal linings such as the intestinal tract and the lung, in this context TGF-β has been shown to be essential for the upregulation of CD103 in this population (R. Suzuki et al. 2002). In non lymphocyte cells, CD103 as also been shown to identify an important subset of tolergenic DCs within the gastrointestinal lymphoid associated tissues (GALTs), most known for their ability to promote the development of Tregs within these tissues discussed in detail later in this chapter. Growing evidence support the use of CD103+ as a excellent marker for activated memory like Tregs that have undergone rounds of proliferation after activation by antigen in a specific context and have heightened suppressive function when compared to CD103- Tregs (Lehmann et al. 2002) (Huehn et al. 2004) (Suffia et al. 2005) (Banz et al. 2003) (McHugh et al. 2002) {Siewert:2007hz}. Furthermore, these studies have lead to CD103+ Tregs being proposed as inflammation seeking Tregs due to the high surface expression of inflammatory chemokine receptors including CCR5 (D. Zhao et al. 2008), which is known to be required for the migration of T lymphocytes into inflamed tissues
(Huffnagle et al. 1999) (Murai et al. 1999).

1.4 Intestinal immune system

This thesis has a particular focus on immune cells residing in the gut and intestinal inflammation therefore an introduction on the specific details of the intestinal (also known as mucosal) immune system is required.

The immune system can be generally divided into two separate entities: the central immune system, which includes primary and secondary lymphoid sites such as the thymus and spleen respectively, and the mucosal immune system, which includes the airways, the intestines and urogenital tract which are vulnerable sites for entry of pathogens due to their proximity to the external environment.

The intestine represents the largest compartment of the immune system containing the largest number of immune cells found in any tissue of the body. The intestine plays the essential role in the uptake of nutrient and fluid yet at the same time must maintain the protective barrier to avoid infection. For this reason the intestinal immune system has evolved intricate mechanisms to distinguish between harmful pathogens, food antigens and natural commensal bacteria (also known as gut microbiota). As the centralised and mucosal immune systems are therefore faced with different challenges they as a result have very distinct characteristics. For example, in contrast to the centralised immune system, the intestinal immune system is a highly tolergenic environment with vast amounts of anti-inflammatory cytokines present including IL-10 and TGF-β.

The mucosal immune system within the intestine consists of two anatomically distinct sites including: organised structures of the gut-associated lymphoid structures (GALT) including the Peyers patches found in the wall of the small intestine, and conversely effector sites directly within the epithelial layers of the intestine including the intraepithelial layer (IEL) and lamina propria, which contain distinct subsets of immune cells (reviewed (Mowat & Agace 2014)).

1.4.1 Gut associated lymphoid tissue (GALT)

As mentioned, the GALTs are localised lymphoid structures within the small intestine the most studied of which includes the Peyers patches (PPs) found within but also the draining lymph nodes of the intestinal tract including the mesenteric lymph node (mLN). These locations are principle sites for priming adaptive immune responses within the intestine.

The main draining lymph node for the GALT is the mLN, which is located alongside the anterior mesenteric artery within the mesentery. In mice, the mLN is usually made up of 4-5 connecting lymph nodes with organized lymphoid structure including T cell and B cell zones. Lymph fluid drained from the small intestine and upper colon are brought to the mLN via the lymphatics. The importance of the mLN in governing oral tolerance to both food antigens and commensal bacteria has been demonstrated by *in vivo* studies in which mice

lacking mLN failed to induce tolerance (Worbs et al. 2006). Additionally, the role of the mLN in preservation of tolerance towards commensal bacteria has been demonstrated in studies in which mice lacking mLNs and repeatedly challenged with commensal bacteria are unable to control the ensuing immune response, resulting in the systemic dissemination of bacteria and splenomegaly and lymphadenopathy (Macpherson & Uhr 2004).

PPs are small-organised lymphoid structures located on the antimesenteric side of the small intestine and are particularly concentrated in the distal ileum. As PPs can pick up luminal antigen and bacteria they are considered to be the immune sensors of the small intestine (reviewed (C. Jung et al. 2010)). Similarly to mLNs, PPs also contain organized architecture with distinct T and B cell zones. It is also common to find active germinal centers within PPs, indicating the continual immune system stimulated by constant exposure to luminal antigens. Recently, PPs have been shown to be the main site by which IgA (class switching of IgA is promoted by IL-5 and TGF-β by intestinal T cells) is produced by plasma B cells contributing to gut protection from pathogen whilst retaining homeostasis and limiting damage (Masahata et al. 2014).

The process of pathogenic recognition and resulting immune response within the mucosal immune system is depicted in Figure 1.8.

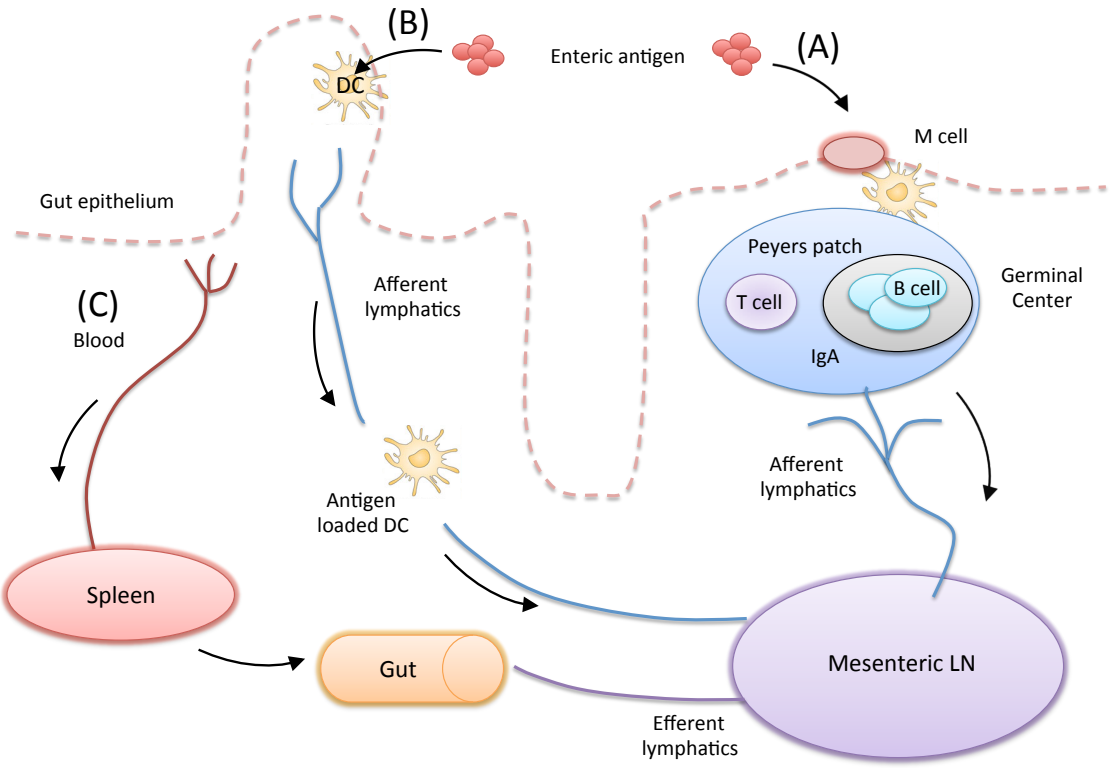

Figure 1.8 Antigen recognition in gut associated lymphoid tissues within the small intestine

Three major routes of antigen acquisition and recognition occur within the small intestine. (A) Enteric antigen is brought into the intestine after digestion of food and fluid by the stomach. M cells that are specialized for the uptake of antigen from the lumen of the intestine and are found strategically placed in the follicle-associated epithelium (FAE) of the PPs. Acquired antigen is transported via M cells to a DC rich sub epithelial dome (SED) where DCs can promote tolerance or activate T cells. Activated T cells can then provide B cell help to promote the production of IgA from plasma cells. Activated T cells may also travel from the PP to the mLN via the afferent lymphatics to further promote immune responses. (B) Specialized intestinal DCs populating the lamina propria extend dendrites through spaces between the epithelial layer to constantly sample antigen. After phagocytosis antigen-loaded DCs travel via the afferent lymphatics to the mesenteric lymph node to stimulate an adaptive immune response or to promote tolerance. (C) luminal enteric antigen from the gut can also enter the intestinal blood supply and travel via the blood into other secondary lymphoid organs such as the spleen. Phagocytosis of antigen delivered to the spleen by splenic DCs may also initiate the immune response. Adapted from (Mowat 2003; Koboziev et al. 2010)

1.4.2 Specialised cell subsets of the intestinal immune system

The intestinal immune system within the gut wall itself is further compartmentalised into two distinct layers including the intraepithelial layer and the lamina propria, both of which are home to unique immune cell populations.

The lamina propria, which consists of loose connective tissue, exists beneath the basolateral (tissue-facing) surface of the gut epithelium. Multiple cells from both the innate and adaptive immune system are found here including specialised DCs, macrophages, neutrophils, NKT cells, mast cells, CD4+ T cells, CD8+ T cells and B cells. In contrast, the intraepithelial layer contains a much more homogenous cell subset in which the most abundant cell types are intraepithelial lymphocytes (IELs), of which are mainly TCRγδ+ T cells.

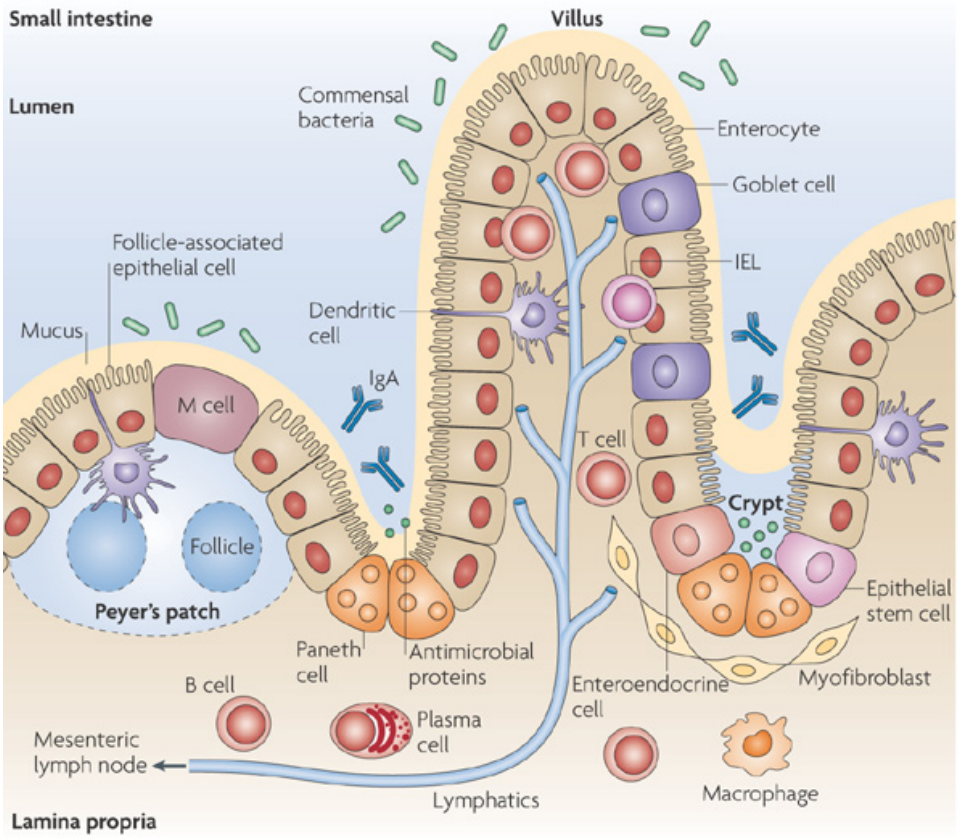

Figure 1.9 Regionalisation of immune cells within the small intestine

A single layer of epithelial cells within the intestine (enterocytes) establishes a protective physical barrier between the commensal bacteria within the intestinal lumen and the lamina propria and defines two specialised immune cell areas within the small intestine. Amongst the epithelial layer are goblet cells that produce mucus as well as epithelial stem cells within sites known as intestinal crypts, which are required to replenish the epithelial layer with new epithelial cells. The single layer of epithelial cells is commonly known as the intraepithelial layer. Distinct subsets of lymphocytes localise between these epithelial cells and are termed intraepithelial lymphocytes (IEL). IELs are specifically located here to detect pathogens but also immediately detect the breach of commensal microbiota. Beneath the epithelial layer exists the lamina propria layer, populated by a highly heterogeneous population of cells including DCs, macrophages, T cells, B cells and plasma cells. The lamina propria layer is connected to the mesenteric lymph node by draining by the afferent lymphatics. Specialised solitary lymphoid follicles known as Peyer's patches are also present within between the intraepithelial layer and the lamina propria in which B and T cell interactions can form resulting in active germinal centres formation and the production of IgA. DCs within Peyer's patches are known to extend dendrites through follicle associated epithelial cells to obtain antigen from the intestinal lumen. Within the lamina propria multiple subsets of immune cells including specific subsets of T and B lymphocytes, IgA producing plasma B cells, macrophages and DCs. *Taken from* (Abreu et al. 2010)

1.4.2.1 Intraepithelial lymphocytes

IEL T cells are found within the epithelial layer of mucosal linings such as the skin, lungs and the lining of the gut located at the basement membrane between enterocytes (gut epithelial cells). This population of cells exists in normal settings at a frequency of 10-15 IEL per 100 epithelial cells (Ferguson 1977).

The study of IEL is a relatively new topic in within the field of mucosal immunology, however in mice IELs can be distinguished into two main groups based on their mechanism of activation and surface marker expression. These two subsets include: natural IEL (previously known as type b) and induced IEL (previously known as type a) (Extensively reviewed (Cheroutre et al. 2011)). These two main subsets, their origin and surface marker expression is detailed in both Figure 1.10 and Table 1.2.

Natural IEL express either TCRαβ or TCRγδ and are CD8αα-/+, importantly they do not express CD4 or CD8αβ heterodimer. Although the origin and development of natural TCRαβ and TCRγδ IELs are debated numerous studies have shown they develop and are activated by self-peptide within the thymus. Studies using athymic mice have shown severe reduction in the number of IEL populating the gut, highlighting an essential role of the thymus in the generation of natural IELs. In contrast, inducible IEL are TCRαβ+ CD4+ CD8aa-/+ or TCRαβ+ CD8αβ+ CD8αα-/+ and arise from TCRαβ+ CD4+ conventional T cells or TCRαβ+ CD8αβ+ T cells within the periphery, specifically within GALTs. Induced IELS are subsequently primed to upregulate gut homing receptors including αEβ7 (CD103) in order to successfully migrate to the appropriate site within the small intestine (Kilshaw & Baker 1988; Cepek et al. 1994). On both natural and inducible subsets the upregulation of CD8αα homodimer only occurs after egress from the thymus and upon colonisation of the gut (Gangadharan et al. 2006) (T. A. Baldwin et al. 2004).

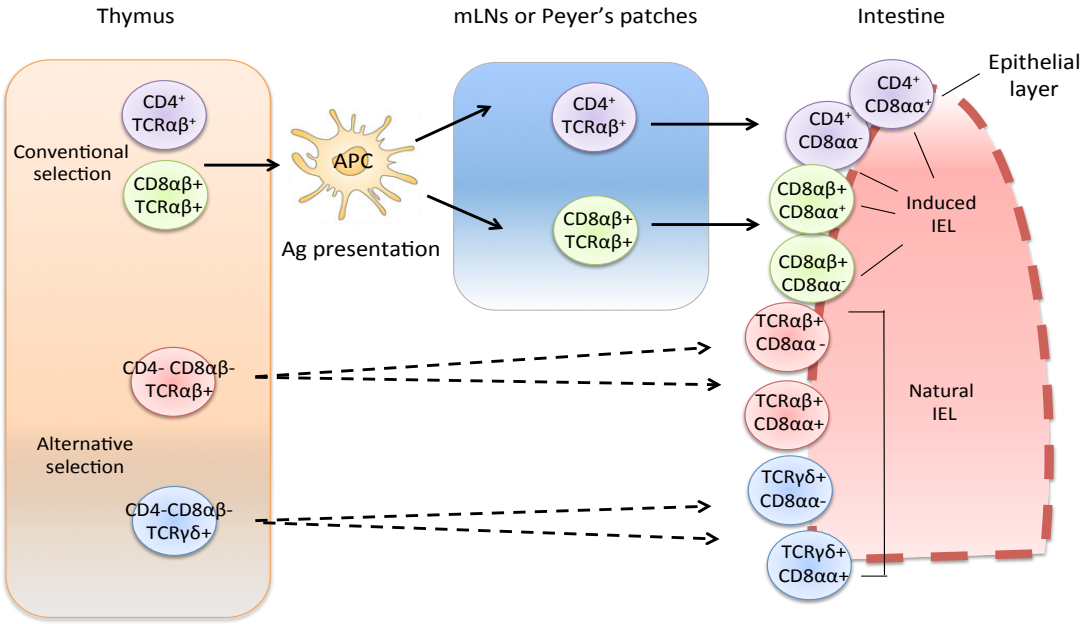

Figure 1.10 Development of natural and induced IEL subsets located within the intraepithelial layer of the small intestine.

Conventional selection within the thymus gives rise to CD4+ TCRαβ+ and CD8αβ+ TCRαβ+ T cells that are activated after antigen recognition by DCs within the mLNs and PPs and subsequently populate the intraepithelial layer as "induced IELs". In contrast, alternative selection within the thymus of CD4-CDαβ- TCRαβ+ and CD4- CD8αβ- TCRγδ+ populate the intraepithelial as "natural IELs". *Adapted from* (Cheroutre et al. 2011)

Subset	Surface marker expression	Activation mechanism
Natural IEL (Type B)	TCRαβ+ CD8αα- TCRαβ+ CD8αα+ TCRγδ+ CD8αα- TCRγδ+ CD8αα+	During development in thymus by self antigen
Induced IEL (Type A)	TCRαβ+ CD4+ CD8αα- TCRαβ+ CD4+ CD8αα+ TCRαβ+ CD8αβ+ CD8αα- TCRαβ+ CD8αβ+ CD8αα+	Arise from TCRαβ+ CD4+ T naïve T cells or TCRαβ+ CD8αβ+ by antigen recognition within the periphery

Table 1.2 Characteristics of IEL subsets in mice

IELs perform multiple immunological functions; as they are located with the epithelium of the gut they are one of the first lines of defense against pathogens to provide immediate responses. IEL also have strong cytotoxic abilities demonstrated by the abundance of cytotoxic granules they contain as well as being key early produces of effector cytokines including IFN-γ, IL-2, IL-17 and IL-4 during a variety of viral and bacterial infections (Shires et al. 2001; Chardès et al. 1994; Müller et al. 2000) . As IELs are antigen experienced (in contrast to naïve T cells) they are able to immediately perform these immunological functions thereby providing rapid responses. In addition to clear roles in the initiation of an immune response, IELs also perform important regulatory functions to maintain gut homeostasis and healthy gut epithelium.

The role for γδ+ T cells in promotion of gut homeostasis has been demonstrated whereby depletion of γδ+ T cells resulting in abnormal gut morphology and reduced IgA production (Fujihashi et al. 1999; Roberts et al. 1996).

1.4.2.2 Immune cells within the lamina propria

As discussed, in contrast to the intraepithelial layer that largely consists of T lymphocyte subsets, the lamina propria is populated by a variety of immune cells including specialised gut DC subsets, B cells, IgA producing plasma cells macrophages, as well as containing T lymphocyte subsets including TCRαβ+ and TCRγδ+ subsets (Figure 1.9). Of the TCRαβ+ subsets both CD4+ and CD8+ subsets also exist within the lamina propria. The CD4+ compartment is highly diverse and subsets are frequently identified on the effector cytokines they produce including IFNγ producing Th1 cells, IL-17 producing Th17 cells and IL-10 producing FoxP3+ Tregs which perform distinct roles within the intestine.

Plasma cells within the lamina propria are also distinct, whilst most plasma cells within the periphery produce IgM, plasma cells within the lamina propria produce IgA (Brandtzaeg & Johansen 2005). Secreted IgA is important for limiting bacterial association upon the epithelial cell surface thereby restricting the penetration of microbiota across the gut epithelium (K. Suzuki et al. 2004).

1.4.3 Specialised DC subsets within the intestinal immune system

As well as the abundance of specialised gut lymphocytes within the intestinal immune system, specialised DC subsets play an important role in the maintenance of tolerance and gut homeostasis, which have been extensively studied in mice (reviewed (A. Iwasaki 2007).

DCs can be found in all lymphoid tissue associated with the intestine including the PPs and mLN as well as being scattered throughout the subepithelial layer including the lamina propria of the small intestine and the colon (Mowat 2003) (Chirdo et al. 2005) (Wilson 2003).

The most frequent DC found within this context are CD103+ DCs (reviewed (Scott et al. 2011)). The CD103+ DC subset have a multitude of unique characteristics, one of which is the ability imprint T and B cells to return to the lamina propria of the small intestine after becoming activated and circulating through the periphery. This is achieved by the expression of retinal dehydrogenase enzymes by CD103+ DCs which catalyses retinoic acid from retinol (Vitamin A) which stimulates the upregulation of gut specific homing molecules including CCR9 and α4β7 on CD8+ T cells and B cells(Johansson-Lindbom et al. 2005) (Johansson-Lindbom & Agace 2007).

Additionally, CD103+ DCs are most notorious for their ability to promote the differentiation of naïve CD4+ T cells into FoxP3+ Tregs via the production of multiple regulatory factors including IL-10, TGF-β and indoleamine-2, 3-dioxygenase (IDO) (S. G. Kang et al. 2007) (Benson et al. 2007).

1.5 Cell signalling downstream of immune receptors

1.5.1 General principles of signalling

Activation of receptors on the cell surface results in cell signalling cascades, this allows external signals or cues to be transmitted into the cell. One of the most common enzymes that potentiate cell-signalling cascades includes protein kinases.

Protein kinases are defined as a group of enzymes that have the ability to catalyse the covalent attachment of a phosphate group to a protein. This reversible process is termed phosphorylation. Phosphorylation works in multiple ways such as the activation, translocation, inhibition or altered binding properties, or the degradation of the altered protein (Ubersax & Ferrell 2007). Protein kinases are categorised into two main groups based on the amino acid residues within proteins that they are able to phosphorylate including tyrosine kinases and serine/threonine kinases.

To regulate or reverse phosphorylation, protein phosphatases exist. The process of de-phosphorylation is crucial for the regulation and the attenuation of

signalling cascades. The process of signalling cascades, phosphorylation and its regulation is used by many cellular systems to control specific cell changes including the activation of transcription factors and ultimately gene regulation to shape how a cell responds to environmental or intracellular cues.

Human mutations and polymorphisms within protein kinases have been linked to multiple human diseases, including multiple components that belong to immune signalling networks (reviewed (Cohen 2014)).

1.5.2 T cell receptor (TCR) signalling

The structure of the TCR and downstream signalling events after TCR activation are illustrated in Figure 1.11.

The TCR is composed of the αβ heterodimer, which is a homodimer of two ζ chains that are linked by a disulphide bond and four CD3 chains (CD3δ, CD3γ, and two CD3ε), which together forms the CD3 complex. Both the CD3 and ζ chains contain a signalling motif - immunoreceptor tyrosine-based activation motif (ITAM) within the cytoplasmic domain (Weiss & Littman 1994). The TCR itself has no intrinsic enzymatic activity and therefore relies on the kinase activity of the SRC kinase family (SFKs) including lymphocyte specific protein tyrosine kinase (Lck) and Fyn which are the first kinases to be activated after TCR activation (Palacios & Weiss 2004) (Salmond et al. 2009). TCR signalling cascades are extensively reviewed in the following references ((Acuto et al. 2008; Smith-Garvin et al. 2009)).

The two most popular models of TCR triggering have been discussed recently (Brownlie & Zamoyska 2013). Following TCR ligation and the interaction of CD4 or CD8 molecules with peptide-MHC class II or MHC class I respectively, Lck is promptly recruited to the vicinity of the TCR/CD3 complex and phosphorylates the ITAM motifs (Veillette et al. 1988) (Shaw et al. 1989). Activation of SFKs is performed by CD45, a tyrosine phosphatase. The activation of SFKs and the phosphorylation of ITAM motifs leads to the recruitment and activation of zeta chain associated protein kinase (ZAP70) (reviewed (Weiss 2010)). After activation and subsequent conformational change ZAP70 is able to phosphorylate multiple targets including the linker for activation of T cells (LAT)

(H. Wang et al. 2010). Significantly, the activation of LAT promotes the recruitment of multiple adaptor molecules resulting in the activation of a diverse range of signalling networks.

The role of SFK family members within T lymphocyte activation, differentiation and within tolerance have recently been reviewed ((Salmond et al. 2009)). Significantly, the importance of Lck within T cell development has been demonstrated in which mice lacking Lck display a profound defect in thymocyte development leading to almost complete lack of peripheral T cells (Molina et al. 1992).

The activation and phosphorylation of LAT allows the recruitment of phospholipase Cγ (PLCγ) that is subsequently activated by interleukin-2 inducible T cell kinase (Idk). Activated PLCγ then catalyses the breakdown of the plasma membrane lipid phosphatidylinositol 4,5-biphosphate (PtdIns $(4,5)P_2$) or otherwise known simply as PIP_2. This generates the second messengers inositol triphosphate (IP3) and diacylglycerol (DAG) (Carpenter & Ji 1999). IP3 production promotes the release of Ca^{2+} from the endoplasmic reticulum (ER) into the cytoplasm and thereby promotes a sustained flux of Ca^{2+} resulting in the activation of calcineurin phosphatase as well as Ca^{2+} - calmodulin dependent kinase (CaMK) (reviewed (Savignac et al. 2007)). The second byproduct of PtdIns$(4,5)P_2$, DAG, activates protein kinase C members, including PKCθ within T lymphocytes and RasGRP. RasGrP subsequently activates Ras which promotes the activation of c-RAF a mitogen activated protein kinase 3 (MAPK3) which is required for the activation of extracellular signalling regulated kinase 1 (Erk1) and ERK2 (Genot & Cantrell 2000). DAG is known to be essential for normal T cell signalling in which loss of DAG related kinases results in profound defects in both thymocyte development but also in peripheral T cell function (Olenchock et al. 2006) (Gharbi et al. 2011). The role of DAG mediated signalling within the immune system is reviewed within the following reference ((Zhong et al. 2008)). DAG regulates the activation of both PKC family members but also the protein kinase D (PKD) family, which is discussed later within this chapter.

Proximal signaling events downstream of the TCR are known be intricately media the strength or threshold of signal, which directly T cell responses (Malhotra & Campelo 2011)

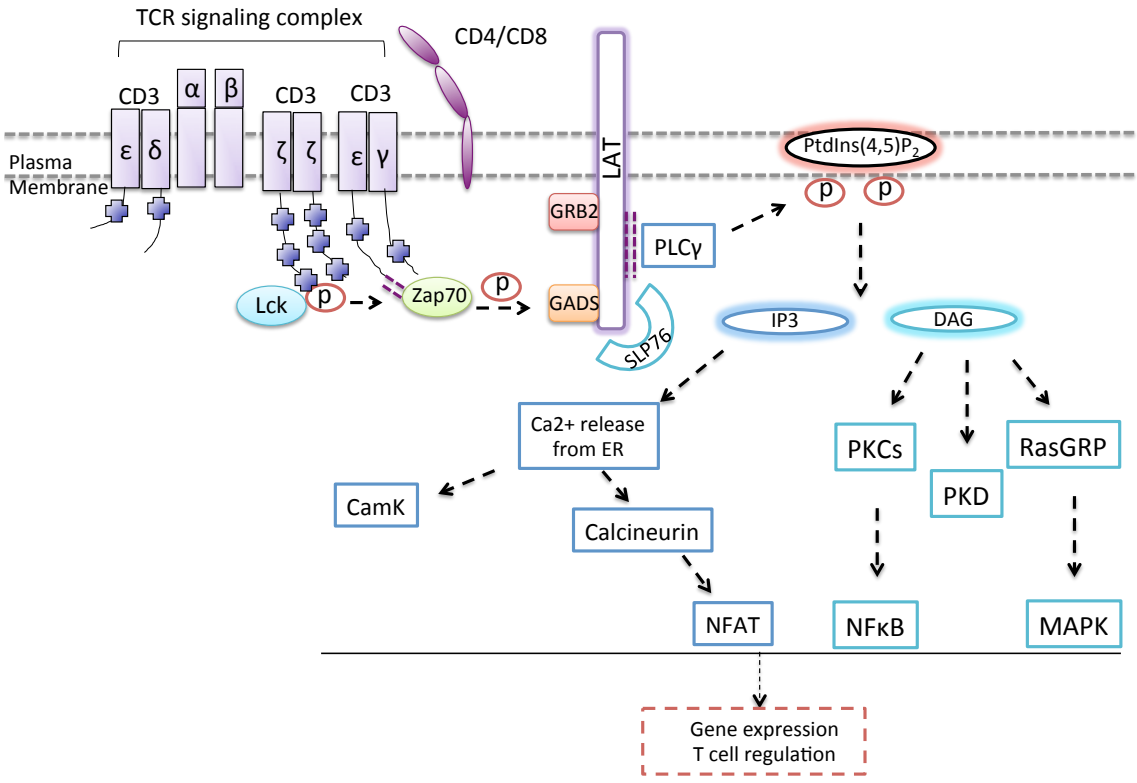

Figure 1.11 TCR signalling

The TCRαβ receptor is made up of the heterodimer of TCRα and TCRβ subunits. Three CD3 units also make up the complex on the cell surface to transmit signals into the cell interior. The γ, δ and ε CD3 contain one single ITAM motif whereas the CD3ζ chains contain 3 tandem ITAM motifs. TCR activation via peptide- MHC complex leads to the activation of Lck and Fyn, which associate with the ITAM motifs of the CD3 complex and subsequently activates PLCγ and Ras-dependent pathways. Activation of these downstream signalling cascades ultimately results in the activation of specific gene expression, which go on to regulate T cell activation responses. *Adapted from* (Smith-Garvin et al. 2009) (Brownlie & Zamoyska 2013).

1.5.3 TLR signalling

In contrast to B and T lymphocytes that express antigen specific receptors including the BCR and TCR, innate immune cells instead use conserved pathogen recognition receptors, the most characterised of which are the TLRs.

The large diversity of responses implemented after activation of a set group of TLRs can be explained by the existence of multiple adaptor proteins

containing TIR domains that are recruited after TLR activation to direct and propagate distinct responses. The mammalian TLR family contains 5 known adaptor proteins including; myeloid differentiation primary response protein 88 (MyD88), TIR domain containing adaptor-inducing interferon-β (TRIF), TIRAP/Mal and TRAM (extensively reviewed (L. A. J. O'Neill & Bowie 2007; Kawai & Akira 2010)). Based on this, TLR signalling can be broadly split into two major groups, MyD88 dependent or TRIF dependent. All TLRs except TLR3 are known to signal through MyD88. Additionally, TLR4 is the only TLR to recruit 4 adaptor proteins and activate both MyD88 and TRIF signalling pathways. TLRs, their adaptor proteins and signalling cascades are illustrated in Figure 1.12.

1.5.4 MyD88 dependent pathway

MyD88 is composed of a death domain (DD) in addition to a TIR domain and is essential for the recruitment to the TIR domain of the receptor.

Upon activation MyD88 recruits and interacts with IL-1 receptor associated kinase 4 (IRAK4), which becomes activated by phosphorylation (Lin et al. 2011) (Warner & Nuñez 2013). IRAK4 goes on to recruit and activate other IRAK family members including IRAK1 and IRAK2 (Kawagoe et al. 2008).

After activation the IRAKs dissociate from MyD88 and interact with TNFR-associated factor 6 (TRAF6). TRAF6 acts as an E3 ubiquitin ligase to promote the formation of a K63-linked polyubiquitin chain on TRAF6 itself. This ubiquitination activates a scaffolding complex allowing TGF-β activated kinase -1 (TAK1), TAB2 and TAB2/3 to come into close proximity to the IKK complex (Sato et al. 2005) (Mendoza et al. 2008). This results in the activation of the Iκκ complex which contains IKK-α, IKK-β and NF-κB essential modulator (NEMO) also known as IKKγ (Kanayama et al. 2004). Subsequently, the phosphorylation of IκBα (an inhibitory protein of NF-κB) allows it to undergo degradation leading to the freeing of NF-κB (Z. J. Chen et al. 1996) (Vallabhapurapu et al. 2008). NF-κB can then translocate to the nucleus to promote gene transcription including induction of several pro-inflammatory genes.

Simultaneously, active TAK1 can activate the MAPK pathway that results in the activation of AP-1, which is crucial for the induction of various cytokine

genes. TAK-1 achieves this by phosphorylating multiple MAP kinases which go onto phosphorylate proteins including ERK1, ERK2, p.38 and c-Jun N-terminal kinases (Jnk) which is discussed later in this chapter.

Distinctively, the activation of TLR7 and TLR9 led to an additional response in addition to classical NF-κB induced cytokines involving the production of type I IFNs. This is achieved in pDCs by MyD88 forming a complex with IRAK-1, TRAF6, TRAF3, IKK-α and interferon regulatory family 7 (IRF7) (Honda et al. 2005). Phosphorylated IRF7 functions to translocate to the nucleus and drive genes that control type I IFN production (Honda et al. 2006).

1.5.5 TRIF dependent pathway

TLR3 and TLR4 utilise TRIF to active an alternative pathway leading to both the activation of NF-κB and IRF3, which promote the transcription of genes controlling pro-inflammatory cytokine production and specifically the production of IFN-β respectively (Yamamoto et al. 2002) (Yamamoto et al. 2003) (Akira & Takeda 2004) .

Activation of TRIF leads to the recruitment of TRAF3 and TRAF6 through TRAF binding motifs. TRIF also recruits a further adaptor molecule receptor interacting protein 1 (RIP1) that undergoes polyubiquitination. This allows another adaptor molecule, TRADD, to bind RIP1 (Ermolaeva et al. 2008) (Pobezinskaya et al. 2008). The utilisation of TRIF downstream of TLR3 and TLR4 ligation leads to the formation of a multiprotein signalling complex consisting of; TRIF, TRAF6, TRADD, Pellino-1 and RIP1 resulting in the activation of both NF-κB and MAPK signalling cascades (Cusson-Hermance et al. 2005) (Kawai & Akira 2010). As mentioned, activation of the TRIF dependent pathway results in the activation of IRF3 promoting the production of IFN-β. This is achieved by the recruitment and assembly of a key signalling complex consisting of the non-canonical IκB kinases (IKKs) including TBK1 and IKKi (IKKε) which subsequently phosphorylate IRF3 promoting its translocation to the nucleus to drive IFN-β production (Hacker & Karin 2006). Importantly, the activation of IRF3 is highly dependent on TRAF 3 activation (Oganesyan et al. 2005).

1.5.5.1 TLR4 activation

TLR4 is the only TLR that is able to recruit 4 adaptor proteins and activate two distinct signalling pathways including the MyD88 and TRIF dependent pathways allowing activation of both the NFκB and IR3 pathways (Kaisho et al. 2001) (Kawai et al. 2001).

LPS can bind to TLR4 in complex with MD2 and CD14 within the plasma membrane resulting in the recruitment of TIRAP/Mal and MyD88 (Dziarski & Gupta 2000). Recruitment of IRAK1/2/4 promotes the activation of TRAF6 and the formation of K63 polyubiquitin chain, which subsequently promotes the activation of TAK1. TAK1 is responsible for the activation of NF-κB and MAPK pathways.

In contrast to other TLRs, TLR4 is subsequently endocytosed from the cell surface and delivered into intracellular vesicles where it can recruit TRAM and TRIF (Husebye et al. 2006) (Zanoni et al. 2011). This results in the recruitment of TRAF3 and the protein kinases TBK-1 and IKKε resulting in the phosphorylation and activation of IRF3. TRIF can also recruit RIP1, which mediates the activation of NFκB and MAPK pathways (Yamamoto et al. 2002).

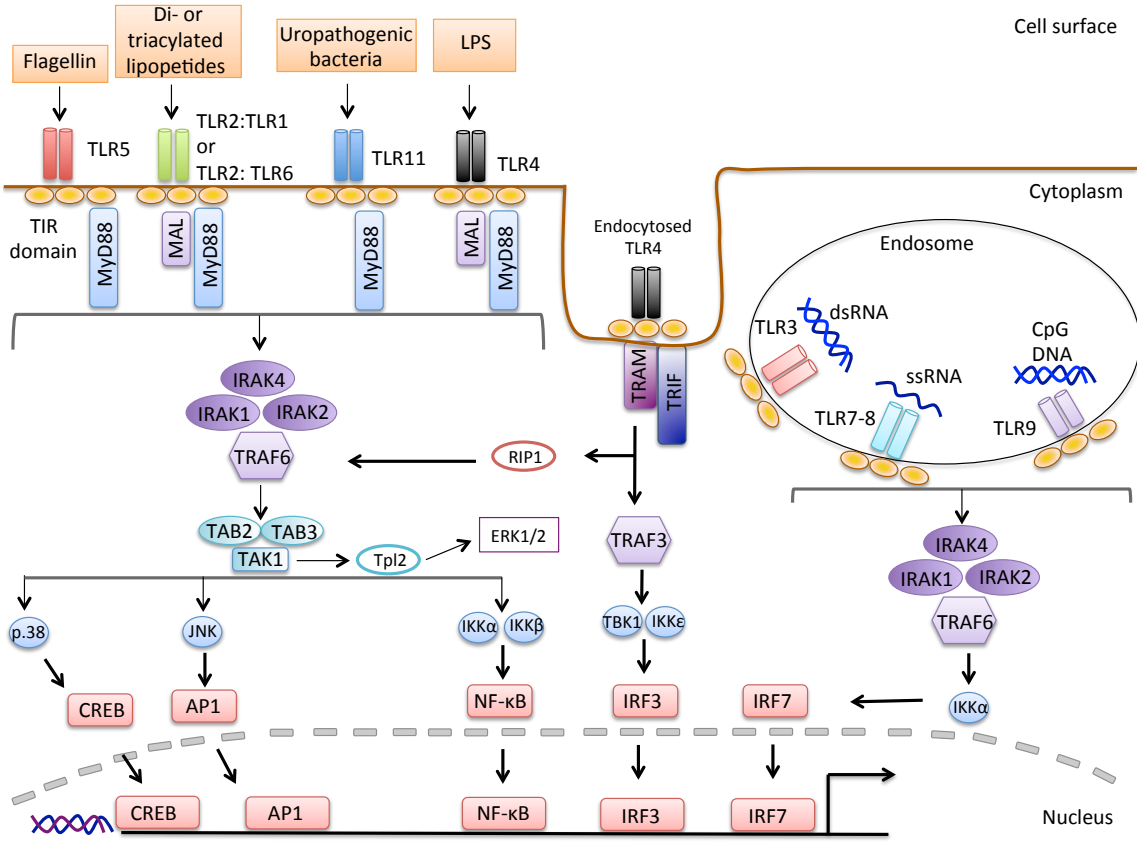

Figure 1.12 TLRs, adaptor proteins and signalling cascades

TLR5. TLR11, TLR4 and heterodimers of TLR2-TLR1 or TLR2-TLR6 bind their ligands on the cell surface whereas TLR3, TLR7-8 and TLR9 are localised to the endosomes within the cell. TLR4 localises at both the plasma membrane and within endosomes. Following TLR ligation the TIR domains of TLRs engage with TIR domain containing adaptor molecules MyD88, TIRAP/Mal, TRIF or TRAM. This engagement propagates downstream signalling cascades that include interaction between IRAK family members and TRAF leading to the activation of MAPKs p.38 and Jnk which mediate the activation of specific transcription factors to drive gene transcription. Additionally, TAK1 indirectly mediates the activation of Tpl2 which is required for ERK1/2 activation downstream of TLR ligation. The two main families of transcription factors activated include the NFκB family and IRF including IRF3 and IRF7. But other transcription factors CREB and AP1. *Adapted from* (Liew et al. 2005)

1.5.6 MAPK signalling

Mitogen activated protein kinases (MAPKs) are serine/threonine kinases with 14 in total which are divided into 7 groups have been identified in mammalian cells (reviewed (Cargnello & Roux 2011)). Conventional MAPKs include extracellular-regulated kinases 1 and 2 (ERK1/2), c-Jun amino (N)-terminal kinases 1/2/3 (JNK1/2/3), p.38 isoforms (α, β, γ and δ), and ERK5. Atypical MAPKs include ERK3/4, ERK7 and Nemo-like kinase (NLK).

1.5.6.1 PRR activation of MAPKs

All PPRs including TLRs, CLRs, NLRs and RLRs upon ligation activate multiple downstream signalling cascades including the NF-κB and MAPKs pathways, both of which are essential in generating an immune response (reviewed (Arthur & S. C. Ley 2013)). MAPK signalling cascades are illustrated in

Figure 1.13.

The activation of MAP3Ks by multiple stimuli, including PPR ligation, results in the activation of downstream MAP2Ks and subsequent activation of MAPKs. Activated MAPKs go to phosphorylate numerous substrates, which broadly include other protein kinases and transcription factors. ERK1, ERK2 and p.38 MAPKs activate activated protein kinase 2 (MK2), MK3 and MK5, ribosomal S6 kinases 1 (RSKs) including RSK1, RSK2 and RSK3, mitogen stress activated kinases (MSKs) and MAPK signal integrating kinase (MNK) MNK1 and MNK2. Jnk1, Jnk2 and Jnk3 activate c-Jun and ATF1 (Raman et al. 2007) (Weston & Davis 2007), finally ERK3 and ER4 activate MK5 (Seternes et al. 2004). In addition, p.38 isoforms and ERK5 can also activate myocyte enhancer factor 2 (MEF2) family of transcription factors (M. Zhao et al. 1999).

The activation of MAPK signalling cascades and their exact role within the immune system are beginning to become elucidate accumulating evidence has highlighted their global requirement for normal cytokine production in myeloid cells. Specifically, recent studies have highlighted the role of MSK1 and MSK as negative regulators of TLR mediated proinflammatory cytokine production (Ananieva et al. 2008), including the inhibition of prostaglandin production within a IL-10 mediated feedback loop after LPS stimulation in macrophages (MacKenzie et al. 2013). RSKs have also been implicated in the endocytosis of

TLR after receptor ligation within DCs (Zaru et al. 2007). Furthermore, MK1/2 are known to be required for TNFα production in macrophages (Kotlyarov et al. 1999). Jnk isoforms have recently been implicated in the mediation of macrophage polarisation (Rincón & Davis 2009). The MEF2 transcription factor family has been implicated in multiple immunological processes including myeloid/lymphoid lineage commitment (Gerstein 2009)but are also implicated in IL-10 cytokine transcription within T lymphocytes (Liopeta et al. 2009).

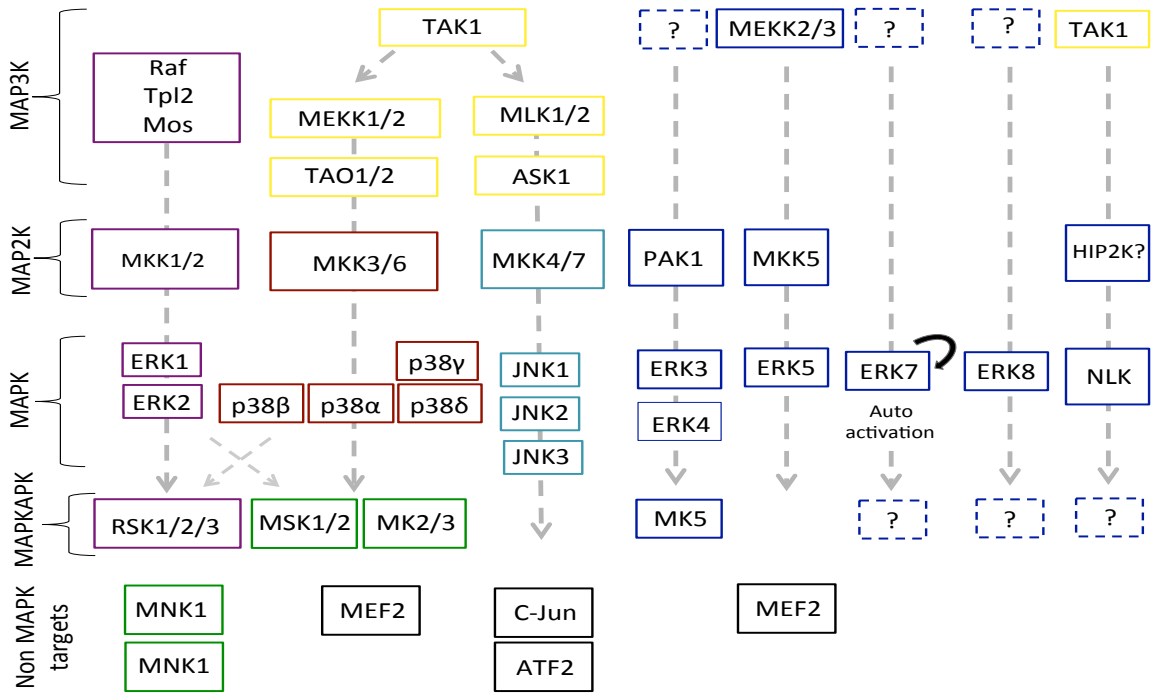

Figure 1.13 Mitogen activated protein kinase signalling pathways

The mitogen activated kinase (MAPK) pathways consist of a cascade comprising of 3 kinases: MAP3Ks that are activated by multiple stimuli, which go on to activate downstream MAP2Ks, which subsequently activate MAPKs. MAPKs have diverse substrates including transcription factors and a family of kinases: MAPKAPKs. Non-MAPK targets such as MNK1/2 and MEF2 are also activated downstream of MAPK cascades. *Adapted from* (Arthur & S. C. Ley 2013).

1.5.6.2 NFκB activation

The NFκB family of transcription factors is a key regulator of inducible gene expression in multiple cellular processes and also within the immune system (reviewed (Hayden & Ghosh 2011) (Ben-Neriah & Karin 2011)). Within the immune system, NFκB plays a crucial role in the production of key mediators including both pro and anti-inflammatory cytokine production (A. S. Baldwin 1996). As such, dysregulation of the NFκB family is commonly associated with multiple human diseases including cancer and autoimmunity (Tak & Firestein 2001).

The NFκB family is includes NFκB1 (p.50/p105), NFκB2 (p52/p100), p65 (RelA), RelB and c-Rel (F. Chen et al. 1999). NFκB can form homo and heterodimers upon activation by upstream signalling cascades after which NFκB

dimers translocate to the nucleus to bind a variety of DNA sequences called κB sites to modulate gene expression.

In most cells, NFκB complexes are in complex with inhibitory IκB proteins including IκBα, IκBβ, IκBε, IκBζ. When signalling pathways are activated, including downstream of TLR activation, the IκB is phosphorylated by IKK complex (IKKα, IKKβ and NEMO) resulting in its tagging for proteasomal degradation (Liu & Z. J. Chen 2010). This releases NFκB from the inhibitory complex, allowing it to translocate to the nucleus where it will subsequently bind to NFκB target sequences within the promoter of NFκB genes (Huang & Miyamoto 2001).

NFκB is known to be critical in multiple aspects of the immune system including lymphoid organogenesis and lymphoid architecture for primary and secondary lymphoid follicle formation, lymphocyte development and indeed down stream of innate immune receptors including TLRs to drive the production of pro and anti-inflammatory cytokines that go to the mediate the immune response (Bonizzi & Karin 2004) (Hayden & Ghosh 2011) (Gerondakis & Siebenlist 2010)

1.5.6.3 Negative regulation of innate immune cell signalling

During an immune response the immune system must also maintain a constant balance between activation and inhibition to prevent the over-activation of an inflammatory response. Due to this, TLR activation and signalling cascades must be tightly regulated. There are multiple such negative regulators within the TLR and other PRR signalling cascades that are broadly split into two major groups; suppressor of cytokine signalling proteins (SOCs) (Yoshimura 2012) and protein inhibitor of activated STAT (PIAS) proteins (Shuai 2006).

1.6 Protein kinase D (PKD) kinases

Protein kinase D (PKD) enzymes are a family of closely related serine/threonine kinases, which in mammals consists of three isoforms: PKD1,

PKD2 and PKD3. PKD was originally described as a member of the PKC family, named PKCμ however was later discovered to have structural, enzymological and regulatory distinct processes from PKC family members (Johannes et al. 1994; A. Hayashi et al. 1999). As such, PKD family members are classed within the CaMK protein kinase superfamily whereas PKC family members exist in protein kinase A, G and C (AGC family) Figure 1.14. Importantly, PKD does not phosphorylate a multitude of known PKC substrates implying that PKD isoforms have distinct substrate specificity and therefore a unique role from PKC isoforms.

PKD is a key-signalling component of the DAG signalling network in which PKD mediates signal transduction by DAG and PLC after activation by PKC mediated or atypical pathways of PKD activation that includes oxidative stress and Src kinases mediated activation. As such, PKD enzymes act as a point of convergence and for integration for multiple signalling cascades.

Signalling via PKD is induced by a remarkable number of stimuli including DAG, phorbol esters, growth factors, GPCR agonists and hormones and antigen receptor stimulation via either the BCR and TCR within lymphocytes (Guha et al. 2002; Matthews et al. 1997; Rozengurt et al. 1997; Zugaza et al. 1996; Zugaza et al. 1997) (Wong & Z.-G. Jin 2005). As a result of this, PKD enzymes have therefore been implicated in a vast array of biological processes including; apoptosis, cell survival, Golgi organization and plasma membrane directed transport, angiogenesis, cancer and immune cell responses (extensively reviewed (Rozengurt 2011)).

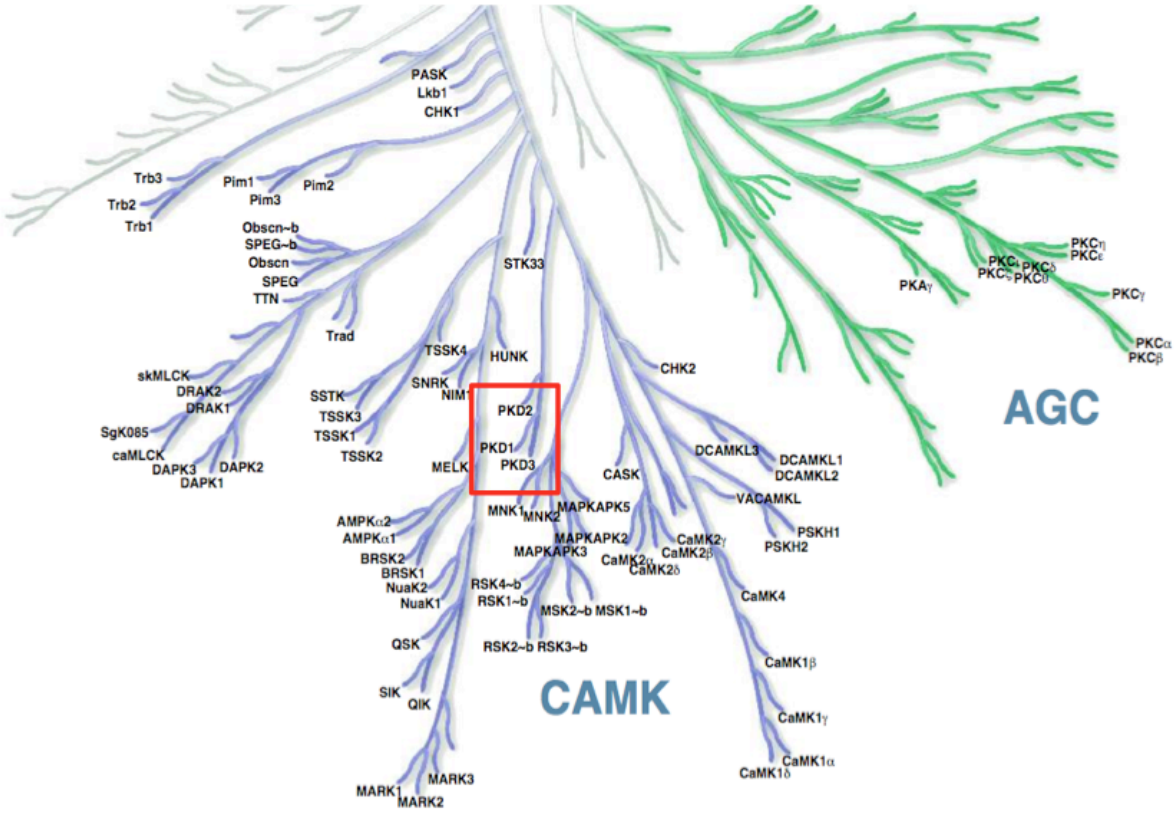

Figure 1.14 Annotation of human kinome of PKD isoforms within CAMK family and PKC isoforms within the AGC family of kinases.

Illustration reproduced courtesy of Cell Signalling Technology, Inc. (www.cellsignal.com)

1.6.1 Isoforms and conservation of PKD family

In mammals 3 PKD isoforms exist, of which, the first member, PKD1 discovered in human and mouse in 1994 (Johannes et al. 1994), followed by PKD3 in 1994 (Valverde, Sinnett-Smith, et al. 1994a) and finally PKD2 in 2001 (A. Hayashi et al. 1999). In contrast to mammals, in the nematode *Caenorhabditis elegans* (C. elegans) there are two PKD homologues including DKF-1 and DKF-2 (Feng et al. 2007; Feng, Ren & Rubin 2006a; Feng, Ren, Wu, et al. 2006b). In *Drosophila melanogaster* (D. Melanogaster) only one PKD homologue is present (Maier et al. 2006). Sequence conservation from insect to mammal is strikingly similar. The conserved nature of the family of kinases indicates an important role for PKD isoforms from basic to complex cellular processes. The evolutionary

development of human PKD isoforms in multiple species can be seen in the PKD family tree (Figure 1.15)

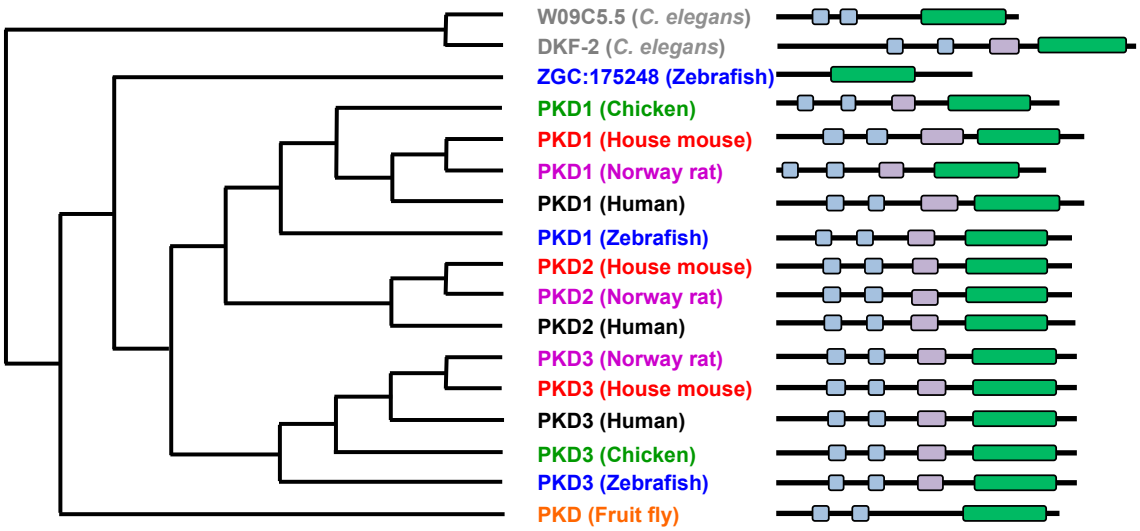

Figure 1.15 Family tree of PKD isoforms and their evolutionary history in multiple species

Illustration reproduced courtesy of www.treefam.com.

1.6.2 Structure and phosphorylation sites of PKD kinases

Although the three-dimensional structure of PKD has not yet been resolved multiple studies have provided insight into defining structural features of PKD isoforms. The three mammalian isoforms of PKD share a similar modular structure consisting of a conserved C-terminal kinase domain, C1a and C1b CRD domains, which are the DAG binding regions of PKD, and a N-terminal regulatory domain containing a pleckstrin homology (PH) domain (Figure 1.16). (A. Hayashi et al. 1999) (Johannes et al. 1994) (Valverde, Sinnette-Smith, et al. 1994b) (Sturany et al. 2001) (Iglesias et al. 1998). Non-phosphorylated PKDs have little catalytic activity and must first of all become activated to go on to activate down-stream substrates to perform its biological functions.

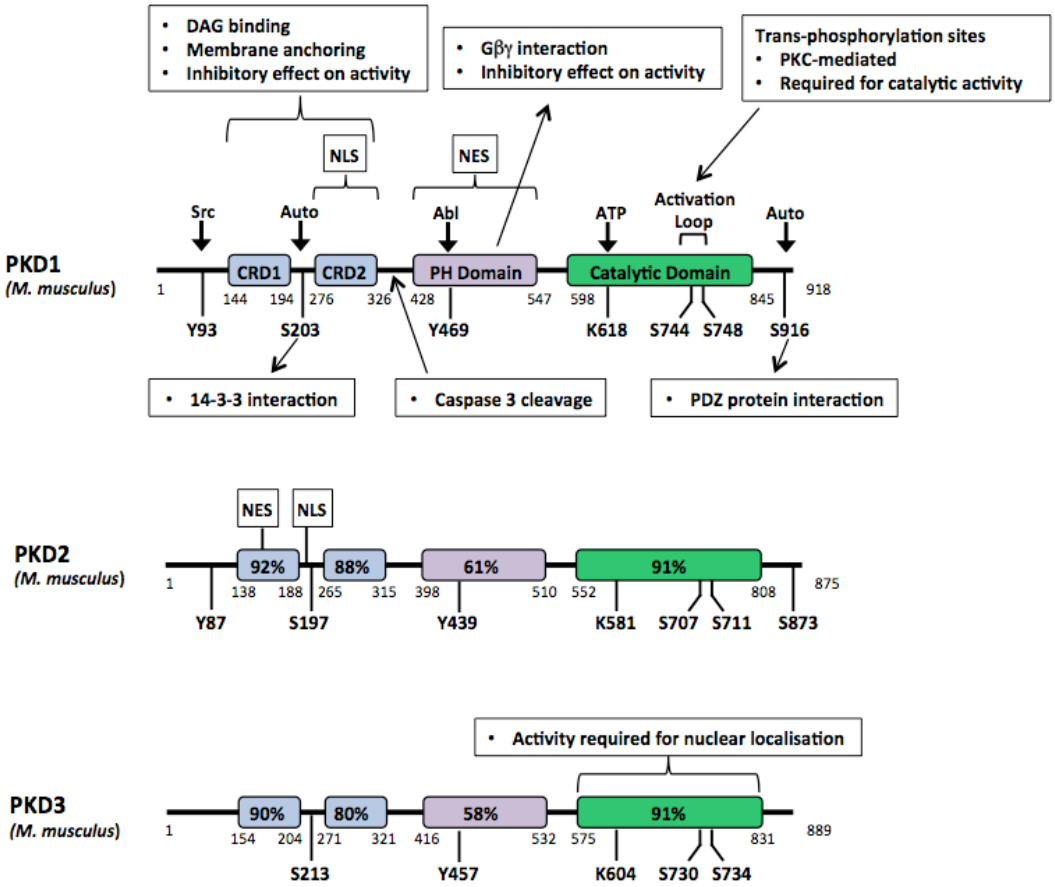

Figure 1.16 Structure of murine PKD isoforms, phosphorylation and regulatory sites and implicated functions

Schematic representation of PKD isoforms. The catalytic domain containing the kinase activation loop is shown in green, PH domain is shown in purple, the regulatory PH domain is shown in purple and cysteine rich domains (CRD), involved in DAG binding, are shown in blue. Phosphorylation sites and their implicated functions are shown. Numbers correspond to the percentage sequence similarity to PKD1 is depicted in each region of PKD2 and PKD3. *Adapted from* (Fu & Rubin 2011) *and* (Rozengurt et al. 2005).

PKD kinases have three major phosphorylation sites including; two serine residues within the activation loop, a tyrosine site within the PH domain and one autophosphorylation loop (except on PKD3). The serine sites within the activation loop include Ser744 and Ser748 of PKD1, Ser706 and Ser710 in PKD2, and Ser730 and Ser734 on PKD3 respectively. These serine residues are directly phosphorylated by up-steam PKC isoforms. Within the PKD1 and PKD2 isoform autophosphorylation sites include a Ser916 site within PKD1, which corresponds to Ser876 on PKD2. Tyrosine residues within the PH domain include Tyr464, Tyr439, and Tyr457 for PKD1, PKD2 and PKD3 respectively. The mechanisms of

PKD activation have been extensively studied and characterised (reviewed (Rozengurt et al. 2005) (Fu & Rubin 2011)). Multiple studies established that PKD becomes activated through the direct phosphorylation of two conserved serine residues within the activation loop by upstream activated PKC isoforms {Waldron:2002ko} (Waldron et al. 1999) (Zugaza et al. 1996). Subsequent autophosphorylation within PKD1 and PKD2 isoforms serves to confer full and sustained activation (Matthews et al. 1999) (Jacamo et al. 2008) (Sinnett-Smith et al. 2009). Key autophosphorylation sites within PKD1/2 isoforms have also been shown to play a role the tertiary structure of the kinase and may play a potential regulatory role for the duration of signaling by PKD (Rybin et al. 2009). The PH domains are known to serve as an essential regulatory function as deletion results in constitutive activity (Iglesias & Rozengurt 1998; Iglesias & Rozengurt 1999). These distinct regions of PKD have high sequence homology between the 3 mammalian isoforms but also in other species. For example, the amino acid sequence homology of the CRD domains and kinase domains between mammalian and *C.elegans* is over 70% identical. Furthermore, the key PKC phosphorylation sites located within the catalytic domain are highly conserved, as they are identical in *C.elegans* and human.

1.6.3 Expression and localisation of PKD kinases

Expression studies assessing PKD isoform mRNA transcription has been performed using in-situ hybridization to accurately assess which isoforms are expressed in specific tissues during mouse embryonic development (Oster et al. 2006). All three PKD family members were shown to be expressed early in development however later embryonic development PKD isoform expression became more differentiated with tissue specific preferential expression of different isoforms. Interestingly, later in embryonic development (E.18.5) PKD2 was shown to become preferentially expressed in the intestinal villi within the lumen of the intestine. This study demonstrates the strikingly different and unique expression patterns of PKD isoforms in certain tissues during embryonic development, further highlighting that PKD cellular and tissue localisation must play a fundamental part in PKD functional properties. In regard to specific PKD

isoform expression within cells has been difficult due to lack of isoform specific antibodies, largely due to the high sequence similarity between the isoforms.

In regard to localisation, PKD isoforms have been shown to undergo rapid redistribution upon stimulation. PKD1 and PKD2 undergo translocation from the cytosol to the DAG rich regions within the plasma membrane (Rey, Young, et al. 2001b). Subsequently, PKD1/2 isoforms relocate from the plasma membrane to the nucleus after PKC mediated activation (Rey, Sinnett-Smith, et al. 2001a). In contrast, PKD3 is constantly shutting between the cytoplasm and the nucleus (Rey et al. 2006). Additionally, pools of PKD isoforms have been reported within the Golgi complex (Yeaman et al. 2004) (Liljedahl et al. 2001) (Malhotra & Campelo 2011) and the mitochondria (Cowell, Döppler, et al. 2009a). The importance of PKD localisation has been demonstrated by studies that have harnessed alternatively targets PKD indicate that the cellular location of PKD kinases elicits different cellular responses in T cells (Spitaler, Emslie, Wood & Cantrell 2006a).

As such, PKD isoforms can regulate downstream targets in multiple locations within the cell and subsequently control a range of cellular activities.

1.6.4 Cell signal transduction pathways of PKD

A plethora of studies have attempted to unravel the exact mechanism by which PKD kinases become activated, often this is dependent on specific cell type, isoform expression and abundance, cellular localisation, and the type of stimulus used. To date, two main mechanisms of PKD activation have been elucidated within the literature, including typical PKD activation by PKC and atypical activation of PKD by oxidative stress and Src mediated pathways.

1.6.4.1 Conventional PKC mediated activation of PKD

Second messengers play a key role during the beginning of multiple signalling pathways including DAG, which acts as lipid secondary messenger in multiple cells (reviewed (Carrasco & Mérida 2007)). Within the adaptive immune system DAG signalling has been shown to be an essential component in

T cell development whereby mice lacking certain diacylglycerol kinases (DGKs) display T cell development defects (reviewed (Zhong et al. 2008)). Several studies have also confirmed the role of DAG signalling in acting as a braking mechanism during immune cell responses where by loss of DAG signalling leads to hyper activation in these cells. (Zhong et al. 2003)

DAG regulates the activation of two major signalling pathways involving PKC family members and PKD. There are 10 PKC family members that are categorised into 3 groups based on their activation requirements; classical PKCs (cPKCs: PKCα, PKCβI, PKCβII and PKCγ), require calcium, diacylglycerol and phosphatidylserine, novel PKCs (nPKC: PKCδ, PKCε, PKCη and PKCθ), require diacylglycerol, phosphatidylserine but are calcium independent, and atypical PKCs (aPKC: PKCζ and PKCι), that only require phosphatidylserine (reviewed (Griner & Kazanietz 2007)). DAG stimulated nPKCs including PKCδ, PKCε, PKCη and PKCθ are potent activators of PKD however Ca^{2+} and DAG activated cPKCs have also been shown to activate PKD (J. Li et al. 2004). cPKC isoforms undergo activation in response to Ca^{2+}, DAG and phorbol ester, in contrast nPKC do not undergo activation in response to increased Ca^{2+} and are only recruited and activated in response to DAG and phorbol ester mimics. Importantly, PKC isoforms similarly to PKD bind DAG via the CRD domains located within the N-terminus (Steinberg 2008) (Rozengurt et al. 2005). DAG therefore also promotes the localisation and redistribution of PKC and PKD kinases during proximal signaling events. Phorbol esters such as phorbol 12,13,-bibutyrate (PDBu), which act as pharmacological mimetic of DAG are commonly used to activate the entire pool of available PKD within experimental studies. The activation of PKD by phorbol ester and DAG was first demonstrated in cell free stimulation studies (Van Lint et al. 1995).

Studies by Rozengurt and colleagues showed that PKC directly interacts with PKD via its PH domain and directly phosphorylates two serine residues within the activation loop of PKD (Zugaza et al. 1996). Within the same studies, it was confirmed that PKD is activated downstream of PKC signalling cascade using specific PKC inhibitor studies that also potently blocked PKD activation despite PKC inhibitors not directly blocking PKD activity itself. Confirmation of a

PKC mediated PKD activation pathway was demonstrated upon cotransfection studies utilising mutant active forms of novel PKCs.

Multiple studies have now extensively characterised the PKC mediated activation of PKD signal transduction pathway. Ligand binding to several reported receptors including seven-transmembrane, tyrosine kinase and G protein coupled receptors, have been shown to result in PKD activation. Ligation of these receptors results in the production of DAG after the hydrolysis of PIP2 by PLC that is membrane bound. Due to its hydrophobic properties direct binding of PKC to DAG retains DAG at the cell membrane facilitating the activation of PKC, which during the accumulation of DAG translocate from the cytosol to the plasma membrane. This binding also allows PKC to undergo dramatic conformational change that releases the pseudosubstrate domain from the substrate-binding site, facilitating substrate binding, phosphorylation and ultimately the activation of downstream signalling molecules (Colón-González & Kazanietz 2006). The accumulation of DAG at the plasma membrane also recruits PKD, which is then activated by PKC.

Further studies have shown that prolonged receptor stimulation, particularly through Gq-couple protein receptor stimulation by bombesin and vasopressin, results in PKD phosphorylation within the activation loop which becomes PKC independent and is then sustained by auto-phosphorylation loop activation (Jacamo et al. 2008; Sinnett-Smith et al. 2009).

1.6.4.2 Atypical PKD activation

PKD has been shown to be a key sensor of oxidative stress by several studies. PKD1 becomes activated after stimulation of cells with multiple induces of oxidative stress including Rotenone, pervanadate, hydrogen peroxide (H_20_2) and diphenyleneiodonium (Storz & Toker 2003) (Storz et al. 2005); (J. Song et al. 2006a) (Waldron et al. 2004); (Cowell, Yan, et al. 2009b); (J. Song et al. 2009). In contrast to DAG accumulation and PKC mediated activation of PKD, oxidative stress within cells has been shown to result in tyrosine phosphorylation at tyrosine sites 463 (PKD1) and tyrosine 694 on PKD2 within the PH domain of PKD. Using RNA interference techniques (RNAi) Storz and colleagues were first

to demonstrate that knock down of endogenous PKD present in HeLa cells rendered them more sensitive to cell death after oxidative stress stimulating treatments (Storz & Toker 2003). The mechanism by which PKD is activated following oxidative stress involves tyrosine kinases including Src activation and subsequent downstream Abl activation, which then directly phosphorylate PKD on tyrosine residues within the PH domain. It has been proposed that this promotes a conformation change whereby the PH domain then uncovers PKD activation loop facilitating phosphorylation of these sites to achieve full kinase activity. Oxidative stress however also leads to the activation of PKC mediating the phosphorylation of PKD on activation loop (Ser744/Ser748) and it was subsequently shown that the nPKC PKCδ isoform mediates this phosphorylation and activation of PKD (Storz et al. 2004).

In regard to the biological function of oxidative stress mediated activation of PKD it has also been shown that activation of PKD in this manner is required for subsequent downstream NFκB activation, this is specific to the oxidative stress pathway as it does not occur via bradykinin or platelet derived growth factor (PGDF) stimulation. Additionally, PKD has been shown to be required for the induction of manganese-dependent superoxide dismutase (mSOD) via NFκB, elucidating a potential mechanism for why knock-down of PKD leads to more cell death in response to oxidative stress (Storz et al. 2005). Collectively, oxidative stress and Src mediated pathway of PKD activation appear to play an important role in the elicitation of signaling pathways that led to the activation NFκB mediated transcription of pro-survival genes. However, the direct targets of PKD that mediates this NFκB response remain to be elucidated.

The two major pathways of PKD activation are summarised in Figure 1.17.

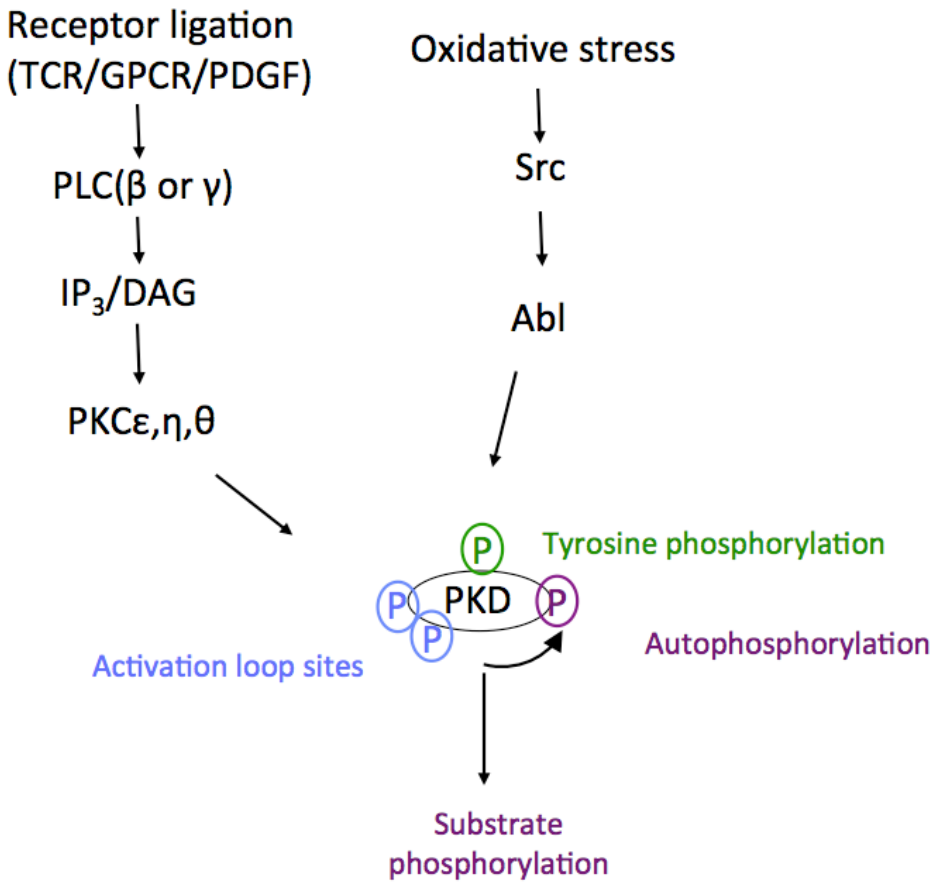

Figure 1.17 Schematic detailing activation of PKD via two main pathways

Multiple receptor ligation have been shown to activate PKD via a PKC dependent pathway including TCR and BCR after antigen recognition and GPCR agonists such as bombesin and angiotensin. Accumulation of DAG activates PKC, which goes on to phosphorylate and activate PKD isoforms within activation loop sites. PKC independent pathways include activation of PKD by oxidative stress pathway via Src-Abl cascade, however phosphorylation of PKD in this pathway is in the form of tyrosine phosphorylation within the PH domain of PKD isoforms. In both instances this leads to auto-phosphorylation in PKD1 and PKD2 isoforms and downstream substrate phosphorylation.

1.6.5 Downstream targets and biological functions of PKD isoforms

Early studies investigating the role of PKD isoforms in cellular processes involved over-expression studies, the use of dual PKC-PKD pharmacological inhibitors and RNAi techniques, which were mainly performed in cell lines. Although these studies were required to ascertain the structure and mechanism of activation of PKD, many of the original papers do not clarify which isoform is

being studied, making the definition of biological roles for specific isoforms of PKD from the early literature difficult.

To date, only a number of direct substrates of PKD have been demonstrated (reviewed (Fu & Rubin 2011)). These include a range of substrates that are known to play diverse biological functions from cell survival and motility to gene transcription and are summarised below in Table 1.3.

Protein	Function	Reference
Class IIa HDACs (4-5-7-9)	Transcriptional de-repression 14-3-3 binding	(Dequiedt et al. 2005) (Vega et al. 2004) (Parra et al. 2005)
PI4KIIIβ	Activation and stabilisation via 14-3-3 binding	{Hausser:2005bx} {Hausser:2006ho}
KI220	Undetermined	{Iglesias:2000ke}
HSP27	Pro survival chaperone activity	(Hutti et al. 2004; Döppler et al. 2005)
CREB	Transcriptional activation	(Yeaman et al. 2004)
CERT	Inhibition of docking with PI4P	{Fugmann:2007et}
SSH1L	Disrupts association with F-actin via 14-3-3 binding	{Eiseler:2009kd}
RIN1	Inhibition of actin remodeling and cell motility	{Ziegler:2011en}
Cortractin	Inhibition of actin remodeling	{Eiseler:2010fz}
SNAIL	Transcriptional de-repression 14-3-3 binding Mediation of adherens-junction formation	{Du:2010kx}
OSBP	Attenuation OSBP Golgi localisation and promotes Golgi fragmentation	{Nhek:2010ht}
IFNAR1	Phosphorylation within degron promotes degradation in CML cells	(Bhattacharya et al. 2011; H. Zheng et al. 2011),

Table 1.3 Key protein kinase D substrates and their functions

The substrate requirement for PKD is dissimilar to that of PKC, with a high selectivity for leucine at the –5 position (substrate consensus L/V/Ix(R/K)XX(S*/T*) (Nishikawa et al. 1997) (Hutti et al. 2004; Döppler et al. 2005). A common feature amongst PKD substrates is that phosphorylation by PKD results in the creation of a 14-3-3 binding site which plays a crucial role in the translocation between cellular locations including the cytoplasm and the nucleus.

Notably, PKD has been shown to phosphorylate class IIa histone deacetylases (HDACs), which includes HDAC4, HDAC5, HDAC7 and HDAC9. Class IIa HDACs catalyse the removal of acetyl groups from lysine residues and are crucial transcriptional regulators (Martin et al. 2007) (X.-J. Yang & Seto 2008). The acetylation of histones by histone acetyltransferases promotes transcription by relaxing chromatin structure, conversely, the removal of acetyl groups results in transcriptional repression. Specifically, class IIa HDACs are recruited to gene promoters by multiple transcription factors including MEF2, runt-related transcription factor (RUNX) and calmodulin binding transcription activator 2 (CAMTA2) and function to repress these genes (Jensen et al. 2009) (McKinsey et al. 2001) (McKinsey et al. 2002) (Taniuchi & Littman 2004) (K. Song et al. 2006b). The phosphorylation of class IIa HDACs results in 14-3-3 binding and their subsequent exportation from the nucleus to the cytoplasm thereby de-repressing transcription. PKD mediated export of class IIa HDACs has been shown to be crucial in multiple cellular processes in various cell types. PKD mediated HDAC phosphorylation has been implicated in cardiac hypertrophy (Vega et al. 2004) and within immune cell signaling (Dequiedt et al. 2005) (Parra et al. 2005) (Matthews et al. 2006).

Collectively, the PKD mediated phosphorylation and therefore regulation of class IIa HDACs serves as a molecular link that connect environmental stimuli to changes within the transcriptome.

(Hausser et al. 2005) (Hausser et al. 2006) (Iglesias et al. 2000) (Fugmann et al. 2007) (Du et al. 2010) (Eiseler et al. 2009) (Eiseler et al. 2010) (Nhek et al. 2010) (Ziegler et al. 2011)

Additionally, as multiple substrates of PKD are fundamentally involved in cell migration pathways, including Hsp27, CREB, class IIa HDACs, PKD activity

has shown to play multiple roles within angiogenesis (reviewed (Evans & Zachary 2011)).

The progression of examining the role of PKD kinases by investigating the consequences of deleting individual isoforms using gene-targeting approaches in mice has allowed investigators to begin to address the true physiological functions of these kinases *in vivo.* The use of transgenic models will allow research to validate what extent PKD *in vitro* studies translate into true physiological roles of PKD kinases *in vivo*. These recent advances have been reviewed within the following reference (Ellwanger & Hausser 2013). The list of biological functions in which PKD isoforms have been implicated is growing, with some examples illustrated in Figure 1.18. It is important to stress that these biological functions and substrates of PKD have been discovered primarily within individual cell types and therefore these substrates cannot be considered as "global" targets of PKD, it is more the case that functions of PKD are highly dependent on cell type but also the cellular localisation of PKD. For example, PKD has been implicated within the Golgi in Hela and HEK293 cells as PKD is found within the Golgi compartments within these cells, whereas in contrast phosphoproteomic analysis has demonstrated that loss of PKD2 in CD8+ CTLs does not affect the phosphorylation of these substrates.

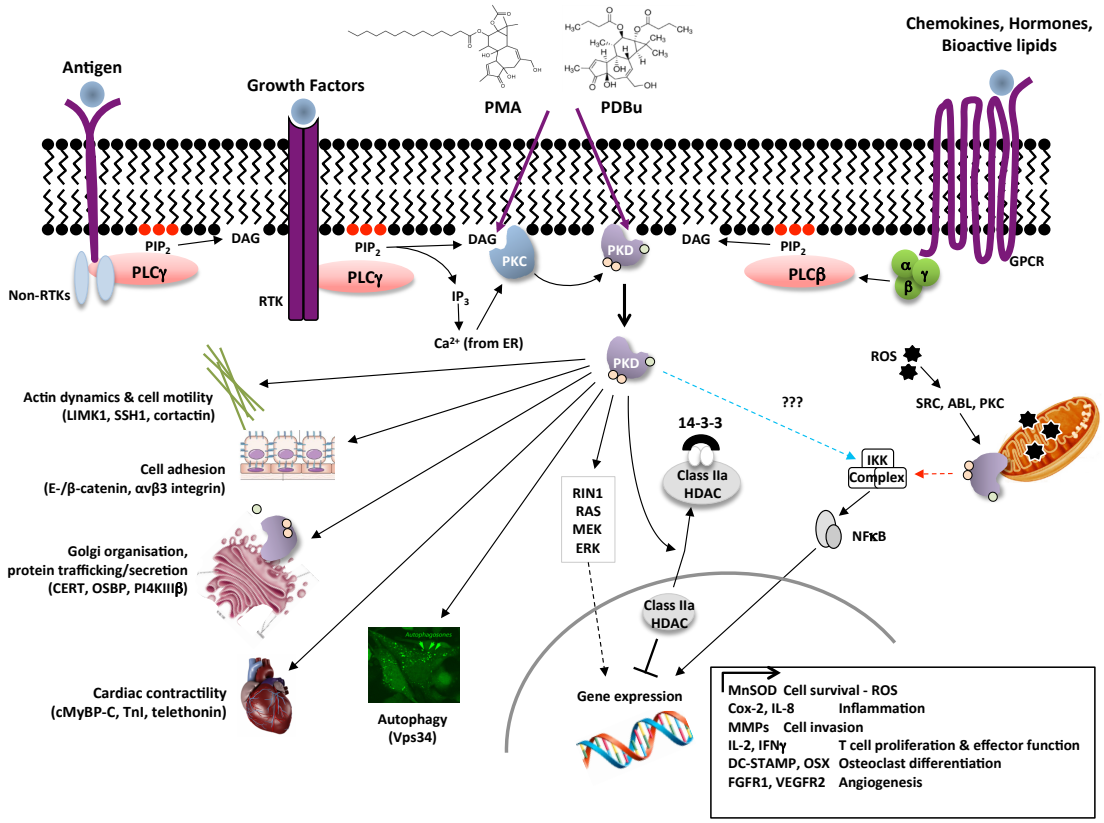

Figure 1.18 PKD is implicated in multiple cellular processes

Evidence exists to support the role of PKD in a large array of essential biological functions within normal and malignant cells. This includes (but is not limited to) cell survival during oxidative stress, inflammation including Cox-2 induction and IL-8 production, cell invasion, successful adaptive immunity, osteoclast differentiation and cell proliferation. It should be noted however that this figure is to give a broad overview of roles PKD has been implicated in and that these substrates are very dependent on the cell type, cellular localisation of PKD (and therefore its access to these substrates) and of course the isoform of PKD under study.
(Figure courtesy of S.A.Matthews)

1.6.6 Role of PKD in cancer development and progression

Although no direct mutations of PKD isoforms in humans have been reported in the literature to lead to disease occurrence, PKD2 was identified as one of the susceptible loci in a genome-wide association study (GWAS) for chronic myeloid leukemia (CML) (Di Bernardo et al. 2008). There is a wealth of literature reporting the dysregulation in the expression and activation of PKD isoforms in the development of cancer albeit with conflicting data, which are summarised below (Table 1.4).

Cancer type	Implication	Reference
Skin cancer	UVB activates keratinocyte PKD1 Reduced papilloma formation in chemical induced carcinogenesis model PKD3 found to mediate chemoresistance	(Arun et al. 2010) (Rashel et al. 2014) (J. Chen et al. 2011)
BCR-Abl+ Leukemia	Tyrosine phosphorylated PKD2 mediates BCR-Abl induced NFκB activation Gabpα expression is required for development of BCR-Abl induced CML and for HSC cell cycle entry Enhanced degradation of the IFNAR1 from cell surface of CML cells	(Mihailovic et al. 2004). (Bhattacharya et al. 2011; H. Zheng et al. 2011)
Colorectal	Combination of small molecule inhibitor of PKD (CRT101) with regorafenib reduces Hsp27 phosphorylation in multiple colorectal cell lines CRT101 compound inhibits tumour growth *in vivo*	(Wei, Chu, Wu, et al. 2014b) (Wei, Chu, Wipf, et al. 2014a)

Pancreatic	PKD2 expression is upregulated and enhances invasion Novel small molecule inhibitor of PKD (CRT101) blocks pancreatic tumour cell growth *in vitro* and *in vivo* Hypoxia activates PKD2 in pancreatic cancer cells and knock down prevents angiogenesis and tumour growth	(Wille et al. 2014) (Ochi et al. 2011) (Harikumar et al. 2010). (Azoitei et al. 2010)
Breast	Epigenetic silencing of PRKD1 gene promoter is correlated with breast tumour invasiveness in patient sample	(Borges et al. 2013)
Prostate	Depletion of PKD3 reduces prostate cancer proliferation *in vivo*	(LaValle et al. 2012).

Table 1.4 Implications for PKD in multiple cancers

1.6.6.1 Potential role of PKD kinases within chronic myeloid leukemia

As this thesis has a particular focus on exploring the role of PKD in chronic myeloid leukemia (CML), it requires a more detailed introduction.

CML is a myeloproliferative neoplasm characterised by a dramatic increase in the infiltration of myeloid cells into the bone marrow, blood and peripheral tissues. CML is most frequently due to chromosomal translocation events that produce the Philadelphia chromosome, whereby a balanced translocation between the c-abl gene on chromosome 9 and the Bcr gene on chromosome 22 occurs, designated as [t(9:22)]. This results in the generation of the fusion oncoprotein Bcr-Abl, which has constitutive tyrosine kinase activity (reviewed (Ahmed & Van Etten 2013)).

The expression of Bcr-Abl in HSCs is central to the pathogenesis of CML and allows the cytokine independent proliferation of myeloid cells, whereby constitutive tyrosine kinase activity leads to dysregulation of key signalling pathways including STAT and NFκB pathways. This has multiple effects on CML

cells including increased proliferation and increased cell survival. Bcr-Abl tyrosine kinase inhibitors (TKIs), such as imatinib, are an effective treatment for CML cells but they are not a 'cure' since they fail to eradicate all Bcr-Abl+ cells and have little effect on leukemic stem cells (LSCs) that drive disease recurrence (Y. Chen & S. Li 2013). Furthermore, drug resistance to TKIs is becoming a more frequent occurrence resulting in blast crisis in patients with CML. As such, combinational therapy strategies are a particular focus of drug research, as more effective treatments are needed to target circulating LSCs (O'Hare et al. 2011) (Graham 2002) (Copland 2006). As a result, further research is required into alternative therapies that actively target LSCs. One such therapy includes the use of interferon alpha (IFNα) either alone or in combination with existing TKIs. IFNα therapy has been previously used with success in a small subset of CML patients with data implicating IFNα induces CML cells to undergo terminal differentiation (Angstreich et al. 2005). This is significant as it allows a window of opportunity for combinational therapy in sensitized cells with the potential to promote the eradication of LSCs.

In regard to PKD expression in CML cells, PKD2 is dominantly expressed in both the K562 CML cell line but also in CML patient samples. However, the extent of IFNα signalling is limited by receptor induced ubiquitination and subsequent degradation of the IFNAR1/IFNAR2 complex from the cell surface (Kumar et al. 2003) (Kumar et al. 2007). It has been shown this process of receptor down-regulation is dysregulated in Bcr-Abl+ cells whereby CML cells express very low levels of IFNAR1, rendering them insensitive to IFNα therapy. Interestingly, PKD2 has been implicated in this process whereby Bcr-Abl has been shown to directly phosphorylate PKD2 on a tyrosine site (Tyr 438) within nthe PH domain causing constitutive activity of PKD in CML cells. Furthermore, PKD2 has been directly linked to the degradation of IFNAR1 by studies showing PKD2 phosphorylates key serine residues (Ser535) on the intracellular domain of (degron) IFNAR1, tagging it for E3 ligase ubiquitination, degradation and removal from the cell surface (Bhattacharya et al. 2011; H. Zheng et al. 2011), depicted in Figure 1.19. Previous studies have also implicated a role for PKD2 in NFκB signalling, which is constitutively active in Bcr-Abl+ CML cells (Mihailovic et al. 2004). Here, PKD2 was elucidated to play a significant role as a docking

protein, as a result of tyrosine phosphorylation within the PH domain, rather than as a direct consequence of its kinase activity.

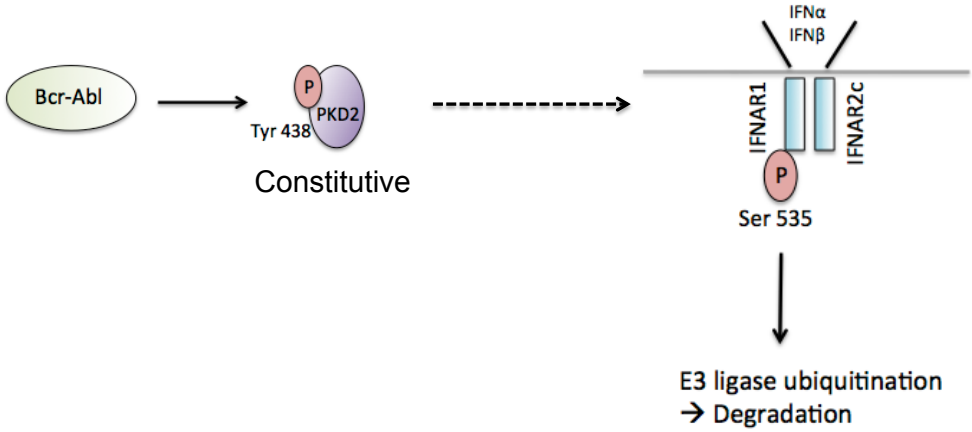

Figure 1.19 PKD2 is implicated in the degradation of the IFNα/β receptor on CML cells

Bcr-Abl oncoprotein activity leads to the dysregulation of multiple normal cellular processes. Bcr-Abl oncoprotein has been shown to constitutively phosphorylate PKD2 on tyrosine 438. PKD2 then goes on to phosphorylate a key serine residue on IFNAR1 degron leading to it being tagged for ubiquitination, subsequent degradation and therefore removal from the cell surface.

Furthermore, two recent studies have shed some light into PKD2 role for CML *in vivo*. The first of which demonstrated that PKD2 was a mediator of Bcr-Abl transformation in CML via GA binding protein (GABP), in which knockdown or inhibition of PKD2 resulted in increased CML cell death. (Z.-F. Yang et al. 2013). Additionally, the same groups have also demonstrated that loss of PKD2 catalytic activity in BCR-Abl induced CML cells protect mice from the development of CML *in vivo* (CML abstract unpublished data).

1.6.7 PKD isoform specific transgenic animals

The first study to harness transgenic mouse models to address the role of PKD kinases, specifically in T cell function *in vivo*, was published in 2003 (Marklund et al. 2003). Germ-line deletion of PKD1 has been shown to be embryonic lethal in studies investigating establishing the role of PKD1 in pathological cardiac remodeling, embryonic lethality was overcome by

conditional deletion of PKD1 catalytic domain in cardiomyocytes specifically (Fielitz et al. 2008). Additionally, homozygous disruption of the key PKC phosphorylation sites of PKD1 (Ser744-748) ($PKD1^{SS/AA}$ mice) also resulted in embryonic lethality (Matthews et al. 2010). In contrast, transgenic mice generated with homozygous mutations in PKD2 activation loop (Ser707-Ser711), deemed catalytic knock-in $PKD2^{SS/AA}$ mice, but also PKD2 gene-trap ($PKD2^{GT/GT}$) mice with deletion of the catalytic domain, of PKD2 were born at Mendelian frequency and indistinguishable from wild type littermates (Matthews et al. 2010). The generation of isoform specific targeted transgenic mouse models demonstrates a clear non-redundant role for intact PKD1 catalytic activity during normal murine embryogenesis.

The generation of PKD transgenic animals specifically lacking catalytic activity is significant as it permits investigation of the roles performed by specific isoform of PKD catalytic function but does not disturb any scaffolding functions. An overview of the current knowledge of existing isoform specific PKD transgenic mouse models and their known phenotypes are shown in Table 1.5.

Mutant allele	Tissue specificity and description	Phenotype	Reference
PKD1^{flox}	Germline deletion (CAG-Cre) Conditional deletion (alpha Myosin heavy chain (MHC)-cre) in cardiomyocytes	Embryonic lethal Decreased heart hypertrophy in response to cardiac stress	(Fielitz et al. 2008)
PKD1$^{SS/AA}$ KI	Targeted knock in to generate kinase dead PKD1 Ser744/748 allele	Embryonic lethal (E9.5)	(Matthews et al. 2010)
PKD2$^{SS/AA}$ KI	Targeted knock in to generate kinase dead PKD2 Ser707/711 allele	Reduced TCR stimulated cytokine production by CD4+ and CD8+ T cells in vitro Reduced T-cell dependent antibody responses using immunisation model Enlarged thymus, spleen and lymph nodes when crossed to TCR-Tg mice (OT I and OT II)	(Matthews et al. 2010) (Navarro et al. 2012)

$PKD2^{SS/AA}$ KI	Targeted knock in to generate kinase dead PKD2 Ser707/711 allele	Dispensable for integrin mediated adhesion and lymph node homing in lymphocytes.	(Matthews et al. 2012)
$PKD2^{GT/GT}$	Gene trap deletion of PKD2 catalytic domain by retroviral insertion into intron 15.	Similar hyper cellularity when crossed to TCR-Tg mice as observed in $PKD2^{SS/AA}$ KI	(Navarro et al. 2012)
$PKD3^{GT/GT}$	Gene trap deletion of PKD3 by retroviral insertion between exon 1-2.	Mice are viable albeit with reduced Mendelian frequency. Decreased vertebral trabecular bone volume and thickness	Unpublished data (S.Matthews) (Rogers et al. 2005)
$PKD3^{KO/KO}$	Bal-Cre mediated excision resulting in loss of protein function by generation of frame shift mutation	Potentially embryonic lethal, no homozygous live born.	Unpublished data (S.Matthews)

Table 1.5 Isoform specific PKD transgenic animal models and their phenotypes

1.6.8 Pharmacological inhibition of PKD

1.6.8.1 Older generation inhibitors used to target PKD

Foundational research attempting to tease apart PKC and PKD functions and downstream targets began with the development of a staurosporin derivative that potently blocked Ca^{2+} dependent PKC isoforms including PKCα and PKCβ1 but also PKD (Gschwendt, dieterich, et al. 1996b). The Go6976 compound arose from previous studies identifying that indolocarbazoles, including the microbial alkaloid staurosporin, potently inhibited PKC isoforms which were at the time a particular focus during phorbol ester induced tumorigenesis research (Martiny-Baron et al. 1993). The development of Go6976 lead to a host of publications attempting to define the distinct functions of PKD that were independent from those previously attributed to PKC isoforms. Many of these studies were achieved by comparing the effects of Go6976 with Go6983, also a derivative from staurosporin that acted as a pan-PKC inhibitor, potently blocking all isoforms of PKC but importantly not PKD. Multiple studies have since used Go6976 to assess the role of PKD in different cells and their biological processes. Go6976 inhibited LPS induced production of inducible nitric oxide synthase (iNOS) and TNFα, ultimately protecting neurons from microglia mediated cytotoxicity. However, Go676 has significant off target effects including inhibition of janus kinases (JAKs) (Grandage et al. 2006).

1-Naphthyl PP1 (1-NA-PP1), a pyrazolopyrimidine that was originally designed for inhibition of mutant src kinase (Bishop et al. 1999) has also been shown to be a potent pan PKD inhibitor, with little effect on PKC isoforms (Tandon et al. 2013). However, although there is little effect on PKC isoforms this compound also has major off targets effects at the concentration required to cause PKD inhibition including >50% inhibition of Src, Lck, CSK, RIP2, p38α MAPK and CK1δ (Bain et al. 2007).

Although these studies provided early insights into the many roles of PKD isoforms, they have provided somewhat conflicting data as to the true roles for PKD in many different cell lines. The ability to dissect and understand true biological functions of PKD is also complicated by lack of selectivity in widely used PKC/PKD inhibitors. In more recent years, small molecular protein kinase

inhibitors have been widely developed and used in research to elucidate cellular signaling pathways. As such, small molecule inhibitors are frequently the focus of research into the generation of therapeutic agents including anti-cancer therapies.

The first report of a potent and specific inhibitor of PKD was identified from National Institute of Health (NIH) small molecule repository library using human PKD1 for high throughput screening assays (HTS). The resulting compound, CID755673, demonstrated potent ability to suppress all 3 PKD isoforms, with no apparent preference (IC_{50}: 0.182nM, 280nM and 227nM for PKD1, PKD2 and PKD3 respectively) (Sharlow et al. 2008). CID755673 was demonstrated to not only be a potent pan-PKD inhibitor but also highly selective, without any inhibition of PKC isoforms in *in vitro* kinase assays. Significantly, it was not ATP competitive, like all other previously described PKD inhibitors. This is advantageous as the ATP binding pocket is highly conserved between kinase families, often resulting in multiple off-target effects, making it difficult to find selective compounds. The development of non-competitive ATP inhibitors offers the possibility to overcome these difficulties. In contrast, non-ATP competitive inhibition exert their effects by causing a conformational shift resulting in the kinase being unable to function rather than competing with high levels of intracellular ATP. Multiple analogues developed from CID755673 were developed to improve potency, this notably included kb NB-142-70, which demonstrated a 7 fold increase in potency for PKD isoforms (IC_{50} values are 28.3, 58.7 and 53.2 nM for PKD1, 2 and 3 respectively). This analogue has been shown to inhibit cell migration and invasion in a prostate cancer cell line (LaValle, Bravo-Altamirano, et al. 2010a). However, additional studies have shown kb NB-142-70 has poor aqueous solubility and is rapidly metabolised in mice (J. Guo et al. 2013).

In addition to CID755673 and its analogues, another potent inhibitor of PKD was developed through further HTSs, however it was shown to have large off target effects (Meredith, Ardayfio, et al. 2010a). The attempt to reduce off target effects led to the development of bipyridyl, BPKDi (2'-(cyclohexylamino)-6-(piperazin-1-yl)-[2,4'-bipyridine]-4- carboxamide) (Monovich et al. 2010). The BPKDi compound was generated at the same time as the Novartis 12a compound

sharing chemical structure and potency, BPKDi will be referred to as 12a from this point onwards. This compound has been shown to be ATP competitive with IC_{50} values of 1nM, 9nM and 1nM for PKD1, PKD2 and PKD3 respectively. Studies have been conflicting with this inhibitor. One study has demonstrated potent inhibition of PKD resulting in reduced phosphorylation and therefore increased nuclear retention of HDAC4 and HDAC5, resulting in a reduction in pathologic cardiac gene expression and reduced myocyte hypertrophy *in vitro* in neonatal rat ventricular myocytes (NRVM). However, Studies attempting to move this compound into *in vivo* animal studies to assess the potentially therapeutic inhibition of PKD for pathological hypertrophy of the heart unfortunately showed little result. (Meredith, Beattie, et al. 2010b). This was attributed to poor bioavailability due to low permeability of the compound (Meredith, Ardayfio, et al. 2010a).

The chemical structures of previous inhibitors to target PKD are summarised in Figure 1.20. Collectively, although these compounds are fairly potent for PKD none of them have made the transition into clinical trials, due to multiple difficulties such as lack of selectivity, poor *in vivo* stability or bioavailability and general toxicity issues. As such, the search for PKD inhibitors with good *in vivo* efficacy is still required.

A

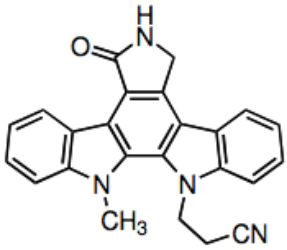

GO6976

B

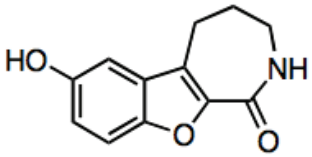

CID75563

C

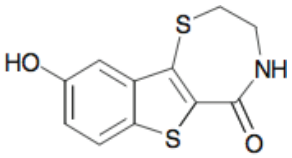

kb NB-142-70

D

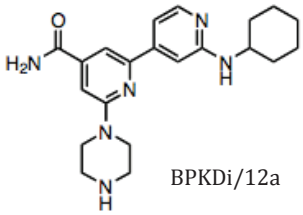

BPKDi/12a

E

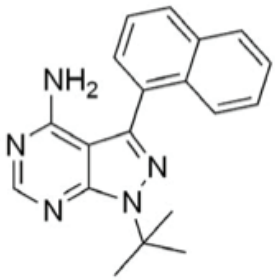

1-NA-PP1

Figure 1.20 Chemical structures of older generation inhibitors of PKD

(A) GO6976 (B) CID75563 (C) kb NB-142-70 analogue (D) BPKDi/12a (E) 1-NA-PP1.
Taken from (LaValle, George, et al. 2010b) (Monovich et al. 2010)*;* (Meredith, Beattie, et al. 2010b) (Grandage et al. 2006).

1.6.8.2 Novel small molecule inhibitors of PKD

In order to improve drug target specificity, cancer research technologies (CRT) have expanded studies for the development of new generation PKD inhibitors with such properties via further HTS studies. This resulted in the

successful generation of two lead compounds: CRT0066101 and CRT0066051. Both chemical structures are shown in Figure 1.21.

CRT0066101 is a pyrazine benzamide, which is structurally distinct from CID75563 It has had significant success in being the first PKD inhibitor to demonstrate good bioavailability *in vivo* (Harikumar et al. 2010). Significantly, oral gavage of this compound led to reduction in tumour size in two separate pancreatic cancer models (Harikumar et al. 2010). In addition to this study, three other studies investigating the therapeutic potential of the CRT0066101 compound have been published, all of which demonstrated promising results for potential use of CRT0066101 for treatment of CML, colorectal and glioblastoma tumors, in both *in vitro* and *in vivo* settings (Z.-F. Yang et al. 2013; Bernhart et al. 2013; Wei, Chu, Wipf, et al. 2014a).

The CRT0066051compound has to our knowledge has only been cited in one study demonstrating its potential therapeutic use in the inhibition of vascular endothelial growth factor (VEGF) induced migration, proliferation and *in vitro* angiogenesis (Evans et al. 2010).

Both past and present compounds used to target PKD, IC50s and the known off-target effects are summarised in Table 1.6.

A B

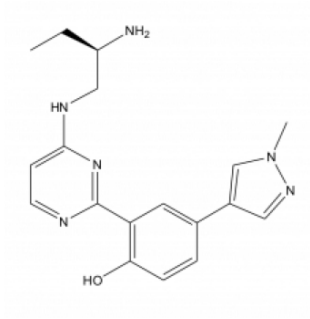

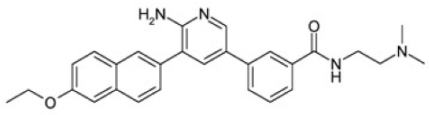

CRT0066101 CRT0066051

Figure 1.21 Chemical structures of new generation inhibitors of PKD

(A) CRT0066101 (B) CRT0066051.
Taken from (Harikumar et al. 2010) (Evans et al. 2010).

Inhibitor	Targets and IC50	Off target effects	References
Go6976	PKCα (2.3nM) PKCβ1 (6.2nM) PKD1 PKD2 PKD3	JAK2 (5nM) JAK3 (30nM) TrkA (130nM) TrkB (370nM)	(Gschwendt, Dieterich, et al. 1996a) (Grandage et al. 2006)
CID755673	PKD1 (0.182nM) PKD2 (280nM) PKD3 (227nM)	GSK3β MAPKAPK2 CK18δ MK2 ERK1	(LaValle et al. 2012).
kb-NB-142-70 (CID755673 analogue)	PKD1 (28.3nM) PKD2 (58.7nM) PKD3 (53.2nM)		(LaValle et al. 2012). { (LaValle, Bravo-Altamirano, et al. 2010a).
1-NA-PP1	PKD1 (154.6nM) PKD2 (133.4nM) PKD3 (109.4nM)		(Tandon et al. 2013) (Bain et al. 2007)
IKK-16	PKD1 (153.9nM) PKD2 (115.0nM) PKD3 (99.47nM)		(Tandon et al. 2013)
BPKDi/12a	PKD1 (1nM) PKD2 PKD3		(Monovich et al. 2010). (Meredith, Ardayfio, et al. 2010a). (Meredith, Beattie, et al. 2010b).

CRT0066101	PKD1 (1nM) PKD2 (2.5nM) PKD3 (2nM)	{Harikumar:2010bz} (Z.-F. Yang et al. 2013; Bernhart et al. 2013; Wei, Chu, Wipf, et al. 2014a)
CRT0066051	PKD1 (1nM) PKD2 (2.5nM) PKD3(1.5nM)	{Evans:2010dt}

Table 1.6 Inhibitors used to target PKD

1.6.9 Role of PKD enzymes in immune system

1.6.9.1 Innate immune cells

In regard to the activation of PKD enzymes in cells from the myeloid lineage and innate arm of the immune system the literature is somewhat limited and conflicting. However, studies have pointed to a clear and conserved role for PKD kinases in innate immunity whereby studies in C. elegans lacking DFK-2A (homologue of PKD) were hypersensitive to death from bacterial pathogens (Ren et al. 2009). This is significant as the study directly links DAG mediated signalling, specifically involving PKD to innate immunity. At present, no studies have yet been published investigating the role of PKD kinases in the development of myeloid cells within the bone marrow or the effect of loss of PKD catalytic activity on the population of myeloid cells within peripheral tissues. Although there is data implicating a role for PKD within myeloid effector functions in which PKD1 has been implicated in PRR signaling within macrophages, DCs and mast cells.

Involvement of PKD kinases in response to PPR or TLR ligation was first highlighted whereby treatment of microglia cells with dual PKC/PKD inhibitor GO6976 was shown to significantly reduce TNFα production in response to LPS (Jeohn et al. 2002). Subsequently, another study implicated PKD1 to be involved

in TLR5 activation in response to bacterial flagellin in HEK293 cells expressing TLR5 constructs (Ivison et al. 2007). PKD1 activation in response to PAM3CSK4, a TLR1/2 agonist has also been shown in bone marrow derived mast cells (BMDMCs), additionally treatment with GO6976 resulted in reduced expression of the chemokine CCL2 mRNA transcript whereas other PKC inhibitors did not (Murphy et al. 2007). Within mast cells, the overexpression of PKD led to enhanced production of IL-13 and TNFα after FceRI stimulation, although it is not clear what PKD isoform is under study (Yamashita et al. 2010).

Specifically, PKD1 has implicated in pathogenic DNA sensing via the TLR9 signalling pathway in BMDMOs (J.-E. Park et al. 2008). Pharmacological inhibition of PKD with Go6976 significantly reduced proinflammatory cytokine production including TNFα, IL-6, and IL-12p40 but also reduced IL-10 production. Additional studies also concluded that PKD1 was required for MyD88 mediated TLR signaling within macrophages and DCs (J.-E. Park et al. 2009b).

More recently, both PKD1 and PKD2 have been reported to be required for the production of chemokines including CXCL8 (IL-8) and CCL20 in response to TLR2, TLR4 and TLR5 in epithelial cells (Steiner et al. 2010).

1.6.9.2 Adaptive immune cells

A wealth of studies has established a prominent role for PKD kinases within the adaptive immune system including T and B lymphocytes. In regard to isoform expression, T and B lymphocytes selectively express PKD2. Upon antigen receptor engagement via the TCR the accumulation of DAG rapidly recruits PKD from the cytosol to the immunological synapse (Spitaler, Emslie, Wood & Cantrell 2006b). Although studies have shown that PKD2 participates in the IL-2 promoter regulation within Jurkat T cells (Irie et al. 2006) PKD is not directly activated by IL-2 (Matthews et al. 2000)Within B lymphocytes PKD activation is essential for class IIa HDAC phosphorylation after BCR ligation (Matthews et al. 2006).

Analysis of T and B cell development within catalytically in-active PKD2 transgenic animals has been shown to be normal. However, PKD2 was

highlighted to have a particular role in T cell effector function in which PKD2 deficient mice are unable to efficiently produce key pro-inflammatory cytokines such as IL-2 and IFNγ. Unsurprisingly, *in vivo* experiments went on to show that PKD2 deficient mice displayed a reduced immune response after immunisation, presumably due to significantly reduced production of IL-2 and IFNγ (Matthews et al. 2010). Further analysis has demonstrated lack of effector function by PKD2 null T lymphocytes is cell intrinsic and not due to abnormal thymocyte development (Navarro et al. 2012).

Although the PKD family has been implicated in regulating the activity of β1 integrins in T lymphocytes (Medeiros et al. 2005), *in vivo* analysis of T lymphocyte homing to lymphoid tissues is not affected within PKD2 catalytically inactive mice (Matthews et al. 2012), demonstrating that PKD2 does not play a key role in integrin receptor expression or integrin mediated adhesion *in vivo*.

More recent studies have taken a wider approach and examined the effect of loss of PKD2 on the phosphoproteome in CD8+ CTLs, which display high levels of basal PKD activity, allowing insight into the role of PKD2 including the positive and negative regulation of cell signalling networks within effector T cells (Navarro, Goebel, et al. 2014b). Significantly, phosphoproteomics in this study revealed that PKD2 regulates approximately 5% of the phosphoproteome in CTL, whether directly or indirectly. Additionally, studies have also demonstrated that PKD2 acts as a ultrasensitive digital amplifier of TCR signaling that mediates cellular responses within CD8+ CTLs (Navarro, Feijoo Carnero, et al. 2014a). Finally, the role of PKD2 has also been addressed in multiple experimental disease models highlighting key roles for PKD2 activity within CD8+ CTLs during the immune response to *Listeria Monocytogenes* yet conversely lack of PKD2 in CD8+ CTLs has been shown to be protective within the development of autoimmune diabetes (Navarro, Feijoo Carnero, et al. 2014a).

1.7 Aims

The aims of this thesis were to investigate for the requirement and role of catalytic activity of PKD kinases in the mammalian immune system, including cells from both the innate and adaptive branches. Specifically, we wished to answer the following research questions:

1) Are novel small molecule inhibitors of PKD indeed specific for PKD and do they share significant off target effects?
2) Which isoforms of PKD are predominantly expressed in primary myeloid cells?
3) Do TLR agonists activate PKD kinases in myeloid cells and does loss of PKD catalytic activity affect effector functions of myeloid cells
4) Is PKD2 catalytic activity required for normal myeloid cell development *in vivo*?
5) What are the effects of loss of PKD2 catalytic activity on T lymphocyte homeostasis within the small intestine and within Treg development, homeostasis and effector function?

Importantly, we wished to address these aims both *in vitro* by using primary murine cells and *in vivo* through the use of isoform specific kinase inactive transgenic mice. As many of the roles of PKD have been defined through the use of pharmacological inhibitors, we additionally sought to characterise and validate new specific small molecule inhibitors for PKD. PKD has been implicated in signalling events downstream of TLR and therefore pathogen recognition in myeloid cells. Therefore we examined the effect of the loss of PKD catalytic activity on myeloid cell effector function after TLR4 ligation, including cytokine production, antigen presentation and subsequent T cell activation. Finally, as a wealth of evidence exists to support a key role for PKD2 in T lymphocyte effector function we examined the loss of PKD2 catalytic activity of PKD in T lymphocyte homeostasis in the small intestine as well as the development of regulatory T cell populations and their effector functions *in vivo*.

2 Materials and methods

2.1 Acknowledgements

I would like to take this opportunity to acknowledge services provided that allowed this thesis to be completed including; Dr Matthew Mackenzie and Dr Mark Anderson who assisted with in multiple experiments including much help with tissue preparation, all staff within the transgenic animal unit who performed all animal care including ear notching and tail bleeds, staff within the International Centre for Kinase Profiling within the University of Dundee for performing *in vitro* kinase screen analysis, staff within Veterinary services at the University of Glasgow including Lynn Stevenson and Dr Francesco Marchesi who completed tissue sectioning, staining and colitis scoring, the flow cytometry core services provided by Dr Rosie Clarke and Ms. Arlene Whigham who performed cell sorting and finally Dr. George Ramsay who helped performed analysis of lymphocyte populations within the small intestine and provided much assistance during the colitis model.

2.2 Materials

All materials used were of the highest quality available. Unless otherwise stated, all chemicals were provided by Sigmal-Aldrich (Poole, Dorset, UK) or VWR (Lutterworth, Leicestershire, UK). All solutions were prepared using deionised water (MilliQ system, Millipore) and where appropriate solutions were autoclaved at 120°C, 15psi for 20 min. All cell culture media including Roswell Park Memorial Institute (RMPI), Dulbecco's Modified Eagle Medium (DMEM) and Iscoves Modified Dulbecco's Medium (IMDM) were purchased from Invitrogen- Life technologies (Paisley, Glasgow, UK). Fetal Bovine Serum (FBS) was purchased from Labtech International Ltd (FB-1090/500). Sodium Dodecyl sulphate-polyacrylamide gel electrophoresis (SDS-PAGE) cell modules and pre-cast gradient gels were purchased from Invitrogen Life Technologies. All

oligonucleotides were purchased from MWG-Biotech UK Ltd. (Peartree Bridge, Milton Keynes, Bucks, UK), sequences are shown in Appendix A.

2.3 Common Solutions

Phosphate Buffered Saline (PBS)	37mM NaCl 2.7mM KCl 4.3mM Na_2HPO_4 1.2mM KH_2PO_4
5x SDS sample buffer	250mM Tris-HCL pH 6.8 30% Glycerol 10% SDS 5% 2β-mercaptoethanol 0.02% Bromophenol blue
PBS-Tween	37mM NaCl 2.7mM KCl 4.3mM Na_2HPO_4 1.2mM KH_2PO_4 0.025% Tween 20
ACK lysing buffer (10x) pH 7.2	1.5M NH_4Cl 100mM $KHC0_3$ 10mM EDTA
Tris-borate-EDTA (TBE) buffer	89mM Tris-Borate 2mM EDTA pH 8.3
MES SDS running buffer (1x)	50ml 20X MES buffer 950ml deionised water
Transfer buffer (1x)	50ml 20x concentrated transfer buffer 100ml methanol

	850ml deionised water
F lysis buffer	10mM Tris-HCl pH 7.05 50mM NaCl 30mM Sodium pyrophosphate 50mM NaF 5μM $ZnCl_2$ 10% (w/v) glycerol 0.5% Triton-x-100
Low salt lysis buffer	50mM Tris-HCl pH 7.8 150mM NaCl pH 7.4 10mM EDTA 50mM NaF 1% Triton-x-100
NP-40 Lysis buffer	50mM HEPES pH 7.0 250mM NaCl 5mM EDTA 5mM NaF 0.5mM Na_3VO_4 1% NP-40
Ear digestion buffer	28nM NaCl 55mM Tris/HCl pH 8.0 0.1% SDS
Blood buffer	Complete mouse media (RMPI) 10mls 1x ACK
MACs buffer	1xPBS 1% FBS 2mM EDTA

FACS buffer	1xPBS
	1% FBS/BSA
	2mM EDTA

2.4 Animals

2.4.1 Maintenance of animal lines

Animals in the transgenic animal unit have a 14: 10 light cycle and are maintained on autoclaved RM3 pelleted diet (SDS Diets, local agent DBM) ad libitum along with autoclaved water ad lib. Animals are housed in accordance with HO CoP, local WEC best practice guidance and project license authority Animals bred and maintained under specific pathogen free conditions in the Wellcome Trust Biocentre at the University of Dundee. The background strain for breeding is the C57Bl/6j jax supplied by Charles River UK, Manston, Kent. All animals were maintained in accordance with the UK Home Office Animals (Scientific Procedures) Act 1986 guidelines, under the license for the project (PPL 60/3972 and PPL 70/8084). The genotypes of mice used within this thesis were as follows: wild type (WT), $PKD1^{WT/KI}$, $PKD2^{KI/KI}$, $PKD1^{WT/KI}$ x $PKD2^{KI/KI}$ double knock-in, PKD2 gene trap knock out mice ($PKD2^{GT/GT}$) and $RAG2^{KO/KO}$. The generation of PKD1 and PKD2 transgenic mice are thoroughly described within the following reference (Matthews et al. 2010))

2.4.2 Biopsy of animals by ear notch

Animals aged 4 weeks were biopsied by taking a small notch from the ear using a dermal punch. The notch served as both a source of DNA for genotyping and for identification of the animal. DNA was extracted from the ear notch and analysed using PCR. Animals within the $PKD2^{KI/KI}$ line were maintained by

biopsy and genotyping of the first litter of a new mating, after which animals were presumed homozygous.

2.4.3 Genotyping of animals by PCR

2.4.3.1 Ear digest for DNA

Ear notches were digested to obtain DNA by incubating with 50µl of ear buffer and proteinase K (1mg/ml) (Sigma) and heated to 55°C for 9 hrs. Proteinase K was then inactivated by addition of 150µl of dH_2O and boiling samples at 100°C for 10 min. Ear digests were then centrifuged at 250 x g for 1 minute to collect debris and genomic DNA was stored at 4°C short term and -20°C long term.

2.4.3.2 Optimisation of PKD1 genotyping assay

Due to various problems with genotyping PKD1 heterozygous mice via PCR, this assay was optimised. New primers were generated using ApE- A plasmid editor software. Successful primers were subsequently validated using verifying PCR products using DNA sequencing by capillary electrophoresis (Lab901 ScreenTape system). Verified sequence alignment of the PCR product with the relevant murine *Prkd1* gene region is shown in Appendix A. This service was provided by Genetics Core Services Unit, Ninewells Hospital, University of Dundee. Validated primers were purchased from MWG-operon and reconstituted in nuclease free water at a concentration of 100µM and diluted to 10µM as required. All primers were stored at -20°C and aliquoted to prevent repeated freeze thawing. Typical reaction mixture used to amplify genomic DNA from WT and $PKD1^{WT/KI}$ mice is shown in Table 2.1 and PCR conditions are shown in Table 2.2 respectively.

Reagent	1 x Volume
10x Buffer (1x f.c)	2.5µl
25mM MgCl (2mM f.c)	2µl
10mM dNTPs (0.4mM f.c)	1µl
1:10 Forward primer (10µM f.c)	1µl
1:10 reverse primer (10µM f.c)	1µl
5u/µl Redtaq (1 unit f.c)	2.5µl
H_20	13.5µl
Genomic DNA	2µl

Table 2.1 A typical PCR reaction mixture used for genotyping WT and PKD1$^{WT/KI}$ mice

Step	Temperature	Time	Cycles
1. Initial denaturation	95°c	3 min	1
2. Denaturation	95°C	30 seconds	34
3. Annealing	62°C	45 seconds	
4. Extension	72°C	1 minute	
5. Final extension	72°C	10 min	1

Table 2.2 Reaction conditions and cycle used to amplify genomic DNA

2.4.3.3 Genotyping of PKD2$^{KI/KI}$ mice by PCR

DNA obtained from ear notching from PKD2$^{WT/WT}$ and PKD2$^{KI/KI}$ mice was amplified using similar methodology to PKD1$^{WT/KI}$ genotyping. Reaction mixtures and PCR amplification cycles described below in Table 2.3 and Table 2.4 respectively.

Reagent	1 x Volume
10x Buffer (1x f.c)	2.5µl
25mM $MgCl_2$ (2mM f.c)	2µl
10mM dNTPs (0.4mM f.c)	1µl
1:10 Forward primer (10µM f.c)	1µl
1:10 reverse primer (10µM f.c)	1µl
5u/µl Redtaq (1 unit f.c)	2.5µl
H_20	13.5µl
Genomic DNA	2µl

Table 2.3 A typical PCR reaction mixture used for genotyping of WT and $PKD2^{KI/KI}$ mice

Step	Temperature	Time	Cycles
1. Initial denaturation	95°c	3 min	1
2. Denaturation	95°C	30 seconds	34
3. Annealing	58°C	45 seconds	

4. Extension	72°C	1 min	
5. Final extension	72°C	10 min	1

Table 2.4 Reaction conditions used to amplify genomic DNA from WT and $PKD2^{KI/KI}$ mice

2.4.4 Genotyping of OT II TCR transgenic mice by blood analysis

Mice were blood biopsied at 25 days of age via tail bleeding. Blood samples were placed in 500µl blood buffer. Red blood cells were lysed in 1ml 1x ACK buffer and incubated at room temperature until samples were no longer cloudy (30 seconds to 3 min). Samples were then washed by adding 2ml of PBS supplemented with 1% FBS or BSA and spun at 250 *x g* for 5 min at 4°C. The supernatant was then poured off and cells were stained with the following antibodies prepared in FACS buffer: CD4-APC and Va2- PE both used at 1:200. Samples were stained for 20 min on ice in 50µl staining buffer, washed with 1ml FACS buffer, centrifuged at 250 *x g* for 5 min, resuspended in 200µl FACS buffer and acquired on BD Verse.

Samples were described as OT II positive if mice had a skewed CD4/CD8 T cell ratio whereby 80-90% of lymphocytes are CD4+, additionally all CD4+ lymphocytes were Vα2+ (Figure 2.1A).

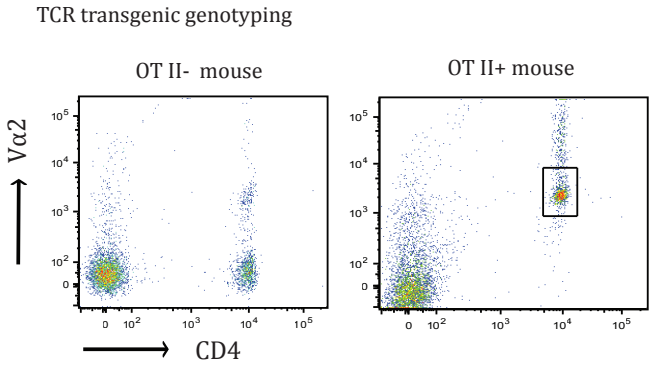

Figure 2.1 Genotyping of OT II TCR transgenic mice by blood analysis using flow cytometry

Homozygous OT II+ lymphocytes double positive for surface staining of CD4 (PE) and Vα2 (APC).

2.5 Preperation of murine tissues

Age (6-12 weeks of age unless otherwise indicated) and sex matched mice were sacrificed using CO_2 and various organs were harvested and prepared for use in downstream applications. All tissues were counted after preparation unless otherwise stated using either a hemocytometer or using the cell counting assay on a BD Verse.

2.5.1 Isolation of thymocytes

Thymus was dissected and cleaned using cold DMEM media. Samples were mashed through cell strainers (70µm, BD) using the hard end of a 5ml syringe (BD) to obtain single cell suspensions, strainers were flushed through with 10ml DMEM media to ensure maximum collection of cells. Samples were centrifuged at 250 *x g* 5 min at 4°C, resuspended in cold DMEM media and kept on ice until use.

2.5.2 Isolation of bone marrow cells

Femurs and tibias were dissected and cleaned thoroughly to remove muscle using PBS and rinsing in 70% ethanol. The end of each bone was removed and bone marrow was isolated by flushing through 10ml sterile PBS with a 23G needle. No red blood cell lysis was carried out when the resulting cell suspension for used within culture, as it is detrimental for isolation of myeloid progenitor cells thus lowering yield of differentiated cells throughout culture. However, for downstream application in flow cytometry red blood cells were lysed by incubation of samples with 1 x ACK buffer for 2 min at room temperature. Cells were then washed in 10ml of complete mouse media and centrifuged at 250 *x g* for 5 minutes.

2.5.3 Isolation of splenocytes

Spleens were dissected and placed between 2 pieces of sterile gauze in 6-well plates. Single cell suspensions were achieved by mashing tissues with 5 ml syringes into cold complete mouse media. Resulting cell suspensions were filtered through 0.45µm filters (Partec, Milton Keynes, UK) into falcons and centrifuged for 5 min at 250 *x g* to pellet cells. Supernatant was removed and spleen preparations were red blood cell lysed using 3ml 1x ACK solution for 2 min at room temperature. Samples were then diluted with 5ml RMPI media and centrifuged for 5 min at 250 *x g* at 4°C. Red blood cell lysis step was performed until cell pellets were no longer red. At this point they were resuspended in 10ml complete mouse media and kept on ice until use.

2.5.4 Isolation of cells from lymph nodes

Lymph nodes including axillary, inguinal and mesenteric, were dissected and placed between 2 pieces of sterile gauze in 6-well plates. Single cell suspensions were achieved by mashing tissues with 1 ml syringes into cold complete mouse media. Resulting cell suspensions were filtered through 0.45µm filters (Partec, Milton Keynes, UK) into falcons and centrifuged for 5 min at 250 *x g* to pellet cells and resuspended in complete mouse media.

2.5.5 Preparation of blood

Blood was obtained through cardiac puncture using 1ml syringe with 23G needle and collected in heparin tubes. Heparin tubes were inverted 3 times to prevent clotting of blood samples, and were kept on ice until use. 100µl blood per stain, per mouse was pipetted into FACS tubes and 1ml 1 x ACK solution was added to allow lysis of red blood cells. Samples were incubated at room temperature for 2 min and 1ml RMPI media was added before centrifuging samples at 250 *x g* for 5 min at 4°C. The red blood cell lysis step was repeated 3 times or until cell pellets were no longer red. Cells were kept on ice before proceeding to FACS staining.

2.5.6 Isolation of lymphocytes from the small intestine

2.5.6.1 Isolation of intraepithelial lymphocytes (IELs)

The small intestine from the proximal duodenum to terminal ileum were dissected free from the mesentery and removed. Small intestines were flushed with 20ml cold 1 x PBS and cut longitudinally. Peyers patches were identified and excised. Intestines were then cut transversely into pieces of approximately 5mm in length and placed in falcons containing 50ml of RPMI media supplemented with 10% FBS and 1mM DTT per individual tissue. Samples were incubated for 30 min whilst shaking at room temperature. Samples were then centrifuged for 5 minutes at 500 x g at room temperature for 5 min. The supernatant was discarded and intestinal pieces were resuspended in 10ml of RMPI media within 50ml falcons. Samples were vortexed for 3 min. At this point, the resulting suspension was passed through a 70µm cell strainer (Griener, Gloucestershire, UK) and supernatant was collected. Remaining intestinal pieces were placed in 10ml RMPI media, vortexed for 3 min and passed through a 70µm cell strainer. The resulting supernatant was centrifuged at 500 *x g* for 5 min at room temperature.

Cells were then resuspended in 40% Percoll (Sigma, Dorset, UK) and overlaid on 80% Percoll and the gradient was centrifuged at 700 x g for 30 minutes at room temperature. Cells that lay at the 40-80% interface are the IEL, which were removed from the Percoll and washed with RMPI media supplemented with complete mouse media.

2.5.6.2 Isolation of cells within the lamina propria

Once the intraepithelial layer had been extracted, the remaining small intestinal pieces were washed twice in PBS before extraction of the lamina propria lymphocyte layer. Pieces were placed in RMPI complete mouse media with collagenase D (0.5mg/ml) (Roche, West Sussex, UK) and DNAse I (100µg/ml) (Sigma). Samples were incubated at 37°C for 1 hr and subsequently vortexed for 3 min before passing through 70µm cell strainers. The resulting supernatant was then mixed with 40% Percoll and centrifuged at 700 x g for 30

minutes at room temperature. Cells were then isolated from the lower layer of 40% Percoll, placed in a fresh falcon. Samples were then washed in complete mouse media and centrifuged for 5 min at 250 x *g* at 4°C. Cells were kept on ice until use.

2.5.7 CD4+ T lymphocyte purification from primary cell suspensions

In order to use a pure population of cells, murine tissues including spleen and multiple lymph nodes including axillary, inguinal and mesenteric lymph nodes were used as prepared.

For positive selection of CD4+ lymphocytes total cell suspension were mixed with CD4+ magnetic beads (Miltenyi) according to manufacturers instructions. Briefly, cell preparations were centrifuged at 250 *x g* for 10 min, the supernatant was removed and 10µl CD4 magnetic beads + 90µl MACs buffer (1xPBS/ 1% FBS/ 2mM EDTA) was added per 10^7 total cells, mixed well and incubated on ice for 30 min. Samples were washed in 40ml MACs buffer and centrifuged for 5 min at 250 *x g*. Labeled cells were resuspended in MACs buffer and positively selected using magnetic separation using autoMACs machine (Miltenyi). Cells were counted and placed on ice until use. Purity of CD4 cells after positive selection was checked by flow cytometry, purity was always >80%.

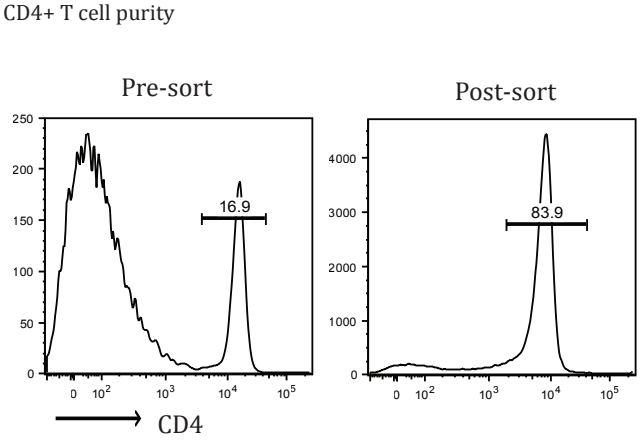

Figure 2.2 CD4+ lymphocyte purity after magnetic purification

CD4+ T lymphocyte purity assessed by CD4 surface staining by flow cytometry.

2.6 Cell culture

2.6.1 Culture of mammalian cell lines

2.6.1.1 RAW264.7 macrophage cell line

Cells were kindly obtained from Simon Arthur laboratory (Cell signaling and Immunology, University of Dundee). Cells were cultured in DMEM media (Invitrogen) supplemented with 10% (v/v) heat-inactivated FBS, 50 units/ml penicillin and 50 μg/ml streptomycin. Cells were cultured at 37°C, 5% CO_2 at 90% humidity and maintained at 70% confluence, according to ATCC guidelines. When 70% cell confluence was reached, cells were scraped into suspension using a cell scraper and flushed to harvest. Cells were split into 1:3 or 1:6 suspensions with media refreshed every 2 days.

2.6.1.2 K562 human CML cell line

Cells were kindly obtained from David Meek laboratory (Division of Cancer Research, University of Dundee). Cells were cultured in RMPI media supplemented with 10% (v/v) heat-inactivated FBS, 50 units/ml penicillin, 50 μg/ml streptomycin and 2mM l-glutamine. Cells were cultured at 37°C at 5% CO2 and maintained at $1x10^6$/ml and the media was renewed every 2-3 days, according to ATCC.

2.6.1.3 Freezing of cell lines

All cell lines were frozen at $5x10^6$ or $10x10^6$ total cells in cyrovials suspended in FBS with 5% (v/v) DMSO (Sigma). Cells were frozen in Mr. Frosty containers at -80°C for 24 hrs. Vials were then transferred to liquid nitrogen containers and stored in liquid nitrogen vapor phase.

2.6.2 Primary cell culture

2.6.2.1 Bone marrow derived macrophages (BMDMs)

Isolated bone marrow cells were resuspended in 20ml DMEM media (Invitrogen) medium supplemented with 10% (v/v) heat-inactivated FBS , 50 units/ml penicillin, 50 µg/ml streptomycin and further supplemented with 10ng/ml macrophage-colony stimulating factor (M-CSF) (R&D systems, Oxford, UK). Cells were cultured for 6 days at 37°C at 5% CO_2 and were supplemented with fresh media containing M-CSF on day 3. Macrophages were harvested on day 6 of culture.

2.6.2.2 Bone marrow derived dendritic cells (BMDCs)

Isolated bone marrow cells were resuspended at a cell density of $1x10^7$/ml. 200µl ($2x10^6$ total) of this suspension was added to the middle of non-tissue treated 10cm plates containing 10ml of RPMI media supplemented with L-glutamine (Invitrogen), 10% (v/v) heat-inactivated FBS, 50 units/ml penicillin (Sigma), 50 µg/ml streptomycin, 50 µM 2-βmercaptoethanol and 10ng/ml granulocyte macrophage colony stimulating factor (GM-CSF) (Peprotech, London, UK). Cells were cultured for 10 days at 37°C at 5% CO_2 and given fresh media containing 10ng/ml GM-CSF on days 3, 6 and 8. BMDCs were harvested on day 10 of culture.

2.6.2.3 Harvesting adherent primary myeloid cells

Unless otherwise stated, cells were harvested by aspirating media and incubating 5ml sterile 2mM EDTA/PBS @ 37°C for 10 min to loosen cell adhesions (Invitrogen). Cells were then flushed up and down repeatedly using a pipette aid to harvest, centrifuged for 5 min at 250 x g. Cells were then counted using a hemocytometer and resuspended at required density in 6, 12 or 24-well non-TC treated plates (BD).

2.7 Stimulation and inhibiton of various cells

2.7.1 Cell lines

2.7.1.1 RAW264.7 macrophage cell line

Cells were harvested by gentle cell scraping, counted and resuspended at required density. For protein samples cells were plated at either $5x10^6$/ml in 12-well tissue culture plates, or $2.5x10^6$/ml in 2ml in 6-well tissue culture plates and allowed to settle for 3 hr before stimulation. For cytokine analysis cells were plated at $1x10^6$/ml in 2ml per well. For phospho-flow analysis cells were plated at $0.5x10^6$/ml the night before and stimulated the following morning.

2.7.1.2 K562 CML cell line

Cells were harvested, counted and resuspended at required density. For protein samples cells were plated at either $5x10^6$/ml or $7x10^6$/ml in 12-well tissue culture plates and allowed to settle for 3 hr before stimulation. For phospho-flow and cell cycle analysis cells were plated at $0.2x10^6$/ml or $0.5x10^6$/ml the night before and stimulated the next morning.

2.7.2 Primary cells

2.7.2.1 Lymph node cells

Lymph nodes were dissected and prepared as previously described. Cells were resuspended to $5x10^6$/ml and plated in 12- or 24-well tissue culture plates. Cells were allowed to settle for 4 hrs at 37°C at 5% CO_2 before stimulation.

2.7.2.2 BMDMs and BMDCs

For protein analysis cells were seeded at either $5x10^6$/ml or $7x10^6$/ml in 12-well non-tissue cultured plates (BD) and allowed to settle for 4 hr before stimulation. For flow cytometry and cytokine analysis cells were plated at $2x10^6$/ml in 2ml in 6-well non-tissue culture treated plates (BD) and starved of M-CSF and GM-CSF overnight before stimulation.

2.7.2.3 Co-culture of CD4+ OT II+ T cells with OVA-loaded BMDCs

BMDCs were generated *in vitro* as previously described from WT and $PKD2^{KI/KI}$ bone marrow. BMDCs were then counted and resuspended complete mouse medium supplement with GM-CSF (10ng/ml) at $2x10^6$ cells per ml and stimulated with or without LPS (100ng/ml) overnight. Cells were harvested the following morning with 4mM EDTA in 1xPBS and loaded with 1µM OVA-peptide, which encompasses an allergenic and antigenic epitope of the ovalbumin protein a I-A(d) MHC class II protein (peptide sequence - SQAVHAAHAEINEAGR) (Anaspec, Fremont, California, USA) and incubated for 90 min. BMDCs were then harvested, counted and resuspended at $0.2x10^6$ cells per ml. BMDCs were then mixed 1:10 with purified CD4+ T lymphocytes obtained from OT II+ mice as previously described and co-cultured for in 24-well plates. Samples were taken every 24 hours for flow cytometry analysis and supernatant was obtained for downstream ELISA application.

2.8 Detection of protein by immunoblotting

2.8.1 Lysis buffers

The following lysis buffers and conditions used depending on cell type to extract soluble proteins are detailed below in Table 2.5. Protease inhibitors were added fresh to lysis buffers before use. Protease inhibitors used are described Table 2.6.

Cell type	Lysis buffer	Cell density
Bone marrow derived dendritic cells	Low salt lysis buffer	$70x10^6$/ml
Bone marrow derived macrophages	NP-40 lysis buffer	$70x10^6$/ml
RAW264.7 cell line	Np-40 lysis buffer	$50\text{-}70x10^6$/ml
K562 human CML cell line	Low salt or RIPA buffer	$50\text{-}70x10^6$/ml
T lymphocytes	F lysis buffer	$100x10^6$/ml
Spleen lymphocyte preparations	F lysis buffer	$100x10^6$/ml
Lymph node lymphocyte preparations	F lysis buffer	$100x10^6$/ml

Table 2.5 Various lysis buffers used in the preparation of cell lysates and final cell density after lysis.

Protease inhibitor	Stock concentration	Final concentration	Solvent	Inhibition of
Leupeptin	5mg/ml	2µg/ml	Water	Cysteine and serine proteases
PMSF	100mM	1mM	Isopropanol	Serine proteases
Pepstatin A	1mg/ml	1µg/ml	Methanol	Aspartic proteases
Na_3VO_4	200mM	1mM	Water	Phosphotases

Table 2.6 Protease inhibitors used in cell lysis buffers

2.8.2 Lysis of cells for protein immunoblotting

2.8.2.1 Suspension cells

After treatment cells were harvested into 1.5ml eppendorfs and centrifuged for 5 min at 250 x g at 4°C. Cell pellets were then washed in 1ml ice cold PBS and centrifuged again for 5 min at 250 x g. Samples were then either snap frozen in liquid nitrogen or lysed in appropriate volume of chosen lysis buffer and protease inhibitors as described in for 30 min on ice with occasional vortexing. Samples were then centrifuged for 20 min at 500 x g at 4°C. The supernatant was removed carefully to avoid disrupting the pellet and placed in fresh eppendorfs. 1 x laemelli buffer supplemented with 1:20 2β-mercaptoethanol was finally added and samples were boiled for 10 min at 100°C. Samples were subsequently stored at -20°C until use.

2.8.2.2 Adherent cells

After stimulation or treatments, cells were harvested by gentle aspiration of media and addition of 1ml per well of ice cold PBS. Cells were harvested into 1.5ml eppendorfs by gentle pipetting and centrifuged for 5 min at 250 x g at 4°C. Samples were either snap frozen in liquid nitrogen or lysed in appropriate volume of chosen lysis buffer and protease inhibitors (table) for 30 min on ice with occasional vortexing. Samples were then centrifuged for 20 min at 500 x g at 4°C. The supernatant was removed carefully to avoid disrupting the pellet and placed into fresh eppendorfs. 1 x laemelli buffer supplemented with 2β-mercaptoethanol was added and samples were boiled for 10 min at 100°C. Samples were subsequently stored at -20°C until use.

2.8.3 Resolution of protein samples on SDS polyacrylamide gel electrophoresis

For western blotting, 30µl of sample for 1.5mm 10 well pre-cast 4-12% gradient gels (Life technologies) or 15µl of sample for 1.0mm 12 well pre-cast 4-12% gels. For each gel 5µl of molecular weight seeblue® prestained marker (Life technologies) was loaded. Pre-cast gels were run with 1X MES buffer (Life technologies) using . Gels were then electrophoresed at 150V for 80-100 min depending on protein size. Proteins were then transferred onto PVDF membrane (Millipore, Seltham, UK)

2.8.4 Transfer of proteins onto PVDF membrane for immunoblotting

Invitrogen life technologies transfer cell modules were used to transfer proteins from the SDS-PAGE gel onto polyvinylidene fluoride (PVDF) membrane (Merek, Millipore). All materials were pre-soaked in transfer buffer (Invitrogen - life technologies) prior to assembly of transfer module. The transfer module comprised of 2 sponges, 2 x 8cm by 8cm 3mm Whatman filter paper (Sigma), the SDS page gel, one 7.5cm by 8cm PVDF membrane (pre-activated by soaking in 100% methanol for 5 min), 2 x 8cm by 8cm Whatman filter paper and 2 further sponges. The module was then filled with transfer buffer. The proteins were transferred at 35V for 1-2 hr depending on protein size.

2.8.5 Western blot antibodies and conditions

Following transfer of proteins onto PVDF membrane protein loading was checked by staining the membrane with Ponceau solution (Sigma) for 5 min and washed in de-ionised water. Membranes were then blocked with 5% (w/v) dried milk (Marvel) in PBS-Tween buffer for 1 hr on a shaker at room temperature. Membranes were then incubated with primary antibody diluted 1:100 or 1:500 in either 5% dried milk/PBS-Tween or 2% BSA/ PBS-Tween as described in

tables (Table 2.7 and Table 2.8). Unbound primary antibody was removed by washing the membrane with PBS-Tween for 3x 5 min shaking, after which membranes were then incubated with appropriate species horseradish peroxidase (HRP) conjugated secondary antibody (company) diluted either 1:10,000 or 1:5000 in either 3% dried milk in PBS-Tween or PBS-Tween only. Various antibodies used to detect both endogenous and phosphorylated proteins are described in Table 2.7. Specific antibodies used to detect PKD isoforms, both endogenous and phosphorylated are detailed in Table 2.8

Antibody	**Species**	**Company**	**Order number**
Pan-AKT	Rabbit	Cell Signaling Technologies	9272S
Phospho- AKT (473)	Rabbit	Cell Signaling Technologies	9272S
β-Tubulin	Mouse	Santa Cruz	SC 5274
Phospho p.38 (T180/Y204)	Mouse	Cell Signaling Technologies	9216S
Phospho ERK1/2 (T202/Y204)	Mouse	Cell Signaling Technologies	9106S
Total ERK1/2 (P44/p42)	Mouse	Cell Signaling Technologies	9102S
Phospho HDAC 4-5-7	Rabbit	Cell Signaling Technologies	3424S
Ικβα (NFKB)	Mouse	Cell Signaling Technologies	9247S
p-105 NFκB Ser933 site	Rabbit	Cell Signaling Technologies	4806S
Phospho-STAT3 (XP)	Rabbit	Cell Signaling Technologies	9145S
Phospho-STAT5 (XP)	Rabbit	Cell Signaling Technologies	4322S
Phospho-S6 (Ribosomal)	Rabbit	Cell Signaling Technologies	2211S

Table 2.7 Cell signaling western blot antibodies

Antibody	Species	Isoform specificity	Company	Order number
Phospho PKD Serine916	Rabbit	PKD1 PKD2	Raised in house	N/A
Phospho PKD Serine 744/748	Rabbit	PKD1 PKD2 PKD3	Cell Signaling Technology	2054S
Phospho PKD Tyrosine 643	Rabbit	PKD1 PKD2	Abcam	AB59415
PKD total	Rabbit	PKD1 PKD2 PKD3	Raised in house	N/A
PKD2 total	Rabbit	PKD2	Calbiochem (Merck Millipore)	ST1042
PKD3 total	Rabbit	PKD3	Bethyl	A300-319A

Table 2.8 Antibodies used to detect PKD isoforms by western blotting

2.9 Flow cytometry

Flow cytometric data was obtained using either an LSR II Fortessa, Canto or Verse (BD). All flow cytometry data was analysed using FlowJo data analysis (Tree star inc).

2.9.1 Flow cytometry solutions

FACS buffer	1 x PBS 2% FBS/BSA

2mM EDTA

Fixation and permeabilisation buffers (eBioscience)

2.9.2 Determination of cell number by flow cytometry

Murine tissues were prepared as stated and their cell number determined by making a 1:10 dilution. Live/dead cells were counted by adding 500µl of PBS supplemented with 50µg/ml DAPI and analysis of cell populations by forward light scatter (FSC) and side scatter (SSC) identifying live cells as a DAPI negative population. Cell counting was performed on BD FACS Verse and cells per ml number was achieved by the following calculation:

Cells/volume * 1000

Total cell number per tissue was then achieved by the following calculation:

Cells per ml * dilution factor * total volume

2.9.3 Compensation controls

All flow cytometry experiments, unless stated otherwise, were performed with compensation controls to correct for spectral overlap in multi-colour and multi-parameter experiments. This included a no stain control and single stained samples for all fluorophores used in the experiment. With the use of tandem dyes the same antibody was used for compensation as used in the experiment. Where non-tandem dyes were used compensation controls were picked to ensure a negative and positive population was present in the stained control. For intracellular staining, including phospho-flow, compensations were also fixated and permeabilised to ensure the same FSC and SSC profiles as experimental samples.

2.9.4 Surface staining

To pellet cells samples were placed in FACS tubes (BD) and spun down at 250 x g in a chilled 4°C centrifuge. The supernatant was poured off and samples were resuspended in Fc blocking solution (eBioscience), this step is necessary to block the binding of antibodies to the FcγR present on cell surfaces which can result in non-specific antibody binding. All samples were incubated with FcγR antibody for 20 min on ice prior to staining. Surface staining was performed using the relevant antibodies at previously determined saturating concentration as described in table (Table 2.9 and Table 2.9). Staining was performed for 20 min on ice in the dark. Cells were washed in FACS buffer and resuspended in FACS buffer before acquisition on stated flow cytometer. A minimum of 10,000 events were collected and stored un-gated after which the data was analysed on FlowJo. Live cells were gated by FSC/SSC profiles and live cells were further confirmed by being DAPI negative.

2.9.5 Detection of Treg populations by intracellular flow cytometry

Age and sex matched mice were sacrificed at 6-8 weeks of age unless otherwise stated. Tissues were dissected and prepared as described, 5-10x10^6 cells were used per mouse per tissue and centrifuged at 250 *x g* for 5 min at 4°C. 5x10^6 cells were used per tissue for compensation controls. Samples were FcγR blocked (eBioscience) 1:70 for 20 min on ice. Samples were then surface stained for CD4-PE-CY7, CD25 –APC-CY7 or CD25 -PerCPCy5.5, and CD103-PE for 30 min on ice concealed from light. Samples were washed in 1ml FACS buffer and centrifuged at 250 *x g* for 5 min at 4°C. Samples were then resuspended fixation/permeabilisation buffer (FoxP3 specific buffer in kit - eBioscience) and incubated at 4°C overnight or for 1 hr at room temperature. Samples were centrifuged at 250 *x g* for 5 min and supernatant was removed. Samples were vortexed and resuspended in 100µl 1x permeabilisation buffer (provided in kit) with FoxP3-APC antibody diluted 1:100. Cells were stained with FoxP3 antibody for 45 min at 4°C in the dark. Samples were washed in 2ml 1x permeabilisation buffer and centrifuged at 250 *x g* for 5 min. Supernatant was removed, samples

were vortexed, resuspended into 300µl FACS buffer and acquired on either BD Canto or BD Fortessa.

2.9.6 Analysis of phospho-proteins by flow cytometry

For analysis of phospho proteins by flow cytometry cells were plated and settled overnight. After stimulation all reagents were kept on ice unless otherwise stated. Unless otherwise stated all experiments contained a negative unstimulated control and a positive control. Depending on the experiment 1-5x10^6 cells were used per sample. For adherent cells the media was immediately aspirated and cells were placed in 200µl of cold IC fixation buffer supplemented with various protease inhibitors including leupeptin, pepstatin and sodium orthovanadate. Cells were then harvested by vigorous pipetting. Cell scraping was never used during phospho flow analysis as it affects the cells FSC and SSC profiles dramatically. For cell suspensions 1:1 volume of cold IC fixation buffer was directly added to the media and cells were harvested into FACS tubes. Cells were fixed for 20 min on ice.

2.9.6.1 Analysis of phospho PKD (p. SER916) and phospho ERK1/2 (p. ERK1/2)

After cells were fixed cells were centrifuged, the supernatant removed and 1ml ice-cold 90% methanol was added whilst vortexing. Samples were permeabilised for 30 min on ice and washed twice with 2ml FACS buffer and centrifuged at 250 *x g* for 5 min at 4°C. Samples were FcγR (blocked for 20 min on ice and stained with either both p-SER916 rabbit antibody used at 1:1000 and p-ERK mouse antibody 1:200 for 30 min at room temperature. Samples were washed twice with FACS buffer and centrifuged at 250 x g for 5 min. Secondary antibodies including anti-rabbit Alexafluor 488 and anti-mouse Alexafluor 647 both used at 1:500 for 30 min at room temperature and concealed from light. Finally cells were washed twice with FACS buffer and acquired on either BD Fortessa or BD Canto.

2.9.6.2 Analysis of phospho STAT5

After cells were fixed cells were washed with 2ml FACS buffer and centrifuged at 250 *x g* for 5 min at 4°C. The supernatant was discarded and 1ml ice cold 1:1 acetone: methanol solution was added whilst vortexing. Samples were either permeabilised for 30 min on ice or overnight at -20°C. Samples were washed twice with 4ml 1xPBS 5% FBS. Samples were FcγR blocked with CD16/32 antibody (Biolegend) for 20 min at room temperature. Samples were then stained with pSTAT5- PE antibody (BD) used at 1:50 for 30 min at room temperature and concealed from light. Finally samples were washed twice with 2ml 1xPBS 5% FBS and acquired on BD Canto.

2.9.7 Analysis of IFNAR1 surface and intracellular expression in K562 CML cells

Chronic myeloid leukemia cells are documented within the literature to display abnormal amounts of intracellular expression of the IFN-α receptor due to enhanced down-regulation from the cell surface. To analyse the effects of PKD inhibitors on the up-regulation of the IFN- α receptor both surface staining and intracellular staining was performed.

2.9.7.1 Surface

$5x10^6$ cells were treated and centrifuged for 5 min at 250 *x g* at 4°C. Samples were then FcRγ blocked for 20 min and stained with an anti-IFN-α receptor human rabbit monoclonal (Abcam, Cambridge,UK) for 30 min on ice. Samples were washed in 1ml FACS buffer and centrifuged. Cells were then stained with 1:500 anti-rabbit AlexaFluor 488 for 30 min at room temperature concealed from light. Finally cells were washed in 2ml FACS buffer and acquired

on BD Canto. Either 20µg/ml DAPI or ToPRO(Invitrogen, Life Technologies) was added to discriminate between live/dead cells.

2.9.7.2 Intracellular

For intracellular detection $5x10^6$ cells were centrifuged at 250 *x g* and resuspended in 200µl of IC fixation buffer (eBioscience) for 20 min at room temperature. Cells were washed in 2ml FACS buffer, cells pelleted and resuspended in 1x permeabilisation (eBioscience) buffer supplemented with FcγR block (eBioscience) and incubated for 20 min at room temperature. Anti-human IFN-α receptor antibody was diluted 1:30 in 1x permeabilisation buffer and 100µl was added per sample and stained for 30 min to 1 hr at room temperature. Cells were washed and resuspended in 1:500 anti-rabbit Alexafluor 488 (Invitrogen Life Techonologies) and stained for 30 min at room temperature concealed from light. Samples were washed in 2ml FACS buffer and acquired on BD Canto.

2.9.8 Analysis of cell cycle by propidium iodide

K562 cells were harvested, their cell number determined and resuspended at required density. For cell cycle analysis, cells were plated at $0.2x10^6$/ml in 24-well tissue culture treated plates and incubated overnight to ensure cells were actively cycling after seeding. Cells were then treated with increasing concentrations of PKD inhibitors, DMSO was used as a vehicle control and media only samples were including as negative controls. Cell cycle was analysed at the following time points; 2, 4, 6, 7 and 8 hr. After treatment cells were harvested into FACS tubes and centrifuged at 250 *x g* for 5 min at 4°C. The supernatant was poured off and cells were gently resuspended by flicking the bottom of the tubes. Cells were suspended in 1ml ice cold 70% ethanol whilst gently vortexing to prevent clumping of cells. Cells were fixed for at least 30 min room temperature or stored at -20°C for up to 4 weeks. Cells were adjusted to $5x10^6$/ml and washed in twice in 1x PBS + 1% v/v FBS. Cells were then pelleted and resuspended in 300-500µl staining buffer which consisted 50µg/ml

propidium iodide (company) and 50µg/ml ribonuclease A in 1x PBS + 1% FBS. Cells were incubated at room temperature and concealed from light for 20 min before acquisition on BD Canto.

2.9.9 Flow cytometry antibodies and their conjugates

Antibody	**Clone**	**Fluorophore**	**Company**
CD4	RM45	PE-Cy7	Biolegend
CD4	RM45	PE	Biolegend
CD4	H129.19	FITC	BD
CD8α	53.6.7	APC- Cy7	eBioscience
CD8α	53.6.7	PerCP Cy5.5	eBioscience
CD8β	eBioH35-17.2	APC	eBioscience
CD11b	M170	APC	Biolegend
CD11b (Integrin αM)	M170	PerCP Cy5.5	Biolegend
CD11c (Integrin αX)	HL3	Pe-Cy7	BD
CD16/CD32 (Fc receptor γ block)	93	N/A	Biolegend
CD19	6D5	APC-Cy7	Biolegend
CD19	6D5	FITC	Biolegend
CD21	7G6	FITC	BD
CD23 (FcεRII)	B2B4	PE	BD
CD25 (IL-2Rα)	PC61	APC-Cy7	Biolegend

CD25 (IL-2Rα)	PC61	PerCP-Cy5.5	Biolegend
CD40	312.3	PE-Cy7	Biolegend
CD44	IM7	PE	BD
CD45	30F11	APC-Cy7	Biolegend
CD45	30F11	APC	Biolegend
CD45	30F11	PE-Cy7	Biolegend
CD45	30F11	PerCP Cy5.5	Biolegend
CD45	30F11	PE	eBioscience
CD45	30F11	FITC	eBioscience
CD69	H1.273	PE	eBioscience
CD45R	RA3-632	PE-Cy7	Biolegend
CD45RB	C363.16A	FITC	eBioscience
CD80	16.10.A1	APC	eBioscience
CD86	GL1	FITC	eBioscience
CD103 (Integrin – αE)	2E7	PE	eBioscience
CD127 (IL-7Rα)	SB-199	PE	Biolegend

Table 2.9 List of CD flow cytometry antibodies and their conjugates

Antibody	Clone	Fluorophore	Company
B220	RA3-632	PerCP-CY5.5	Biolegend
B220	RA3-632	PE	eBioscience
B220	RA3-632	FITC	BD
B220	RA3-632	APC	eBioscience
F4/80	BM8	PE	Biolegend
FoxP3	FJK16S	APC	eBioscience
Ly6-C	1G7.G10	APC	Miltenyi Biotec
Ly6-G	RD6-85C	FITC	eBioscience
GL-7 (Ly-77)	GL-7	FITC	BD
MHC class II (I-A/I-E)	M5/114.15.2	APC-Cy7	Biolegend
p-STAT5	47	PE	BD PhospFlow
Siglec-H	eBio440c	FITC	eBioscience
TCR αβ	H57-597	APC	BD
TCR αβ	H57-597	PE	eBioscience
TCR αβ	H57-597	PerCP - Cy5.5	eBioscience
TCRγδ	GL3	APC	Biolegend
TCRγδ	GL3	PE	BD
Thy1.1	53.2.1	APC	Biolegend

Table 2.10 List of non-CD antibodies used and their conjugates

2.10 Enzyme Linked Immunosorbant Assay (ELISA)

2.10.1 Reagents and solutions

ELISA coating buffer	1x PBS
ELISA blocking and diluting buffer	1xPBS 2% BSA
Wash buffer	1xPBS-Tween
Substrate solution	TMB solution (eBioscience)
Stop solution	1M H_2SO_4

2.10.2 ELISA procedure

2.10.2.1 Sample preparation

After treatment cells were collected in 2ml eppendorfs and centrifuged for 5 min at 250 *x g* at 4°C. Supernatants were then transferred into fresh eppendorfs and stored in aliquots to prevent freeze thawing.

2.10.2.2 Sandwich ELISA

For analysis of cytokine production 96-well plates were coated with the antibodies described in Table 2.11. All coating antibodies were used at 1:1000 as per manufacturers instructions in 1x PBS and 100µl was used per well coating immuno maxisorp 96-well flat-bottomed plates (Thermo Scientific, Leicestershire, UK) and incubated at 4°C overnight. Plates were washed three times in PBS-Tween and non-specific binding was removed by blocking plates with 200µl 2% BSA in PBS per well. Samples were mixed thoroughly and diluted in 2% BSA/PBS-Tween and specific cytokine standards were also plated. Plates were incubated overnight at 4°C, after which they were washed in PBS-Tween repeatedly. Cytokine specific biotin-conjugated antibodies (same as primary antibody but biotin conjugated) were diluted 1:1000 with 2%BSA/PBS-Tween

and incubated at room temperature for 2 hr rocking. Plates were then washed three times in PBS-Tween and incubated with anti Avidin-HRP (eBioscience) diluted in 2%BSA/PBS-Tween 1:1000 for 1 hr at room temperature with gentle rocking. Plates were then washed a final 5 times in PBS-Tween and 100µl 1xTMB substrate (eBioscience) was used per well for detection. Plates were allowed to develop for 5-10 min until standards were developed to a similar level to experimental samples. The reaction was stopped using 50µl 2M sulphuric acid per well, initiating a colour change from blue to yellow. Plates were then read at 450nm on microplate spectrometer. Cytokine production was determined using the relevant recombinant mouse cytokine standard curve.

2.10.2.3 ELISA antibodies

Capture antibody	Clone	Dilution	Company
IFN-γ	AN-18	1:1000	eBioscience
TNF-α	1F3F3D4	1:1000	eBioscience
IL-2	78071	1:1000	Biolegend
IL-6	MP5-20F3	1:1000	eBioscience
IL-10	JES5-16E3	1:1000	eBioscience
IL-12p40 subunit	C15.6	1:1000	Biolegend

Table 2.11 Capture antibodies used in ELISA assays

2.10.2.4 Cytokine standards

Murine TNF-α, IFN-γ, IL-6 and IL-10 standards were purchased from eBioscience. Murine IL-2 and IL-12p40 standards were purchased from Biolegend. All standards were stored and used according to manufactures instructions, standards were always used fresh and diluted in 1% BSA/PBS. To create a standard curve standards were diluted two fold.

2.11 *In vivo* colitis model

2.11.1 Cell sorting for naïve T cells and Treg populations

Spleens from age and sex matched WT and PKD2 $^{KI/KI}$ mice were dissected and prepared as previously described. Cells were then purified for CD4+ lymphocytes using a CD4 isolation kit (Miltenyi) according to manufacturers instructions. Briefly, cell number was determined and cells were centrifuged for 10 min at 300 *x g.* 400µl MACs buffer + 100µl of biotin antibody cocktail was added per 10^7 cells, mixed well and incubated for 5 min at 4°C. Next 300µl MACs buffer plus 200µl of anti-biotin beads were added, mixed well and incubated for 10 min at 4°C. Cells were then sorted using an autoMACs machine (Miltenyi) using depletion. Cell number was determined and cells were Fc blocked 1:70 before staining with the following antibody cocktail; CD4-PerCP-Cy5.5, CD25-APC, CD45RB-FITC, all diluted 1:100 in hanks buffered salt solution (HBSS) supplemented with 1% FBS. Cells were stained for 20 min on ice and washed in 4ml HBSS before centrifuging at 250 *x g* at 4° C for 5 min. Cells were finally resuspended in HBSS/1% FBS and filtered through 50µm filcons (BD) into cell sorting tubes. Naïve T cells were sorted by definition of CD4+ CD25- CD45RB ^{high} whereas regulatory T cells were defined as CD4+ CD25+ CD45RB-. Cells were collected into sterile RMPI media supplemented with 20%FBS and 50 units/ml penicillin.

2.11.2 Intraperitoneal injection of lymphocytes into RAG2$^{KO/KO}$ hosts

For this study 20 male homozygous RAG2$^{KO/KO}$ mice were used and split into 4 groups of n= 5 per group. Cells transferred into each group are detailed in table (Table 5.1). All mice had body weight recorded on day 0 before cells were injected. Sorted cells were injected into the peritoneal cavity using 29g 1ml insulin needles (Terumo, Somerset, UK).

2.11.3 Analysis of body weight

Mice were weighed weekly until signs of illness appeared after which point they were then weighed and monitored daily. When mice lost 20% of their total body weight they were sacrificed using CO_2.

2.11.4 Generation of tissue sections and Hematoxylin and Eosin (HE) staining

Samples including sections of the mesenteric lymph nodes were taken ex-vivo from age and sex matched mice and collected in 10% neutral buffered formalin. Tissue samples were then embedded in paraffin blocks, sliced into 4µm thick sections which were subsequently stained using Hematoxylin and Eosin (HE) and assessed microscopically by a pathologist.
The University of Glasgow Veterinary Diagnostic Services kindly provided these services; pathologist Dr Francesco Marchesi assessed microphotographs.

2.11.5 Colitis scoring

Briefly, lesions were assessed with a multi-parametric grading system consisting of a modified version of previously reported colitis score systems (Coccia et al. 2012) (Izcue et al. 2008). Grading was performed by two independent pathologists under blind assessment. Assessment and grading of histological changes used as indication of colitis severity are described below.

Colitis scoring parameters	Score
Histological changes	
Epithelial hyperplasia and goblet cell depletion	
Inflammatory cell infiltration within lamina propria	0 = no changes
Presence of crypt abscesses	1= mild
Mucosal erosion/ ulceration	2 = moderate
Submucosal to transmural inflammatory cell infiltration	3 = marked
PMNs infiltration	
	0 = absent
Number of neutrophils	1= low numbers
	2 = moderate numbers
	3 = large numbers
Extent of tissue affected	
Extent of tissue involved with epithelial and	0 = no change
inflammatory changes	1= <30%
	2 = 30-60%
	3 = >60%

Scores for all six parameters listed above were added to give a total

inflammation score for each individual section of 0–18. Finally, an overall colonic lesions score for each mouse was calculated as the average of the total scores from the sections of proximal and distal colon.

2.12 Real time - quantitative PCR (RT- qPCR)

2.12.1 RNA preparation, purification and quantification

$5x10^6$ cells were harvested and washed in 1ml ice cold PBS, centrifuged for 5 min at 250 *x g*. Cell pellets were lysed in 350µl RLT cell lysis buffer (Qiagen). Samples were then stored at -80°C until further use. For RNA purification samples were first homogenized whereby samples were transferred into cell shredders (Qiagen) and centrifuged for 1 min at 1300 x g. Resulting lysates were prepared using RNA easy kit (Qiagen) according to manufacturers' instructions. RNA was eluted in 50µl of RNase free water. The eluted RNA was stored at -80°C until further use.

1µl purified RNA was measured using a nanodrop (Thermo Scientific) according to manufactures instructions. Absorbance was between at 260nm and 280nm and RNA sample concentration was determined by Nano drop software.

2.12.2 cDNA preparation by reverse transcription

1µg of isolated RNA was reversed transcribed to cDNA using qScript cDNA synthesis kit, which contained an optimised blend of random oligo (dT) primers and qScript reverse transcriptase, which is a mixture of engineered MML RT and a ribonuclease inhibitor protein. 1µg to 10pg total purified RNA was diluted into 15µl nuclease free water plus 4µl qScript reaction mix and 1µl of qScript reverse transcriptase per reaction (Table 2.12). cDNA was then amplified using thermo cycles described Table 2.13.

Reagent	1 x Volume
Nuclease-free water	10µl
qScript reaction mix (5x)	4µl
qScript Reverse Transcriptase	1µl
RNA	5µl
Total volume	15µl

Table 2.12 cDNA reaction master mix

Step	Temperature	Time	Cycles
1	22°C	5 min	1
2	42°C	30 min	1
3	85°C	5 min	1

Table 2.13 cDNA amplification cycles

2.12.3 RT-qPCR assay

Quantitative PCR was performed in 384 well-plate format (Bio-Rad, Hertfordshire, UK) using SYBR Green based detection (Takara, Saint-Germain-en-Laye, France) in a Bio-Rad CFX384 thermo cycler. Each reaction comprised of 14µl reaction containing 6µl of diluted template cDNA (15ng per well), 0.5µl (10µM) sense primer and 0.5µl (10µM) antisense primer, 7µl of SYBR Green supermix. Samples were heated to 95°C for 30 seconds and then underwent 49 cycles of 95°C for 1 second and 60°C for 25 seconds. This was followed by 95°C for 1 min, 65°C for 1 min then 0.5°C increments every 5 seconds to calculate a melt curve. Each reaction was performed in duplicate. CD45 was used for normalisation and relative mRNA levels calculated using the following equation:

$$\text{Relative mRNA expression} = 2^{(C_{t,\,CD45} - C_{t,\,GOI})}$$

Where 2 is primer efficiency, C_t is the threshold cycle, CD45 is the reference gene and GOI of gene of interest.

2.13 Statistical methods and analysis

All quantified data was processed in Microsoft Excel (Mac 2011). Statistical evaluation was performed in Prism 5 (Mac OS X). Prism was used to generate all bar and line graphs, dot plots and column graphs. Unless otherwise stated statistical tests used to determine significant differences were unpaired students T-test or where indicated one-way ANOVA with *post-hoc* Dunnet test or two-way ANOVA with Bonferroni *post-hoc* test. Differences were considered significant when $p \leq 0.05$.

For annotation purposes the following convention was used for significance:

ns = $p > 0.05$

* = $p \leq 0.05$

** = $p \leq 0.01$

*** = $p \leq 0.001$

**** = $p \leq 0.0001$

3 Charaterisation of new generation small molecule pharmacological inhibitors of the PKD family

3.1 Introduction

The PKD family has been implicated in multiple biological pathways and cellular processes including angiogenesis, proliferation, cell survival, cell motility and within various inflammatory pathways all of which are intricately linked to development and progression of cancer, and targeting PKD family members has become a particular focus for potential therapeutic target in cancer therapy through drug development. Within the current literature the focus on the therapeutic use of inhibition of PKD has focused largely on therapeutic use of PKD inhibition within pancreatic and prostate cancer cell lines (Wille et al. 2014) (Ochi et al. 2011) (Harikumar et al. 2010) (LaValle et al. 2012).

Previous inhibitors of PKD have had limited success *in vivo* largely due to poor bioavailability and numerous off target effects. New and highly specific small molecule inhibitors of PKD have since been developed and one compound has shown significant promise in an *in vivo* model of pancreatic cancer due to improvements in bioavailability (Harikumar et al. 2010). Significantly this potentially allows the movement of PKD inhibitors into clinical trials for the first time. However, more knowledge is required to determine the potential effects these inhibitors may have on the immune system if they are to be used as anti-cancer drugs.

Accordingly, this chapter describes data exploring the specificity of novel small molecule inhibitors of PKD derived through the use of *in vitro* kinase assay screening. This screening process importantly also revealed off target effects on other kinases demonstrated by all three compounds. Additionally, we wished to address if pharmacological inhibition of PKD with these novel inhibitors would correspond with data within the literature obtained by knockdown of PKD and indeed data observed from PKD transgenic mice. In regard to the therapeutic potential of using novel compounds to target PKD within malignant cells, we

chose to direct our studies towards examining the effects of these compounds on chronic myeloid leukemia (CML) cells as PKD2 has been specifically implicated in development and/or progression of CML, therefore potentially opening the exciting avenue for combinational therapies within CML via PKD inhibition.

3.2 Results

3.2.1 Characterisation of novel small molecule inhibitors of PKD via in vitro kinase screen analysis

Kinase inhibitors are powerful tools for the dissection of intricate signaling pathways, as well as being a strong focus of therapeutic interest within disease settings such as cancer and autoimmunity. In the past 10 years the U.S Food and Drug Administration (FDA) have approved 15 small molecular inhibitors and five anti-kinase antibodies for therapeutic use (Grant 2009). However, as many kinase inhibitors target the highly conserved ATP binding pocket, many inhibitors act on multiple kinases. As such, off target effects can often skew results and make the process of attributing an effect to a single kinase difficult.

With the development of new, more specific small molecule inhibitors of PKD we first sought to validate the specificity of these inhibitors for PKD and to assess off target effects on other kinases. To achieve this, inhibitors were screened using *in vitro* kinase assays against a panel of 124 protein kinases, including PKC isoforms (PKCα, PKCγ and PKCζ) and other CaMK family members. This is an important control as older PKD inhibitors have been shown also to target PKC activity (Gschwendt, Dieterich, et al. 1996a) (Grandage et al. 2006) (Meredith, Ardayfio, et al. 2010a).The protocol used, and substrate peptide sequences for assessing *in vitro* kinase activity have been described previously, samples were measured in duplicate (Bain et al. 2007). In order to remain consistent with the literature, a cut-off point of less than 20% remaining activity was chosen to define significant off target effects on other kinases (Bain et al. 2003). Full kinase screens of all three compounds can be see in Appendix B.

3.2.1.1 Novartis 12a compound

The 12a compound demonstrated significant inhibition of PKD1 (≤ 20% remaining activity) at 1μM concentration, shown in red in Figure 3.1. Other significant off target effects were observed including: MINK1, DYRK3, NUAK1 and CAMK1, percentage inhibitions and standard deviations are described in Table 3.1.

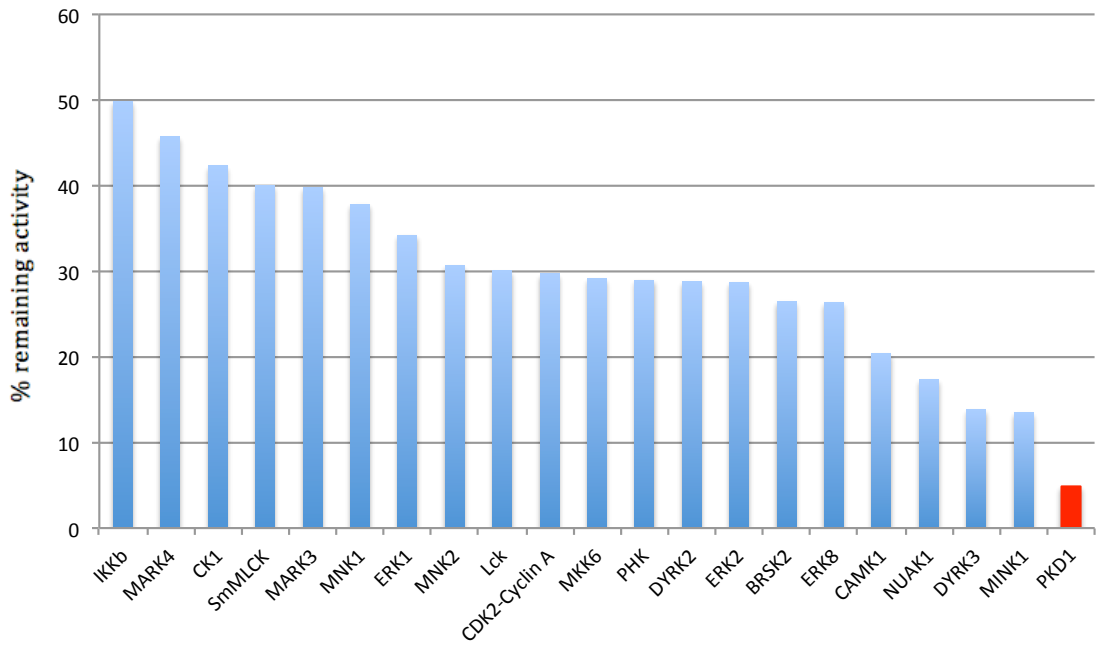

Figure 3.1 Kinase profile report for Novartis 12a compound screen at 1μM

5 out of 124 kinases screened were reduced ≤ 20% remaining activity in an *in vitro* kinase assay using a single dose of 1μM 12a compound (PKD1 is shown in red)

Kinase	12a 1μM % Activity remaining
PKD1	5
MINK1	13
DRYK3	14
NUAK1	17
CAMK1	20

Table 3.1 Kinase profile report for Novartis 12a compound screen at 1μM

5 out of 124 kinases included in *in vitro* kinase assay are reduced to ≤ 20% remaining activity with 1μM. of 12a compound.

Additionally, the 12a compound was also screened at a higher concentration of 10μM. As can be seen in Table 3.2 this greatly increased the occurrence of off target effects with 25/124 kinases significantly inhibited (≤20% remaining activity). Furthermore, this did not only increase off target effects it also produced greater inhibition of 5 kinases other than PKD at this concentration including CAMK1, MINK1, RSK1, PKBb and ERK8.

Kinase	12a 10μM
	% Activity remaining
CAMK1	2
MINK1	2
RSK1	2
PKBb	3
ERK8	4
PKD1	5
PHK	5
ERK2	6
MNK2	6
MNK1	7
DYRK3	7
BRSK2	8
Lck	9
SmMLCK	10
MARK4	10
ERK1	10
DYRK2	10
CDK2-Cyclin A	11
TSSK1	12
MARK3	15
MKK6	16
CK1	18
PRK2	19
AMPK	20
DYRK1A	21

Table 3.2 Kinase profile for Novartis 12a compound screened at 10μM

25 out of 124 kinases screened were reduced to less than 20% remaining activity in an in vitro kinase assay using a single dose of 10μM 12a compound.

3.2.1.2 CRT0066101 compound

The CRT0066101 (CRT101) compound screened at 1μM showed significant inhibition of PKD (Figure 3.2). Other kinases inhibited at this concentration included 9 out of 124 kinases tested including DYRK3, CLK2, PIM3, PIM1, ERK8, SIK2, CDK9-cyclin T1 and CDK9- cyclin A, percentage activity remaining and standard deviations are shown in Table 3.3. Importantly no significant inhibitions of PKC isoforms (including PKCα, PKCγ and PKCζ) were observed at this concentration. Interestingly, significant off target effects on serine/threonine protein kinase isoforms 1 and 2 (PIM1 and PIM3) may be explained by the 2-(4-aminopyridin-2-yl) phenol moiety in CRT101, which is also present in bi-substrate small molecular kinase inhibitors of PIM1(Ekambaram et al. 2013).

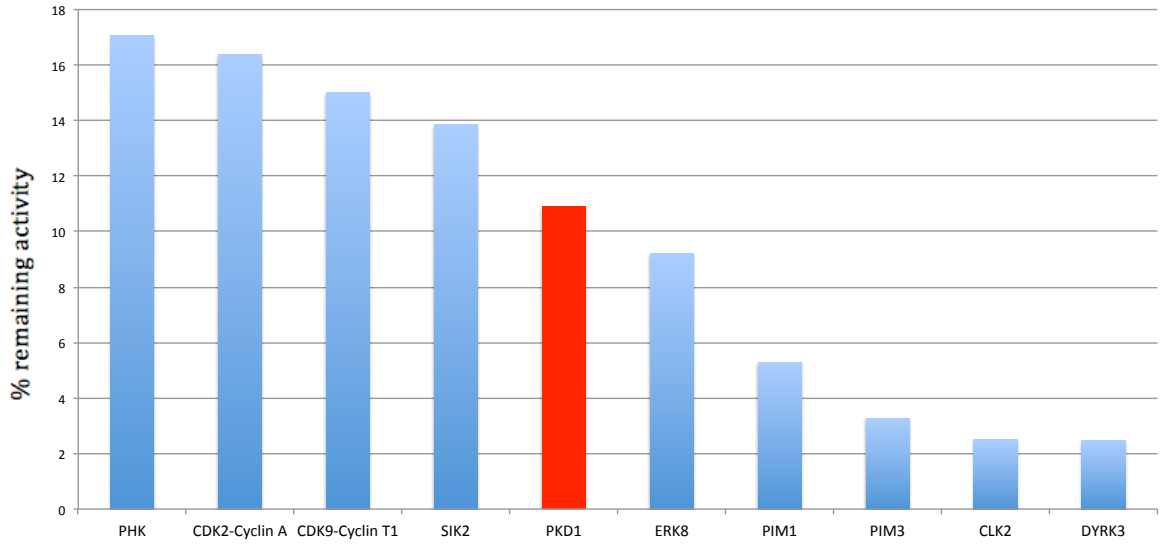

Figure 3.2 Kinase profile for CRT0066101 compound screen at 1μM

10 out of 124 kinases screened were reduced to less than 20% remaining activity in an *in vitro* kinase assay using a single dose of 10μM 12a compound. PKD1 is shown in red.

Kinase	CRT0066101 1μM % Activity remaining
DYRK3	2
CLK2	3
PIM3	3
PIM1	5
ERK8	9
PKD1	11
SIK2	14
CDK9-cyclin T1	15
CDK2-cyclin A	16
PHK	17

Table 3.3 Kinase profile for CRT0066101 compound screen at 1μM

6 out of 124 kinases screened were reduced to less than 20% remaining activity in an *in vitro* kinase assay using a single dose of 1μM CRT101 compound.

3.2.1.3 CRT0066051 compound

The CRT0066051 (CRT051) compound screened at 2.5μM showed significant inhibition of PKD shown in Figure 3.3. Other kinases inhibited at this concentration included 6 out of 124 kinases tested including GCK, BRK, MAP4K5, MAP4K3 and MINK1, percentage activity remaining and standard deviations are shown in Table 3.4. Importantly no significant inhibitions of PKC isoforms (including PKCα, PKCγ and PKCζ) were observed at this concentration.

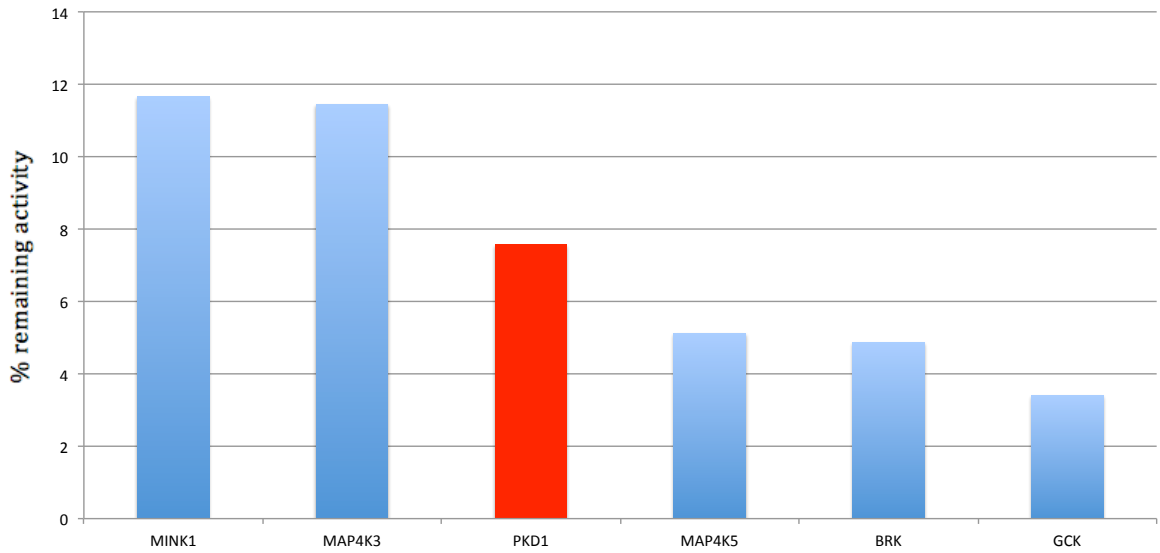

Figure 3.3 Kinase profile for CRT051 compound at 2.5μM

6 out of 124 kinases screened were reduced to less than 20% remaining activity in an *in vitro* kinase assay using a single dose of 2.5μM CRT051 compound.

Kinase	CRT051 2.5μM % Activity remaining
GCK	3
BRK	5
MAP4K5	5
PKD1	8
MAP4K3	11
MINK1	12

Table 3.4 Kinase profile for CRT051 compound at 2.5 μM

6 out of 124 kinases screened were reduced to less than 20% remaining activity in an *in vitro* kinase assay using a single dose of 2.5μM CRT051 compound.

3.2.2 Comparative analysis of off target effects of current PKD inhibitors

In order to distinguish between specific PKD inhibition and off target effects frequently found with small molecule inhibitors we compared off target effects seen with new compounds 12a, CRT101 and CRT051.

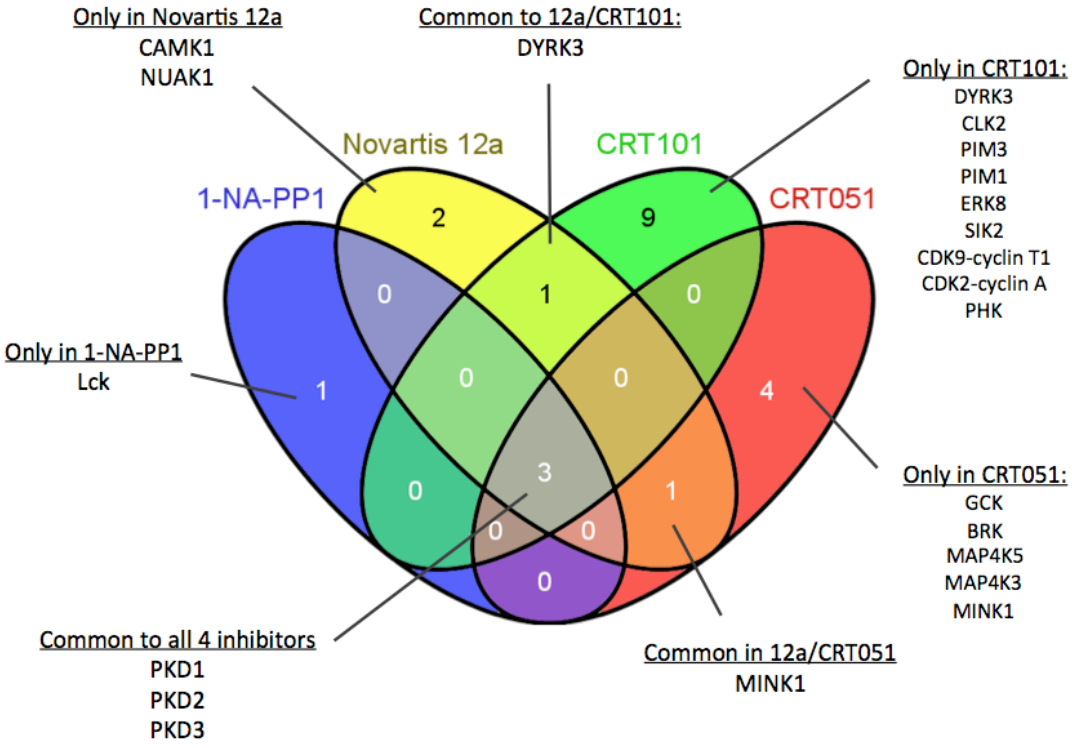

Figure 3.4 Comparative analyses of novel small molecular inhibitors of PKD and common off target effects

Shown are the protein kinases that are inhibited by >80% by indicated inhibitors in *in vitro* activity assays using purified kinases.

Using the kinase screen data obtained, we were able to compare specific kinase inhibition by our three novel PKD inhibitors as well as older generation inhibitors such as 1-NA-PP1. As illustrated in Figure 3.4, although each inhibitor does display off target effects on other kinases inhibition of PKD isoforms was the only common target of all 4 inhibitors. With these data we are able to confidently conclude that the effects seen with by all three PKD novel inhibitors are highly likely to be due to specific PKD inhibition and not to off target effects

on other kinases. In conclusion, these data demonstrate that inhibition of all three PKD isoforms is shown to be a common trait amongst the 4 small molecule inhibitors.

3.2.3 Pharmacological inhibition of PKD using new generation inhibitors reduce cytokine production in murine T lymphocytes

Having demonstrated that the three novel small molecule inhibitors are indeed highly specific for PKD and they do not share any of the same off-target effects, we next wanted to investigate if PKD inhibitors lead to biological consequences that would be expected from the loss of PKD activity. It has previously been shown that lack of PKD2 catalytic activity in T lymphocytes leads to significantly reduced cytokine production *in vitro* after TCR engagement (Matthews et al. 2010). Therefore we hypothesised that pharmacological inhibition of PKD should also led to reduced cytokine production from murine T lymphocytes after TCR triggering. To achieve this, T lymphocytes obtained from WT murine lymph nodes were pretreated with increasing concentrations of 12a, CRT101 and CRT051 for 1 hour before TCR triggering using anti-CD3. As can be seen in Figure 3.5A-B, treatment of T lymphocytes with the 12a compound lead to a 3 fold reduction in the production of key cytokines including IFN-γ and IL-2 after 24 hours after TCR triggering. Results with the CRT101 compound also lead to a significant reduction of both IL-2 and IFNγ in a more dose dependent manner (Figure 3.5C-D). The highest concentration used (5μM) of CRT101 lead to a 5-fold reduction of IL-2 and a 3 fold reduction in production of IFNγ. . Finally, we observed the same results with CRT051, with a significant dose-dependent reduction in cytokine production (Figure 3.5E-F); 10-fold reduction in IL-2 and 31-fold reduction in IFNγ respectively.

Importantly, this was not simply due to toxicity of increasing concentrations of 12a, CRT101 and CRT051 as minimal cell death was observed by propidium iodide (PI) staining when compared to DMSO vehicle controls (data not shown). Collectively, these data show that PKD inhibition mimics the biological effects observed by previously published data.

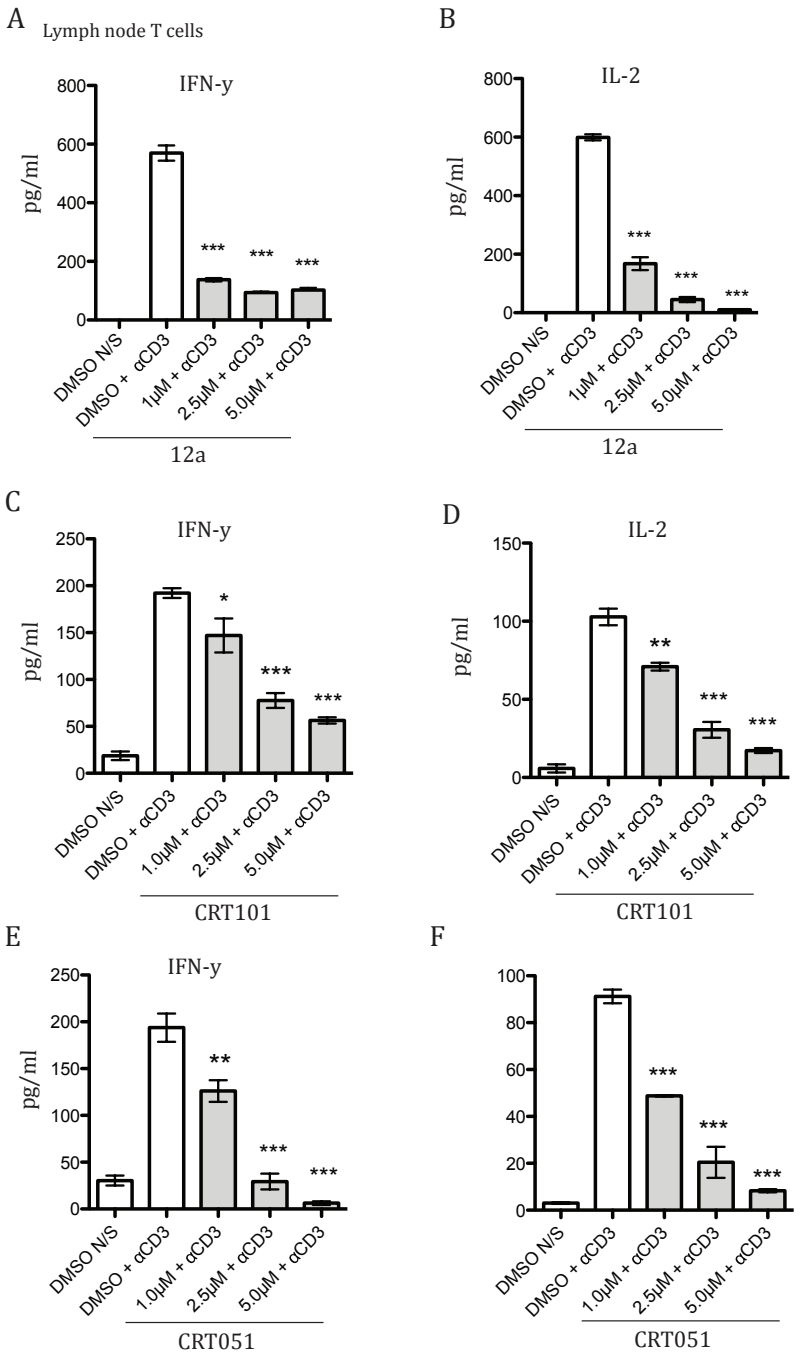

Figure 3.5 Effects of PKD inhibition on murine T cell cytokine production

Production of IFN-γ and IL-2 within the supernatant of WT T cells assessed by ELISA after pretreatment for 1 hour with increasing doses of compounds as indicated (A) 12a (B) CRT101 and (C) CRT051 24 hours after TCR triggering via αCD3 (500ng/ml). *= p≤ 0.05, ** = p≤0.01, *** = p≤0.001 compared with DMSO vehicle treated controls by one-way ANOVA with *post-hoc* Dunnetts test. (Representative experiment from 2 independent experiments, error bars represent SEM from technical replicates from one experiment).

3.2.4 Exploring the use of PKD inhibitors in CML

As discussed within the introduction, CML is a myeloproliferative disorder that occurs most frequently as a result chromosomal translocation events resulting in the formation of the oncoprotein Bcr-Abl, which has constitutive tyrosine kinase activity. This leads to the dysregulation of numerous signaling pathways, such as PI3K/AKT/mTOR, RAS/RAF/MEK/ERK and JAK/STAT/ (Holyoake & Helgason 2015). Unregulated activity of these pathways supports the cytokine independent drive of cell survival and cell proliferation of CML cells and promotes disease progression. One therapeutic approach is to examine and target these dysregulated intracellular signaling pathways that are caused by Bcr-Abl oncogene in order to uncover novel therapeutic targets. Current therapies involving TKIs including imatinib experience significant levels of drug resistance and although TKIs have proved highly successful within the clinic, they do not eradicate LSCs, therefore TKI therapy is a lifelong treatment and for this reason, new therapeutic targets are required (O'Hare et al. 2011) (Graham 2002) (Copland 2006).

Involvement of PKD2 in numerous aspects of intracellular signaling pathways within CML, including direct phosphorylation of PKD2 via Bcr-Abl has been demonstrated previously. PKD2 has also been shown to be the dominant isoform expressed in Bcr-Abl+ LAMA85 human CML cells, in this context PKD2 displayed constitutive tyrosine phosphorylation within the pleckstrin homology domain (PH) and mediates Bcr-Abl induced NF-κB activation (Mihailovic et al. 2004). More recently, studies have uncovered a role for PKD2 in the constitutive degradation and subsequent removal of the IFNAR1 from Bcr-Abl+ CML cell surface. This is significant as interferon alpha (IFNα) therapy has been shown to be curative in a small subset of patients. This development has generated interest in using multi-targeted therapies for CML to reintroduce more efficient IFNα therapy in combination with TKIs therapy (Kujawski & Talpaz 2007). Accordingly, we sought to ask the following questions; what role(s) do PKD enzymes play in CML signaling pathways? Do human CML cells display basal PKD activity? Does pharmacological inhibition of PKD affect cell cycle progression, up-regulation of the IFNAR1 or p. STAT5 levels in CML cells?

To address these questions we chose to use the human K562 Bcr-Abl+ CML cell line as they provided a useful starting point displaying several characteristics of those seen in CML patients such as low surface expression of the IFNAR1 chain yet high amounts of this receptor are found intracellularly (Figure 3.6A). It is important to mention that we chose to assess IFNAR1 expression via flow cytometry due to the ability to quantitatively detect surface expression, rather than simply detect protein degradation via western blotting. The Bcr-Abl oncogene promotes the activation of multiple signaling pathways including the constitutive phosphorylation of STAT5. In this context constitutive p. STAT5 has been shown in multiple studies be a critical component in the maintenance of CML cells (Gesbert & Griffin 2000) (Hoelbl et al. 2010) (Anon 2011; Hantschel et al. 2012). Within the K562 cell line we observed high levels of constitutive p. STAT5 (Tyrosine 694 site) activity within cell culture by phospho-flow cytometry (Figure 3.6B).Comparing the p. STAT5 levels to another non CML human malignant B cell line (Raji), we saw high levels of p. STAT5 in unstimulated K562 cells which was completely absent in the Raji cell line (Figure 3.6C), supporting the use of the human K562 CML cell line as an appropriate model for human CML.

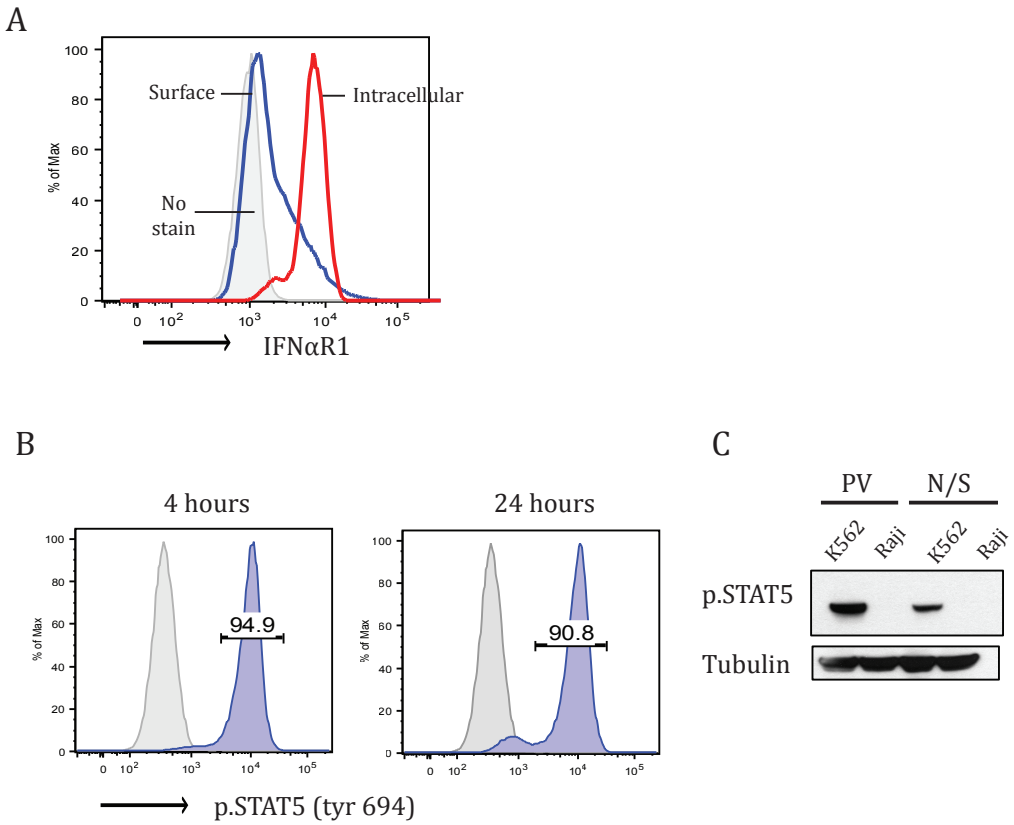

Figure 3.6 K562 human CML line display common characteristics of CML cells

(A) Representative flow cytometry of surface and intracellular IFNAR1 in K562 cell line (n=3). (B) Flow cytometry of intracellular constitutive p. STAT5 (tyrosine 694 site) activity in culture with no cell stimulation, 4 hours and 24 hours after passage of cells in culture (n=2). (C) Western blot of p. STAT5 (Tyr694) and β-tubulin as equal loading control of K562 cell lysates and Raji cell lysates unstimulated or treatment with pervanadate (10nM) for 10 minutes. Data obtained from 2 independent experiments.

3.2.4.1 Activation and inhibition of PKD in K562 CML cells

The activation status of PKD in K562 CML cells including inhibition of PKD by compounds 12a, CRT101 and CRT051 was assessed. In agreement with reported literature, PKD2 was observed as the dominant isoform expressed in CML cells by blotting with an antibody specific for the PKD2 isoform compared alongside murine lymphocytes obtained from WT spleen (Figure 3.7A)

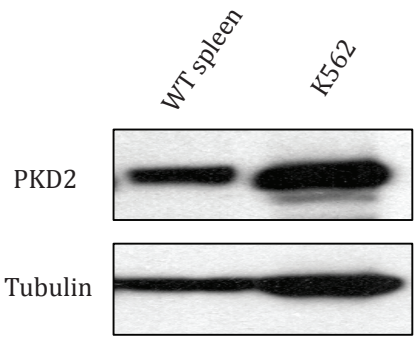

Figure 3.7 PKD2 isoform is expressed in human K562 CML cell line

Western blot of WT murine spleen sample and K562 CML cell line lysates detecting PKD2 with PKD2 specific antibody (Calbiochem) with β-tubulin as loading control (n=2).

In regard to activity of PKD, CML cells have been shown to display constitutive tyrosine phosphorylation (tyrosine 438) within the pleckstrin homology domain (PH) directly mediated by the Bcr-Abl oncoprotein. This phosphorylation does not lead to the activation of PKD and rather has been described as potentially serving as a docking site for the mediation of signaling complexes rather than directly activating NF-κB (Mihailovic et al. 2004). Other reports also demonstrate constitutive p. SER916 activity within CML cells, including K562 cells, furthermore this basal activity was severely reduced upon treatment of K562 cells with the CRT101 compound (Z.-F. Yang et al. 2013). We therefore assessed PKD activity in K562 cells via flow cytometry to examine p. SER916 levels after treatment of unstimulated cells with 5μM of PKD inhibitors including 12a, CRT101 and CRT051. As can be seen in Figure 3.8, we did not observe any reduction in the level of p. SER916 upon treatment with 12a, CRT101 or CRT051 demonstrating that K562 had no detectable levels of PKD activity, certainly within the autophosphorylation site of SER916.

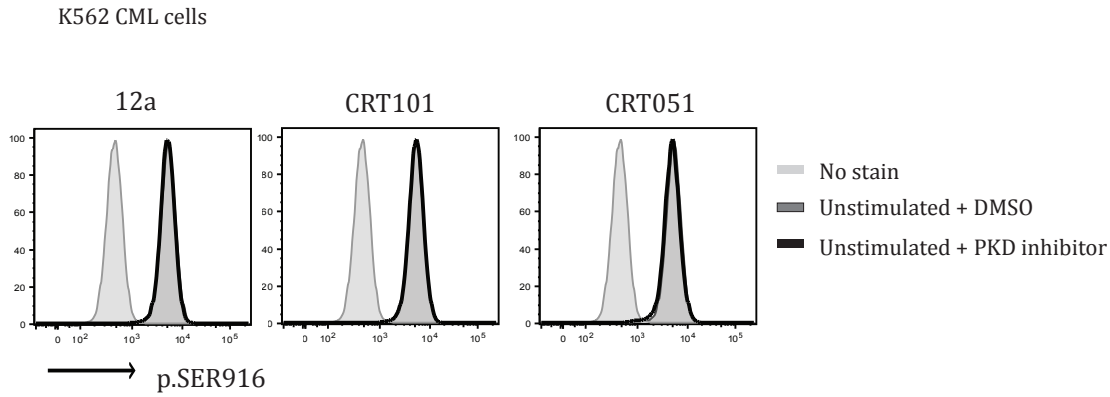

Figure 3.8 K562 CML cells do not display any basal PKD phosphorylation on SER916 site

Assessment of basal intracellular p. SER916 levels within K562 CML cells detected by flow cytometry in unstimulated cells treated with DMSO as a vehicle control or treated with 5μM of PKD inhibitors 12a, CRT101 and CRT051 for 1 hour. Data is representative of 3 independent experiments.

To assess the activation of PKD in K562 CML cells we next used phorbol ester (PdBu) to induce the activation of PKD, which was upregulated in a similar fashion to that seen in T lymphocytes in published data. Strong PKD activity, indicated by p. SER916 within autophosphorylation loop, was seen 15 minutes after stimulation, peaking at 30 minutes and beginning to decline at 60 minutes when assessed by flow cytometry (Figure 3.9A). This was also seen using western blot analysis (Figure 3.9B).

Interestingly, pervanadate was a weak inducer of PKD activity (p. SER916), which we first used as a positive control (data not shown), possibly a further indication of lack of basal PKD activity as pervanadate is a irreversible protein phosphatase inhibitor which upon application to cells prevents dephosphorylation therefore serving as a strong positive control within phosphorylation experiments. In regard to this, any basal PKD phosphorylation within K562 cells should accumulate with treatment of pervanadate, which we did not observe. As pervanadate was a poor positive control we used PdBu in all subsequent experiments within K562 CML cells.

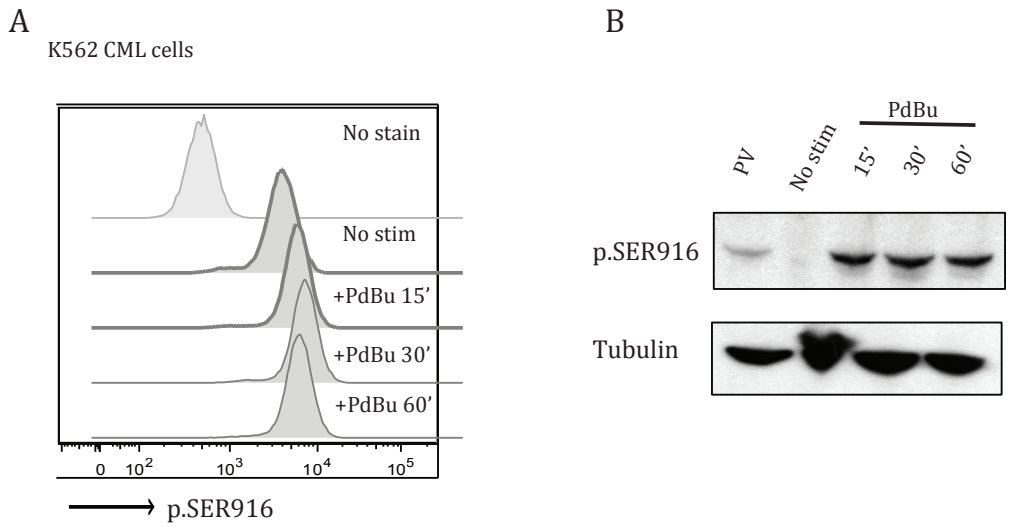

Figure 3.9 Activation and inhibition of PKD activity in K562 CML cells stimulated with phorbol ester

(A) Flow cytometry of intracellular p. SER916 PKD activity in K562 CML cell line stimulated with PdBu (200nM) for indicated time points (B) Western blot of p. SER916 after stimulation with PdBu (200nM) with indicated time points . Data representative of 3 independent experiments.

To study the ability of PKD inhibitors to block phorbol ester mediated activation of PKD we pre-treated K562 CML cells with increasing concentrations of 12a, CRT101 and CRT051 compounds before stimulation cells with phorbol ester for 30 minutes, a previously optimised time point where maximum PKD autophosphorylation upon Ser916 site was observed. We decided to assess this by phospho-flow cytometry, as it was a more informative and quantitative method than western blotting. As can be seen in Figure 3.10A-C all three PKD inhibitors robustly inhibited PKD activation in a dose dependent manner. This data is also represented as MFI values as shown in Figure 3.11.

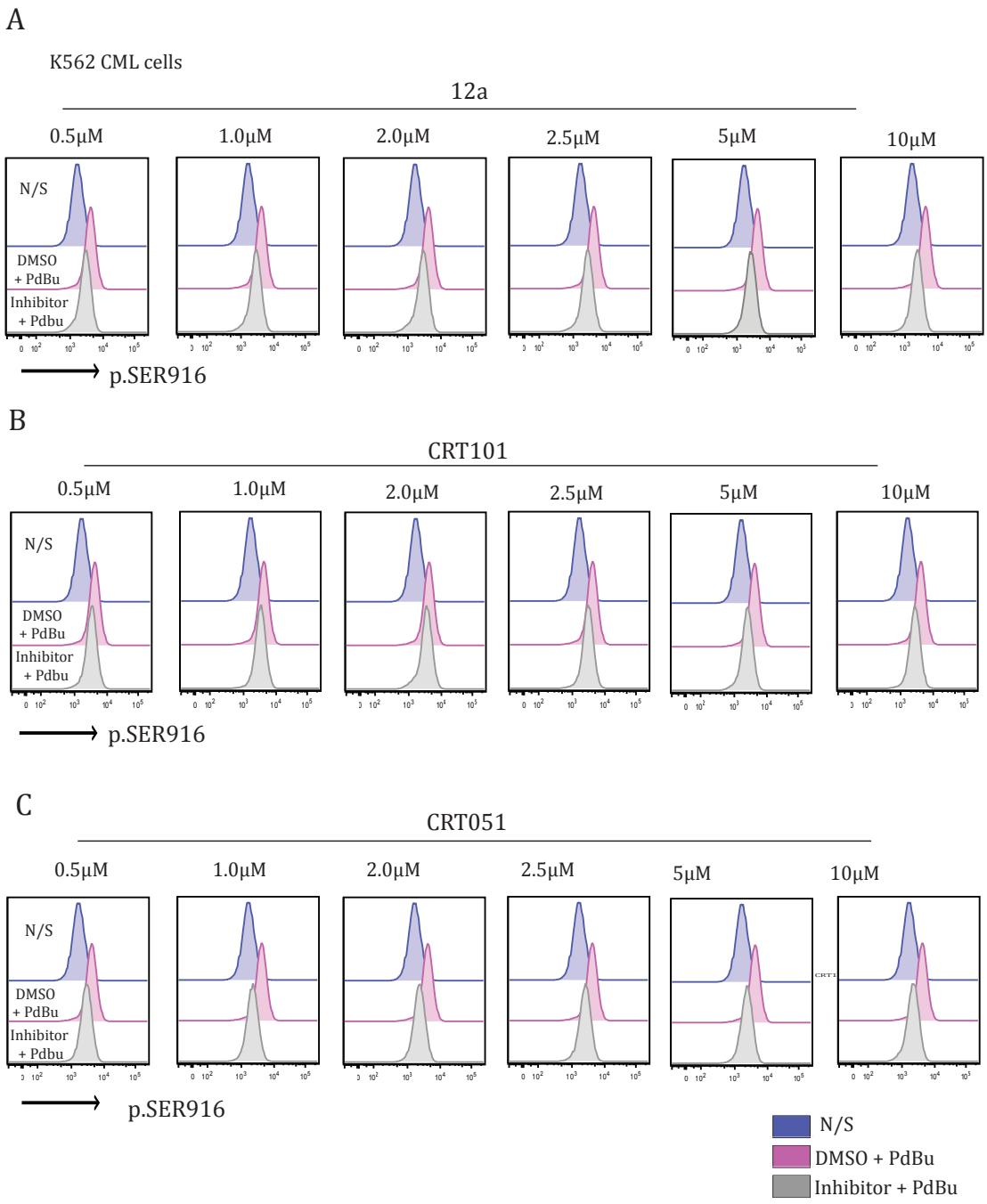

Figure 3.10 All 3 PKD inhibitors robustly inhibit PKD activation in response to PdBu in a dose dependent manner in K562 CML cells

Phospho-flow cytometry analysis of p. SER916 PKD activity in K562 CML cells pre-treated with increasing concentrations of (A) 12a (B) CRT101 (C) CRT051 before stimulation with PdBu (200nM) for 30 minutes, DMSO was used as vehicle control. Data obtained from 2 independent experiments.

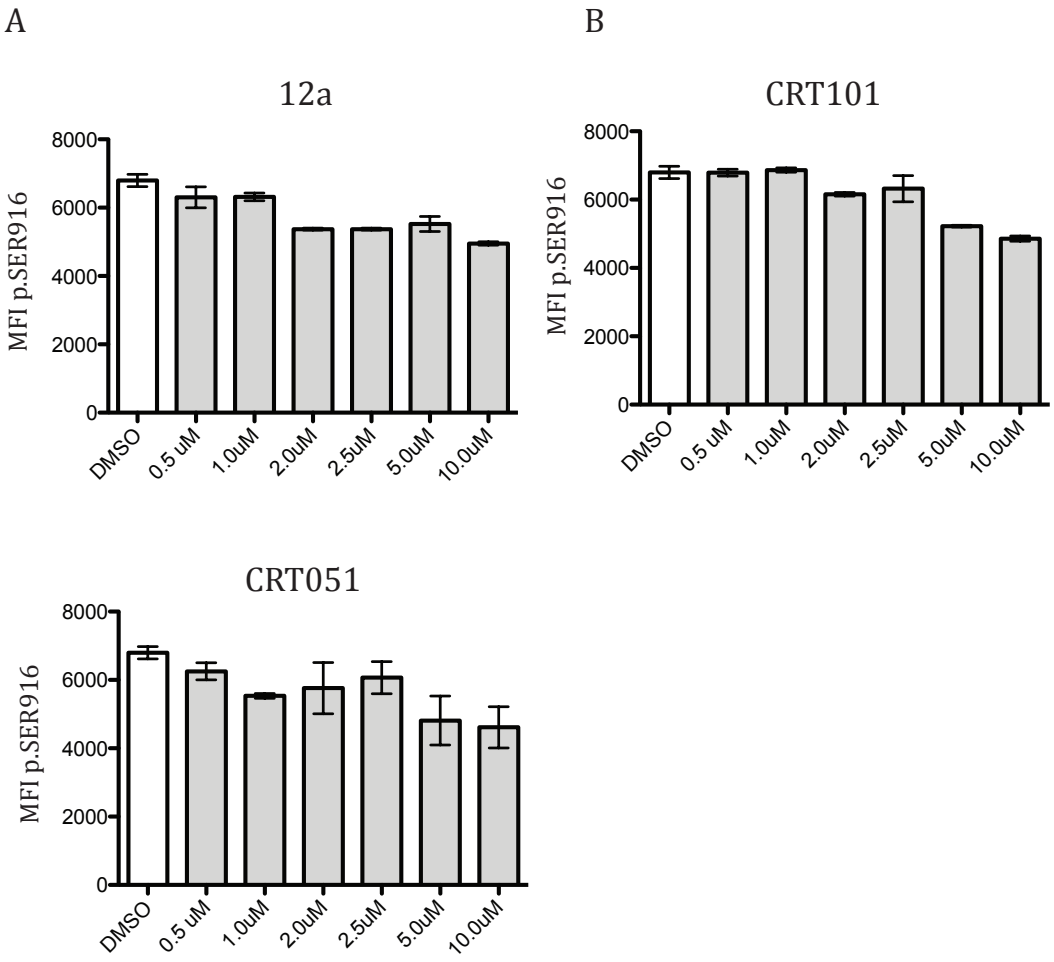

Figure 3.11 PKD inhibitors reduced induction of p.SER916 after PdBu stimulation in K562 cells

MFI of p. SER916 within K562 cells after treatment with increasing doses of (A) 12a (B) CRT101 and (C) CRT051. Data obtained and combined from two independent experiments.

These experiments were also expanded to combine p. ERK1/2 staining as a positive control of successful cell stimulation. As can be seen in Figure 3.12A-B, all three PKD inhibitors used at 5μM for 1 hour robustly prevented p. SER916 PKD activity yet p. ERK1/2 activation in response to phorbol ester stimulation remained intact. Although it should be noted that treatment with CRT051 compound did reduced p.ERK1/2 levels this is most likely due to off target effects present with this compound, however p.ERK1/2 levels still demonstrated that cells had successfully been stimulated with phorbol ester. This is also

demonstrated in Figure 3.12C whereby activation of p.SER916 was blocked in K562 CML cells but key PKC transphosphorylation sites remained functional.

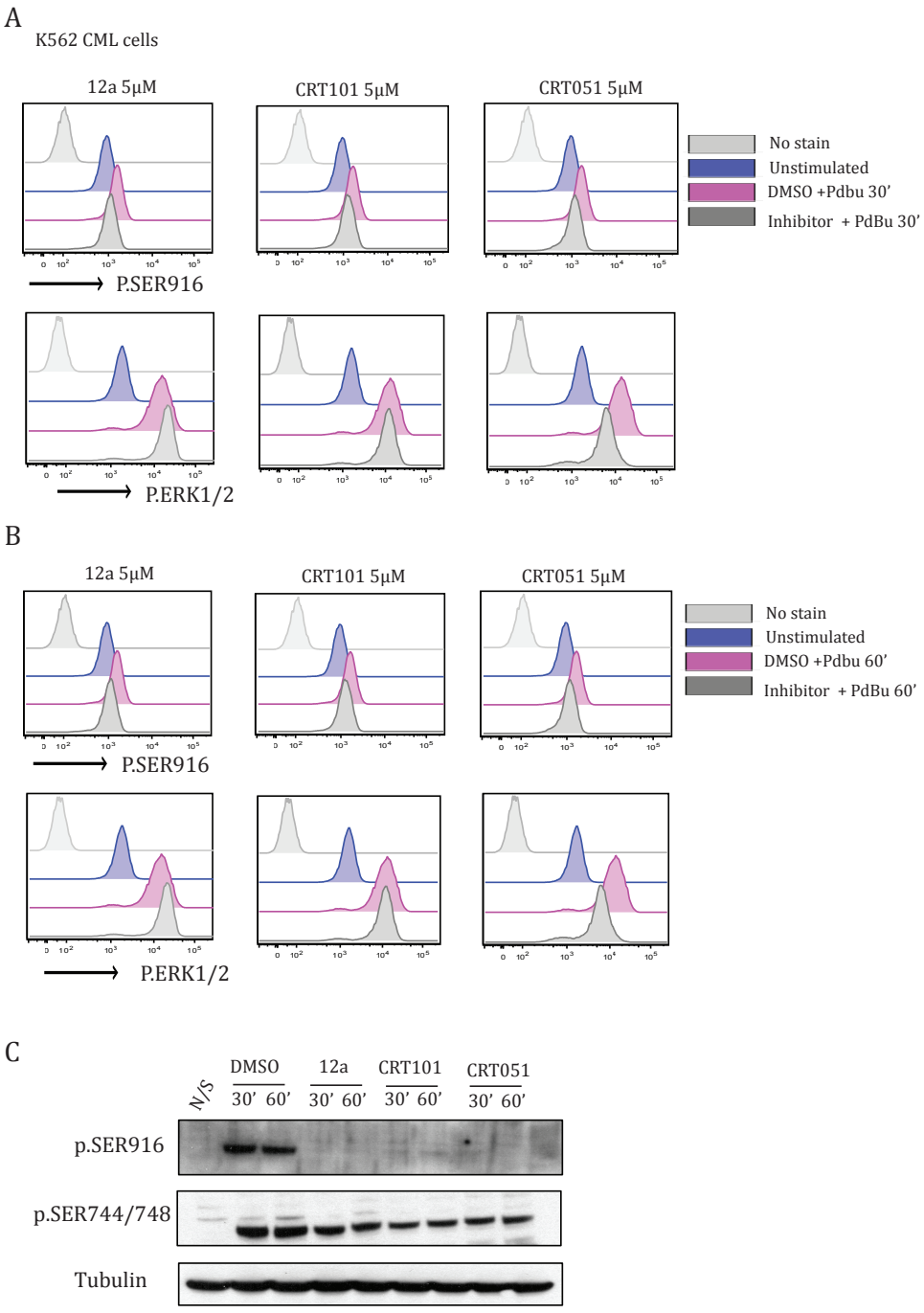

Figure 3.12 PKD inhibitors block PKD autophosphorylation in K562 cells but do not inhibit phosphorylation of key PKC sites on PKD

Phospho-flow cytometry analysis of p. SER916 and p. ERK1/2 in K562 cells pre-treated with 5μM 12a, CRT101 and CRT051 for 1 hour before stimulation with PdBu (200nM) for: (A) 30 minutes (B) 60 minutes. (C) Western blot of P.SER916

and p.SER744/748 in K562 cells. Data is representative of 3 independent experiments performed in duplicate.

Collectively, these results demonstrate that 12a, CRT101 and CRT051 compounds efficiently inhibit the activation of PKD, specifically the autophosphorylation site p. SER916, in a dose dependent manner, which is detectable by both phospho-flow cytometry and western blotting. Importantly, key PKC-mediated transphorylation sites (p. SER744/748) remained functional indicating these compounds do not affect up-stream PKC signaling.

3.2.4.2 Pharmacological inhibition of PKD in K562 CML cells causes cell cycle arrest

Consistent with previously published data assessing toxicity of CRT101 in K562 CML cells (Z.-F. Yang et al. 2013), unpublished data from our group agrees that all 3 PKD inhibitors, 12a, CRT101 and CRT051 were toxic in increasing concentrations to K562 CML cells.. This was assessed using PI staining after incubation with increasing doses of inhibitors for 24 hours. From this analysis IC50's were obtained; 12a IC_{50} 26.4±1.5μM, CRT101 IC_{50} 7.3 ± 0.7μM, CRT051 4.0±0.4μM. Significant cellular cytotoxicity was also noted in other experiments with the inclusion of live/dead dye including DAPI and PI staining in flow cytometry experiments using PKD inhibitors. In order to investigate the mechanism of cellular cytotoxicity we performed cell cycle analysis using PI staining in K562 CML cells under increasing concentrations of PKD inhibitors. Optimisation of these experiments lead us to exclude CRT051 from cell cycle studies due to the rapid cell death observed (within 5 hours) after incubation with the inhibitor, most likely due to off target inhibition of constitutive p. STAT5 signaling that exists within these cells, which is discussed later in this chapter.

To ensure cells were indeed undergoing normal cell cycle activity, K562 cells were plated 12 hours before treatment. Cell cycle analysis was performed

by treatment of cells with increasing concentrations of 12a or CRT101 compound for 7 hours with media only and DMSO used as controls. Figure 3.13B shows that culture of K562 CML cells with increasing concentration of 12a lead to a significant increase in the percentage of cells in G1 phase at 5μM concentration, representative histogram is shown in Figure 3.13A. In contrast, K562 cells treated with 2.5-5.0μM 12a showed significant decrease in the % of cells in S phase (Figure 3.13C). Finally, 12a compound had no significant effect on the % of cells in G2 phase (Figure 3.13D).

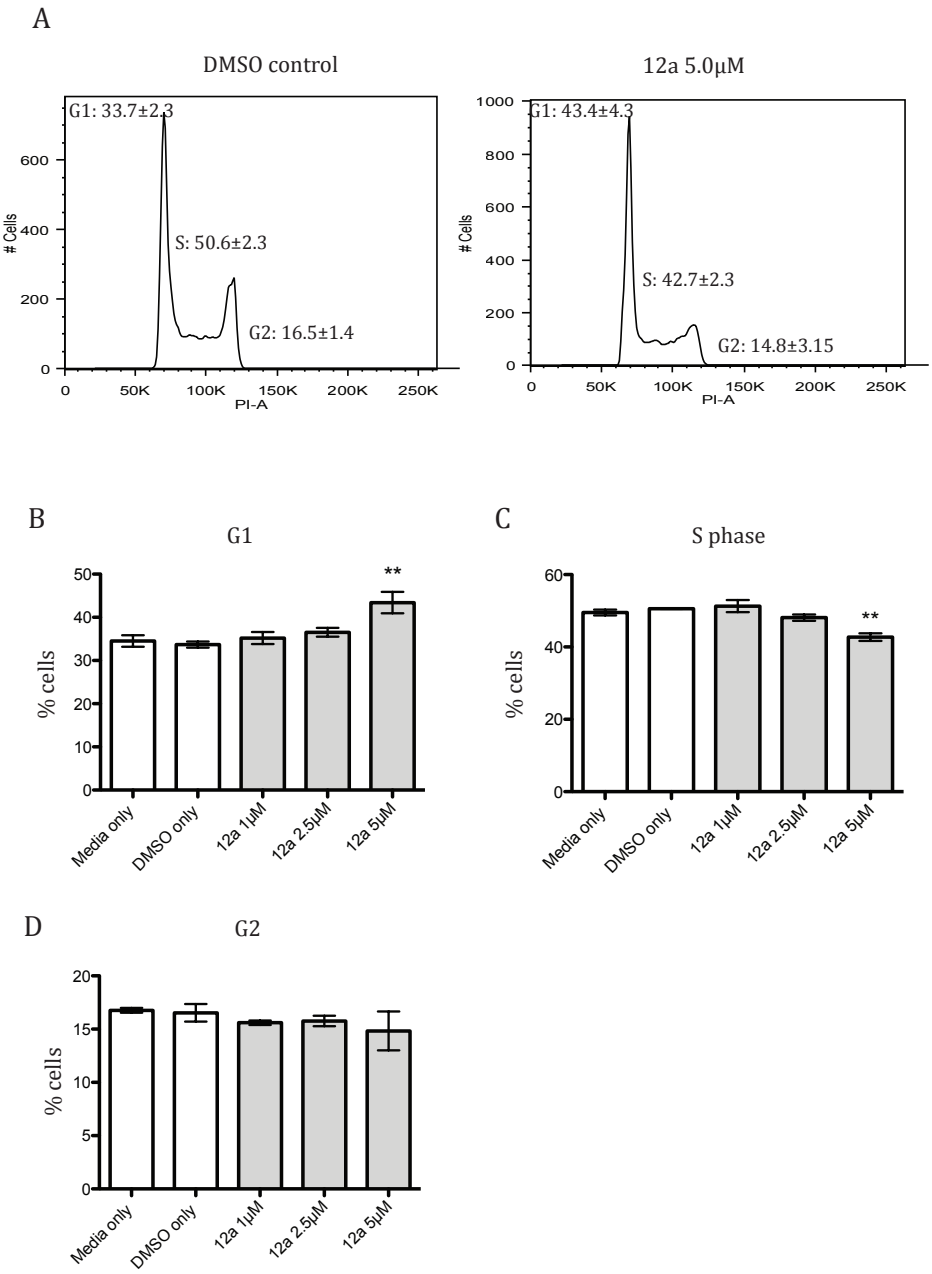

Figure 3.13 Cell cycle analysis of K562 CML cells under increasing concentrations of Novartis 12a

(A) Representative histograms of cell cycle analysis performed by PI staining 7 hours after treatment with either DMSO as vehicle control or 5.0μM 12a compound. Average % of cells in each stage of cell cycle with SD is displayed (n=3) (B) Combined data showing % cells in G1 after treatment with media only, DMSO or increasing concentrations of 12a compound (1.0μM, 2.5μM or 5.0μM. (C) % cells in S phase (D) % cells in G2 phase. Flow cytometry software that uses an algorithm to fit Gaussian curves to each phase was used, since it is more objective than setting markers by eye. ** = p≤0.01 analysed by one-way ANOVA with *post hoc* Dunnet test. Data obtained from 3 independent experiments.

We then assessed the effect of CRT101 on K562 CML cell cycle. This compound had slightly different effects on the cell cycle profiles of K562 cells after 7 hours of culture whereby at 2.5μM and 5μM concentrations the % of cells in G1 was significantly reduced (Figure 3.14 B), also shown as representative histograms in Figure 3.14A. Assessment of S phase revealed a significant increase in the % of cells found in S phase after treatment with 2.5μM and 5μM of CRT101 compound. Finally no differences in the cell cycle profile for G2 phase were observed in cells treated with increasing concentrations of CRT101 compound.

These results collectively reveal that most likely cause of cell cytoxicity within K562 CML cells after treatment of PKD inhibitors 12a and CRT101 is due to effects upon the cell cycle.

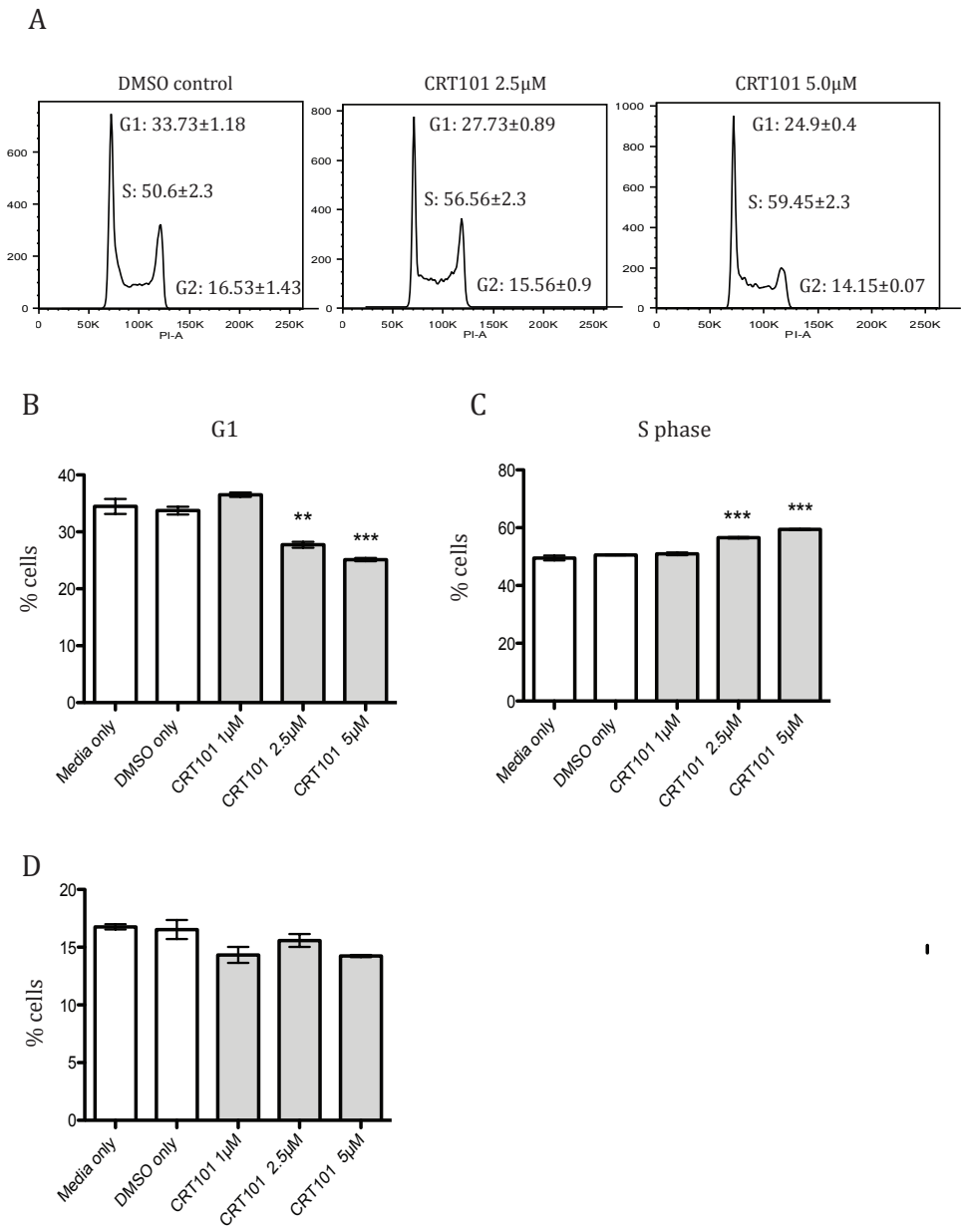

Figure 3.14 Cell cycle analysis of K562 CML cells under increasing concentrations of CRT101

(A) Representative histograms of cell cycle analysis performed by PI staining 7 hours after treatment with either DMSO as vehicle control or 2.5µM and 5.0µM CRT101 compound. Average % of cells in each stage of cell cycle with SD is displayed (n=3). (B) Combined data showing % cells in G1 after treatment with media only, DMSO or increasing concentrations of 12a compound (1.0µM, 2.5µM or 5.0µM. (C) % cells in S phase (D) % cells in G2 phase. Flow cytometry software that uses an algorithm to fit Gaussian curves to each phase was used, since it is more objective than setting markers by eye. ** = p≤0.01and *** = p≤0.001 analysed by one-way ANOVA with *post hoc* Dunnet test. Data obtained from 3 independent experiments. Data obtained from 3 independent experiments.

3.2.4.3 Analysis of the role of PKD in constitutive p. STAT5 phosphorylation in CML cells

As all three novel PKD inhibitors cause toxicity at increasing doses and cause cell cycle arrest, we wanted to investigate underlying mechanisms. The transcription factor STAT5 has been shown to be an essential mediator of the pathogenesis and survival of CML cells. CML cells including the K562 cell line have constitutively active and phosphorylated STAT5, which drives the transcription of multiple key survival genes such as BCL-x, and cyclin D (Hoelbl et al. 2010). Although there is published literature that PKD inhibitor CRT101 causes cell cycle arrest in K562 and human patient CML cells, no mechanism to explain the resulting cell death has yet been elucidated (Z.-F. Yang et al. 2013). Therefore, we decided to address if the pharmacological inhibition of PKD had any effect on the level of constitutive p. STAT5 in CML cells. To achieve this we used phospho-flow cytometry with p. STAT5 staining after incubation with increasing concentration of PKD inhibitors. Analysis of p. STAT5 activity in K562 CML cells after treatment with increasing concentrations of 12a compound had no effect on p. STAT5 activity within 4 hours treatment, which was similar to DMSO vehicle controls (Figure 3.15A-C). Conversely, treatment with increasing concentrations of CRT051 compound resulted in a significant reduction of p. STAT5 levels within K562 CML cells at 4 hours, shown by phospho-flow (Figure 3.15D) and by western blot (Figure 3.15E). These data are also shown plotted as MFI values in Figure 3.16.

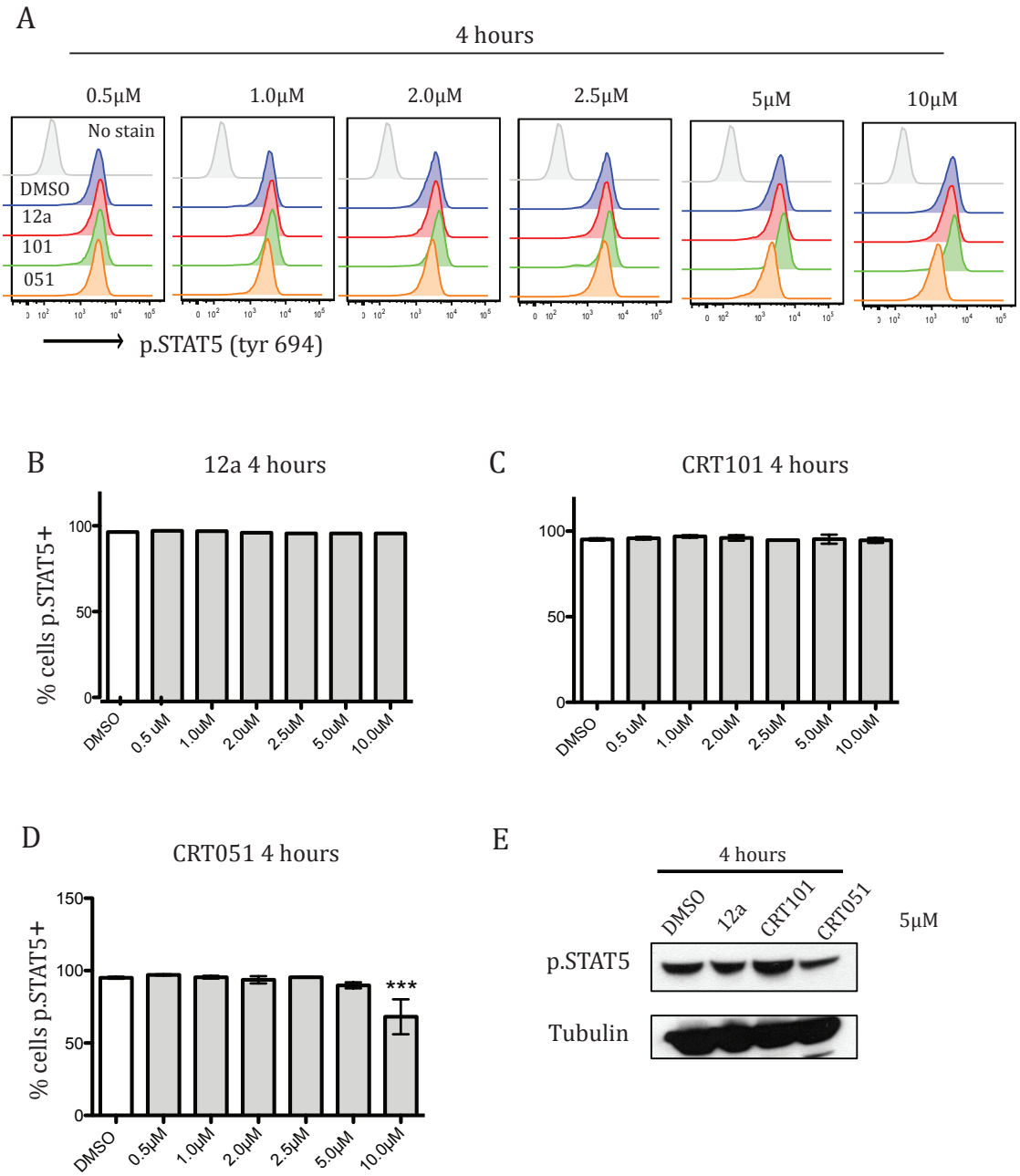

Figure 3.15 Assessing effects of PKD inhibitors on constitutive p. STAT5 activity in K562 CML cells

(A) Representative histogram of intracellular p. STAT5 levels in K562 cells assessed by flow cytometry after treatment of cells with increasing concentrations of PKD inhibitors 12a, CRT101 and CRT051 for 4 hours. Combined data showing analysis of % K562 cells positive for p. STAT5 after 4 hours with increasing doses of (B) 12a. (C) CRT101 and (D) CRT051. (E) Western blot of p. STAT5 activity in K562 cells after treatment with 5μM PKD inhibitors for 4 hours. *** = p≤0.001 analysed by one-way ANOVA with *post hoc* Dunnet test. Data obtained from two independent experiments.

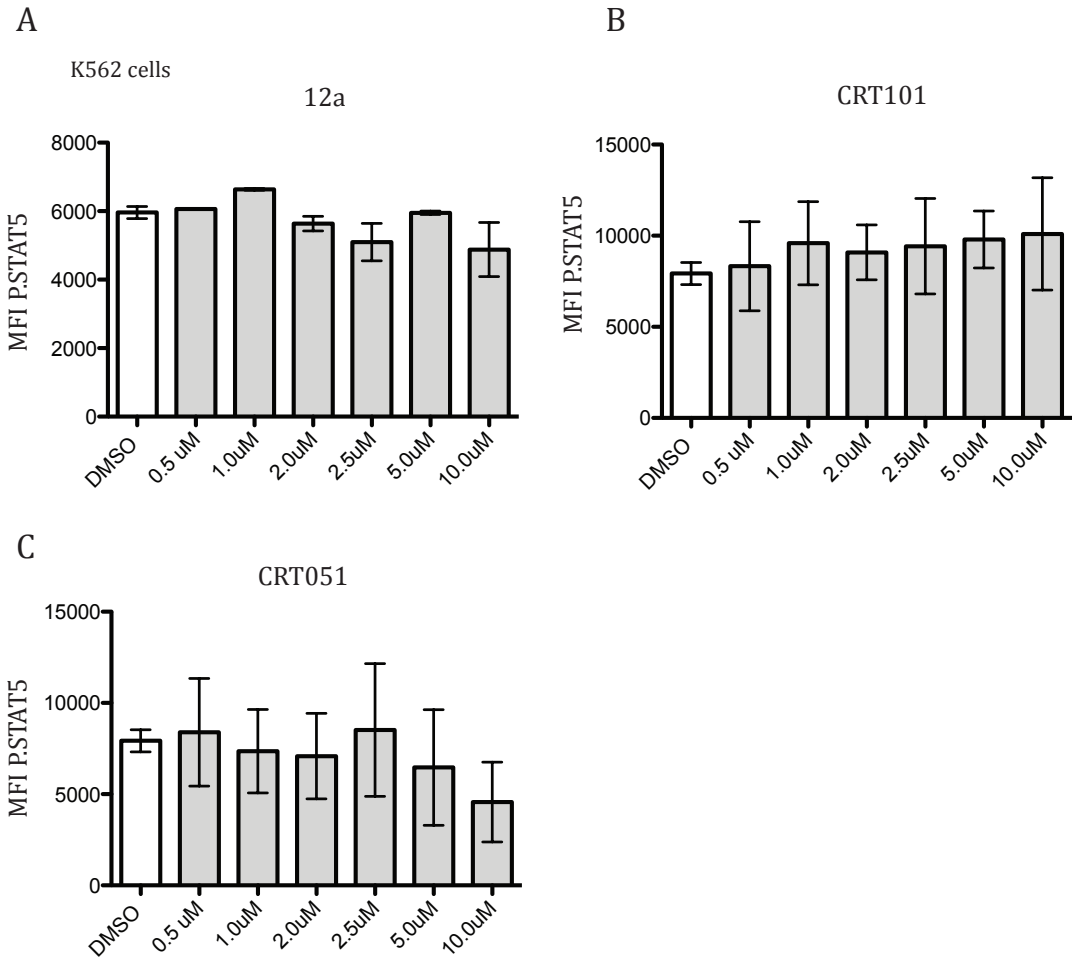

Figure 3.16 p.STAT5 levels shown as MFI 4 hours after treatment with PKD inhibitors

Combined MFI data of p.STAT5 staining in K562 cells after 4 hours treatment increasing concentration of PKD inhibitors including (A) 12a (B) CRT101 and (C) CRT051. Data obtained from 2 independent experiments.

Consequently, we extended our time point to 24 hours, excluding the 12a compound from our studies and instead focusing on newer CRT compounds. Preliminary data of K562 cells after 24 hours with increasing doses of CRT101 compound we noticed subtle increases in p. STAT5 in K562 CML treated cells (Figure 3.17A-B) with increasing concentrations when compared to DMSO treated controls. As expected from initial 4 hour time points with CRT051 compound, the number of cells positive for p. STAT5 was severely decreased with higher concentrations of CRT051 including 5μM and 10μM (Figure 3.17C)

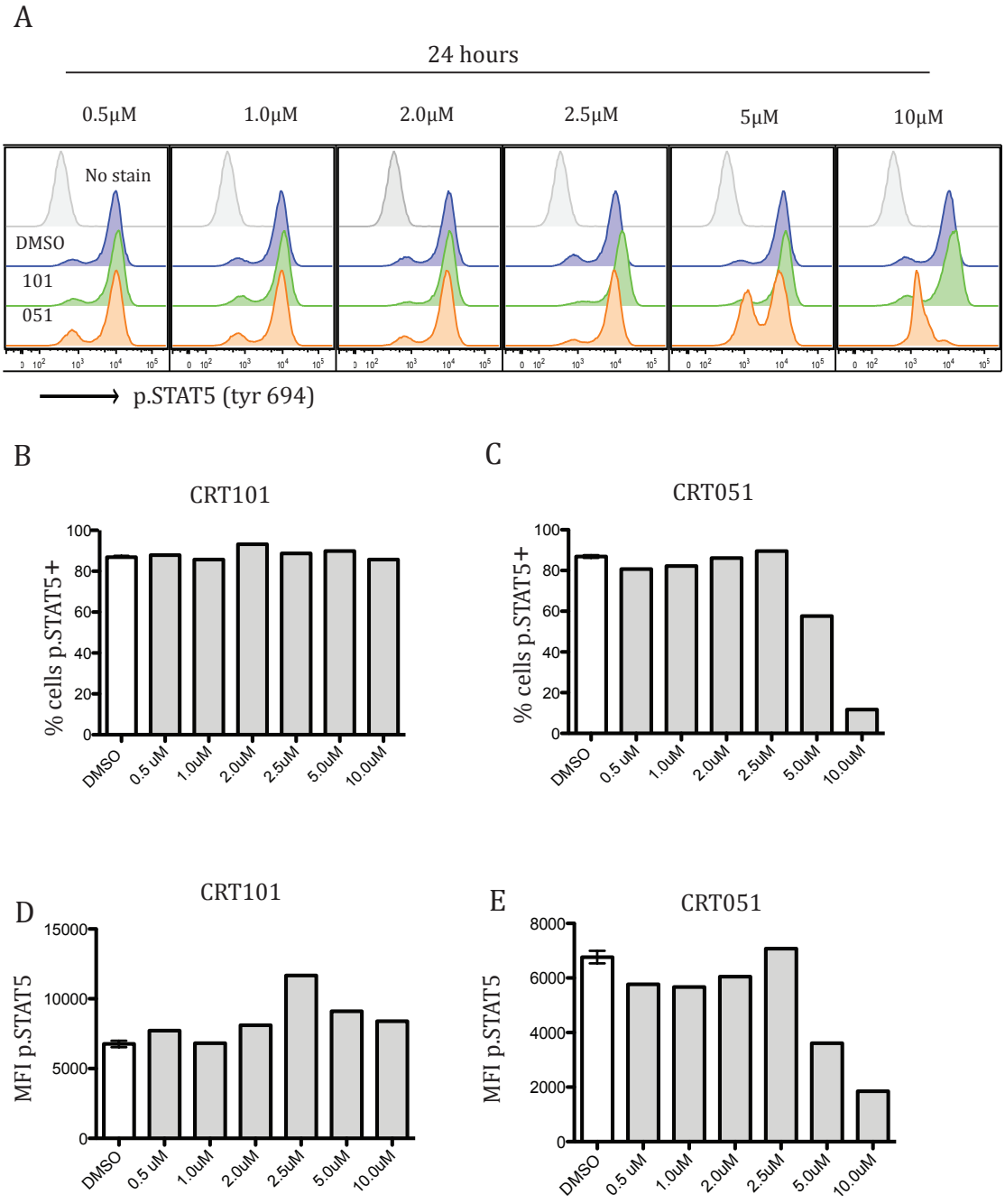

Figure 3.17 Analysis of p. STAT5 activity after treatment with increasing doses of PKD inhibitors for 24 hours

(A) Flow cytometry of p. STAT5 activity in K562 CML cells after treatment with increasing doses of PKD inhibitors CRT101 and CRT051 for 24 hours. % cells pSTAT5+ after 24 hour incubation with increasing concentrations of (B) CRT101 and (C) CRT051. (D) MFI p.STAT5 levels after treatment with CRT101 for 24 hours. (E) MFI p.STAT4 levels after treatment with CRT051 for 24 hours. Preliminary data showing data from 1 independent experiment.

3.2.4.4 Pharmacological inhibition of PKD promotes the up-regulation of the IFNAR1 on the cell surface of CML cells

Data published by Zhang et al have demonstrated that knockdown of PKD2 resulted in the increase of the IFNAR1 on the cell surface of CML cells, offering the potential therapeutic advantage to sensitise CML cells to IFNα therapy. This is of particular significance in the case of patients who have developed drug resistance to TKIs and require further treatment options. Moveover, there is evidence that IFNα therapy can sensitise LSCs that are resistant to conventional TKI therapy and contribute to disease regression (Kujawski & Talpaz 2007). We wanted to investigate if pharmacological inhibition of PKD with small molecular inhibitors also replicated results seen with knockdown of PKD. To achieve this we used 12a, CRT101 and CRT051 compounds in increasing concentrations for 18 hours using flow cytometry to assess cell surface expression of IFNAR1 on K562 CML cells. We also incorporated the use of a live/dead dye in these experiments to assess IFNAR1 on live cells only. 12a, CRT101 and CRT051 had modest effects on the up-regulation of IFNAR1 at higher doses including 2.5μM and 5μM compared to DMSO vehicle controls (Figure 3.18A-C). This was particularly difficult to assess due to high levels of toxicity at higher doses of PKD inhibitors at later time points including 24 and 48 hours (data not shown).

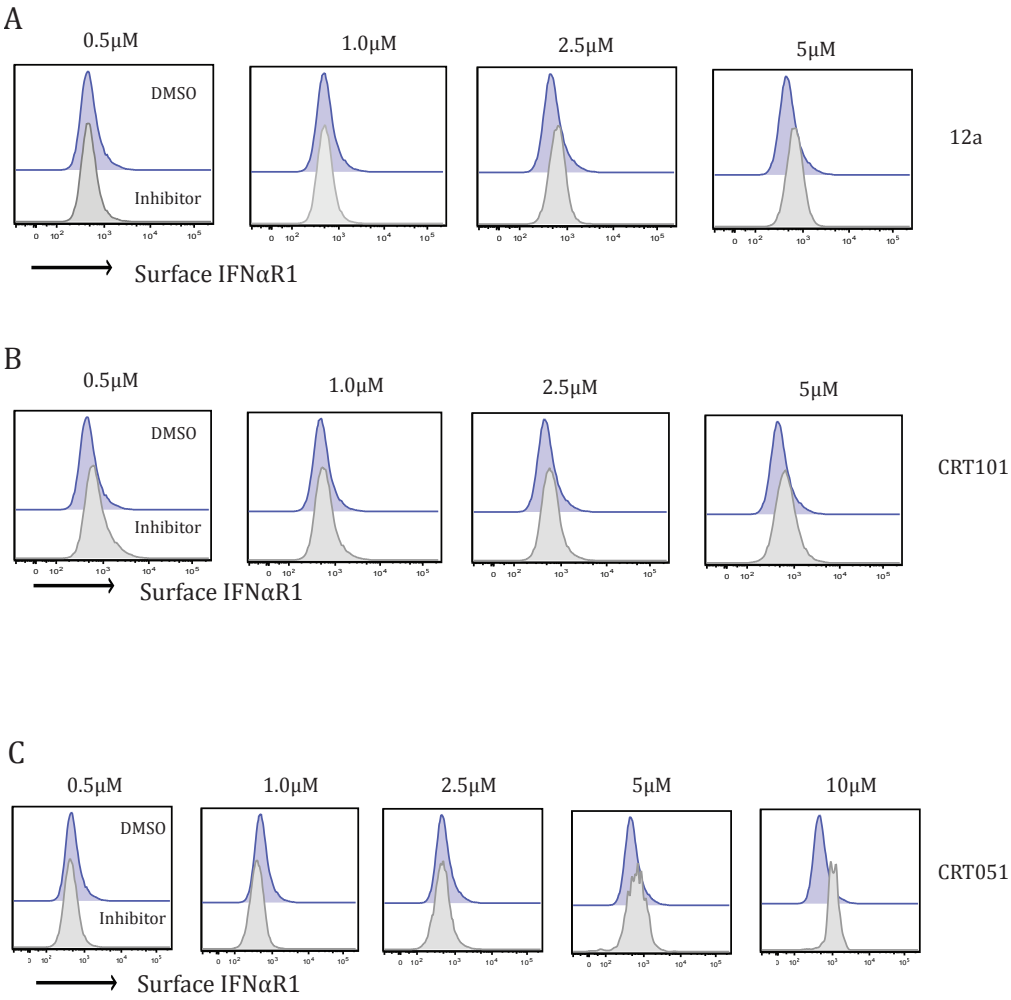

Figure 3.18 PKD inhibitors cause a dose dependent up-regulation of IFNAR1 on the cell surface of K562 cells

(A) Flow cytometry analysis of IFNAR1 expression on cell surface of K562 CML cells after treatment with 12a compound at increasing concentrations for 18 hours. PI staining was used to gate on live cells and DMSO was used as a vehicle control. (B) IFNAR1 expression after treatment with increasing concentrations of CRT101 compound. (C) IFNAR1 expression after treatment with increasing concentrations of CRT051 compound. Representative experiment from 3 independent experiments.

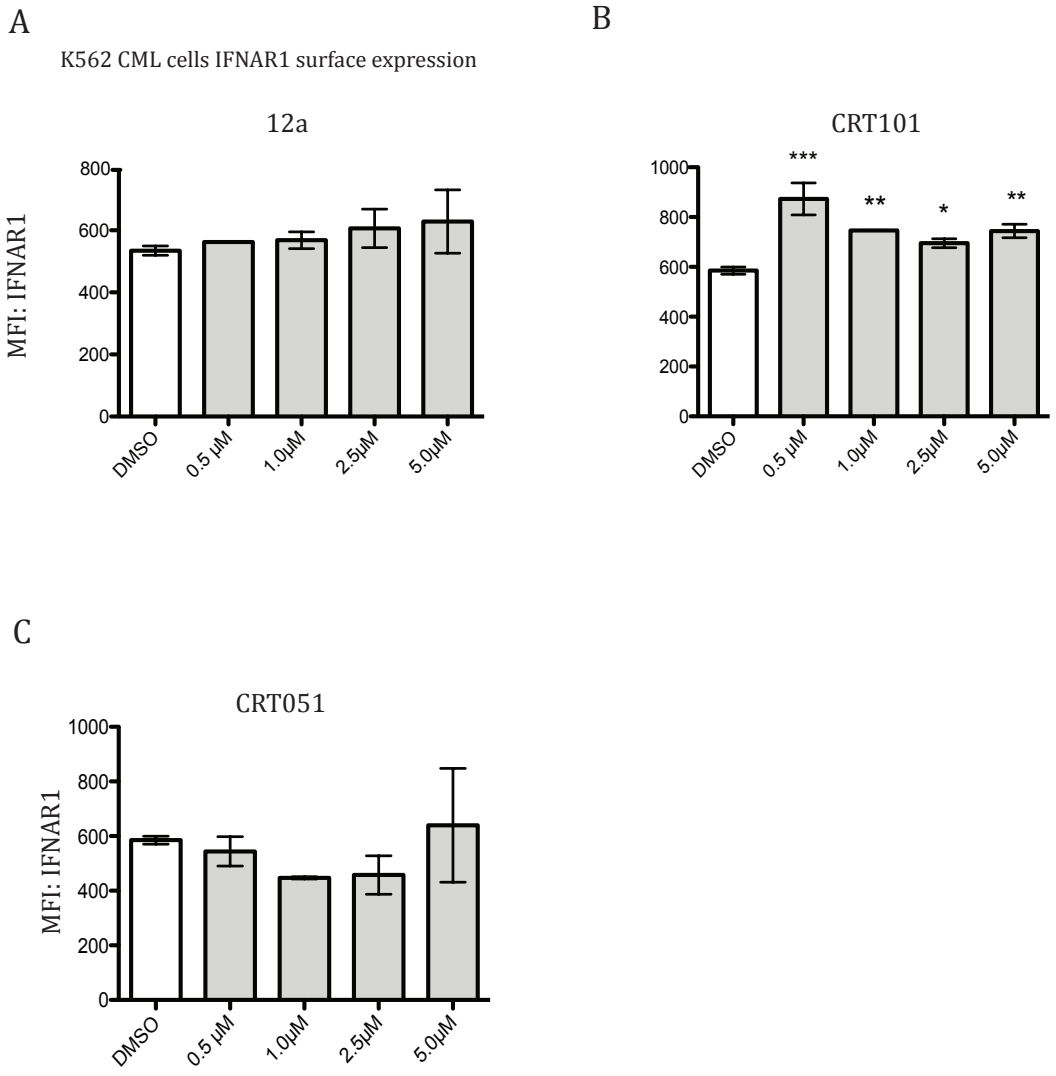

Figure 3.19 Analysis of IFNAR up-regulation on cell surface of K562 CML cells after pharmacological inhibition of PKD

Analysis of IFNAR1 expression on the cell surface by flow cytometry of K562 cells after treatment with increasing concentrations of PKD inhibitors, graphs show MFI (A) 12a (B) CRT101 (C) CRT051. *= p≤ 0.05, ** = p≤0.01, *** = p≤0.001 compared with DMSO treated controls by one-way ANOVA with *post-hoc* Dunnetts test. Combined data from 3 independent experiments.

3.3 Discussion

The data in this chapter explore the specificity and biological effects of novel small molecule inhibitors of PKD. Our results show that compounds 12a, CRT101 and CRT051 are indeed specific for PKD and although individually they display off target effects on other kinases they comparatively do not share any off-target effects. Importantly, all three inhibitors did not inhibit the *in vitro* kinase activity of multiple PKC isoforms including PKCα, PKCγ and PKCζ. This is significant, as it distinguishes these newer inhibitors from previous reports using dual PKC/PKD inhibitors such as Go6976 allowing more selective targeting of PKD and its downstream substrates despite the fact that significant off target effects remain. Furthermore, our comparative analysis of data obtained from our *in vitro* kinase analysis in combination with published data illustrate that although each compound display individual off target effects they are not shared between all three compounds. These results subsequently allowed us to confidently explore the effect of pharmacological inhibition of PKD with the rationale that any biological effects observed should be shared between the three compounds and to allows us to reliably describe it as a consequence of PKD inhibition specifically.

Our subsequent studies detailed the characteristics of PKD inhibition that compounds 12a, CRT101 and CRT051 demonstrated within primary murine T lymphocytes and malignant myeloid cells including human K562 CML cells.

Pharmacological inhibition of PKD within murine T lymphocytes demonstrated that catalytic activity of PKD after TCR ligation is essential for IFNγ and IL-2 production in agreement with previous reports showing impaired cytokine production in PKD2$^{KI/KI}$ animals lacking specifically PKD2 catalytic activity (Matthews et al. 2010). Previous reports within the literature have further revealed that PKD catalytic activity is required downstream of TCR ligation for the recruitment of RNA polymerase II (Pol II) to the IFNγ transcriptional start site (Navarro, Feijoo Carnero, et al. 2014a). To determine if is the case in regard to the effect pharmacological inhibition of PKD on the recruitment of Pol II to the IFNγ and IL-2 start sites could be examined in the future. The implication of PKD kinases within cytokine production is not limited

to TCR induced cytokine production as studies using pharmacological inhibition or knockdown of PKD in prostate cancer cell lines and epithelial cell lines have also reported a reduction in the production of IL-6 and IL-8 (LaValle, Bravo-Altamirano, et al. 2010a; Hao et al. 2009).

Previous reports within the literature implicate a role for PKD within multiple aspects of including CML development and CML cell survival (Mihailovic et al. 2004) (Z.-F. Yang et al. 2013) (Bhattacharya et al. 2011; H. Zheng et al. 2011). Additionally, PKD2 has been shown to be expressed within K562 Bcr-Abl+ CML cell line, in agreement with our data. However, one discrepancy within these results are reports also describe constitutive PKD activity (p.SER916 site) after direct phosphorylation by the Bcr-Abl oncoprotein, which we do not observe either by western blot or more sensitive methods such as phospho-flow cytometry. This is in contrast to data previously published and data generated within our lab that demonstrates high basal activity of PKD (p. SER916) in murine T lymphocytes (Matthews et al. 2010) and within primary murine myeloid cells (discussed within the chapter 4). Although one study has demonstrated that Bcr-Abl phosphorylation the tyrosine residues within the PH domain of PKD rather than inducing p. SER916 autophosphorylation sites (Mihailovic et al. 2004). To determine if PKD inhibitors block tyrosine phosphorylation in K562 CML cells could be addressed in the future by using immunoprecipitation techniques to purify PKD2 and assess tyrosine phosphorylation. Although constitutive activity is absent in our experiments, PKD was strongly induced within K562 cells in response to phorbol ester.

The lack of constitutive activity of PKD within K562 Bcr-Abl+ CML cells made it difficult to address potency of these inhibitors to block PKD. Therefore to overcome this, we assessed the ability of PKD inhibitor compounds 12a, CRT101 and CRT051 to block phorbol ester induced activation, a potent activator of PKD. The pharmacological inhibition of PKD demonstrated that, within human K562 CML cells, all three small molecule inhibitors of PKD potently block PKD activation in response to phorbol ester, in a dose dependent manner. Importantly, key PKC mediated transphorylation sites were unaffected by all three compounds.

Previous reports on PKD2 in CML cells have found that knockdown or pharmacological inhibition of PKD (with the CRT101 compound) led to inhibition of cell cycle progression, with a significant reduction in cells within S phase (Z.-F. Yang et al. 2013). Our data displays discrepancy with these results, in which treatment of cells with the CRT101 compound led to a significant increase in the number of cells in S phase. This conflict in data may be due to two possibilities. Firstly, the Yang et al study does not give a time point used for treatment with CRT101 although cell cycle analysis is frequently analysed at 24 hour time points, however our analysis was performed at 7 hours as we had previously observed significant cell death. Secondly, studies within cell lines such as the K562 CML cell line must be approached with caution due to clonal variation between different laboratories as a result of the acquisition of mutations over time due to repeated passaging. Furthermore, based on the kinase profiling data, it is plausible that effects we observed within cell cycle analysis after inhibition of PKD in K562 CML cells with CRT101 is in part due to its inhibition on CDK9 and CDK2 which are known to be a regulators of S-phase entry via the binding of cyclin A (McDonald 2005) (Hu et al. 2001).

Although K562 CML cells and indeed CML patient cells are known to express constitutive phosphorylation of p. STAT5 no studies have yet examined the effect of PKD inhibition upon p. STAT5 within CML cells. Treatment within CML cells 12a, CRT101 and CRT051 compounds revealed inconsistent results between compounds in which 12a had no effect, CRT101 subtly increased and CRT051 profoundly decreased p. STAT5 levels, it is highly plausible that discrepancies are most likely to be off target effects displayed by individual compounds. Referring to data obtained within in vitro kinase screen analysis offers potential insights into results in regard to the increase in pSTAT5 levels upon treatment with CRT101. Notably, PIM1 and PIM3 kinases are significantly reduced within the kinase screening profile for CRT101. PIM1 has been shown to be involved the negative feedback loop for p. STAT5 levels, whereby PIM1 phosphorylates and activates suppressors of cytokine signaling (SOCs) proteins which act to suppress p. STAT5 signaling. Additionally, the 2-(4-aminopyridin-2-yl) phenol moiety in CRT101 is also present in small molecule inhibitors of PIM1

(pimozide), which has also been studied in the context of p. STAT5 within CML cells (Nelson et al. 2011).

Previous reports have demonstrated that PKD2 plays a key role in mediating the enhanced internalisation and degradation of the IFNAR receptor from the surface of CML cells (Bhattacharya et al. 2011; H. Zheng et al. 2011). This is reportedly by phosphorylation of a serine residue (Ser535) within the degron of the IFNAR1 by PKD2. Treatment of K562 CML cells within novel inhibitors of PKD yielded mixed results in which we only observed significant increase in surface expression of IFNAR with the CRT101 compound, although again due to toxicity of these compounds in K562 CML cells this was problematic to study. Due to this, we could not reliably validate the role of PKD activity within the IFNAR1 internalisation within CML cells with the use of pharmacological techniques.

4 Exploring the expression and function of PKD isoforms in primary myeloid cells

4.1 Introduction

In the previous chapter I have introduced novel data characterising the specificity of three novel small molecule inhibitors of PKD and their biological effects within T lymphocytes and a CML cell line. As we established the PKD2 isoform was indeed expressed in human K562 CML cells, we also wished to address PKD isoform expression in primary murine myeloid cells, including DCs and macrophages. In regard to expression within different lineages of immune cells the PKD2 isoform is known to be predominantly expressed in T and B lymphocytes in the adaptive immune system, moreover, PKD2 is selectively activated after TCR triggering with cognate antigen and rapidly translocate from the cytoplasm to the plasma membrane within the immunological synapse (Matthews et al. 2010) (Spitaler, Emslie, Wood & Cantrell 2006b).

Within cells of the innate immune system specific PKD isoform expression remains largely unaddressed, although PKD1 is reported to be the dominant isoform expressed within mast cells (Murphy et al. 2007). Previous investigation into PKD isoform expression has been problematic due to the high level of homology between family members leading to a lack of antibodies that do not cross-react . To overcome this problem, we largely focused on the use of isoform specific PKD transgenic animal models. Additionally, a global aim within this thesis was to focus on the use of isoform specific kinase dead mice to investigate the true biological functions of PKD kinases. The justification to use a catalytically in-active kinase transgenic model rather than a total protein knock-out was that they represent a more accurate tool to directly assess the role of PKD kinase activity by examining a direct consequence of loss of phosphorylating ability and therefore the effect on the regulation of downstream substrates, rather than affect potential scaffolding functions. As such, it is important to emphasise that the only PKD knockout cells used in this thesis were

$PKD2^{KO/KO}$, which served as controls for isoform expression experiments and to confirm antibody specificity. It is also important to note that as well as loss of PKD activity upon stimulation of cells with PKD activating factors, catalytically inactive mutant cells have also lost basal kinase activity which may also play a significant role in cellular processes.

In addition to isoform expression, we also wished to utilise PKD transgenic animal models to investigate the consequence of loss of isoform specific PKD catalytic activity on myeloid cell development *in vivo.* At present, no studies have yet established the requirement for PKD catalytic activity in the development of myeloid cells within the bone marrow or peripheral lymphoid tissues such as the spleen. In regard to the adaptive immune system, previous reports have shown that loss of PKD2 catalytic activity has been shown to be dispensable for the development of T and B-lymphocytes *in vivo* (Matthews et al. 2010).

Although the loss of PKD2 catalytic activity has been shown be dispensable for T cell development it has been shown to be required for normal T cell effector functions such as cytokine production including IL-2 and IFNγ, which has direct consequences on the immune response *in vivo*. Immunised $PKD2^{KI/KI}$ mice displayed significantly reduced humoral responses, presumably due to abhorrent T cell response caused by reduced production of effector cytokines. More recent evidence has also highlighted a role for PKD2 activity within the immune response *in vivo* whereby loss of PKD2 activity in CD8+ CTL results in an impaired response to Listeria Monocytogenes (*L. Monocytogenes*), yet loss of PKD2 catalytic activity was protective in a model of autoimmune diabetes (Navarro, Feijoo Carnero, et al. 2014a). Are PKD kinases also required for normal effector responses on innate immune cells? The evidence for this question within the literature is limited, however, studies within *C.elegans* have pointed to a clear and conserved role for PKD kinases in innate immunity whereby animals lacking the DFK-2A homologue of PKD were hypersensitive to death from bacterial pathogens (Ren et al. 2009). In the context of activation of PKD downstream of PRR ligation, previous reports include activation of PKD via TLR1/2 in BMDCs (Murphy et al. 2007), and TLR9 in murine macrophages (J.-E. Park et al. 2008). Further studies also reported requirement for PKD1 in all

MyD88 mediated TLR signalling within a macrophage cell line and BMDCs (J.-E. Park et al. 2009b).

Despite providing insight into the potential role of PKD and their downstream substrates in innate immunity, significant limitations to these past studies exist as they are often performed in cell lines using overexpression techniques and assessed using non-specific dual PKC/PKD inhibitors. Therefore, much of this research needs to be validated in primary cells and *in vivo* to ascertain the true contribution of PKD kinases to these processes.

Accordingly, within this chapter I will present data exploring if PKD kinases play a true physiological role in normal myeloid cell development and function including: PKD isoform expression within primary myeloid cells, the effect of loss of catalytic activity in myeloid cell development within the bone marrow and myeloid cell populations within the spleen and finally the role of PKD catalytic activity within effector function of primary myeloid cells.

4.2 Results

4.2.1 Exploring PKD isoform expression in primary myeloid cells

PKD isoform expression has been examined in both murine T and B cells (Matthews et al. 2010) (Matthews et al. 2006), with PKD2 preferentially expressed in these cell types, however, no studies have specifically addressed isoform expression in cells within the innate immune system, although, studies have concluded that PKD2 is the main isoform expressed in two CML cell lines (Mihailovic et al. 2004). Additional insights into PKD isoform expression at the mRNA level can be assessed by using data from the immunological genome project (Immgen), whereby gene expressional profiles are generated from different immune cells by RNA-sequencing (Ilumina). PKD expression in multiple immune cells within the adaptive immune system (assessed ex-vivo) including CD19+ B lymphocytes, CD4+ and CD8+ T lymphocytes can be seen in Figure 4.1. These data agree with literature which demonstrates that PKD2 is selectively and dominantly expressed within lymphoid tissue and indeed adaptive cells of the immune system (Matthews et al. 2010). In regard to myeloid cells, RNA-

sequencing data from Immgen reveal dominant expression of PKD in splenic DCs, yet comparable levels of PKD1 and PKD2 expression in splenic neutrophils (Figure 4.2).

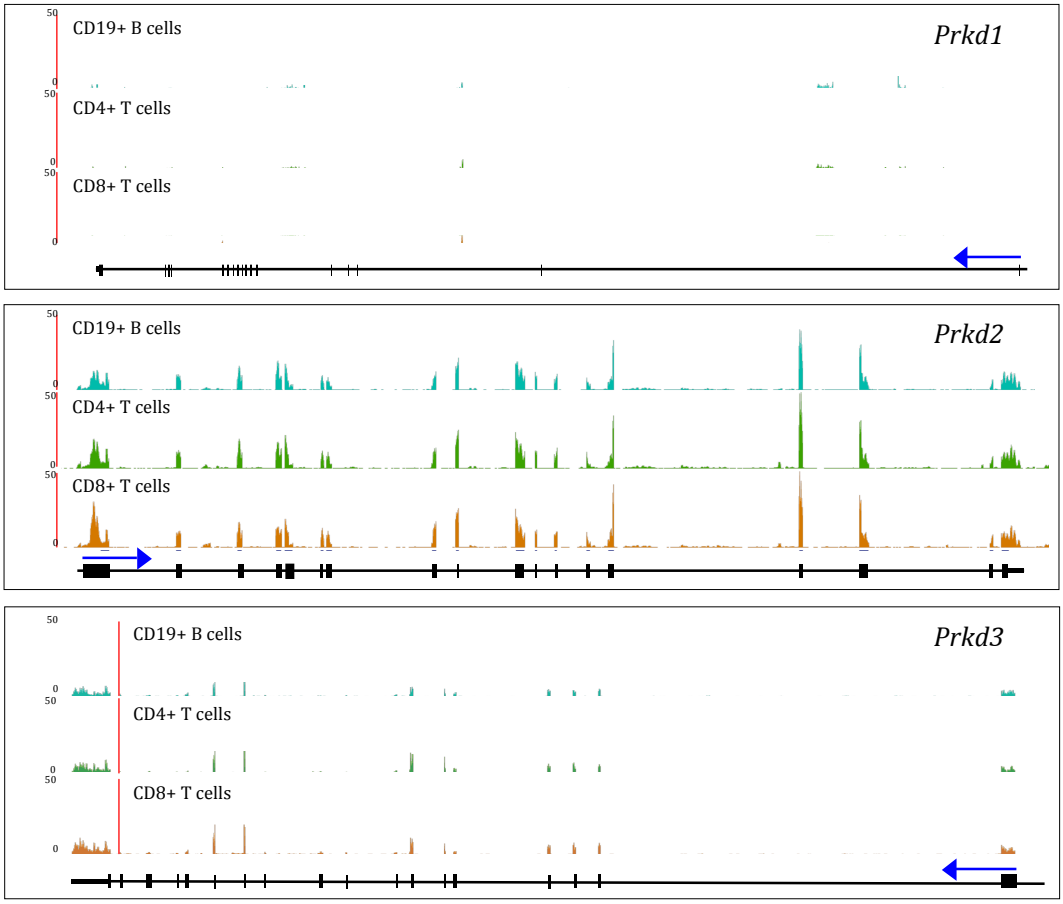

Figure 4.1 PKD RNA isoform expression in CD19+ B lymphocytes, CD4+ and CD8+ T lymphocytes.

RNA sequencing data showing analysis of exons of PKD1, PKD2 and PKD3 isoforms found within either CD19+ B lymphocytes, CD4 and CD8+ T lymphocytes
Data obtained from www.immgen.com

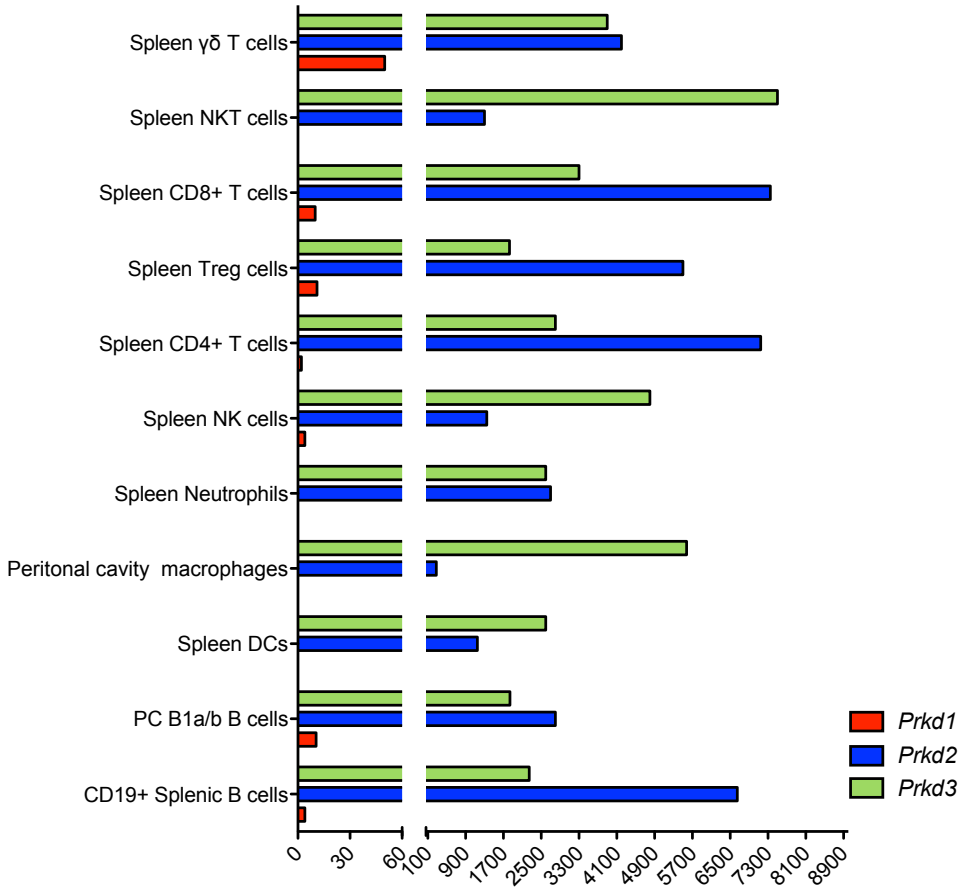

Figure 4.2 RNA sequencing data displaying PKD isoform expression in multiple immune cells.

Data obtained from www.immgen.com

To begin to assess protein expression of PKD isoforms within cells of the innate immune system, including DCs and macrophages. As DCs and macrophages are small populations within murine tissues we therefore first expanded these cell populations *in vitro* using previously described methods, allowing for generation of larger cell numbers of a more homogenous cell population. Bone marrow derived macrophages (BMDMOs) and bone marrow derived dendritic cells (BMDCs) were expanded *in vitro* after bone marrow isolation using GM-CSF (P Matheu et al. 2008) and M-CSF (Manzanero 2011) respectively and cultured for the indicated time.

In order to accurately assess which isoforms of PKD are expressed in primary myeloid cells we used isoform specific kinase inactive (KI) or isoform specific knock out (KO) cells generated from various PKD isoform specific

transgenic animals. This included cells generated from the bone marrow of wild type (WT), PKD1 kinase inactive heterozygous ($PKD1^{WT/KI}$) (as homozygous mutation is embryonic lethal), PKD2 kinase inactive homozygous ($PKD2^{KI/KI}$), double kinase-inactive cross mice ($PKD1^{WT/KI}$ x $PKD2^{KI/KI}$) and finally PKD2 gene trap knock out ($PKD2^{KO/KO}$). The generation of double-kinase dead mice was to assess any significant activity of PKD3 by depletion of the pool of inducible PKD1 and PKD2 isoforms. Furthermore, PKD3 has been shown to have extremely low abundance in T lymphocytes (Matthews et al. 2010).

Firstly, before using *in vitro* generated cells to examine PKD isoform expression we wanted to address if BMDC and BMDMO generated from all transgenic PKD mice were phenotypically comparable to cells derived from WT bone marrow. This analysis addresses two fundamental questions. Firstly, is specific PKD isoform activity required during the generation and expansion of myeloid cell *in vitro*? And secondary, are myeloid cells generated from isoform specific PKD bone marrow comparable to reliably determine PKD isoform expression.

By the end of the culture period WT BMDC typically express high levels of CD11c and MHC class II, which is frequently used for phenotyping BMDCs generated *in vitro* (Inaba et al. 2009). Our data demonstrates that BMDCs generated from the bone marrow of various PKD transgenic mice all displayed comparable levels CD11c and MHC class II to WT BMDCs (Figure 4.3A). Microscopically, BMDCs generated from PKD mutant mice were morphologically comparable to WT BMDCs (data not shown). Additionally, analysis of total cell number ($x10^6$) from both the bone marrow on day 0 and total cell number by day 10 of culture from all PKD transgenic mice were comparable to WT counts (Figure 4.3B-C). These data importantly demonstrates that PKD1 and PKD2 catalytic activity, or indeed in the case of loss of PKD2 protein in the case of $PKD2^{KO/KO}$ cells, is dispensable for the development or expansion of BMDCs *in vitro.* It is also possible to presume that in light of these results BMDC precursors are presumably unaffected within the bone marrow of various PKD mutant mice. Moreover, these confirmed the use of BMDCs generated from PKD mutant bone marrow to confidently assess which PKD isoform predominantly expressed thus validating our experimental approach.

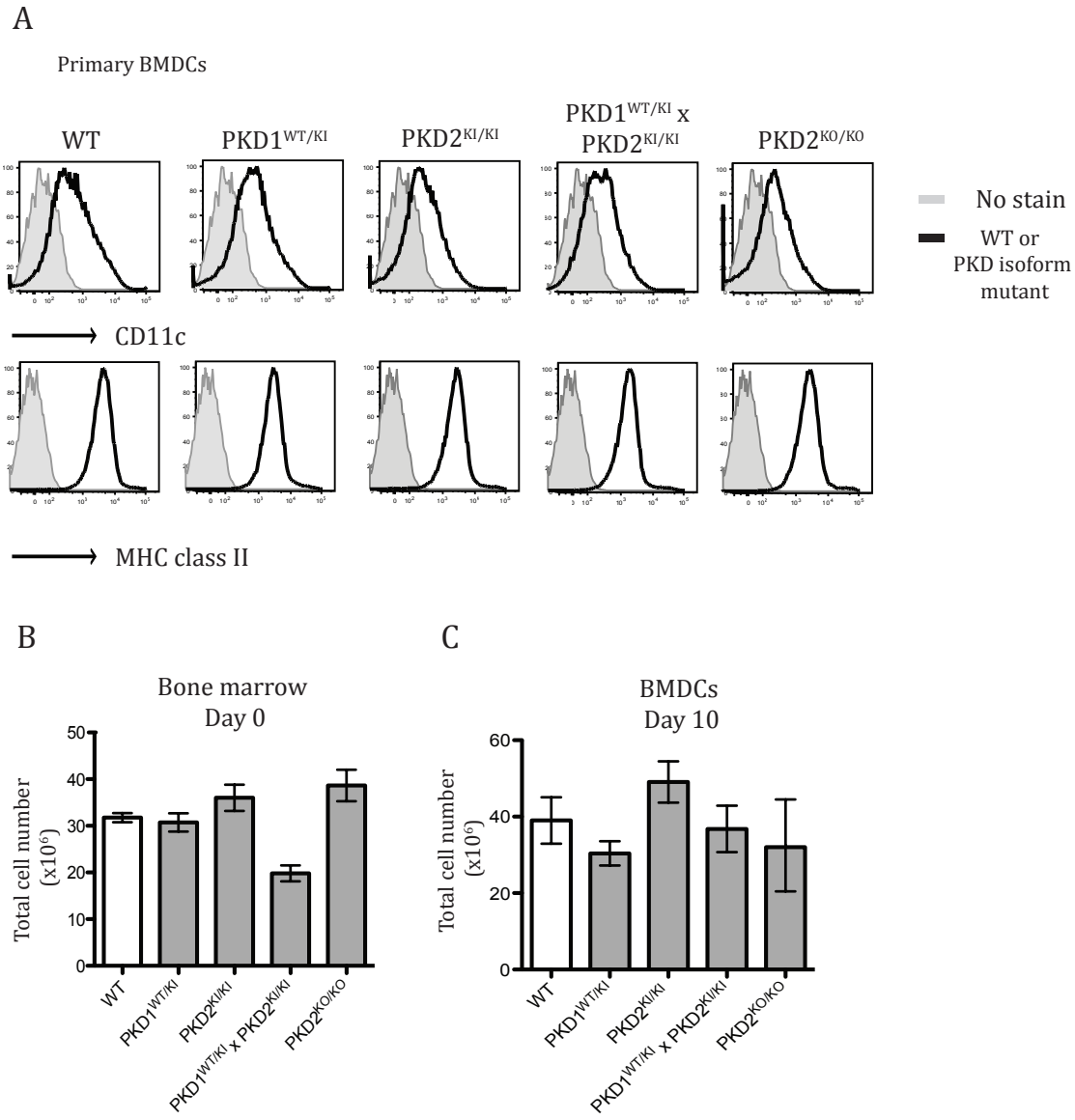

Figure 4.3 Generation and phenotypical analysis of murine BMDCs generated *in vitro* from WT and PKD mutant mice

(A) Flow cytometry analysis of CD11c and MHC class II surface expression on live cells within BMDC on day 10 of culture generated from WT and PKD mutant bone marrow as indicated (n=3). (B) Total cell number (x10^6) from day 0 bone marrow (n=3). (C) Total number (x10^6) of BMDC generated by day 10 of culture. Error bars represent SEM (n=3 biological experiments 9 mice total).

Using the same experimental approach, we moved on to validate and phenotype BMDMOs generated from the bone marrow of PKD transgenic mice. In contrast to BMDCs, BMDMO phenotypically express F4/80 and CD11b upon the cell surface after the culture period (X. Zhang, Goncalves, et al. 2001a).

BMDMO generated from all PKD mutant bone marrow were phenotypically comparable to WT BMDMOs (Figure 4.4A). Microscopically, BMDMOs generated from PKD mutant bone marrow were comparable to WT BMDMOs (data not shown) and the total cell number generated by day 6 of culture from PKD mutant bone marrow was comparable to BMDMOs generated from WT bone marrow (Figure 4.4B-C).

Collectively these data demonstrate that loss of PKD1 or PKD2 catalytic activity does not affect the generation of BMDCs or BMDMO *in vitro*.

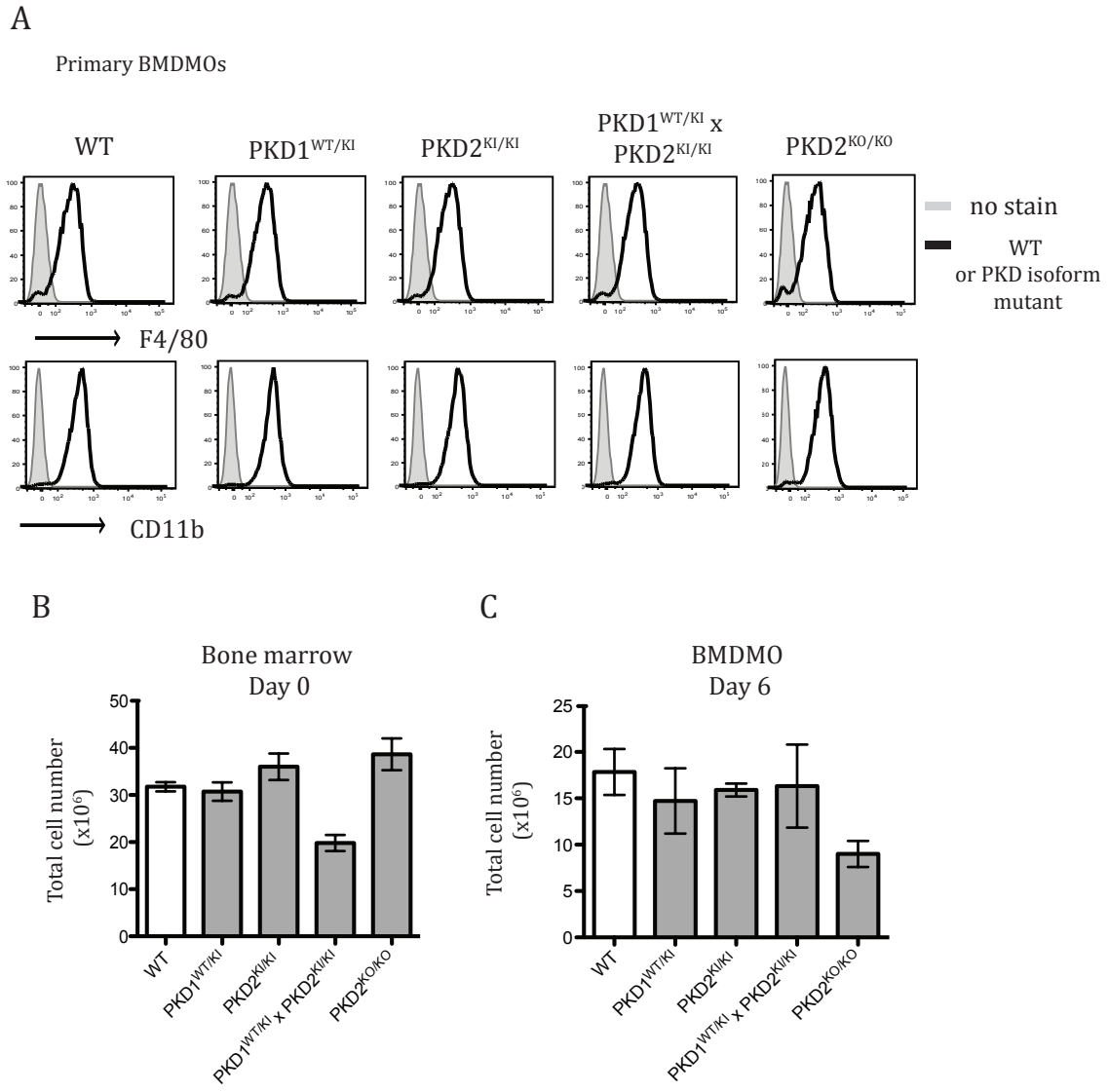

Figure 4.4 Generation and phenotypical analysis of murine BMDMO generated *in vitro* from WT and PKD mutant mice

(A) Representative flow cytometry analysis of F4/80 and CD11b surface expression on day 6 of culture in BMDMOs generated from WT and PKD mutant mice as indicated (B) Total cell number (x10^6) from day 0 bone marrow before BMDMO generation (n=3). (C) Total number (x10^6) of BMDMO generated by day 6 of culture. (n=2 biological experiments 7 mice total).

After phenotypic validation of *in vitro* differentiated primary myeloid cells we sought to determine PKD isoform expression. In order to identify isoforms by western blot, two phospho-specific antibodies against PKD were strategically used. Briefly, p. SER916 antibody recognises the p. SER916 site within the autophosphorylation loop of PKD1 and PKD2 isoforms but not PKD3

(as it lacks an autophosphorylation domain). The p. SER744/748 antibody in contrast recognises PKD1, PKD2 and PKD3 indistinguishably as it recognises trans-phosphorylation residues SER744/748 within the catalytic domain of PKD, which are conserved sites shared by all three isoforms.

Using a combination of these antibodies, cells that lack either catalytic activity of $PKD1^{WT/KI}$, $PKD2^{KI/KI}$ or by depleting the PKD pool even further by use of $PKD1^{WT/KI}$ x $PKD2^{KI/KI}$ mice we confirmed that PKD2 was the dominant isoform expressed in primary murine BMDC by western blot (Figure 4.5A). We achieved this by treatment of cells with pervanadate, a strong phosphatase inhibitor, to induce maximal phosphorylation of all present PKD isoforms. It was clear that heterozygous mutation of PKD1 catalytic activity had little effect on the level of p. SER916 and p. SER744/748, indicating that PKD1 is expressed in low levels. However homozygous mutation of PKD2 within the catalytic domain led to a dramatic reduction in the signal of both p. SER916 and p. SER744/748, which was also true within double knock-in mice $PKD1^{WT/KI}$ x $PKD2^{KI/KI}$. Any detectable expression of PKD3 would be observed in these cells with the p. SER744/748 antibody, which we could not detect. As catalytic activity is severely reduced rather than absolutely abolished in $PKD2^{KI/KI}$ mice, we included BMDCs generated from $PKD2^{KO/KO}$ bone marrow as an additional control. Within $PKD2^{KO/KO}$ BMDCs we could not detect any p. SER916 signal and very low levels of p. SER744/748, in agreement with $PKD2^{KI/KI}$ cells. Finally, p. ERK1/2 was used within these experiments as a positive control of successful cell stimulation, which was evident in all stimulated samples.

We went on to expand these experiments to assess PKD isoform expression in a single cell based assay using phospho-flow cytometry as a more sensitive and quantitative approach to detect p. SER916 levels in BMDC. To achieve strong phosphorylation of all PKD isoforms we stimulated cells with phorbol ester for 30 minutes. As can be seen in Figure 4.5B, $PKD1^{WT/KI}$ BMDCs had comparable levels of p. SER916 activation in response to phorbol ester when compared to WT cells. In contrast, when we compared $PKD2^{KI/KI}$ BMDCs to WT BMDCs we observed an almost 2-fold reduction in the level of p. SER916 upon treatment with phorbol ester. Furthermore, $PKD1^{WT/KI}$ x $PKD2^{KI/KI}$ and $PKD2^{KO/KO}$ BMDCs displayed a 2-fold and 3-fold reduction respectively in the level of p.

SER916 in response to phorbol ester when compared to WT BMDC. Importantly, all cells displayed successful activation as demonstrated by p. ERK1/2 levels, which we co-stained for as a positive control of successful cell stimulation, although p. ERK1/2 levels were reduced in $PKD1^{WT/KI}$ x $PKD2^{KI/KI}$ and $PKD2^{KO/KO}$ BMDCs.

It is also worthwhile mentioning that data from western blots identifying isoform expression of PKD in BMDCs also demonstrated that PKD has high basal phosphorylation within the p. SER916 site in unstimulated samples. This observation is consistent with previous reports of high basal phosphorylation of PKD in other immune cells including CD8+ CTLs (Matthews et al. 2010).

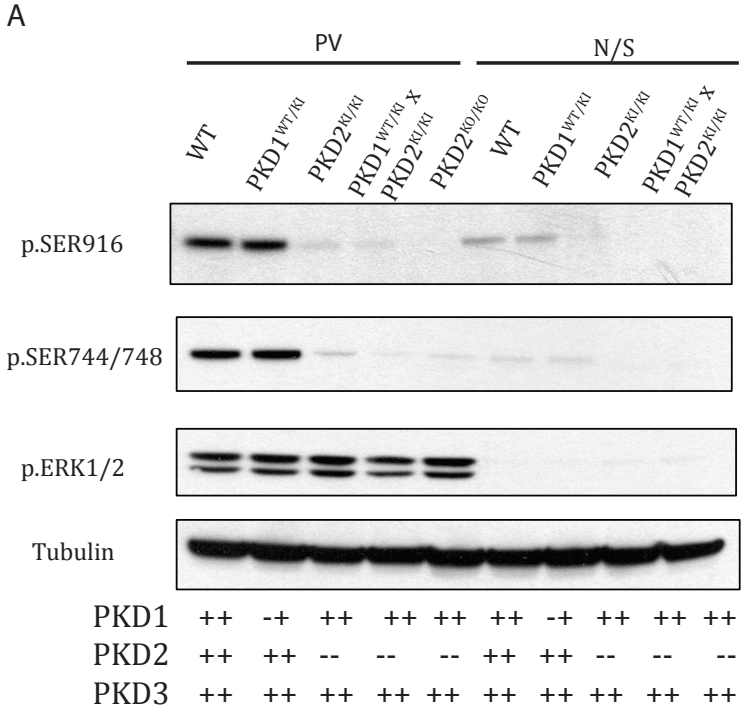

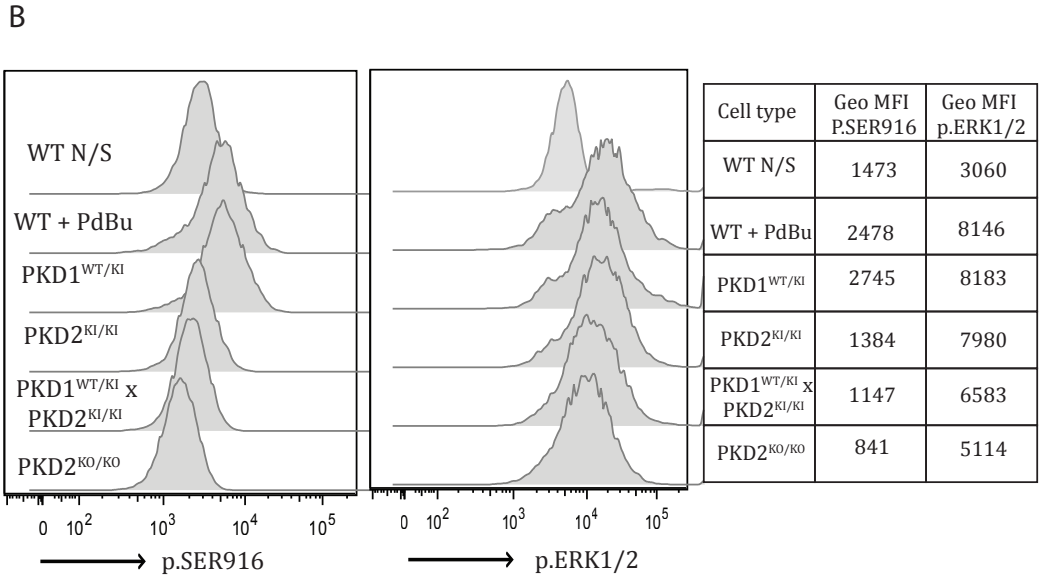

Cell type	Geo MFI P.SER916	Geo MFI p.ERK1/2
WT N/S	1473	3060
WT + PdBu	2478	8146
$PKD1^{WT/KI}$	2745	8183
$PKD2^{KI/KI}$	1384	7980
$PKD1^{WT/KI}$ x $PKD2^{KI/KI}$	1147	6583
$PKD2^{KO/KO}$	841	5114

Figure 4.5 PKD2 is the dominant isoform expressed in primary BMDCs.

(A) Western blot analysis of primary BMDCs generated from WT and PKD mutant mice as indicated unstimulated and stimulated with pervanadate (10nM) for 10 minutes and blotted with p. SER916, p. SER744/748, p. ERK1/2 and β-tubulin as loading control (B) Analysis of intracellular p. SER916 and p. ERK1/2 by phospho-flow cytometry in BMDCs from WT and PKD mutant mice as indicated after stimulation with PdBu (200nM) for 30 minutes. Geometric mean fluorescence intensity (MFI) are shown within the table. Data representative from 3 independent experiments n= 7 mice per genotype.

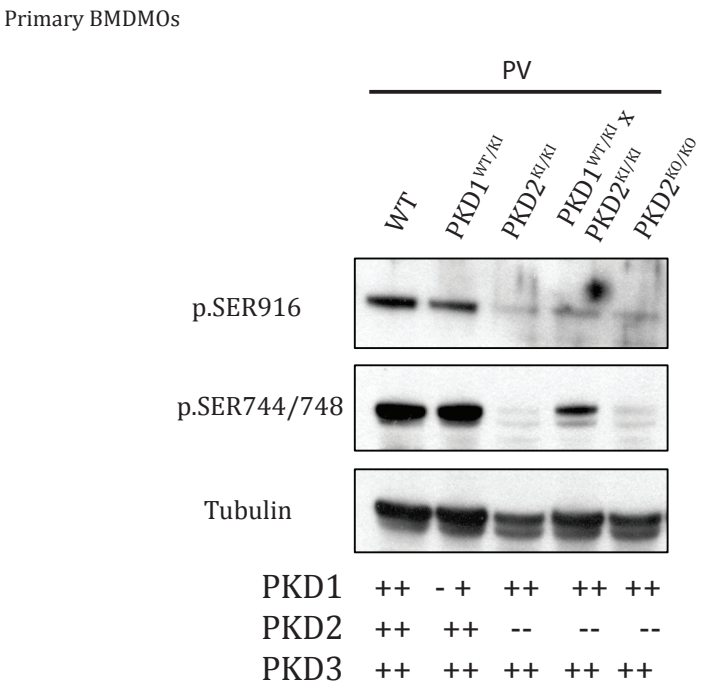

Figure 4.6 PKD2 is the dominant isoform expressed in primary BMDMOS

Western blot analysis of primary BMDMOs generated from WT and PKD mutant mice as indicated treated with pervanadate (10nM) for 10 minutes for detection of p. SER916, p. SER744/748 and β-tubulin. Representative data from 2 independent experiments, n=2 mice per genotype.

Using the same experimental approach, we also confirmed that PKD2 was also the dominant isoform expressed in BMDMO with western blotting (Figure 4.6A). Unfortunately attempts to reproduce this result using phospho-flow were unsuccessful, possibly due to differences in the required fixation and permeabilisation process of BMDMO compared to BMDC. However, it is clear from western blot data that PKD2 is indeed the dominant isoform in similar respect to BMDC where we only observe a reduction in the level of p. SER916 signal in BMDMOs that have either lost PKD2 catalytic activity ($PKD2^{KI/KI}$ and $PKD1^{WT/KI}$ x $PKD2^{KI/KI}$) or indeed in $PKD2^{KO/KO}$ mice.

During our studies two separate companies have generated new and more specific total PKD2 antibodies and we sought to validate the specificity of these antibodies. To achieve this we took a similar approach to previous

experiments whereby we used WT and various PKD mutant mice bone marrow to generate BMDC and BMDMO. One antibody failed to detect any protein at a predicted PKD size (100-120 kDa) and was therefore no longer used in our studies (ST175 antibody (Millipore)). In contrast, a second PKD2 antibody (Calbiochem) proved to accurately detect endogenous PKD2 levels in both BMDMO and BMDC (Figure 4.7A-B) that was severely reduced in $PKD2^{KI/KI}$ or $PKD2^{KO/KO}$ samples. Cells from WT spleen were also included to provide as a reference point for PKD2 expression.

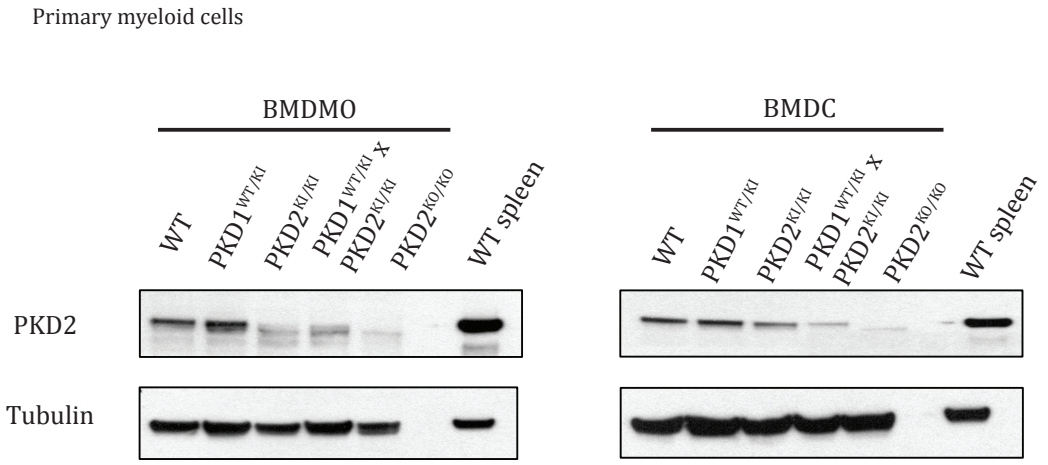

Figure 4.7 PKD2 expression in various myeloid cells using PKD2 specific antibody that differentially recognises PKD2 only.

Western blot analysis of untreated WT splenocytes and WT and PKD mutant BMDMOs and BMDCs as indicated for detection of PKD2 and β-tubulin. Western blot representative of 2 independent experiments.

Collectively these data demonstrate for the first time that PKD2 is the dominant isoform expressed in both primary myeloid cells including murine BMDCs and BMDMO, in agreement with data published from adaptive immune cells. Additionally, these data also demonstrate that both PKD1 and PKD3 isoforms are expressed at very low levels in murine myeloid cells. Importantly, these data demonstrates that abundance of the protein level of distinct isoforms of PKD do not increase after introducing loss of function mutations into one

isoform in a compensatory manner. For example, we do not see an increase in the abundance of PKD1 or PKD3 in both $PKD2^{KI/KI}$ and $PKD2^{KO/KO}$ cells.

Having addressed isoform expression in primary myeloid cells, we next sought to explore the kinetics of PKD activity in response to various stimuli including TLR activation. To assess this, we sought to make further use of the phospho-flow cytometry techniques that were used to assess isoform expression in primary myeloid cells as this provides higher sensitivity over western blotting and has the ability to assess PKD activity at a single cell level. This approach has been successfully used to analyse the activity of PKD in mature T cells in response to TCR engagement (Navarro et al. 2012). The advantage of assessment of PKD activity via phospho-flow cytometry was highlighted in recent publications whereby studies have shown that depending on the context of cell stimuli, e.g. phorbol ester activates the total cellular pool of PKD2, whereas in response to TCR ligation only some cells activate PKD, differences in activation kinetics of PKD can be seen, which are indistinguishable via conventional western blotting. We therefore sought to apply this technique to assess PKD activation in myeloid cells

4.2.2 Assessing PKD activity by p. SER916 phospho-flow is specific for PKD

Before routinely using p. SER916 antibody during a series of phospho-flow experiments we sought to confirm that this antibody specifically detected changes in PKD activity. In particular, we also wished to assess this in primary myeloid cells, which are notoriously auto-fluorescent when used during flow cytometry or microscopy.

To validate the use of p. SER916, we used BMDCs generated from WT, $PKD2^{KI/KI}$ and $PKD2^{KO/KO}$ bone marrow, unstimulated and stimulated with phorbol ester for 30 minutes (Figure 4.8A), p.ERK1/2 was used a positive control. It can be seen that WT BMDC stimulated with phorbol ester have a clear shift demonstrating increase of p. SER916 levels, in contrast, p.SER916 levels within $PKD2^{KI/KI}$ and $PKD2^{KO/KO}$ BMDCs remained unchanged in stimulated samples despite strong p.ERK1/2 activation.

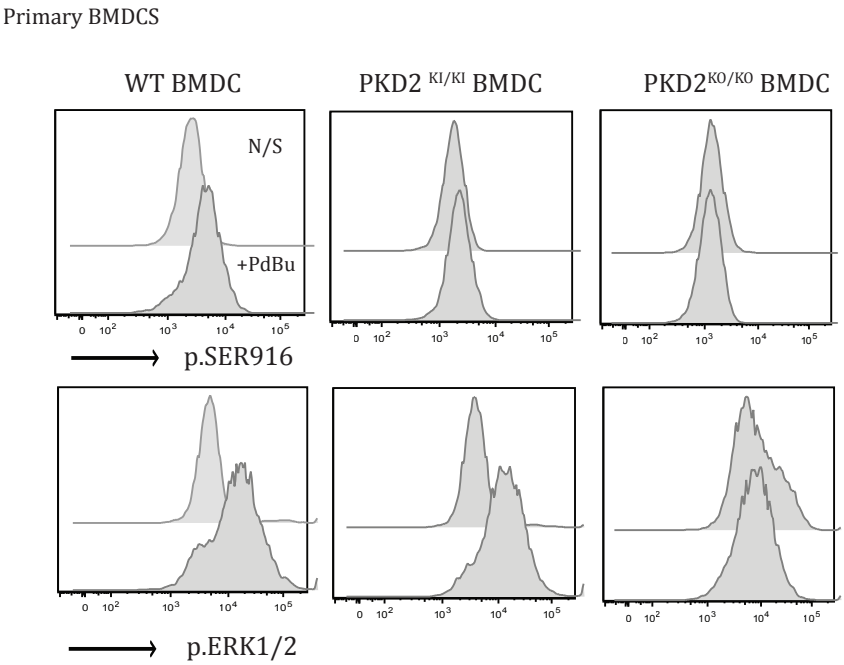

Figure 4.8 p. SER916 PKD antibody effectively detects activation of PKD using phospho flow in primary BMDC.

Phospho flow analysis of p. SER916 PKD and p. ERK1/2 in BMDC generated from WT and PKD mutant mice unstimulated and stimulated with PdBu (200nM) for 30 minutes. Representative flow data shown from 2 independent experiments.

4.2.3 Basal activity, activation and inhibition of PKD in myeloid cells

During initial experiments investigating PKD activity and regulation in myeloid cells it became apparent that primary myeloid cells displayed obvious basal PKD activity. We began to characterise this basal activity within myeloid cells using a murine macrophage cell line, RAW264.7 cells, using phospho-flow cytometry. Treatment of RAW264.7 cells with phorbol ester for 30 minutes induced an increase in p.SER916 levels whereas treatment of RAW264.7 cells with PKD inhibitor 12a compound led to an obvious reduction when compared to untreated samples (Figure 4.9A). We also confirmed specificity of p. ERK1/2 staining in RAW264.7 by treatment of RAW264.7 cells with MEK (MKK1; MAPK kinase) inhibitor PD184352, which selectively suppresses the ERK pathway (Mody et al. 2001). As can be seen in Figure 4.9B, RAW264.7 cells treated with 1μM PD184352 displayed obvious reductions in the level of p. ERK1/2, whereas cells treated with phorbol ester had increased p.ERK1/2 activity. Additionally,

the reduction of basal p.SER916 levels was not limited to one PKD inhibitor as treatment of unstimulated RAW264.7 cells with all three PKD inhibitor compounds including 12a, CRT101 and CRT051 for 1 hour led to a reduction in detectable levels of p. SER916 (Figure 4.9C). PKD inhibitor compounds and the MAPK inhibitor were subsequently used in all phospho-flow experiments as controls.

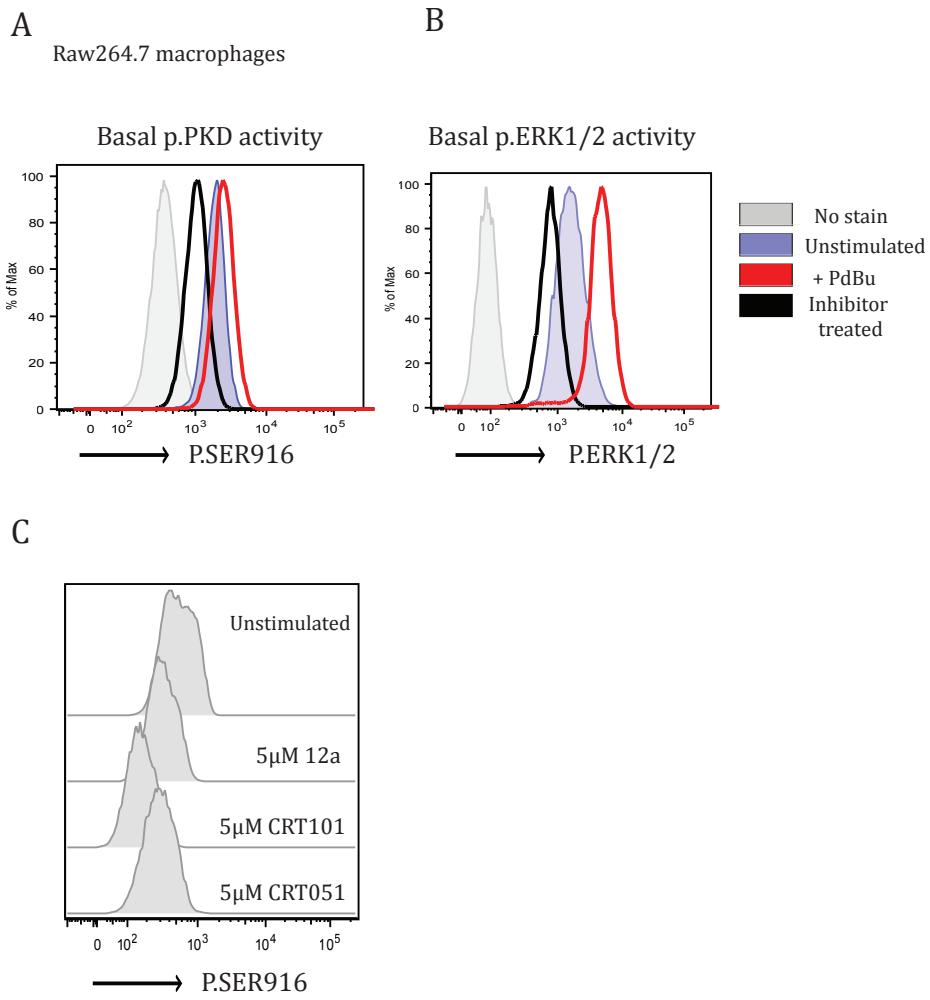

Figure 4.9 Basal PKD and p. ERK1/2 phosphorylation in RAW264.7 macrophages

(A) Flow cytometry of p. SER916 PKD activity in cells treated with 5μM 12a for 1 hour or stimulated with PdBu (200nM) for 30 minutes (B) Flow cytometry of p. ERK1/2 in cells treated with MAPK inhibitor PD184352 (1μM) for 1 hour or stimulated with PdBu for 30 minutes (C) Flow cytometry assessing p. SER916 in unstimulated cells treated with 5μM of PKD inhibitors 12a, CRT101 and CRT051 for 1 hour. Representative flow cytometry data from 3 independent experiments.

Following this, we also wanted to assess basal phosphorylation levels of PKD in primary myeloid cells including BMDCs. This was achieved using a two-fold approach, firstly by comparing unstimulated WT BMDCs with PKD2$^{KI/KI}$ BMDCs then secondly by using pharmacological inhibition of PKD in WT BMDCs. As can be seen in Figure 4.10A, unstimulated PKD2$^{KI/KI}$ BMDCs show an obvious reduction in the level of p. SER916 when compared to WT BMDCs. This change in basal activity is comparable to WT BMDC treated with 5μM of CRT051, which blocks p. SER916 activity (Figure 4.10B).

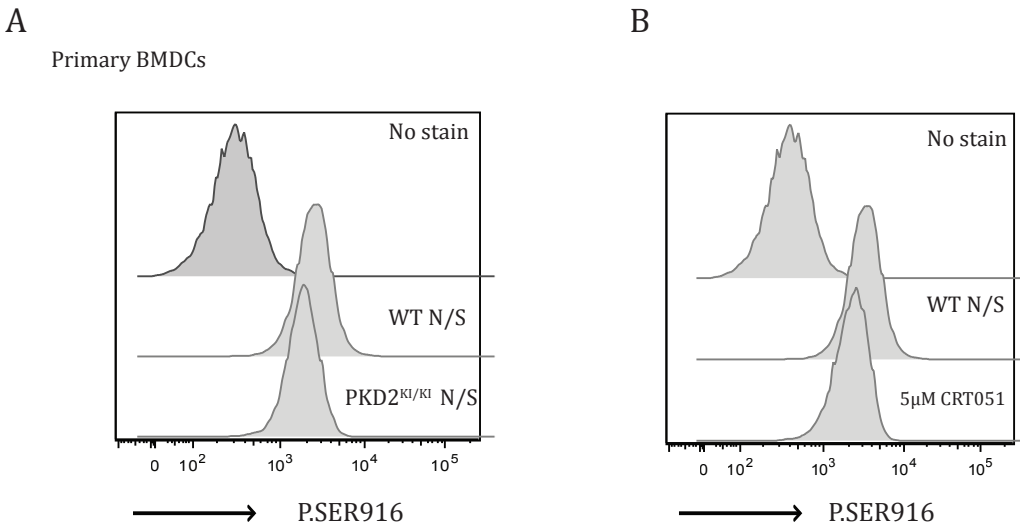

Figure 4.10 Basal PKD activity in primary BMDCs

(A) Detection of intracellular p. SER916 by flow cytometry in non-stimulated (N/S) WT BMDC and PKD2$^{KI/KI}$ BMDCs. (B) Detection of intracellular p. SER916 by flow cytometry of WT BMDCs non-stimulated (N/S) and WT BMDCs treated with 5μM CRT051 PKD inhibitor for 1 hour. Representative data from three independent experiments.

Following the observation that the macrophage cell line RAW264.7 cells had basal PKD activity we went on to investigate the activation and kinetics of PKD activation in these cells. Firstly we examined activation of PKD after stimulation with phorbol ester. Upon stimulation we saw strong activation of PKD (p.SER916) at 15 minute time point, this strong activation was maintained

at 45 minutes stimulation (Figure 4.11A). We also observed robust activation of p.ERK1/2.

After confirming we could accurately assess activation of PKD via p. SER916 in RAW264.7 macrophages we moved on to assess the efficiency of PKD inhibitors to block the induction of phorbol ester induced PKD activation. RAW264.7 cells treated with phorbol ester from 15-45 minutes show strong activation of PKD p. SER916 which correlated with an increased in levels of p.ERK1/2 levels (Figure 4.11A). In contrast, RAW264.7 cells pretreated with 5μM of 12a, CRT101 or CRT051 for 1 hour fail to strongly induce p.SER916 levels upon phorbol ester treatment yet p.ERK1/2 activation remains intact (Figure 4.11B).

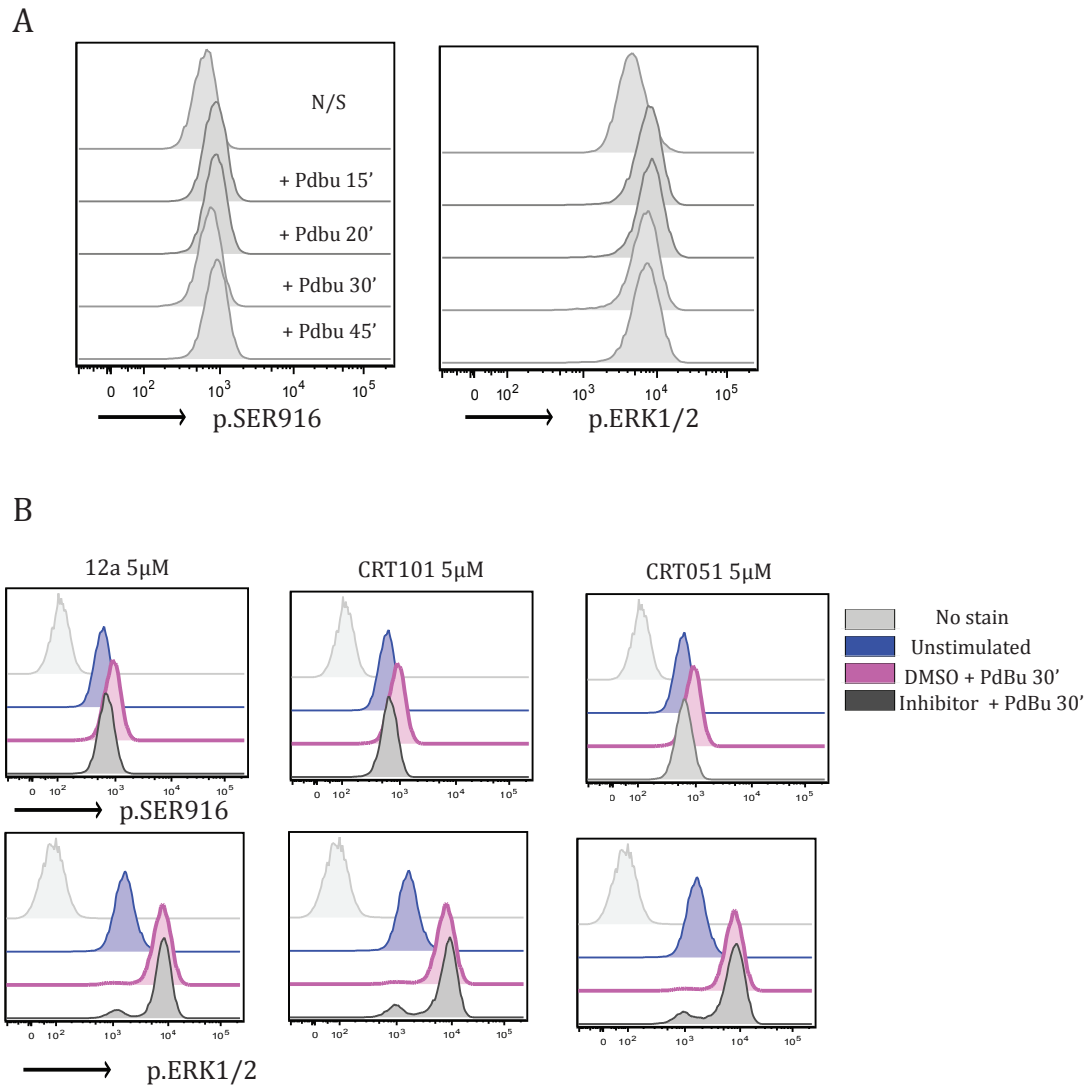

Figure 4.11 Activation and inhibition of PKD activity in RAW264.7 macrophages using small molecule inhibitors of PKD.

(A) Detection of intracellular p. SER916 PKD activity by flow cytometry in RAW264.7 macrophages with PdBu (200nm) for indicated time points, p. ERK1/2 was used as an indication of successful activation of cell signalling pathways (n=3). (B) Flow cytometry analysis of p. SER916 PKD and p. ERK1/2 activity after pre-treatment of cells for 1 hour with 5µM of PKD inhibitor compounds 12a, CRT101 and CRT051 before 30 minute stimulation with PdBu (200nM), DMSO was used as a vehicle control (n=3).

Collectively, these data demonstrates that various myeloid cells including RAW264.7 cell line and primary BMDCs display high levels of basal PKD activity as assessed by level of P.SER916. This basal activity can be removed by mutation of the serine residues within PKD2, as demonstrated with PKD2$^{KI/KI}$ cells but pharmacological inhibition of PKD by three different compounds also has a

similar effect. Additionally, we did note some off target effects of all three PKD compounds in regard to ERK1/2 signalling pathways highlighting that caution should be used with these compounds.

4.2.3.1 Assessing activation of PKD by TLR ligation

After establishing tools to accurately and confidently identify activation of PKD within myeloid cells, we sought to address PKD activation in response to PRR ligation. Additionally, we also wanted to address the role of PKD in the effector functions of myeloid cells including cytokine production. As discussed, previous reports have implicated PKD within innate immune cells including PKD activation downstream of various PRRs including TLRs that use the adaptor protein Myd88 within myeloid cells but also epithelial cells (Ren et al. 2009). (Ivison et al. 2007) (J.-E. Park et al. 2008) (Murphy et al. 2007) Steiner:2010gm}. The emerging evidence that PKD isoforms are involved in inflammatory signaling and cytokine production in innate immune cells led us to address these observations with PKD transgenic animals but also with more specific pharmacological inhibitors for PKD.

To begin to address this, we assessed if PKD becomes activated in response to TLR4 ligation by lipopolysaccharide (LPS) within RAW264.76 cells largely due to the ease of generation of larger cell numbers during culture, in contrast to lower cell numbers generated by generating cells *in vitro* from murine bone marrow. Stimulation of RAW264.7 cells with LPS for indicated time points led to a slight increase in PKD activation when assessed by p. SER916 flow cytometry. p.ERK1/2, levels were used as a positive control within these experiments as p.ERK1/2 is known to be activated downstream of TLR4 ligation (Weinstein et al. 1992). Indeed within our experiments LPS resulted in activation of p.ERK1.2 (Figure 4.12A).

Furthermore, increasing dose of LPS (100ng/ml - 1μg/ml) did enable us to see a stronger PKD activation when assessed by p. SER916 flow cytometry (data not shown). These results were comparable upon western blot analysis of

p. SER916 and p.ERK1/2, although high basal levels of p.SER916 within RAW264.7 cells make western data more difficult to assess (Figure 4.12).

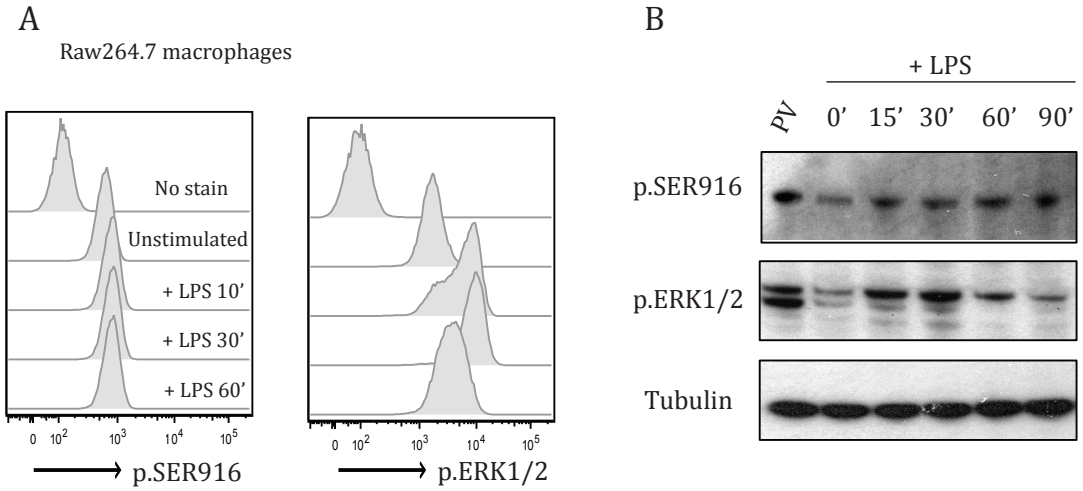

Figure 4.12 LPS stimulation via TLR4 does not strongly activate PKD in RAW264.7 macrophages

(A) Flow cytometry analysis of intracellular p. SER916 and p. ERK1/2 in RAW264.7 macrophages stimulated with LPS (500ng/ml) for indicated time points (B) Western blot analysis of RAW264.7 macrophages stimulated with LPS (500ng/ml) for indicated time points and blotted for p. SER916, p. ERK1/2 and β-tubulin as loading control.

PKD activation in response to TLR ligation in primary BMDCs was also investigated. WT BMDCs stimulated with LPS for 15-90 minutes showed a slight activation to LPS via p. SER916 induction when assessed by western blotting (Figure 4.13A). Furthermore, phospho-flow cytometry also demonstrated that whilst phorbol ester stimulation strongly induced p. SER916 in BMDCs, LPS stimulation did weakly induce p. SER916 (Figure 4.13B). We also expanded these cell stimulations to include TLR3 and TLR9 ligation in addition to TLR4. As can be seen in Figure 4.13C, we saw a weak activation of p. SER916 on PKD by LPS stimulation however TLR3 or TLR9 stimulation with either PolyI:C or CPG respectively did not activate p.SER916. Finally, expanding our time point to assess PKD activation in response to LPS did not reveal any time-dependent activation of PKD by phospho-flow at between 15-90 minutes although again we did observe a weak activation of PKD by LPS (Figure 4.13D).

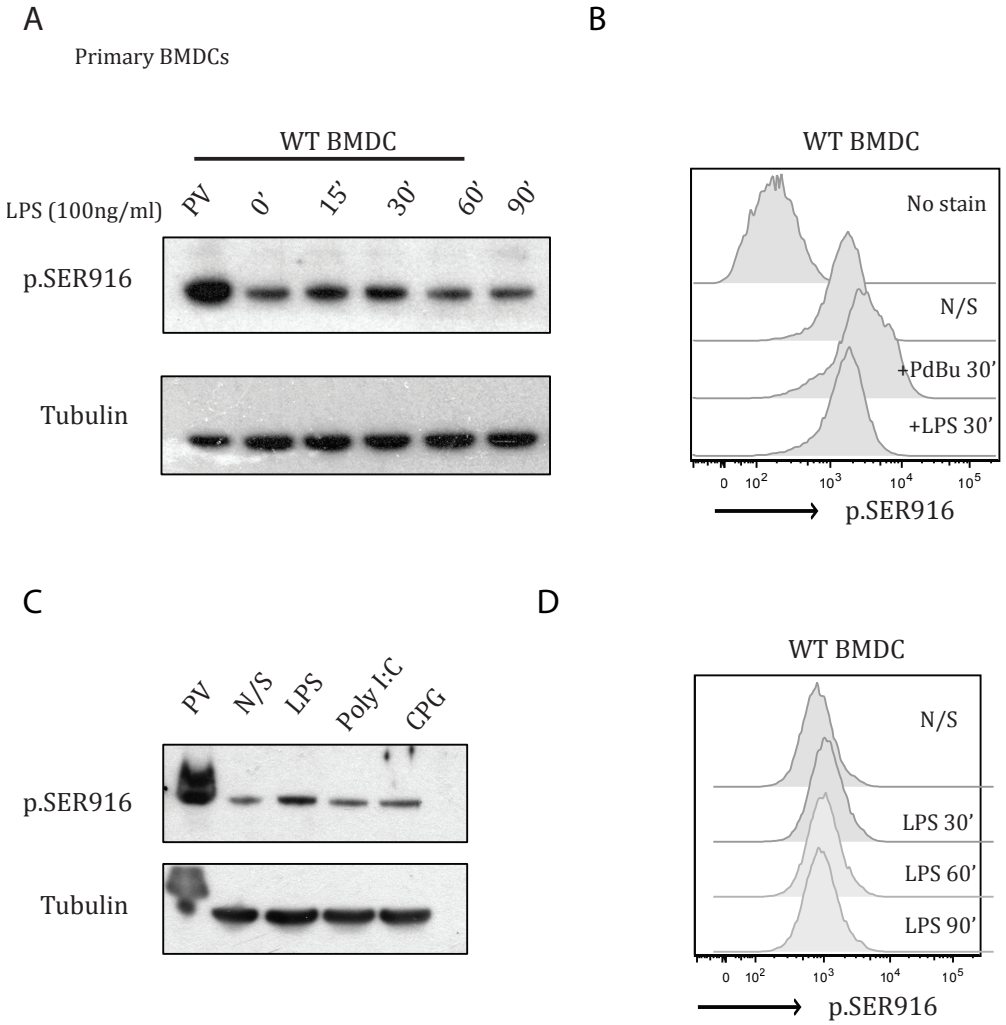

Figure 4.13 TLR3 TLR4 and TLR9 ligation does not strongly activate PKD in primary BMDCs

(A) Western blot of WT BMDCs stimulated with LPS (100ng/ml) for indicated time points and blotted for p. SER916 and β-tubulin, 10-minute pervanadate (10nM) stimulation was used as a positive control. (B) Assessment of intracellular p. SER916 by flow cytometry in WT BMDCs after stimulation with PdBu (200nM) and LPS (100ng/ml) for 30 minutes. (C) Western blot of WT BMDCs stimulated with LPS (100n/ml), poly I:C (50μg/ml) and CPG (1μM) for 30 minutes and blotted for P.SER916 and β-tubulin. (D) Flow cytometry of intracellular p. SER916 in WT BMDCs stimulated LPS (100ng/ml) for indicated time points. Data is representative of 3 independent experiments.

Previous reports have linked PKD activation to multiple TLRs, however no studies have investigated if PKD is activated downstream of other PPRs such as C-type lectins. Dectin-1 is one such C-type lectin that recognises β-glucan, a component of yeast cell wall, and activates downstream signalling pathways mediating an immune response to fungal pathogens (Taylor et al. 2006). Zymosan is a preparation from the yeast cell wall which is frequently used to study Dectin-1 responses, it should be noted however that zymosan also promotes TLR2 activation in cooperation with Dectin-1 (Brown & Gordon 2001) (Brown et al. 2002) (Gantner et al. 2003). Emerging evidence has demonstrated that stimulation of DCs with zymosan triggers an intracellular calcium (Ca2+) flux, mediated by PLCγ (Xu et al. 2009). Studies have also shown that PKD activation can occur not only by accumulation of DAG but also by elevation of Ca2+, in absence of other cell stimulation (Kunkel et al. 2007). Accordingly, we sought to explore whether stimulation of myeloid cells using zymosan led to activation of PKD.

Our preliminary data reveals robust activation of PKD in response to zymosan stimulation in both RAW264.7 macrophages (Figure 4.14A) but also within primary BMDMOs (Figure 4.14B). We also observed phosphorylation of class IIa HDACs (4-5-7), a known downstream substrate of PKD in both RAW264.7 macrophages and primary BMDMO.

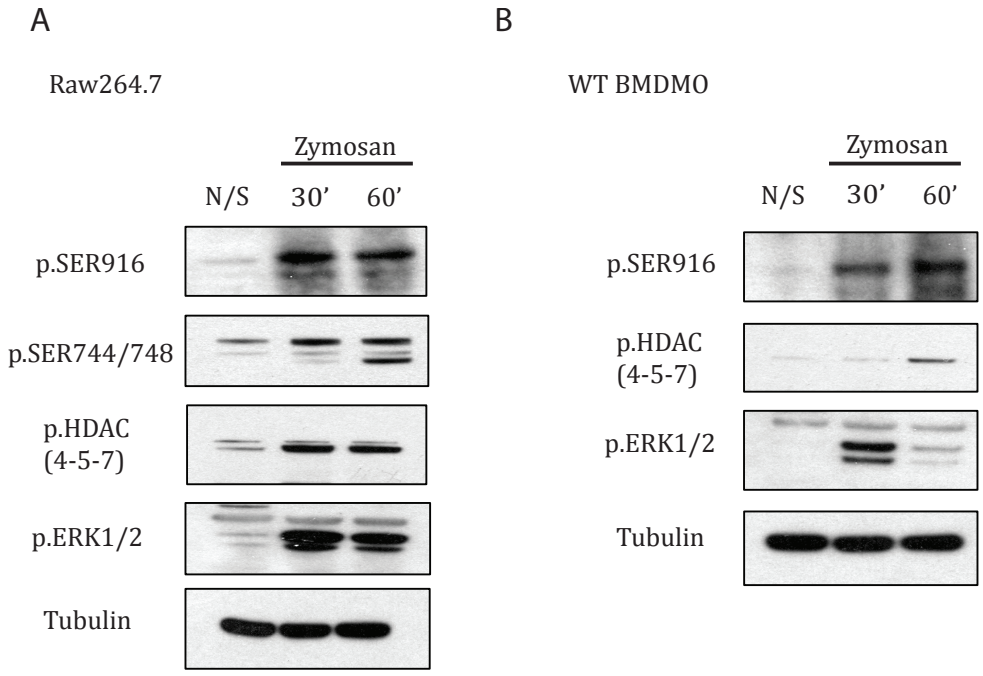

Figure 4.14 Zymosan activates PKD in Raw264.7 macrophages and primary BMDMOs

(A) Western blots of Raw264.7 macrophages stimulated with zymosan (200mg/ml) for indicated time points and blotted for p. SER916, p. SER744/748, p.HDAC (4-5-7), p.ERK1/2 and β-tubulin (n=2). (B) Representative Western blots of WT BMDMOs stimulated with zymosan (200mg/ml) for indicated time points and blotted for p. SER916, p. HDAC (4-5-7), p. ERK1/2 and β-tubulin. Preliminary data is from one independent experiment. *Cell lysates kindly provided by Vicky McGuire, University of Dundee.*

Collectively, these data reveals the surprising result of poor activation of PKD by TLR4 ligation in both the macrophage cell line RAW264.7 but also in primary BMDCs, by both assessed by western blotting but also with more sensitive methods including phospho-flow cytometry. Furthermore, TLR3 or TLR9 ligation within RAW264.7 cells did not result in a strong induction of PKD. Interestingly however, preliminary data suggest robust activation of PKD upon stimulation with zymosan, which activates the C-type lectin Dectin-1 and TLR2.

4.2.4 Pharmacological inhibition of PKD reduces cytokine production in myeloid cells

It has been reported within the literature that knockdown of PKD or pharmacological inhibition of PKD leds to reduced cytokine production in myeloid cells (J.-E. Park et al. 2009b). We also wanted to address if this was the case with novel and more specific inhibitors of PKD. To achieve this we first treated RAW264.7 cells with increasing doses of 12a, CRT101 and CRT051 compounds for 1 hour before treating with 500ng/ml LPS for 24 hours, analysing production of IL-10 and IL-6 cytokines within the supernatant. Unfortunately IL-12p40 production could not be assessed in any experiments using RAW264.7 cells as do not secrete IL-12 in response to LPS treatment (Matsuura et al. 2003). Treatment of RAW264.7 cells with increasing concentrations of each compound resulted in significant reduction in the production of IL-10 in a dose dependent manner (Figure 4.15 A-C). Additionally, all three compounds also resulted in a significant reduction of LPS induced IL-6 production, although this reduction was not in a dose-dependent manner (Figure 4.16A-C).

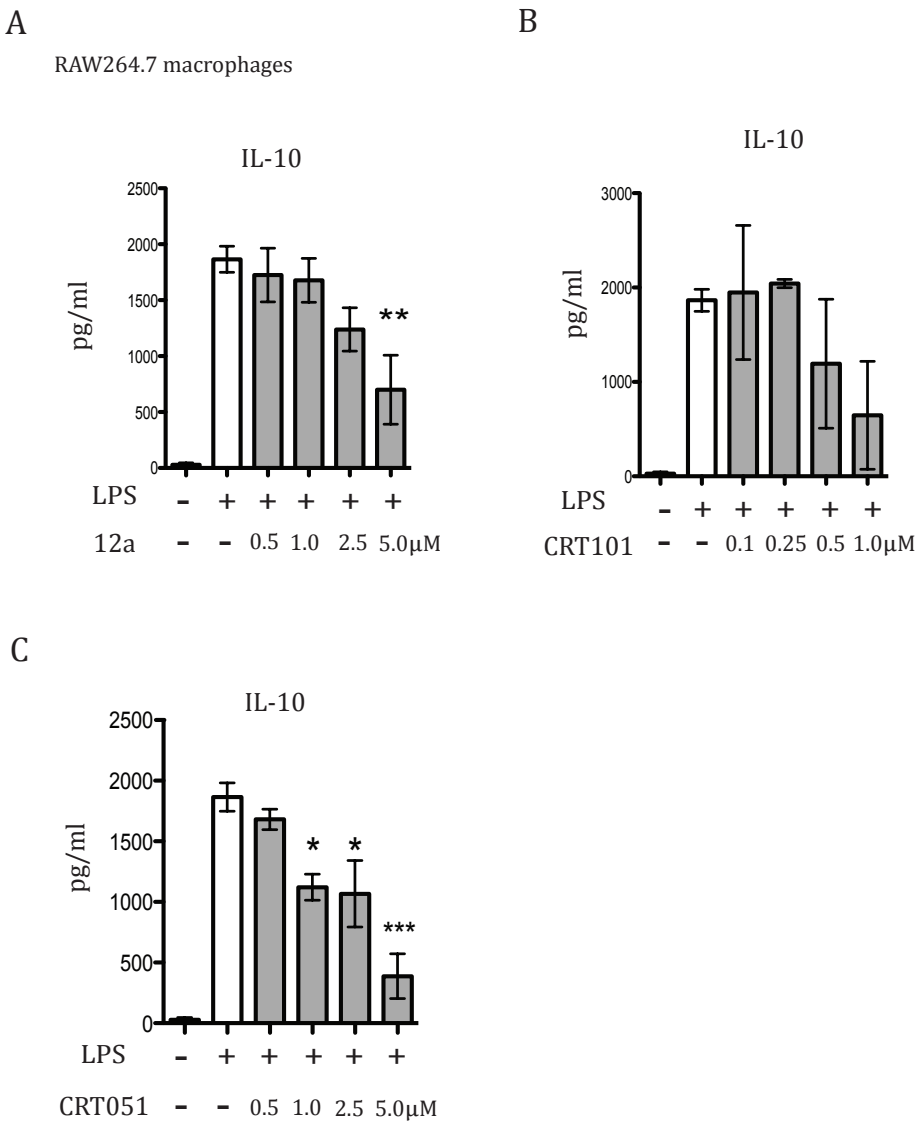

Figure 4.15 PKD inhibitors reduce LPS induced cytokine production in RAW264.7 cells

Analysis of IL-10 production by RAW264.7 macrophages by ELISA in cells treated with increasing concentrations of (A) 12a (B) CRT101 and (C) CRT051 and stimulated with LPS (500ng/ml). *p≤0.05, ** p≤0.01, p≤0.001 analysed by one-way ANOVA with Dunnett *post-hoc* test. Error bars represent SD. (Representative data of 3 independent biological experiments).

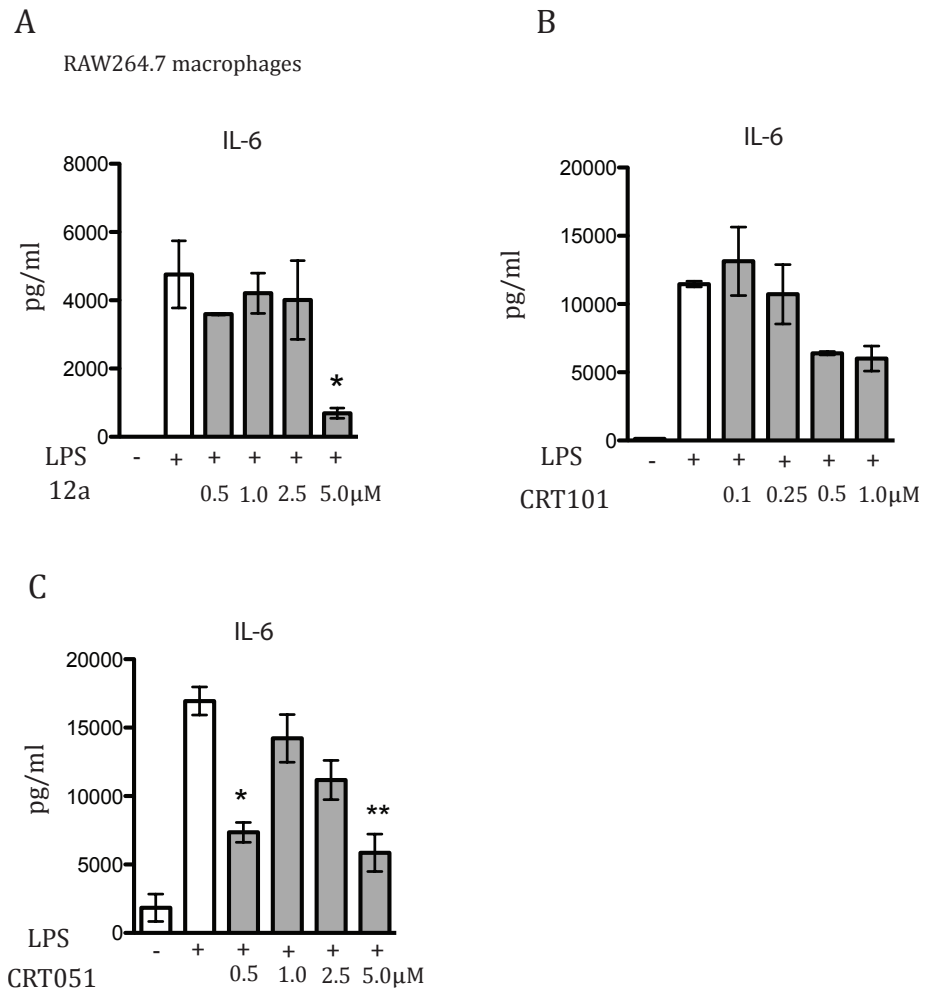

Figure 4.16 PKD inhibitors reduce LPS induced IL-6 production in RAW264.7 cells

Analysis of IL-6 production by RAW264.7 macrophages by ELISA in cells treated with increasing concentrations of (A) 12a (B) CRT101 and (C) CRT051 and stimulated with LPS (500ng/ml). *p≤0.05, ** p≤0.005 analysed by one-way ANOVA with Dunnett *post-hoc* test. Error bars represent SD (Representative data of 3 independent biological experiments).

Collectively, these data reveals that the pharmacological inhibition of PKD by three structurally distinct compounds results in significantly reduced cytokine production, including IL-10 and IL-6, in response to LPS in RAW264.7macrophages. In agreement with data shown in the previous chapter, pharmacological inhibition of primary T- lymphocytes also demonstrated significantly reduced cytokine production, including IL-2 and IFN-γ in response

to TCR stimulation, signifying a general role for PKD mediated cytokine production downstream of multiple immune receptors.

4.2.5 Analysis of myeloid cell development in PKD2$^{KI/KI}$ mice

In regard to murine mature lymphocyte development, loss of PKD2 catalytic activity is dispensable for normal B and T cell development in the bone marrow and thymus respectively (Matthews et al. 2010). In regard to PKD isoform expression in murine myeloid cells, within this chapter we have demonstrated that comparable to cells from the adaptive immune system, PKD2 is also dominantly expressed in innate immune cells including DCs and macrophages. Although we observed no differences within the phenotype of cells from the culture of both BMDCs and BMDMO's from PKD2$^{KI/KI}$ *in vitro* we wished to address if loss of PKD2 catalytic activity had any effect on the development of myeloid cells in PKD2$^{KI/KI}$ mice within the bone marrow, or indeed with subsequent homing to peripheral lymphoid tissues such as the spleen.

To address this we assessed two major DC populations found within the bone marrow and spleen including cDCs and pDCs, which can be assessed by expression of cell specific markers. As previously discussed, the term cDCs largely refers to all other DC subsets that are not pDCs. cDCs have an enhanced ability to sense infection and tissue injury and largely function to capture, process and present environmental antigen, whether pathogenic or self-antigen, to promote an immune response or tolerance respectively, to T cells. In contrast, pDCs represent a small subsets of DCs that play a significant role in anti-viral immunity, largely due to the presence of endosomal TLR7 and TLR9 for detection of foreign nucleic acid, as well as their ability to produce large amounts of type I IFN, including IFNα and IFNβ. In regard to development within the bone marrow, different groups have uncovered evidence that both cDCs and pDCs in mice arise from a clonogenic precursor and differentiate within the bone marrow under instruction of specific cytokines and transcription factors. After differentiation, cDCs and pDCs migrate from the bone marrow to the periphery. Additionally, the role of PKD catalytic activity for the development of neutrophils

remains unaddressed within the literature therefore we assessed neutrophil and macrophage development *in vivo* within the bone marrow and subsequent population of these myeloid subsets within the spleen of PKD2$^{KI/KI}$ mice.

4.2.5.1 Analysis of the development of conventional and plasmacytoid DCs in PKD2$^{KI/KI}$ mice tissues

Analysis of tissue size from PKD2$^{KI/KI}$ mice revealed no obvious differences in total cell number (x10^6) obtained from the bone marrow or the spleen, demonstrating that loss of PKD2 catalytic activity does not affect cellularity of these lymphoid tissues (Figure 4.17A). During these experiments we did note a visible and significant increase in size and cellularity of mesenteric lymph nodes and Peyers patches within the small intestine of PKD2$^{KI/KI}$ mice, which is discussed in the next chapter.

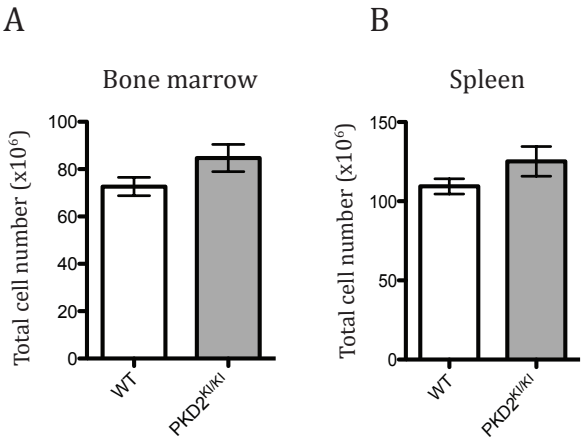

Figure 4.17 Analysis of tissue size in PKD2$^{KI/KI}$ mice

Total cell number (x106) obtained from age and sex matched WT and PKD2$^{KI/KI}$ mice; (A) Bone marrow (B) Spleen. Error bars represent SD (data of 3 independent biological experiments n= 9 mice per group).

Next, we assessed the development of cDC and pDC subsets within the bone marrow of PKD2$^{KI/KI}$ *ex-vivo*. cDCs were defined as CD11c^{high} Siglec-H^{low} and pDCs were defined as CD11c^{high}Siglec-H^{high} and MHC class II^{low}. Figure 4.18A-B, shows development of both cDCs and pDCs within the bone marrow of PKD2$^{KI/KI}$ mice were normal when compared to WT mice with no significant changes in the % frequency of either cell subset. Furthermore, MHC class II expression on PKD2$^{KI/KI}$ pDCs was also comparable to WT pDCs (Figure 4.18C).

The cDC subset can also be further divided into two populations including CD4+ cDCs and CD8+ cDCs, both of which carry out unique functions within the immune system. CD4+ cDC have been shown to have strong tendencies to activate CD4+ T cells (Allenspach et al. 2008) (Mount et al. 2008), whereas CD8+ cDCs are well known for their ability to perform cross presentation of antigen which is important in anti-viral immune responses but for maintenance of tolerance towards self (Haan et al. 2000) (Schliehe et al. 2011). We assessed these populations in the bone marrow of PKD2$^{KI/KI}$ mice and observed no significant difference in the % frequency of either CD4+ or CD8+ cDC subsets (Figure 4.18D-E).

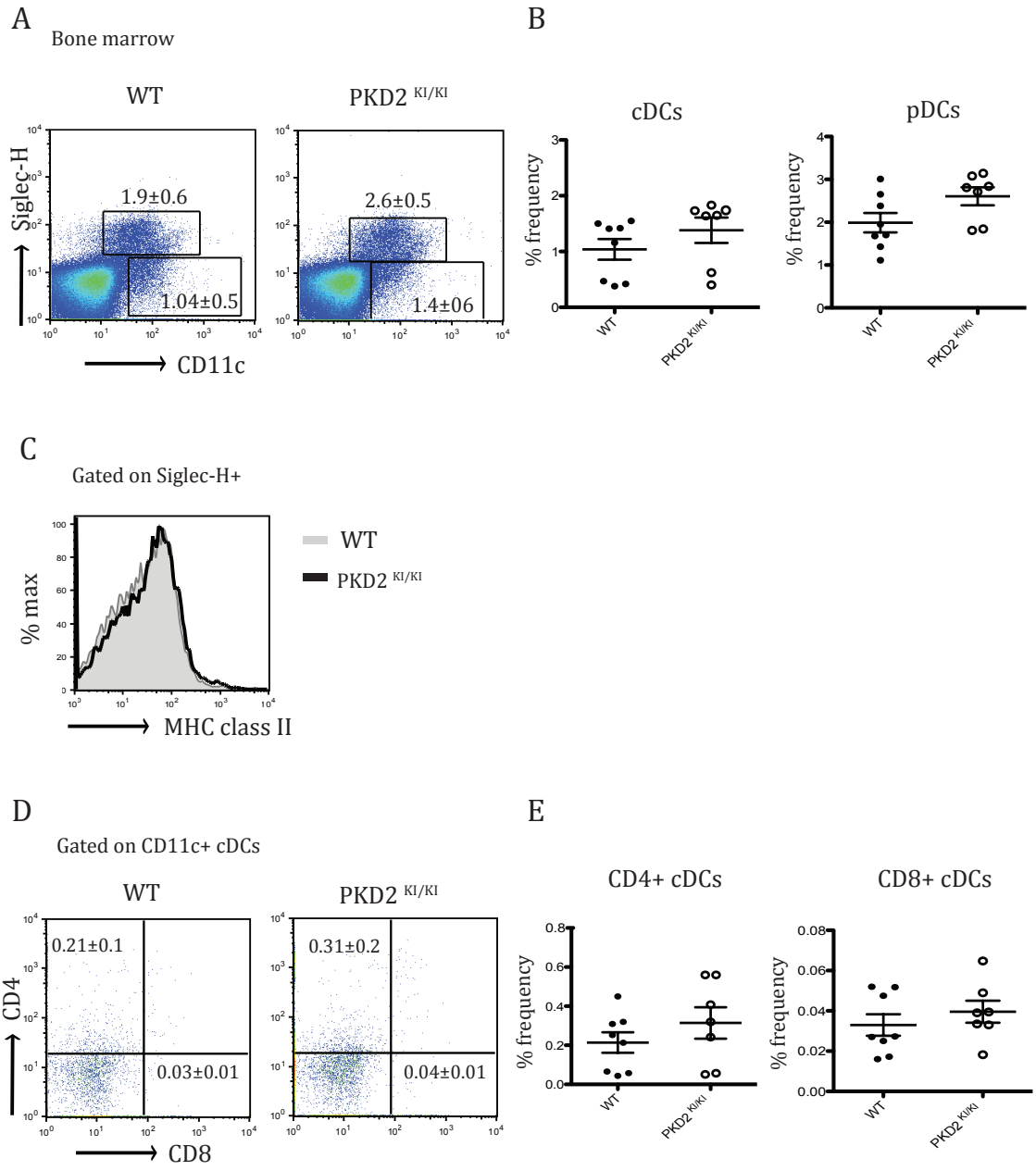

Figure 4.18 Conventional and plasmacytoid DC subsets are normal within the bone marrow of PKD2$^{KI/KI}$ mice

(A) Representative dot plots showing cDC and pDC subsets within the spleen of WT and PKD2$^{KI/KI}$ mice shown by Siglec-H and CD11c surface expression by Flow cytometry. Numbers represent average % frequency and SD. (B) Combined data showing % frequency of cDCs and pDC (C) Overlayed representative histogram of WT and PKD2$^{KI/KI}$ pDCs showing expressing of MHC class II on the cell surface (D) Representative dot plots showing CD4+ and CD8+ cDC subpopulations (gated on CD11c) within bone marrow of WT and PKD2$^{KI/KI}$ mice. (E) Combined data showing % frequency of CD4+ cDCs and CD8+ cDCs. Error bars represent SD. Data is from 3 independent biological experiments, n=8 mice per genotype.

After confirming that the development of DC subsets within the bone marrow of $PKD2^{KI/KI}$ mice were comparable to WT mice we sought to assess these populations within the spleen. This offered insight into the requirement for PKD2 catalytic activity for normal migration of these subsets from the bone marrow to peripheral lymphoid tissues. Figure 4.19A-B shows that both cDC and pDC % frequencies within the spleen of $PKD2^{KI/KI}$ mice were normal when compared with WT mice. It is known that pDCs upon migration from the bone marrow into the periphery upregulate surface expression of MHC class II. This process is also normal in $PKD2^{KI/KI}$ pDCs when compared to WT pDCs within the spleen (Figure 4.19C). Additionally, we assessed CD4+ and CD8+ cDC subsets within the spleen and found no difference in the % frequencies of these populations in PKD2KI/KI mice when compared to WT mice (Figure 4.19D-E).

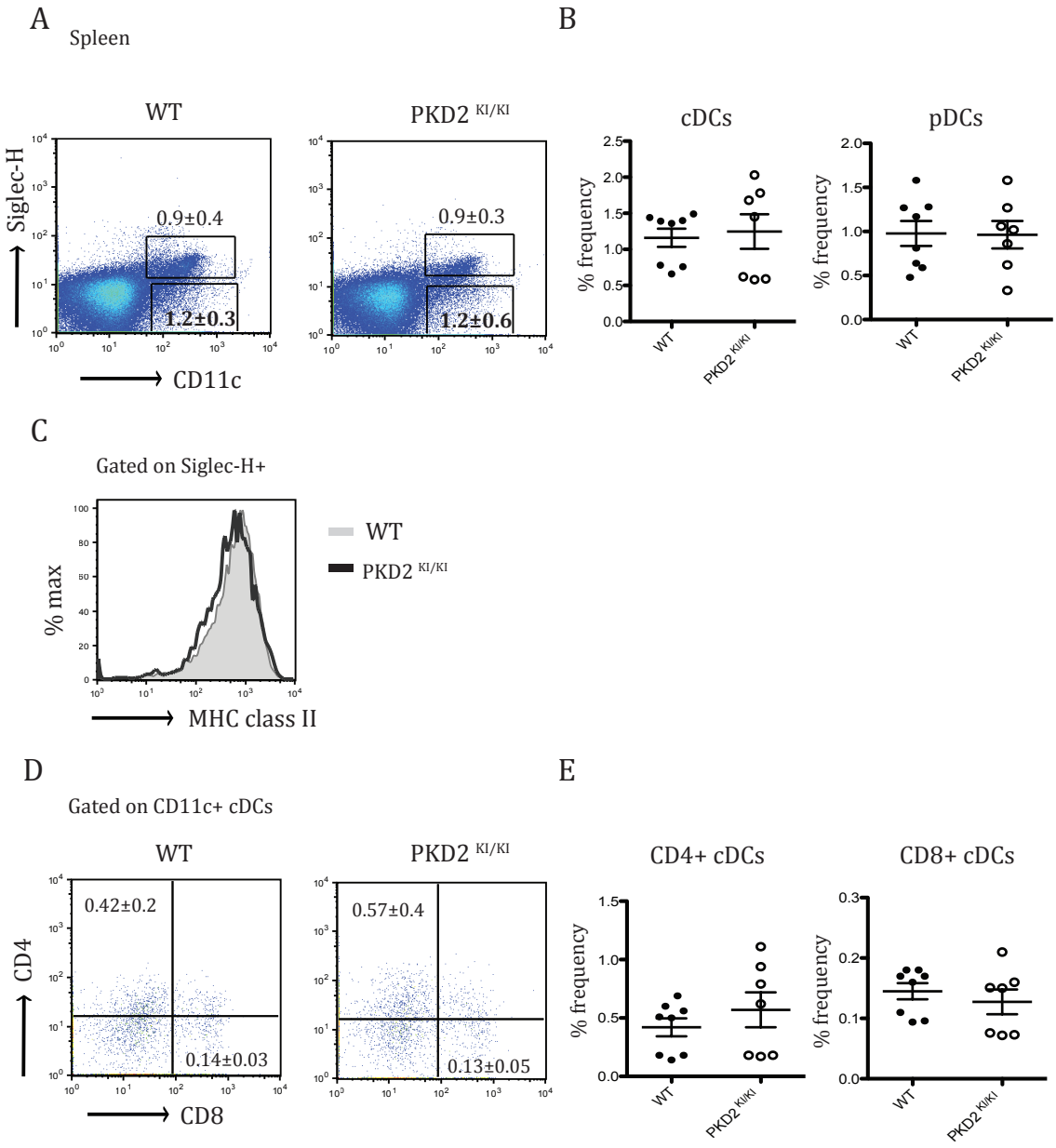

Figure 4.19 Conventional and plasmacytoid DC subsets are normal within the spleen of PKD2$^{KI/KI}$ mice

(A) Representative dot plots showing cDC and pDC subsets within the spleen of WT and PKD2$^{KI/KI}$ mice shown by Siglec-H and CD11c surface expression by Flow cytometry. Numbers represent average % frequency and SD. (B) % frequency of cDCs and pDC (C) Representative histogram of WT and PKD2$^{KI/KI}$ pDCs showing expressing of MHC class II on the cell surface (D) Representative dot plots showing CD4+ and CD8+ cDC subpopulations (gated on CD11c) within bone marrow of WT and PKD2$^{KI/KI}$ mice. (E) Combined data showing % Frequency of CD4+ cDCs and CD8+ cDCs. Error bars represent SD. Data obtained from 3 independent biological experiments n= 8 mice per genotype.

Collectively, these data reveals no obvious requirement for PKD2 catalytic activity within the development or differentiation of two major DC subsets, including cDCS (both CD4+ and CD8+ subsets) and pDCs within the bone marrow but also in regard to their migration and maintenance within the spleen.

4.2.5.2 Analysis of macrophage and neutrophil population in PKD2$^{KI/KI}$ mice

In addition to DC development within the bone marrow, other cells of the myeloid lineage also develop and differentiate from the bone marrow including neutrophils and macrophages. After demonstrating that major DC subset development within the bone marrow of PKD2$^{KI/KI}$ is normal we also sought to address neutrophil and macrophage populations. To assess this we used flow cytometry, neutrophils were defined as Ly6G^{high} CD11b+ and macrophages were defined as Ly6G^{low} CD11b^{+} F4/80^{+}. As can be seen in Figure 4.20A-B, assessment of both neutrophil and macrophage populations within the bone marrow of PKD2$^{KI/KI}$ mice revealed no differences when compared to WT mice.

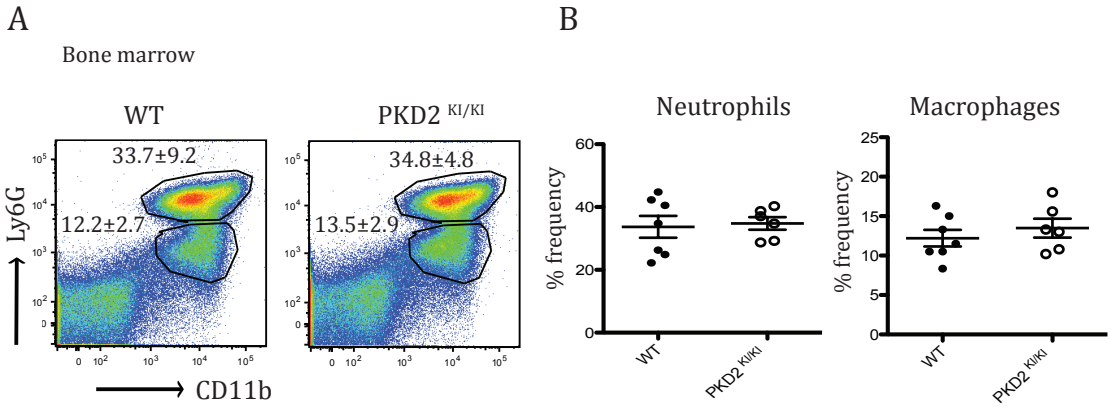

Figure 4.20 Macrophage and neutrophil populations are normal within the bone marrow of PKD2$^{KI/KI}$ mice

(A) Representative dot plots showing macrophage and neutrophil populations with the bone marrow of WT and PKD2$^{KI/KI}$ mice shown by Ly6G and CD11b surface expression by Flow cytometry. Numbers represent average % frequency and SD. (B) Combined data showing % frequency of neutrophils and

macrophages Data is pooled from 3 independent experiments n= 7 mice per genotype.

Neutrophil and macrophages populations within the spleen of PKD2$^{KI/KI}$ mice were also assessed and no differences in these populations when compared to WT mice were seen (Figure 4.21).

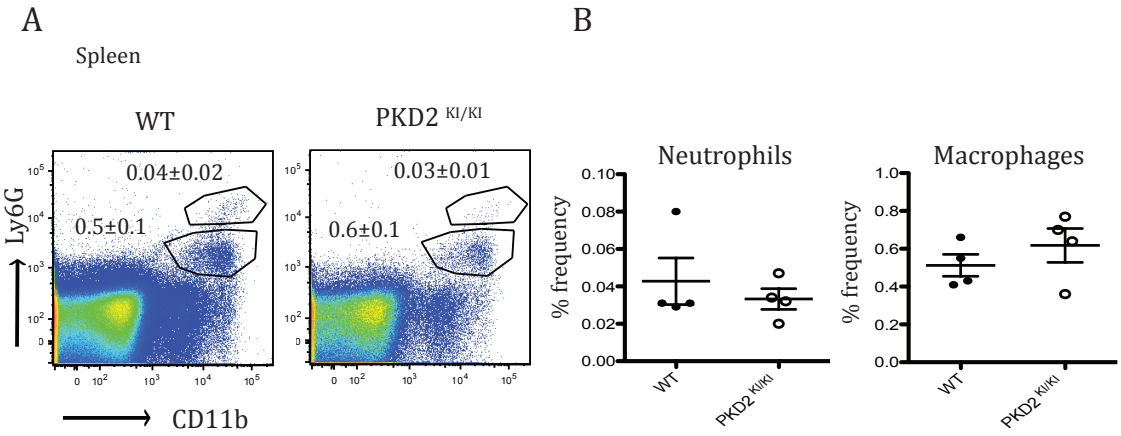

Figure 4.21 Macrophage and neutrophil populations are normal within the spleen of PKD2$^{KI/KI}$ mice

(A) Representative dot plots showing macrophage and neutrophil populations with the spleen of WT and PKD2$^{KI/KI}$ mice shown by Ly6G and CD11b surface expression by Flow cytometry. Numbers represent average % frequency and SD. (B) Combined data showing % frequency of neutrophils and macrophages. Error bars represent SD. Data obtained from 2 independent biological experiments n= 4 mice per genotype.

These data show that the loss of PKD2 catalytic activity does not affect the development of multiple myeloid lineage cells including cDC and pDC DC subsets, neutrophils and macrophages within the bone marrow. Additionally, PKD2 catalytic activity is dispensable for normal population of these myeloid subsets within secondary lymphoid organs such as the spleen.

4.2.5.3

4.2.6 Analysis of myeloid cell development in PKD1$^{WT/KI}$ x PKD2$^{KI/KI}$ double mutant mice

We also performed a similar analysis on myeloid cell development of cDCs, pDCs, neutrophils and macrophages within the bone marrow and spleen of PKD1$^{WT/KI}$ x PKD2$^{KI/KI}$ double mutant to assess the impact of depletion of the available PKD pool even further. Assessment of total cell number (x10^6) of bone marrow cells and spleen revealed that total cellularity of PKD1$^{WT/KI}$ x PKD2$^{KI/KI}$ mice was comparable to WT tissues.

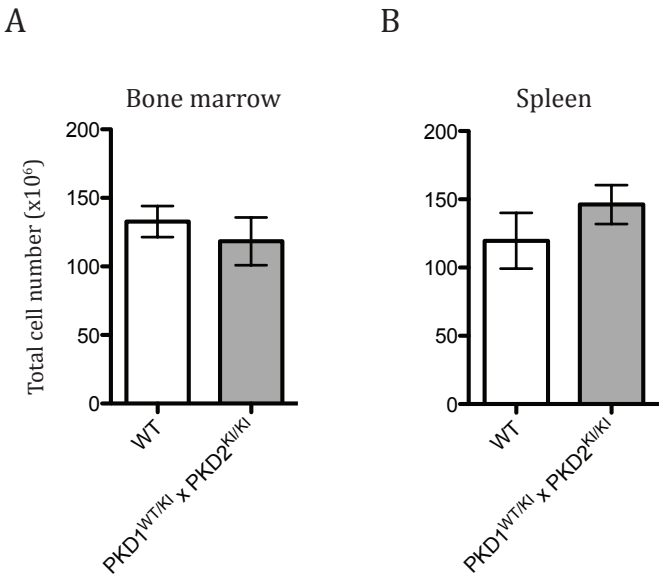

Figure 4.22 Analysis of tissue size in PKD1$^{WT/KI}$ x PKD2$^{KI/KI}$ mice

Total cell number (x106) obtained from age and sex matched WT and PKD1$^{WT/KI}$ x PKD2$^{KI/KI}$ mice of; (A) Bone marrow (B) Spleen. Error bars represent SD. Data combined from 3 independent experiments n= 9 mice per group.

4.2.6.1 Analysis of development of conventional and plasmacytoid DC populations in PKD1$^{WT/KI}$ x PKD2$^{KI/KI}$ mice

Overall assessment of cDC and pDC subset populations within the bone marrow of PKD1$^{WT/KI}$ x PKD2$^{KI/KI}$ revealed no differences when compared to WT mice (Figure 4.23A-C). Additionally, CD4+ and CD8α+ cDC populations were

unaffected within the bone marrow of PKD1$^{WT/KI}$ x PKD2$^{KI/KI}$ mice (Figure 4.23B).

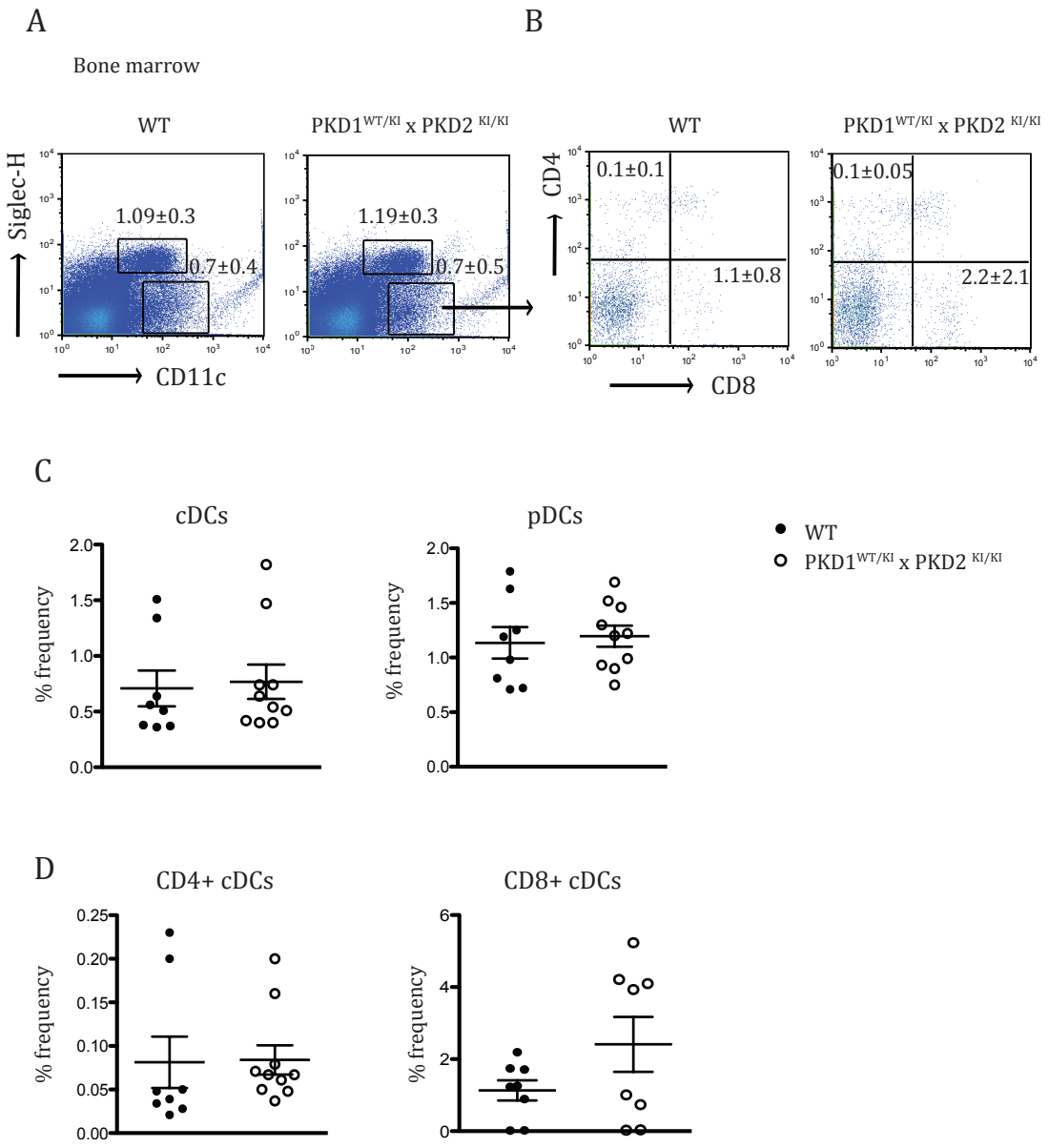

Figure 4.23 Conventional and plasmacytoid DCs within bone marrow of PKD1$^{WT/KI}$ x PKD2$^{KI/KI}$ mice are normal

(A) Representative dot plots showing cDC and pDC subsets within the bone marrow of WT and PKD1$^{WT/KI}$ x PKD2$^{KI/KI}$ mice shown by Siglec-H and CD11c surface expression by flow cytometry. Numbers represent average % frequency and SD. (B) Representative dot plots showing CD4+ and CD8+ cDC subpopulations (gated on CD11c) within bone marrow of WT and PKD1$^{WT/KI}$ x PKD2$^{KI/KI}$ mice. (C) Combined data showing % frequency of cDCs and pDC (D) %

frequency of CD4+ and CD8+ cDC Error bars represent SD. Data from 3 independent experiments n=8 mice per genotype.

Assessment of these populations within the spleen of $PKD1^{WT/KI}$ x $PKD2^{KI/KI}$ also revealed no difference when compared with populations within WT spleen including cDCs, pDCs and CD4+ CD8α+ cDC populations (Figure 4.24A-D).

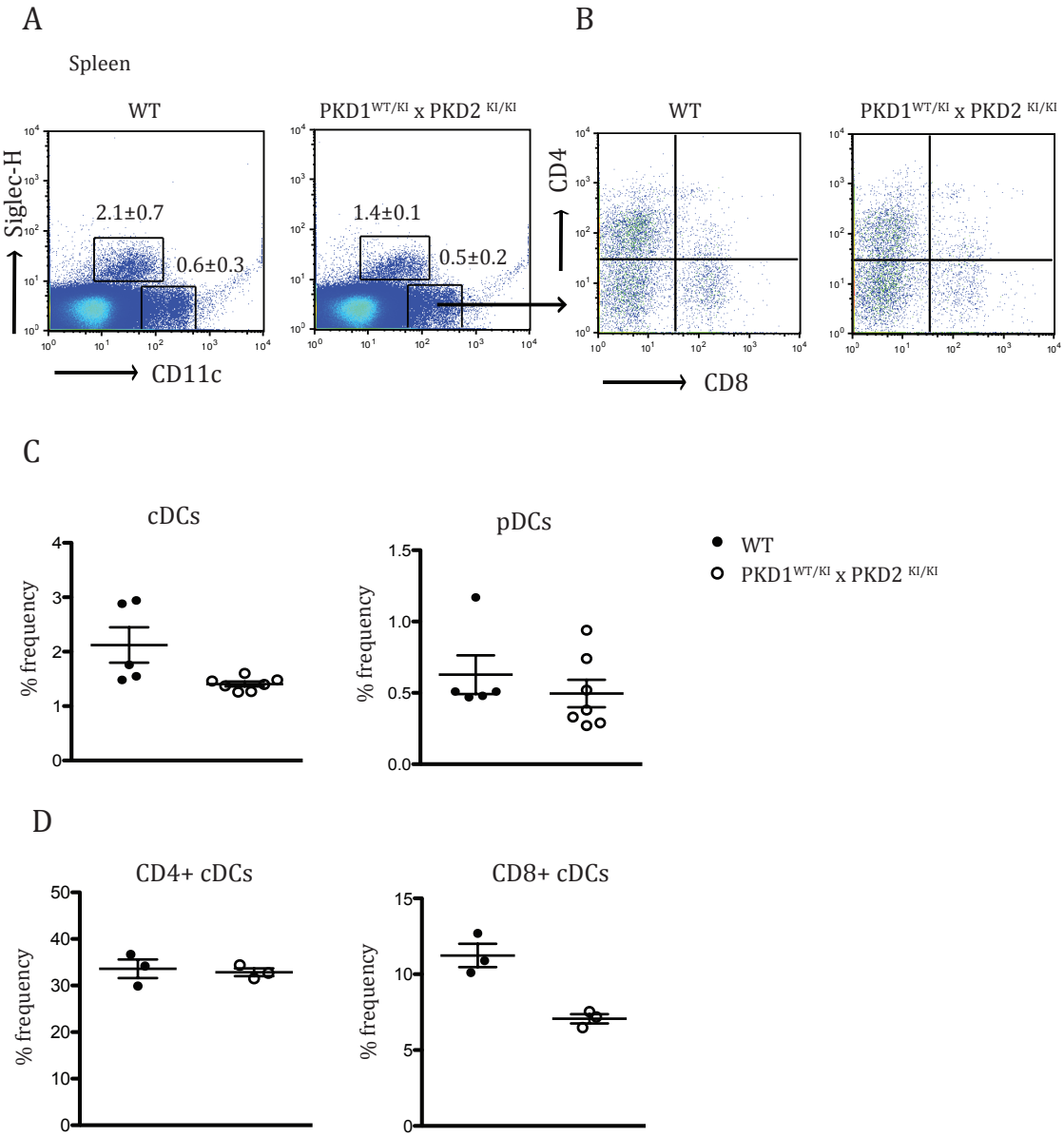

Figure 4.24 Conventional and plasmacytoid DC subsets are normal within the spleen of PKD1$^{WT/KI}$ x PKD2$^{KI/KI}$ mice

(A) Dot plots showing cDC and pDC subsets within the spleen of WT and PKD1$^{WT/KI}$ x PKD2$^{KI/KI}$ mice shown by Siglec-H and CD11c surface expression by flow cytometry. Numbers represent average % frequency and SD. (B) Dot plots showing CD4+ and CD8+ cDC subpopulations (gated on CD11c) within spleen of WT and PKD1$^{WT/KI}$ xPKD2$^{KI/KI}$ mice. (C) % Frequency of cDCs and pDC (D) % frequency of CD4+ and CD8+ cDC Error bars represent SD. Data from 3 independent experiments n=8 mice per genotype.

4.2.6.2 Analysis of the development of macrophage and neutrophil populations within PKD1$^{WT/KI}$ x PKD2$^{KI/KI}$ mice

Additionally we also assessed neutrophil and macrophages within both the spleen and bone marrow of PKD1$^{WT/KI}$ x PKD2$^{KI/KI}$ mice and observed no differences in either of these populations in either the bone marrow or the spleen when compared with WT mice (Figure 4.25A-B,Figure 4.26A-B)

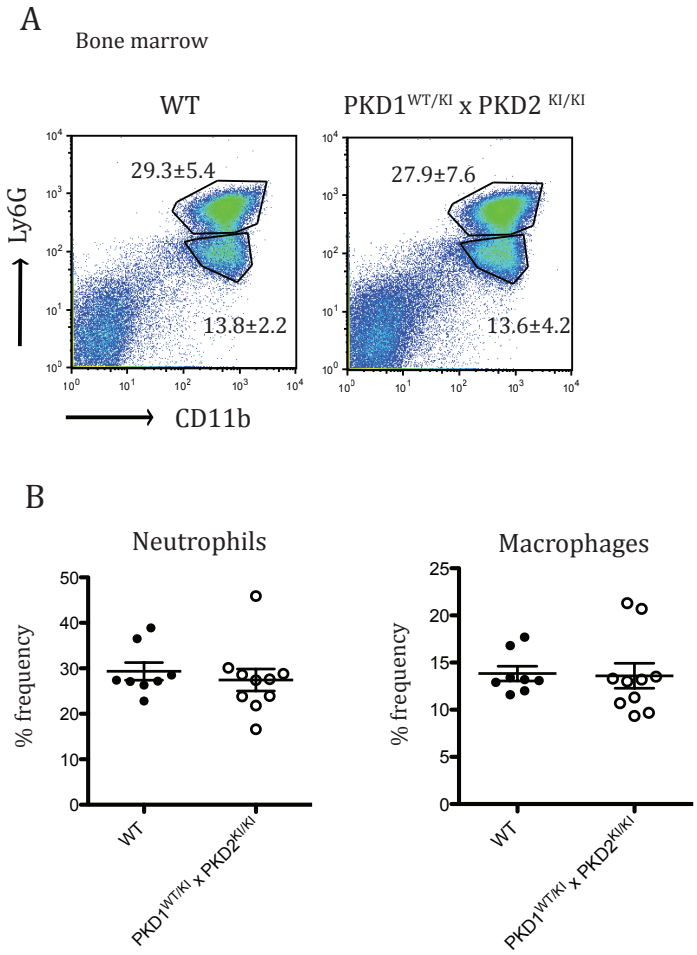

Figure 4.25 Macrophage and neutrophil populations are normal within the bone marrow of PKD1$^{WT/KI}$ x PKD2$^{KI/KI}$ mice

(A) Representative dot plots showing macrophage and neutrophil populations with the bone marrow of WT and PKD1$^{WT/KI}$ x PKD2$^{KI/KI}$ mice shown by Ly6G and CD11b surface expression by flow cytometry. Numbers represent average % frequency and SD. (B) Combined data showing % frequency of neutrophils and macrophages Error bars represent SD. Data from 3 independent experiments n=8 mice per genotype.

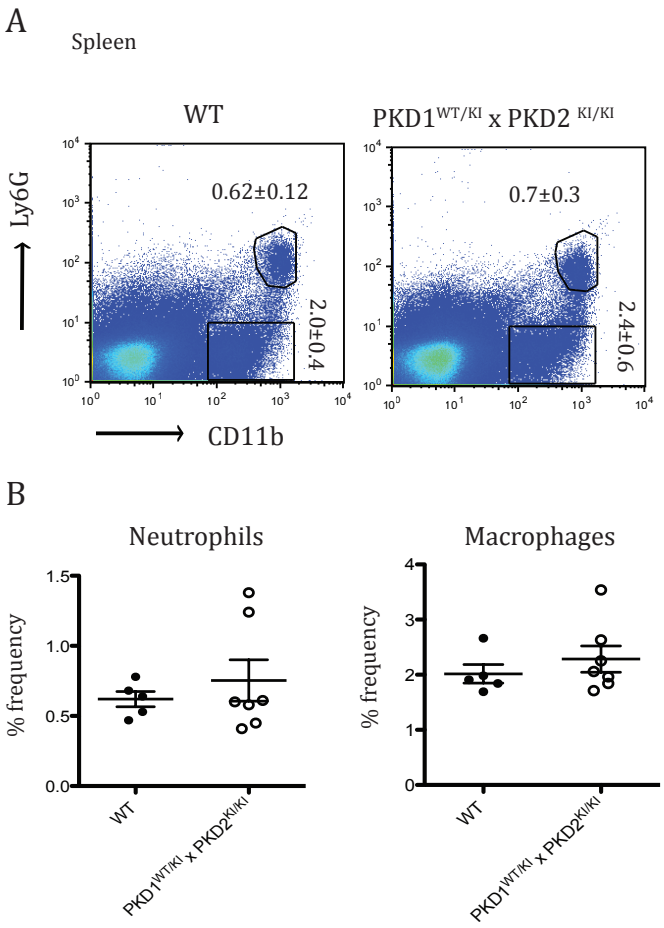

Figure 4.26 Macrophage and neutrophil populations are normal within the spleen of PKD1$^{WT/KI}$ x PKD2$^{KI/KI}$ mice

(A) Representative dot plots showing macrophage and neutrophil populations with the spleen of WT and PKD1$^{WT/KI}$ x PKD2$^{KI/KI}$ mice shown by Ly6G and CD11b surface expression by flow cytometry. Numbers represent average % frequency and SD. (B) Combined data showing % frequency of neutrophils and macrophages. Error bars represent SD. Data from 3 independent experiments n=8 mice per genotype.

4.2.7 Investigating the loss of PKD2 catalytic activity on effector functions of BMDCs *in vitro*

Having established PKD2 is the dominant isoform expressed in BMDCs yet loss of catalytic activity of PKD is dispensable for the development of various myeloid cells *in vivo* we sought to address the role of PKD2 catalytic activity in effector functions of these cells. Within T lymphocytes although the loss of PKD2 catalytic activity did not affect T cell development, multiple studies have shown that PKD2 catalytic activity is essential for normal T lymphocyte function *in vitro*

and *in vivo* (Matthews et al. 2010) (Navarro et al. 2012) (Navarro, Feijoo Carnero, et al. 2014a). Although we have demonstrated that PKD is not strongly activated by LPS stimulation; LPS induces the activation of multiple downstream effector functions within BMDCs including the upregulation of key surface molecules and the production of pro-inflammatory cytokines such as IL-6 and IL-12p40. Previous studies have implicated PKD in integrin expression and recycling (Medeiros et al. 2005), in contrast PKD2 has been shown to be dispensable for normal lymphocyte homing *in vivo* (Matthews et al. 2012), however the role of PKD2 catalytic activity for the expression of key integrins on the cell surface of BMDCs remains unaddressed. Integrin expression upon BMDCs is essential during antigen presentation is known to be crucial for normal T cell activation. $PKD2^{KI/KI}$ BMDCs expressed comparable levels of multiple integrins including CD11c, CD11b, CD11a, CD18 as well as normal levels of MHC class II when compared to WT BMDC (Figure 4.27A).

To assess if PKD2 catalytic activity was required for BMDC effector function we stimulated WT and $PKD2^{KI/KI}$ BMDCs with LPS for 24 hours. As can seen in Figure 4.27B-E, upregulation of key costimulatory molecules upon the cell surface of $PKD2^{KI/KI}$ BMDCs were significantly higher than WT BMDCs. Additionally, assessment of cytokine production revealed comparable levels of IL-6 production by $PKD2^{KI/KI}$ BMDCs however IL-12p40 production was significantly increased (Figure 4.27F-G).

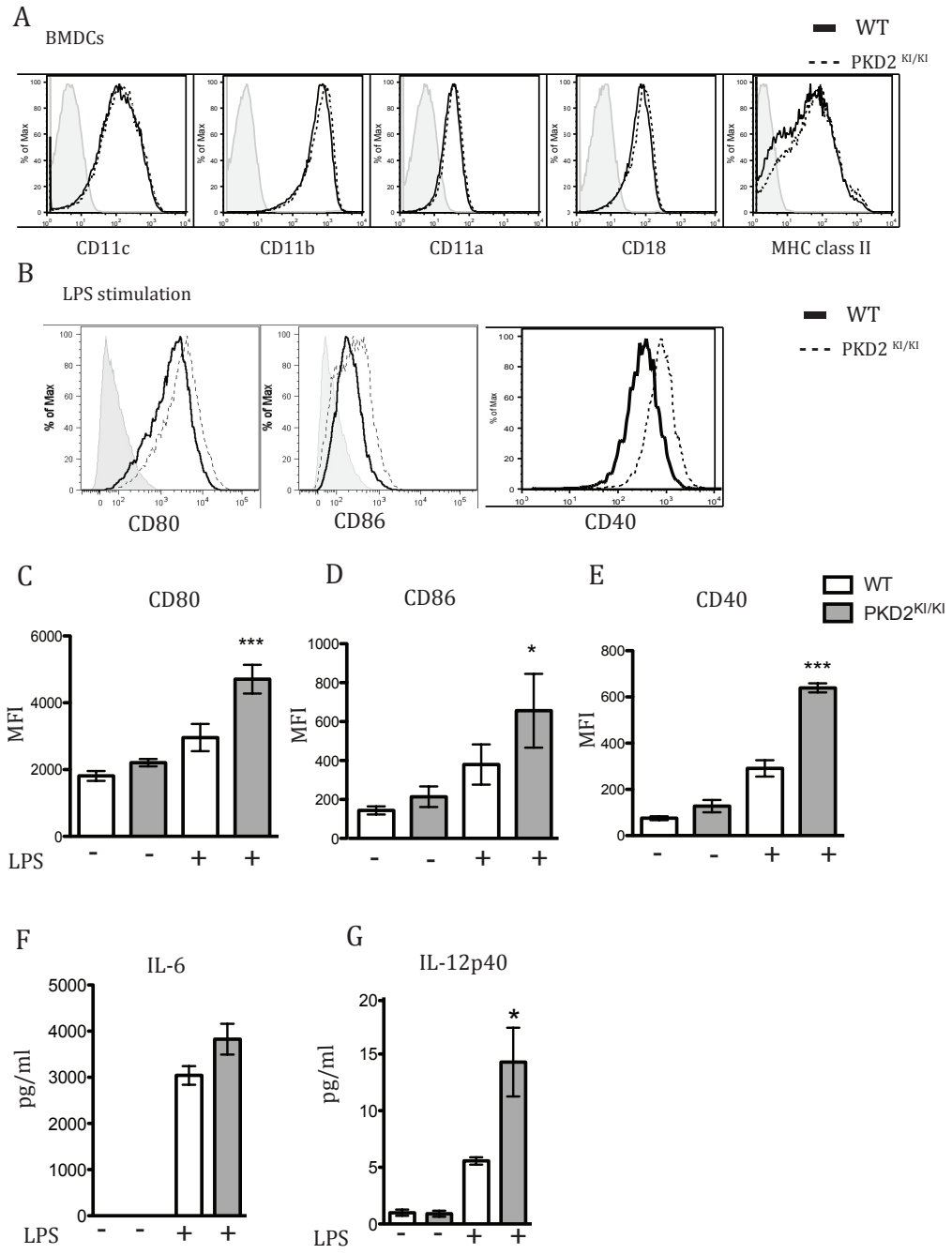

Figure 4.27 Analysis of integrin expression and LPS induced activation of PKD2$^{KI/KI}$ BMDCs

(A) Flow cytometry of integrin expression upon the surface of WT and PKD2$^{KI/KI}$ BMDCs including CD11c, CD11b, CD11a, CD18 and MHC class II. (B) Representative histograms of upregulation of costimulatory molecules on cell surface of WT and PKD2$^{KI/KI}$ BMDCs after 24 hours stimulation with LPS (100ng/ml). Geo MFI of costimulatory molecules including (C) CD80 (D) CD86 and (E) CD40. ELISA analysis of cytokine production after activation with LPS (100ng/ml 24 hours) (F) IL-6 production (pg/ml) and (G) IL-12p40 production (pg/ml). (C-G is pooled data from 3 independent experiments n= 9 mice total) Error bars represent SEM.

4.2.8 PKD2$^{KI/KI}$ BMDCs can activate T lymphocytes using an *in vitro* activation model

As we had observed an overactive phenotype upon activating PKD2$^{KI/KI}$ BMDCs with LPS we next sought to address if these alterations were biologically significant. One way to address this was to examine the ability of PKD2$^{KI/KI}$ BMDCs to activate T lymphocytes. To do this we chose to use the TCR transgenic OT II+ system, a well-characterised model to study DC mediated T cell activation *in vitro* in which T cells from OT II+ transgenic mice express a TCR specific for chicken ovalbumin (Sheng et al. 2008). To assess the functionality of BMDCs lacking PKD2 catalytic activity BMDCs generated in vitro from WT and PKD2$^{KI/KI}$ mice were untreated or stimulated with LPS overnight to promote activation. BMDCs were then loaded with OVA peptide and co-cultured (1:10) with naïve OT II+ CD4+ T cells for 4 days. T cell activation by peptide loaded WT and PKD2$^{KI/KI}$ DCs was assessed by flow cytometry every 24 hours. Commonly used activation markers to assess T cell activation include CD44, CD69, CD62L and CD25 (IL-2Rα) (Shipkova & Wieland 2012). As can be seen in Figure 4.28A-E, T cell activation by peptide loaded PKD2$^{KI/KI}$ BMDCs were comparable to peptide loaded WT BMDCs when we assessed CD44, CD69, CD62L and CD25 upregulation on T cell surface.

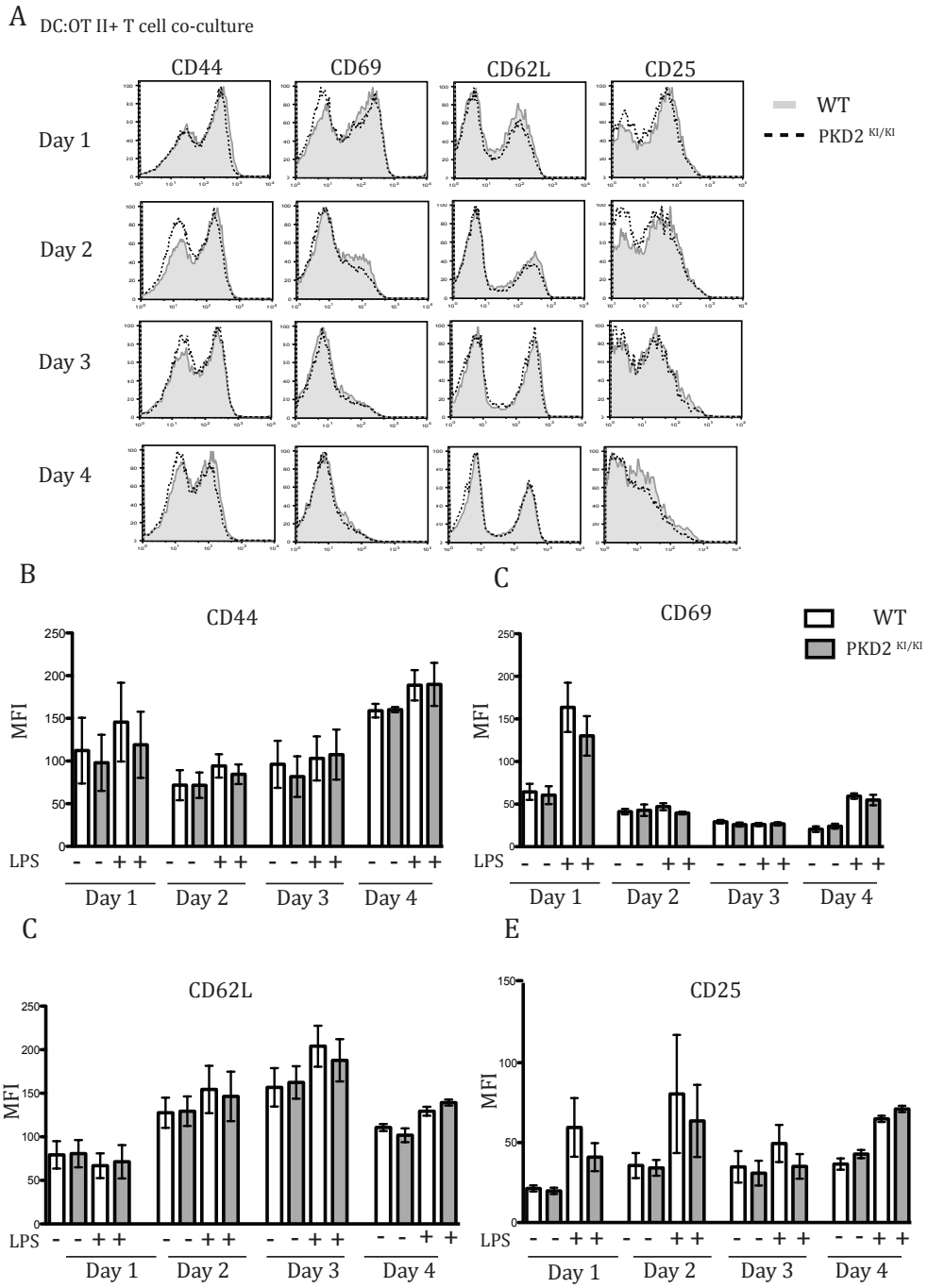

Figure 4.28 Analysis of OT II+ T cell activation from WT and PKD2$^{KI/KI}$ OVA loaded BMDCs

Analysis of OT II+ T cell activation cell surface markers including CD44, CD69, CD62L and CD25 (IL-2R) (A) Representative histograms of OT II+ T cells activation markers assessed by flow cytometry after co-culture for indicated time point with OVA-peptide loaded (1μM) WT and PKD2$^{KI/KI}$ BMDCs stimulated with LPS (100ng/ml) overnight. MFI of (A) CD44 expression (C) CD69 (D) CD62L and (D) CD25 (IL-2R). Representative data of two independent experiments with 5 mice total per genotype assessed.

Additionally, we also cytokine production by activated T cells by harvesting supernatant every 24 hours and assessed IL-2 and IFNγ production, which are abundantly produced in response to TCR ligation. As can be seen in Figure 4.29A, IL-2 production by OT II+ T cells co-cultured with peptide-loaded $PKD2^{KI/KI}$ BMDCs was comparable to WT BMDCs at all indicated time points. However, when we assessed IFNγ production OT II+ T cells that were co-cultured with peptide-loaded $PKD2^{KI/KI}$ BMDCs produced significantly more IFN-γ by day 3 and day 4 (Figure 4.29B).

4.2.8.1

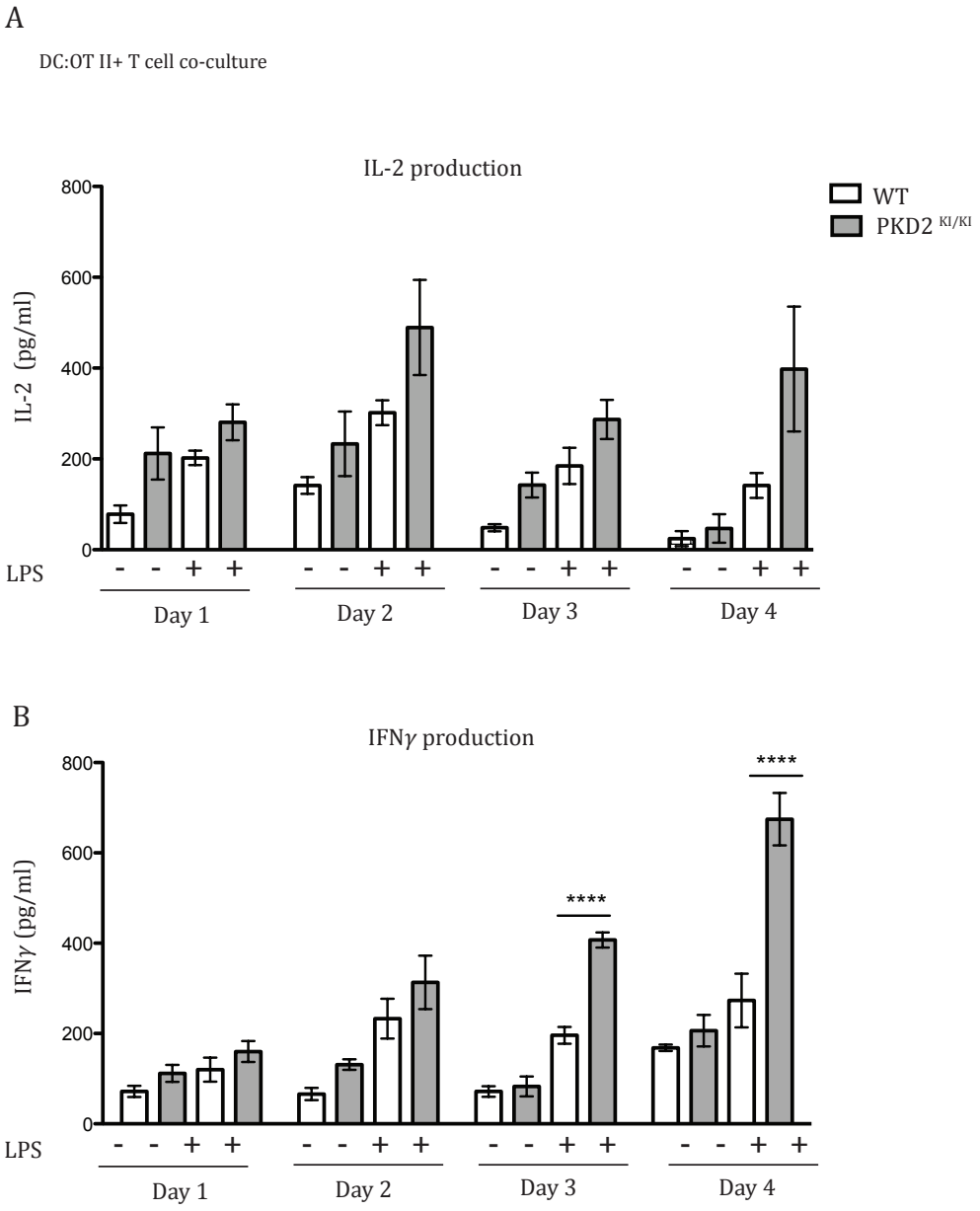

Figure 4.29 Cytokine production by OT II+ CD4+ T cells after co-culture with WT and PKD2$^{KI/KI}$ BMDCs

Cytokine production of IL-2 (A) and IFNγ (B) by sandwich ELISA after co-culture of naïve OT II+ CD4+ T cells with unstimulated or LPS (100ng/ml) treated WT and PKD2$^{KI/KI}$ BMDCs loaded with OVA-peptide (1μM) over indicated time points. **** p≤0.0001 analysed by two-way ANOVA with Bonferroni *post-hoc* test. IL-2 data combined data from 2 independent experiments. IFNγ data is preliminary from one independent experiment.

Collectively, these data reveal a potential regulatory role for PKD2 catalytic activity after activation by LPS, as demonstrated with heightened upregulation of key costimulatory markers and with heightened production of proinflammatory cytokine IL-12p40. These differences did not generally impact on the ability of $PKD2^{KI/KI}$ BMDCs to perform antigen presentation or T lymphocyte activation in an *in vitro* model although did we did observed significantly higher IFNγ production by day 3 and day 4 of co-culture.

4.3 Discussion

The aim of this chapter was to explore the importance of PKD isoforms in the development and effector functions of myeloid cells. Previous studies have reported that PKD1 is required for successful signaling downstream of TLRs utilising the Myd88 dependent pathway within both RAW264.7 cells and primary BMDMOs (J.-E. Park et al. 2009b). One discrepancy within our results when compared to the current literature is that we observe that PKD2 is the predominant isoform expressed within primary BMDMOs and BMDCs. This is consistent with RNA-sequencing data from Immgen that report that PKD2 is predominantly expressed in various innate immune cells. In general within the mammalian immune system PKD2 appears to be selectively and predominantly expressed (Matthews et al. 2010). To determine if PKD1 is predominantly expressed in mast cells as previously reported (Murphy et al. 2007), the generation of bone marrow derived mast cells from PKD transgenic mice could be carried out in the future. The successful generation of both BMDCs and BMDMO from PKD1 and PKD2 transgenic mice demonstrated that these isoforms are not required for the normal expansion of these cell subsets *in vitro.*

Previous studies have reported high basal phosphorylation within T lymphocytes, which was also the case for BMDMOs and BMDCs (Navarro, Goebel, et al. 2014b). Importantly, we observed a reduction of basal PKD activity demonstrated in in both $PKD2^{KI/KI}$ and $PKD2^{KO/KO}$ cells or through pharmacological inhibition of PKD. One possible reason for the high level of basal PKD activity could be due to intracellular reactive oxygen species (ROS), that is expressed in high levels within macrophages and DCs (Y. Zhang et al. 2013) (Del Prete et al. 2008). In particular it is known that the generation of BMDCs with

GM-CSF results in phenotype of DC comparable to that of TNFα and inducible NO synthase-producing (TIP) DC, which has high abundance of ROS (Sheng et al. 2010; Matsue et al. 2003). Interesting, mitochondrial-derived ROS is known to promote DAG generation and subsequent recruitment and activation of PKD (Cowell, Döppler, et al. 2009a).

Previous studies have demonstrated the activation of PKD downstream of MyD88 dependent TLR activation and for the successful production of cytokines including IL-6 and IL-12p40 within various myeloid cells as well as epithelial cells (J.-E. Park et al. 2008) (Yamashita et al. 2010) (Murphy et al. 2007) (J.-E. Park et al. 2009b) (Steiner et al. 2010). In contrast to previously published literature, we did not detect any strong activation of PKD by TLR stimulation including TLR4 or TLR9 in either RAW264.7 macrophage cell line or BMDCs. Interestingly, our preliminary data indicates that zymosan is a strong inducer of PKD in myeloid cells. Stimulation with zymosan is known to trigger ROS production (Goodridge et al. 2007) and induce intracellular Ca^{2+} flux mediated by PLCγ (Xu et al. 2009), both of which have been shown to activate PKD however not within a myeloid cell context. Furthermore, zymosan extracts activate TLR2 in cooperation with dectin-1. Future studies will be required to address the mechanism of PKD activation in response to zymosan. One way to approach this would be to strategically compare zymosan stimulated cells with depleted zymosan, which solely activates dectin-1, and TLR2 only agonists such as PAM2CSK4. Furthermore, it would be interesting to assess if cytokine production in cells lacking $PKD2^{KI/KI}$ cells in response to zymosan stimulation. Investigation into the effect of the loss of PKD2 catalytic activity within anti-fungal immunity using in an *in vivo* infection model such as *Pneumocytsis carinii* and *Crpytococcus neoformans* infection, could be carried out in the future (Nakamura et al. 2007).

Although within our studies LPS stimulation did not strongly induce PKD activity the pharmacological inhibition of PKD in RAW264.7 cells led to a significant decrease in IL-10 and IL-6 production after LPS stimulation. Previous studies have demonstrated that reduced IFNγ production in T lymphocytes is due to reduced recruitment of RNA Pol II to the IFNγ transcriptional start site (Navarro, Feijoo Carnero, et al. 2014a). Future studies

could assess the recruitment of RNA Pol II to transcriptional start site of IL-6 and IL-10 after pharmacological inhibition of PKD in RAW264.7 cells to assess if this is the mechanism behind reduction in cytokine production by these cells.

Previous studies have demonstrated that loss of PKD2 catalytic activity is dispensable for T and B lymphocyte development *in vivo,* the role of PKD kinases remains unaddressed within myeloid cell development *in vivo.* Our data demonstrates for the first time that both PKD1 and PKD2 catalytic activity is dispensable for the development of multiple innate immune cells within the bone marrow including cDC, CD4+ and CD8α+ cDC subsets, pDCs, neutrophils and macrophages. Furthermore, the population of these subsets was normal in peripheral lymphoid tissue including the spleen.

Although previous studies have attempted to address the role of PKD kinases in the effector functions in myeloid cells including primary BMDMOs and BMDCs, these studies frequently address the role of PKD via knockdown or pharmacological inhibition with poor specificity PKD inhibitors such as the Go6976 compound.

These data suggests although PKD may not be activated in response to TLR4 stimulation with LPS, PKD2 may be involved in the negative regulation of this response *in vitro* as indicated by our data in which loss of PKD2 catalytic activity led to the overactive response of BMDCs to LPS stimulation. Previous studies have implicated a role for PKD in activation of the deubiquitinase A20 (also know as TNFα induced protein (TNFAIP3)), although these studies were performed using transfection of A20 and PKD into a beta islet cell line (βTC3) and it was not clear which isoform was used (Liuwantara et al. 2006). Assessment of whether the over activation status we see within the $PKD2^{KI/KI}$ BMDCs affected T lymphocyte activation using an in-in vitro activation model that demonstrate that T cell activation was normal, as indicated by normal activation markers such as CD69, CD44, CD62L and CD25. However, we did note significantly increased production IFNγ by day 3 and day 4 by T cells stimulated with activated $PKD2^{KI/KI}$ BMDCs compared to activated WT BMDCs. One caveat of this T cell activation model is the inability to distinguish between DC produced IFNγ and T lymphocyte produced IFNγ. One way to overcome this problem would be to use intracellular cytokine staining allowing identification of IFNγ

produced by T cells only. Interestingly, studies investigating mice lacking A20 specifically within DCs develop autoimmunity characterised by increased conversion of CD4+ naïve T cells into Th1 phenotype in which Th1 cells produced significantly more IFNγ as well as increased generation of plasma cells (Kool et al. 2011).

Future studies could investigate if that PKD mediates anti-inflammatory responses within innate immune cells after PRR ligation and assess the regulation of A20 within $PKD2^{KI/KI}$ BMDCs.

5 Investigating the role of PKD2 catalytic activity in gut homeostasis, regulatory T cells and colitis

5.1 Introduction

In the previous chapters, I have taken a particular focus on the role of PKD kinases, more specifically the PKD2 isoform, in the development and effector functions of myeloid cells *in vitro* and *in vivo*. Within the mammalian immune system it is well established that thymocytes and peripheral T lymphocytes also predominantly express PKD2 which is selectively activated after TCR activation (Matthews et al. 2000; Matthews et al. 2010; Navarro, Feijoo Carnero, et al. 2014a; Spitaler, Emslie, Wood & Cantrell 2006b). TCR signaling is known to be essential for both T cell development within the thymus and controlling the function of effector T cells during a successful adaptive immune response (Smith-Garvin et al. 2009). Equally important is the role of TCR signaling in the process of deletion of self-reactive T cells, known as central tolerance (reviewed Mathis & Benoist 2004), although this is not completely effective as demonstrated by presence of self-reactive T cells within the periphery (Bouneaud et al. 2000). Therefore, T cell tolerance within the periphery must be maintained by additional mechanisms, these include induction of Tregs (reviewed extensively (Josefowicz et al. 2012)) and T cell clonal anergy, a state of T cell unresponsiveness induced by TCR stimulation that occurs in the absence of co-stimulation (Schwartz 2003) (Appleman & Boussiotis 2003).

DAG signaling is an essential component of downstream TCR signaling events as demonstrated by loss of DGKs (DAG kinases), such as DGKα or DGKζ, which results in reduction in normal peripheral T cells (R. Guo et al. 2008). Furthermore, it has also been shown that loss of DGKα or DGKζ led to enhanced T cell activation and prevents induction of anergy (Riese et al. 2011) (Olenchock et al. 2006).

PKD family members are key receptors and secondary messengers of DAG and integrates signals from DAG and PKC (Q. J. Wang 2006). In this context, PKD2

in T lymphocytes has been shown to be required for IL-2 and IFNγ production after TCR triggering, highlighting an essential function of PKD2 in effector T cell responses and humoural immune responses *in vivo* (Matthews et al. 2010). Studies attempting to address lack of T cell effector function went on to show that although PKD2 catalytic activity is not required for normal T cell selection (shown by transcriptome analysis), but rather PKD2 null T cells are simply unable to switch to effector T cell status in response to TCR stimulation (Navarro et al. 2012). However, it is clear that in this context PKD2 also plays a role in negative regulation of T cell proliferation both $PKD2^{KI/KI}$ or $PKD2^{KO/KO}$ mice crossed onto both the TCR-transgenic OTI and OTII strains (which select for CD8+ and CD4+ T cells respectively) had striking hypercellularity of thymus and as a consequence of these mice also displayed splenomegaly and lymphoid hyperplasia. Subsequent studies have defined PKD2 as a digital amplifier in TCR mediated signalling, and was shown to be required for normal CD8+ CTLs in response to *L.Monocytogenes* however lack of PKD2 was protective in an autoimmune model of diabetes (Navarro, Feijoo Carnero, et al. 2014a) Furthermore, recent studies have taken a wider approach to assess phosphoproteomics within $PKD2^{KO/KO}$ CD8+ CTLs (Navarro, Goebel, et al. 2014b). The main proteins affected by loss of PKD2 included those involved in transcription, cell cycle, RNA processing, chromosomal organisation. Additionally, novel substrates of PKD2 identified in CTLs included the E3 ligase C-Cbl and the tyrosine protein phosphatase non receptor type 22 (Ptpn22), which is known to be crucial for the TCR to discriminate between strong and weak peptides (Salmond et al. 2014).

The development of Tregs has been shown to absolutely require TCR signalling within the thymus where $CD4^+$ T cells with self reactive TCRs respond strongly to self antigen resulting in the upregulation of the FoxP3 transcription factor and development into nTreg (reviewed extensively (Hsieh et al. 2012)). More recently the role of TCR signaling has been addressed in Tregs, which arise from CD4+ T cells within the periphery. Here, TCR signaling was shown to be required for suppressive capacity of Tregs where loss of TCR signaling in peripheral Tregs resulted in the development of severe autoimmunity and

moribund by day 13, highlighting the requirement for TCR signaling for Treg function within the periphery *in vivo* (Levine et al. 2014).

In this chapter I will present our analysis on the effect of loss of PKD2 catalytic activity in gut associated tissues and lymphocyte populations. Although there is abundant information available about the role PKD2 plays in CD8+ and CD4+ T cell subsets, it is unknown if PKD2 catalytic activity may play in the induction of the development of Tregs, their maintenance within the periphery or their effector function. To understand whether PKD2 catalytic activity is required for Treg development, we decided to assess Treg populations within the tissues of $PKD2^{KI/KI}$ mice. Furthermore, we addressed if functionality was impaired in PKD2 $^{KI/KI}$ Tregs by using a well-characterised T cell transfer colitis model to address if any changes observed were due to cell intrinsic or extrinsic mechanisms in an *in vivo* model.

5.2 Results

5.2.1 PKD2 KI mice display enlarged mucosal associated tissues

5.2.1.1 Mesenteric lymph node

As mentioned previously, during charaterisation of myeloid populations within PKD2 $^{KI/KI}$ mice it was observed that mesenteric lymphoid tissues were significantly enlarged (Figure 5.1A-B). Analysis of total live cell counts via flow cytometry revealed a significant 2-fold increase in total cell numbers harvested from PKD2 $^{KI/KI}$ mesenteric lymph nodes, WT total cell counts $18.08x10^6$±3.8 PKD2 $^{KI/KI}$ total cell counts $42.8x10^6$ ± 12.56 (Figure 5.1C). In contrast to normal cell counts obtained from other peripheral lymphoid tissues of PKD2 KI mice, including inguinal and axillary lymph nodes as well as the spleen, this increase in size and cellularity was unique to mesenteric lymph node tissues (Figure 5.1D-E). Interestingly, this observation was also true for double knock-in mice ($PKD1^{WT/KI}$ x $PKD2^{KI/KI}$), however presence of PKD1 heterozygous mutation did not exacerbate this phenotype indicating it is specifically the loss of PKD2 catalytic activity driving this phenotype (data not shown).

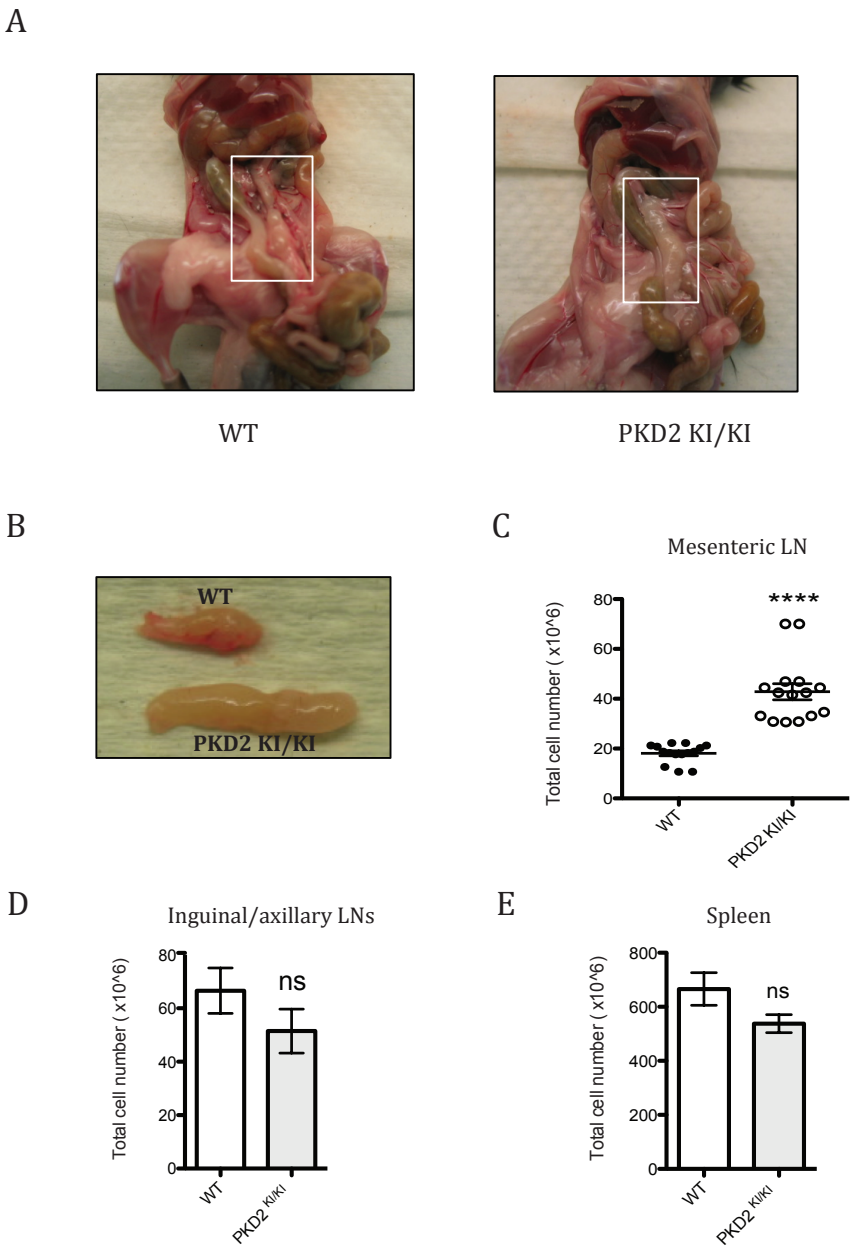

Figure 5.1 PKD2 KI/KI mice display significantly enlarged mesenteric lymph nodes but display normal non-GALT associated tissue size

(A) Representative images depicting mesenteric lymph nodes *ex vivo* from WT and PKD2$^{KI/KI}$ mice. (B) Representative images depicting excised mesenteric lymph nodes from age and sex matched WT and PKD2 $^{KI/KI}$ mice. (C) Mesenteric lymph node live total cell counts (x10^6) from aged and sex matched WT and PKD2$^{KI/KI}$ mice (D) Combined inguinal/axillary lymph nodes live total cell counts (x10^6) ((E) Combined spleen live total cell counts (x10^6) Error bars represent SD. Data obtained from 4 independent experiments, n=15 mice total). **** = p≤0.0001 analysed by students t test.

Next, we wanted to explore if PKD2$^{KI/KI}$ mice displaying enlarged mesenteric lymph nodes displayed any associated histopathology. To achieve this, samples including sections of the mesenteric lymph nodes were taken *ex vivo* from age and sex matched WT and PKD2$^{KI/KI}$ mice and collected in 10% neutral buffered formalin. Tissue samples were then embedded in paraffin blocks, sliced into 4-µm thick sections which were subsequently stained using Hematoxylin and Eosin (HE) and assessed microscopically by a pathologist. *These services were kindly provided by the University of Glasgow Veterinary Diagnostic Services, microphotographs were assessed by pathologist Dr Francesco Marchesi.*

WT mice displayed typical features expected to be found within mesenteric lymph nodes including the presence of cortical lymphoid follicles without well-developed germinal centres. As discussed within the introduction, it is known that GALT associated tissues tend to have some degree of active germinal centres due to ongoing tolerance towards food antigen and commensal bacteria within the gut microbiota.

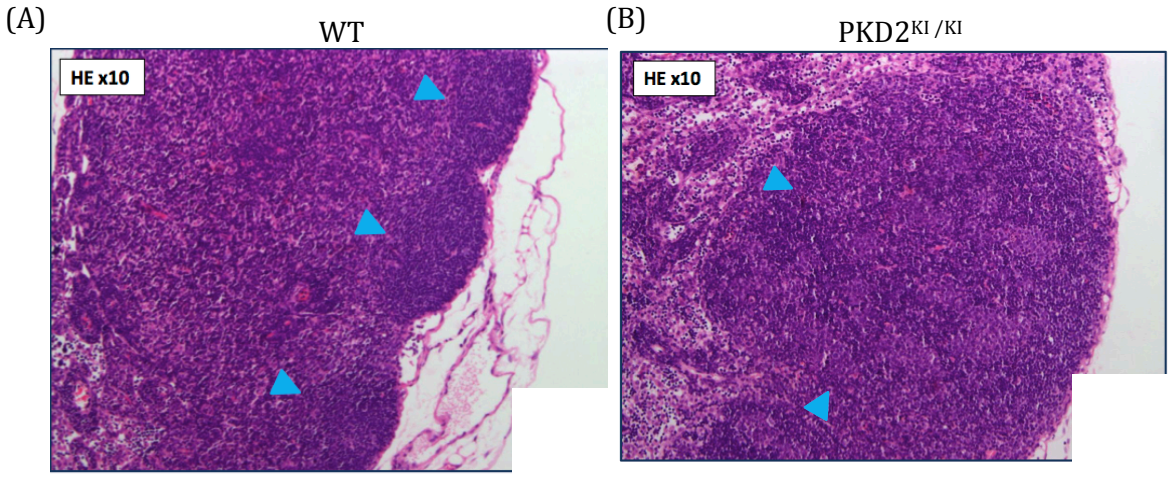

Figure 5.2 Histological features of WT and PKD2$^{KI/KI}$ murine mesenteric lymph nodes

(A) Histological sections of mesenteric lymph node from WT mice stained with HE (10x magnification. Blue arrows indicate cortical lymphoid follicles without well developed germinal centres (B) Histological sections of mesenteric lymph node sections from PKD2$^{KI/KI}$ mice stained with HE (10x magnification). Blue arrows indicate cortical lymphoid follicle with expanded germinal centres, which are characterised by a slightly irregular architecture.

We also wanted to assess lymphocyte populations within the enlarged mLN tissue of $PKD2^{KI/KI}$ mice. As we had observed an expansion of germinal centres within the mLN of $PKD2^{KI/KI}$ mice, we decided to explore any changes in B cell populations *ex vivo* by flow cytometry. As can be seen in Figure 5.3A-B, we observed a significant increase in the % frequency and total cell number ($x10^6$) of B lymphocytes (CD19+ B220+) within the mLNs of $PKD2^{KI/KI}$ mice when compared to WT mice. To explore potential reasons behind enlarged germinal centres and significantly increase B cells within the mLN we also stained B cells for GL-7 (also known as Ly-77), which is a well-known marker of germinal center B cells (Laszlo et al. 1993). This revealed no difference in the surface expression of GL-7 on $PKD2^{KI/KI}$ B cells when compared with WT B cells within the mLN (Figure 5.3D-E)

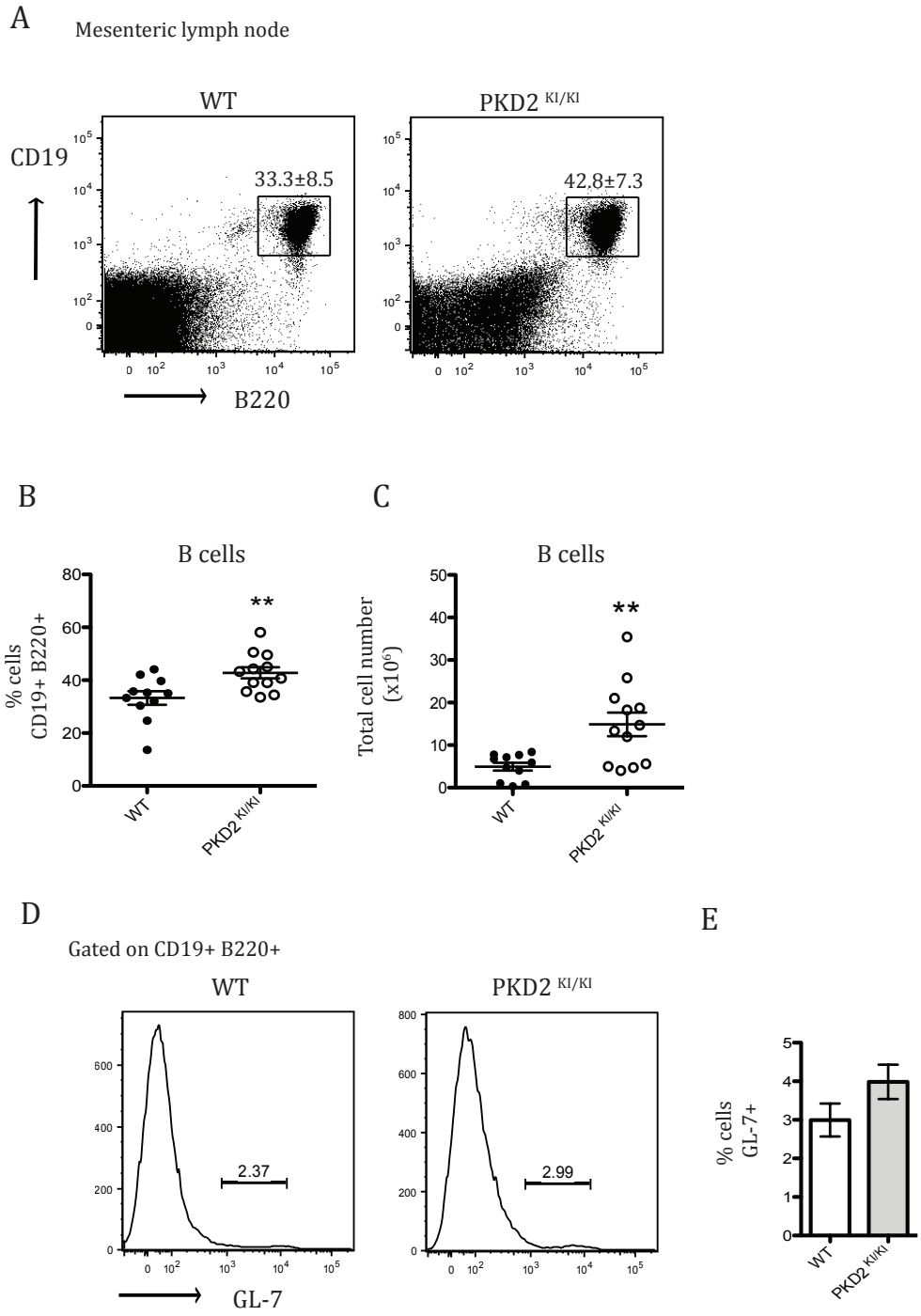

Figure 5.3 B lymphocytes are increased within mLN tissue of PKD2 KI/KI mice

(A) Dot plots showing live B cells populations within mLN of WT and PKD2KI/KI mice by CD19 and B220 surface expression by flow cytometry. Numbers represent average % frequency and SD. (B) % frequency of live B cells (CD19+ B220+) within mLN (C) Total cell number (x10^6) of B cells within mLN. (D) Histogram showing GL-7 surface marker expression on B cells (gated on live CD19+ B220+ lymphocytes). (E) % of live B cells (CD19+ B220+) expressing GL-7 surface marker. Error bars represent SD. Data obtained from 4 independent experiments, n=12 mice per genotype. ** = p≤0.01 analysed by students t test.

We also examined T cell populations within the mLN of WT and PKD2$^{KI/KI}$ mice including TCRαβ+ and TCRγδ+ cells but also TCRαβ+ CD4+ and TCRαβ+ CD8+ lymphocytes. As can be seen in Figure 5.4A-B, the % frequency of TCRαβ+ and TCRγδ+ T cell subsets within the mLN of PKD2$^{KI/KI}$ mice was comparable to WT mice. Although when we compare total cell number of these subsets, all populations with PKD2$^{KI/KI}$ mice are inherently increased due to the significant increase we observe with the total cellularity of the mLN tissue.

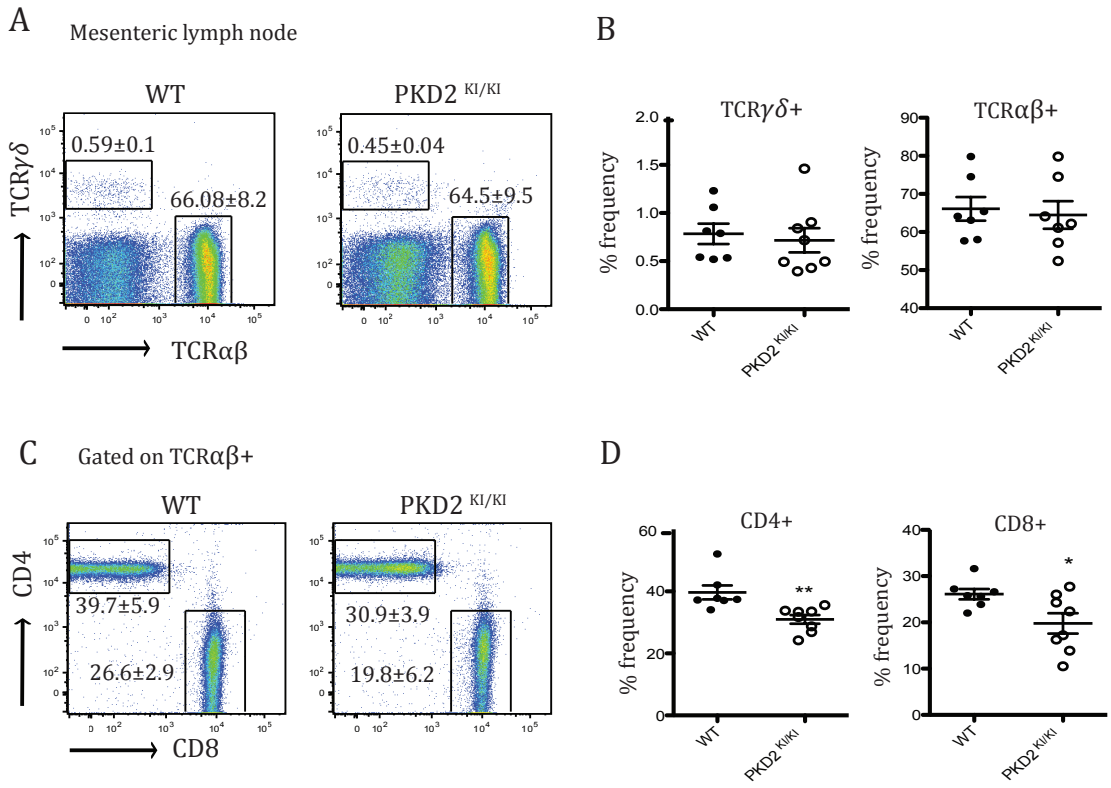

Figure 5.4 T cell populations within mLN of PKD2 $^{KI/KI}$ mice

(A) Dot plots showing live T cells populations within mLN of WT and PKD2 KI mice by TCRαβ and TCRγδ surface expression by Flow cytometry. Numbers represent average % frequency and SD. (B) % frequency of live TCRαβ+ and TCRγδ+ T cell subsets (C) Dot plots showing live TCRαβ+ CD4+ and CD8+ surface marker expression (D) % frequency of live TCRαβ+ CD4+ and CD8+ T cell subsets. Error bars represent SD. Data obtained from 3 independent experiments n-6 mice per genotype. * = p≤ 0.05 and ** = p≤0.01 analysed by students t test.

5.2.1.2 Peyers patches

During assessment of *ex vivo* tissues it was observed that in addition of enlarged mesenteric lymph nodes Peyers patches found within the small intestine were also visibly larger within PKD2$^{KI/KI}$ mice Figure 5.5.

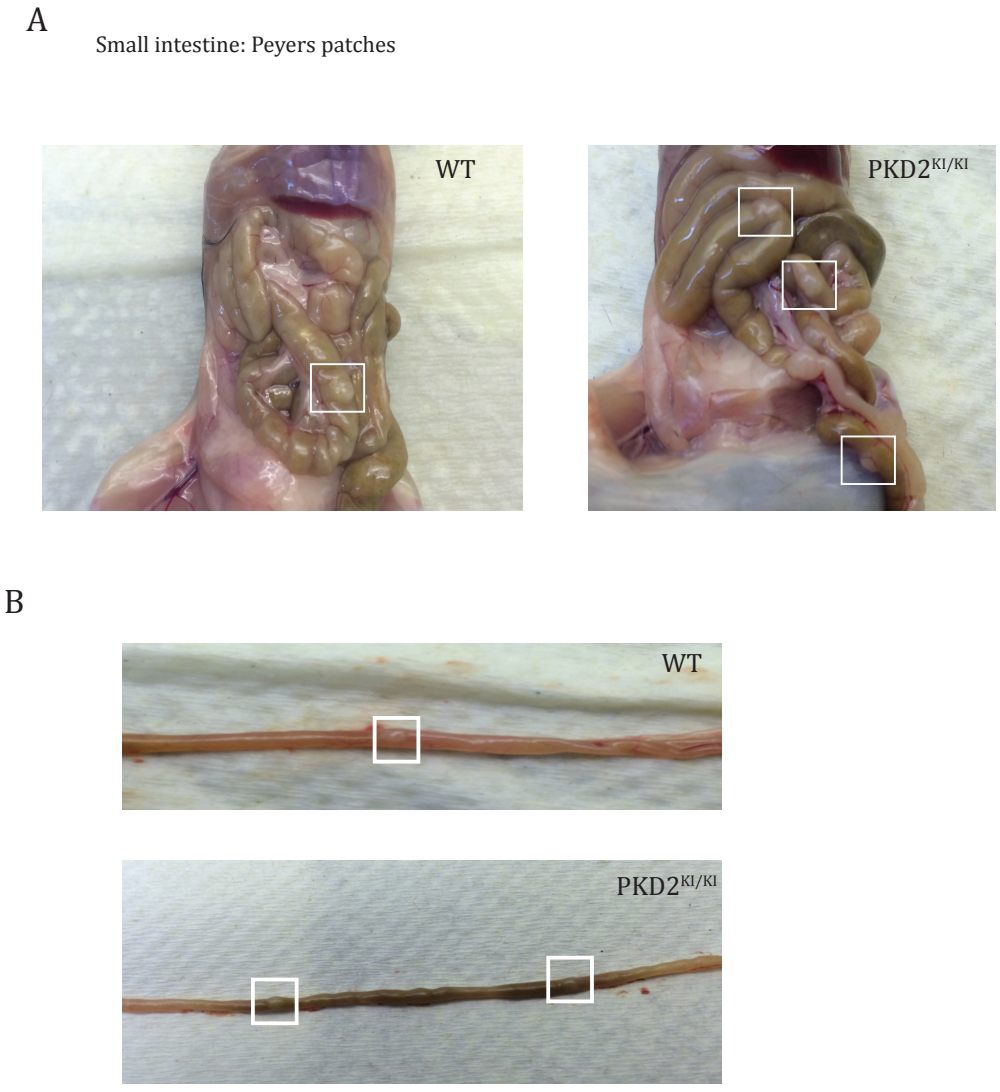

Figure 5.5 Peyers patches are enlarged in PKD2$^{KI/KI}$ mice

(A) Representative images of Peyer's patches within the small intestine of WT and PKD2$^{KI/KI}$ mice ex vivo indicated by white boxes. (B) Excised small intestine and presence of Peyer's patches in WT and PKD2$^{KI/KI}$ mice indicated by white boxes.

Following this observation we wanted to investigate the potential reason behind increased size of GALT tissues. Importantly, we also wanted to address if these were indeed enlarged Peyers patches, containing immune cell subsets, and were not for example intestinal polyps. Furthermore, we also wanted to investigate if the enlarged PPs in PKD2$^{KI/KI}$ mice displayed any histopathology associated with the increase in tissue size. To achieve this, samples including sections of the transverse small intestine containing Peyers patches were taken *ex vivo* from age and sex matched WT and PKD2$^{KI/KI}$ mice and collected in 10% neutral buffered formalin. Tissue samples were then embedded in paraffin blocks, sliced into 4-µm thick sections which were subsequently stained using HE and assessed microscopically by a pathologist.

Morphologically PPs are separated into 3 main domains: the follicular area, the interfollicular area and the follicle associated epithelium. The follicular and interfollicular domains consist of PPs lymphoid follicles containing germinal centres, which contain multiple immune cells, including proliferating B cells, follicular dendritic cells (FDCs) and macrophages. The structure and function of PPs within human and murine immune systems are reviewed in depth elsewhere (Neutra et al. 2001) (C. Jung et al. 2010). This follicle area is surrounded by a subendothelial dome (SED), which contains B cells, T cells, DCs and macrophages. Peyers patches tend to be domed in shape due to developing germinal centres forming the core of each follicle. Histopathology sections revealed the presence of typical architectural features of PPs within WT mice small intestine, including cortical lymphoid follicles containing small or underdeveloped germinal centres (Figure 5.6A), indicated with blue arrows. In contrast, histology sections from the small intestine containing enlarged PPs from PKD2$^{KI/KI}$ mice displayed moderately expanded germinal center (Figure 5.6A). Furthermore, upon closer examination at higher magnification, it can be seen that WT PPs have typical follicular structures with small germinal centres (Figure 5.6B) whereas PPs from PKD2$^{KI/KI}$ mice displayed slightly irregular architecture within the moderately expanded germinal centres (Figure 5.6C).

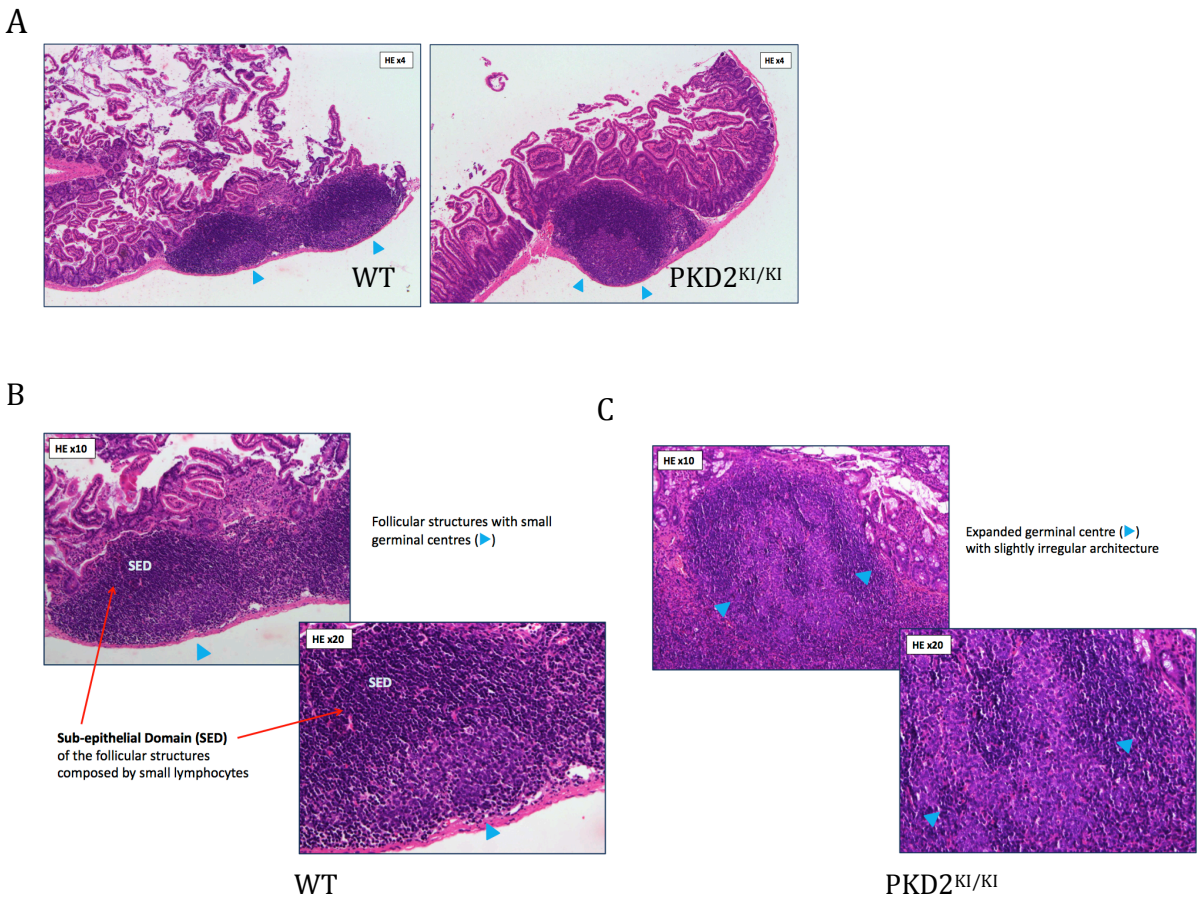

Figure 5.6 Histological features of WT and PKD2$^{KI/KI}$ mice Peyers patches within the small intestine

(A) Comparison of sectioned WT and PKD2 KI small intestine Peyers patches (4x) stained with H+E, images show germinal centres indicated by blue arrows (4x). (B) Sectioned WT Peyers patches show follicular structures with small germinal centres (4x). (C) PKD2 KI small intestine Peyers patches show follicular structures with slightly expanded germinal centres.

To study the effect of loss of PKD2 catalytic activity on lymphocytes within GALT tissues PPs were isolated from age and sex matched WT and PKD2 $^{KI/KI}$ mice and lymphocyte populations were assessed using flow cytometry. Although PPs were visibly larger simply by eye, it was difficult to get accurate cell numbers from these tissues, as they are notoriously difficult to remove in one piece from the small intestinal tract due to their small size. However, it was possible to prepare samples for flow cytometry. Analysis of B cell populations via CD19+ B220+ surface marker staining revealed that frequency of B cells within

PKD2 $^{KI/KI}$ PPs were not significantly different from WT tissue (Figure 5.7A-B). Additional staining of B cells with GL-7, revealed significantly higher expression of this cell surface marker on B cells within PKD2$^{KI/KI}$ PPs (Figure 5.7C-D). These results collectively show that loss of PKD2 catalytic activity leads to an apparent increase in PP tissue size and that germinal centers within these tissues are moderately expanded with activated B cells expressing significantly more GL-7 (2 fold increase). This indicates that B cells within PKD2 $^{KI/KI}$ may potentially be more activate or possibly over responding to antigen (whether food proteins, commensal bacteria or pathogenic bacteria).

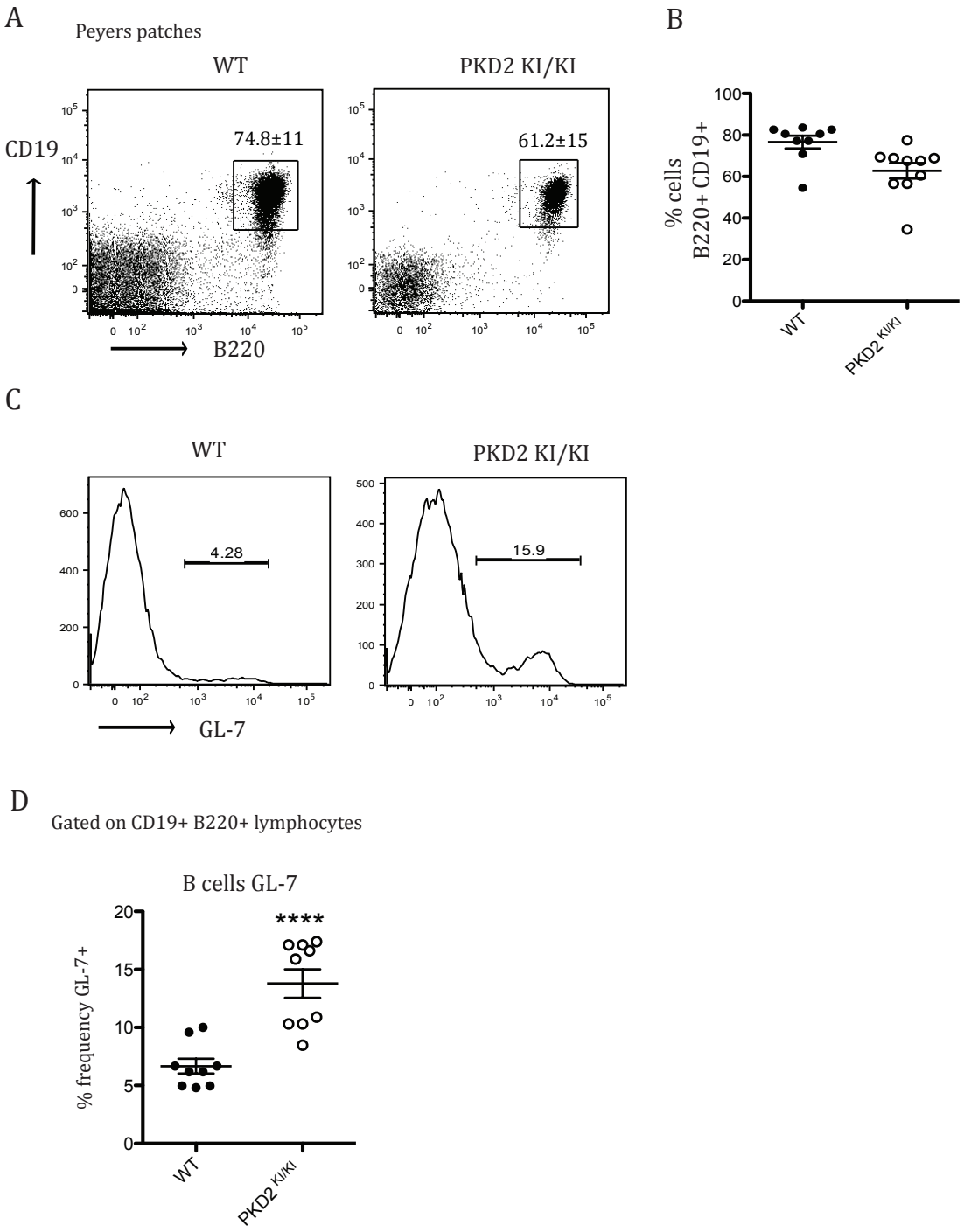

Figure 5.7 B cells within Peyers patches of PKD2 $^{KI/KI}$ mice have increased expression of GL-7

(A) Representative dot plots showing live B cells populations within PPs of WT and PKD2 KI mice by CD19 and B220 surface marker expression by Flow cytometry. Numbers represent average % frequency and SD (B) Combined data showing% Frequency of live B cells in PPs (C) Histogram showing GL-7 surface marker expression on B cells (gated on live CD19+ B220+ lymphocytes) (D) % B cells positive for GL-7 expression. Error bars represent SD. Data obtained from 3

independent experiments, n= 9 mice per genotype. **** = p≤0.0001 analysed by students t test.

In regard to T cell populations within PPs the frequency of T cell subsets within this tissue were grossly normal. Analysis of TCRαβ+T cells within PPs of $PKD2^{KI/KI}$ mice were not significantly different to WT, representative Flow cytometry dot plots are shown in Figure 5.8A and % frequency of cells is shown in Figure 5.8C. In contrast, % frequency of TCRγδ+ population was significantly decreased within PPs of $PKD2^{KI/KI}$, as indicated in representative dot plots in Figure 5.8A and % frequency in Figure 5.8C.

These data importantly demonstrates that enlarged PP tissue within $PKD2^{KI/KI}$ mice were indeed PPs rather than the presence of intestinal polyps as they contained cell subsets, including B cells and typical T cell subsets, that would be expected of gut associated lymphoid tissue.

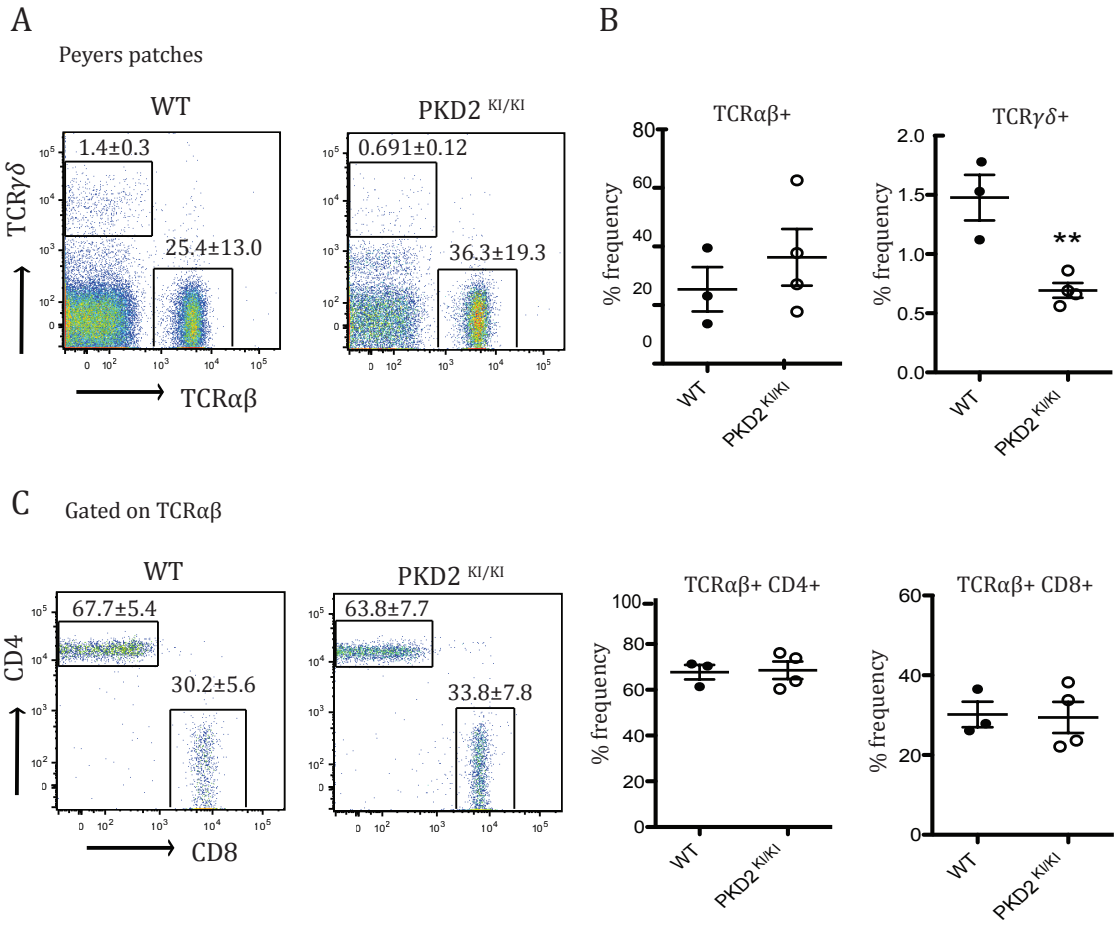

Figure 5.8 T cell populations within enlarged PPs of PKD2$^{KI/KI}$ mice

(A) Representative dot plots showing live T cell subsets within PPs of WT and PKD2$^{KI/KI}$ mice by TCRαβ and TCRγδ surface expression by Flow cytometry. Numbers represent average % frequency and SD (B) Dot plots showing CD4+ and CD8+ populations (gated on TCRαβ+ T cells) in PPs of WT and PKD2$^{KI/KI}$ mice. (C)% frequency of T cell subsets in PPs of WT and PKD2$^{KI/KI}$ mice. Error bars represent SD. Data obtained from 2 independent experiments n= 3 mice per WT group and 4 mice per PKD$^{KI/KI}$ group. ** = p≤0.01 analysed by students t test.

5.3 PKD2$^{KI/KI}$ mice have increased abundance of Tregs in multiple tissues

Although the role of PKD2 has been explored in regard to lymphocyte development and function, including both B and T cells, the potential role for PKD2 in the development of natural and induced regulatory T cells subsets has remained unaddressed. It is known that TCR signaling is essential for not only the development of nTreg cells within the thymus, but is also intricately required for the development of Tregs and their suppressive function within the periphery to maintain tolerance and homeostasis (Levine et al. 2014) (Hsieh et al. 2012). Tregs are also produced in response to environmental cues within the periphery; strong inducers of Treg include the presence of cognate antigen alongside TGF-β and IL-10 and lack of co-stimulation (Bilate & Lafaille 2012) (Hsieh et al. 2012). Tregs have become a large area of therapeutic exploration due to their potent the suppressive capacities and potential use in a variety of autoimmune diseases. This is significant as if PKD inhibitors are to be used in the clinic it is imperative to understand the potential role of PKD2 catalytic activity within cells of the immune system.

5.3.1 Tregs within the spleen and mesenteric lymph node of PKD2$^{KI/KI}$ mice

Upon assessment of CD4^{+} CD25^{+} FoxP3^{+} Treg populations within the spleen, we observed a significant 2-fold increase in the % frequency of Tregs specifically within PKD2$^{KI/KI}$ mice, which was not observed in PKD1 $^{WT/KI}$ mice (Figure 5.9A-B).

This was also true for total cell number; PKD2$^{KI/ KI}$ mice displayed a 2.4 fold increase in the total number of Tregs within the spleen compared to WT counterparts. Additionally, IL-2Rα (CD25) expression was normal in PKD2$^{KI/KI}$ Tregs (Figure 5.9D).

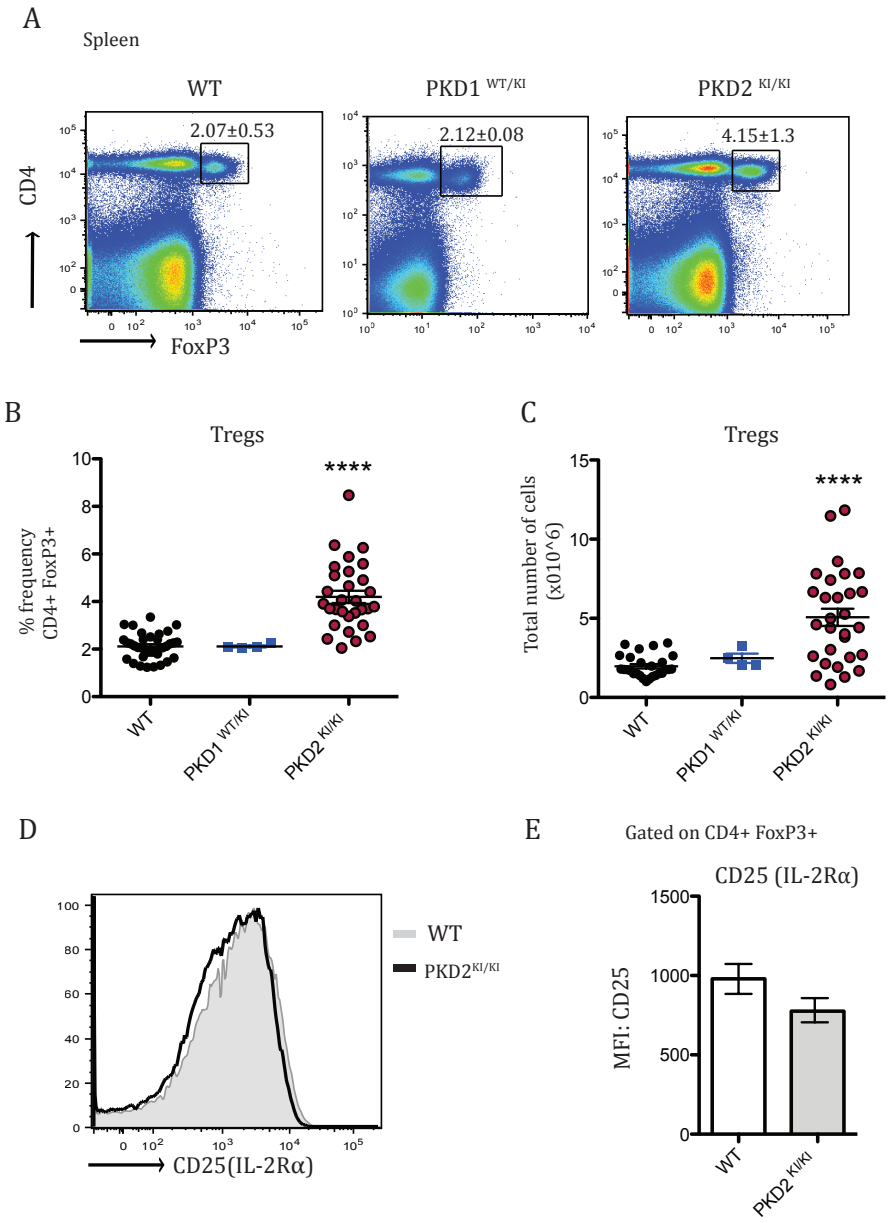

Figure 5.9 Induced Tregs are significantly increased in the spleen of PKD2 $^{KI/KI}$ mice

(A) Representative dot plots showing induced Treg (Treg) populations within spleen of WT, PKD1$^{WT/KI}$ and PKD2$^{KI/KI}$ mice by CD4 surface expression and intracellular FoxP3 expression by Flow cytometry. Numbers represent average % frequency and SD. (B) Combined data showing % frequency of CD4+ CD25+ FoxP3+ Tregs within the spleen (C) Total cell number (x10^6) of CD4+ CD25+ FoxP3+ Treg within the spleen. (D) Mean fluorescence intensity (MFI) of CD25 expression on CD4+ FoxP3+ gated lymphocytes. Error bars represent SD. Data obtained from 5 independent experiments n= 25 WT mice, 4 PKD1$^{WT/KI}$ mice and 25 PKD2$^{KI/KI}$ mice. **** = p≤0.0001 analysed by students t test.

We next assessed the number of CD4$^+$CD25$^+$ FoxP3$^+$ Tregs within the mLNs of WT and PKD2$^{KI/KI}$ mice. As can be seen in Figure 5.10A, % frequency of

Treg populations are also significantly increased (1.3-fold) within the mLNs of PKD2$^{KI/KI}$ mice, although this increase is more modest than that observed in the spleen, it is statistically significant. Furthermore, when taking into account the increased size of mLN tissue itself within PKD2$^{KI/KI}$ mice and assessed total number of Tregs we observed a 3.4 fold increase (Figure 5.10D).

These data shows that the increase in Tregs subsets observed in PKD2$^{KI/KI}$ mice is not limited to one lymphoid site but rather a general increase in the total number of Tregs within PKD2$^{KI/KI}$ mice. This phenotype is therefore unlikely simply homing or migratory problem in which Tregs within PKD2$^{KI/KI}$ mice are unable to migrate between tissues and lymphoid sites.

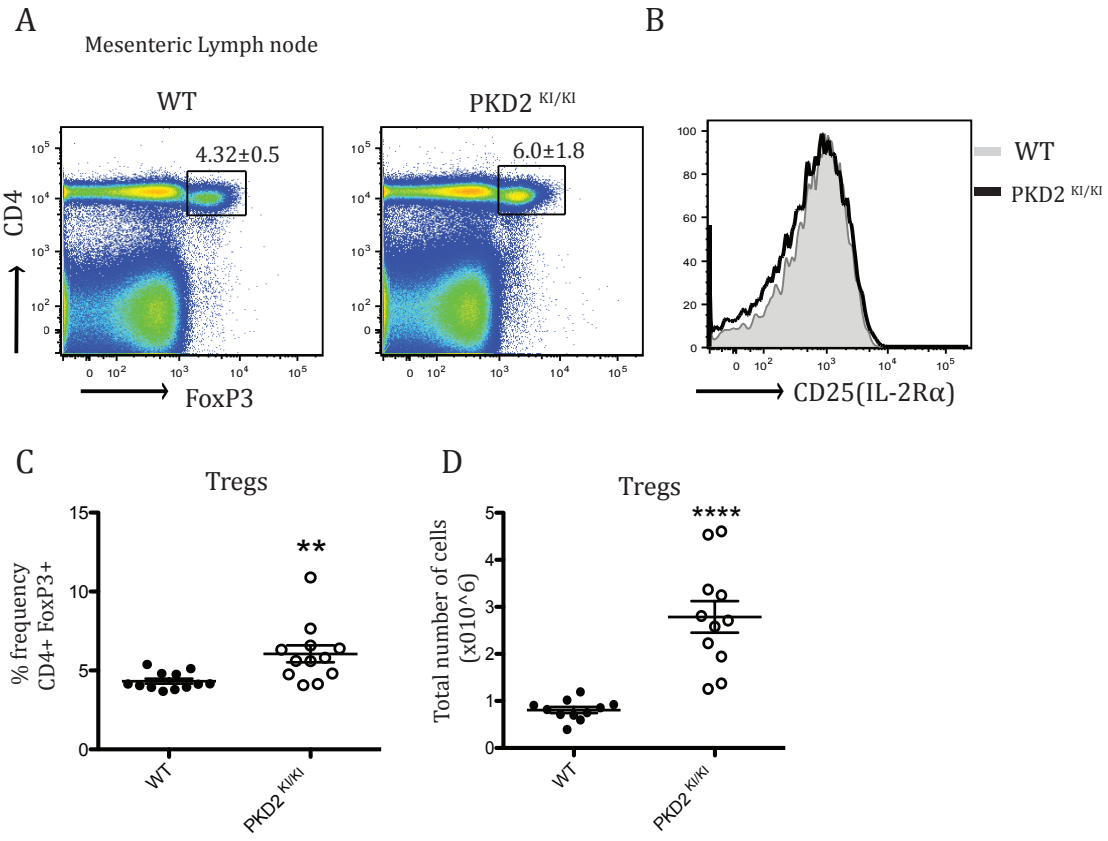

Figure 5.10 Tregs are increased in the mesenteric lymph nodes of PKD2 $^{KI/KI}$ mice

(A) Representative dot plots showing Treg populations within mesenteric lymph nodes of WT and PKD2$^{KI/KI}$ mice by CD4 surface expression and intracellular FoxP3 expression by Flow cytometry. Numbers represent average % frequency and SD. (B) Histogram showing overlayed expression of FoxP3 in WT and PKD2$^{KI/KI}$ CD4+ gated lymphocytes (C) Combined data showing % frequency of CD4+ CD25+ FoxP3+ Tregs within mLN (D) Total cell number (x10^6) of CD4+ CD25+ FoxP3+ Treg within mLN. Error bars represent SD. Data obtained from 4 independent experiments n= 12 mice per genotype. ** = p≤0.01 and **** = p≤0.0001 analysed by students t test.

5.3.2 Thymus

After examining the presence of increased Tregs in tissues including the mesenteric lymph nodes, Peyers patches, spleen and inguinal and axillary lymph nodes of PKD2$^{KI/KI}$ mice, we wanted to address if this difference was due to increased output of precursors of peripheral Tregs (nTregs) within the thymus. nTregs are developed after TCR activation via recognition of cognate self-

peptide, presented by medullary thymic epithelial cells (mTEC) and medullary thymic DCs that express the autoimmune regulator (AIRE) (Nomura & Sakaguchi 2007) (Gallegos & Bevan 2004). Strength of TCR signal is also known to be key within this stage to determine cell death versus development of nTreg (Bour-Jordan & Bluestone 2009).

To assess if increased abundance of peripheral Tregs in $PKD2^{KI/KI}$ mice was indeed a result of increased output of Treg subsets, thymi from age and sex matched mice were prepared and assessed for Treg populations via Flow cytometry. CD4 and CD25 surface marker expression were used to define Treg populations as well as intracellular staining for FoxP3. These data demonstrated that the frequency of nTreg cells within the thymus were normal, shown by assessing CD4+ FoxP3+ populations (Figure 5.11A). This was clearly demonstrated by both the percentage frequency and total number ($x10^6$) of $CD4^+$ $CD25^+$ $FoxP3^+$ cells in thymus of $PKD2^{KI/KI}$ mice compared to age and sex matched WT controls (Figure 5.11B-C)

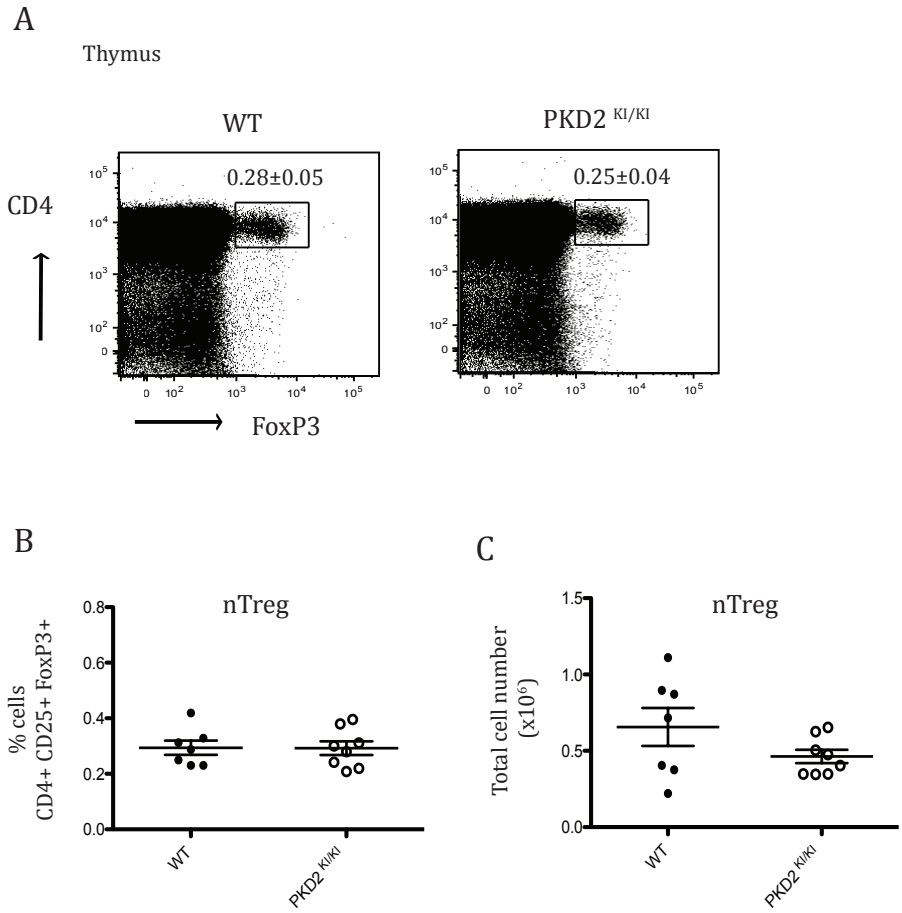

Figure 5.11 nTregs within the thymus of PKD2 $^{KI/KI}$ mice are normal

(A) Representative dot plots showing natural Treg (nTreg) populations within thymus of WT and PKD2$^{KI/KI}$ mice by CD4 surface expression and intracellular FoxP3 expression by Flow cytometry. Numbers represent average % frequency and SD. (B) % frequency of CD4+FoxP3+ T cells within the thymus (C) Combined data showing total cell number (x10^6) of CD4+ CD25+ FoxP3+ nTregs in thymus. Error bars represent SD. Data obtained from 3 independent experiments, n=7 mice per genotype.

Furthermore, assessment of T cell subsets within the thymus of PKD2 KI/KI mice revealed no differences in % frequency of TCRαβ+, TCRγδ+, TCRαβ+ CD4+ or TCRαβ+ CD8+ (Figure 5.12A-D). These data are consistent with previous publications in which loss of PKD2 catalytic activity did not affect T cell development *in vivo* (Matthews et al. 2010).

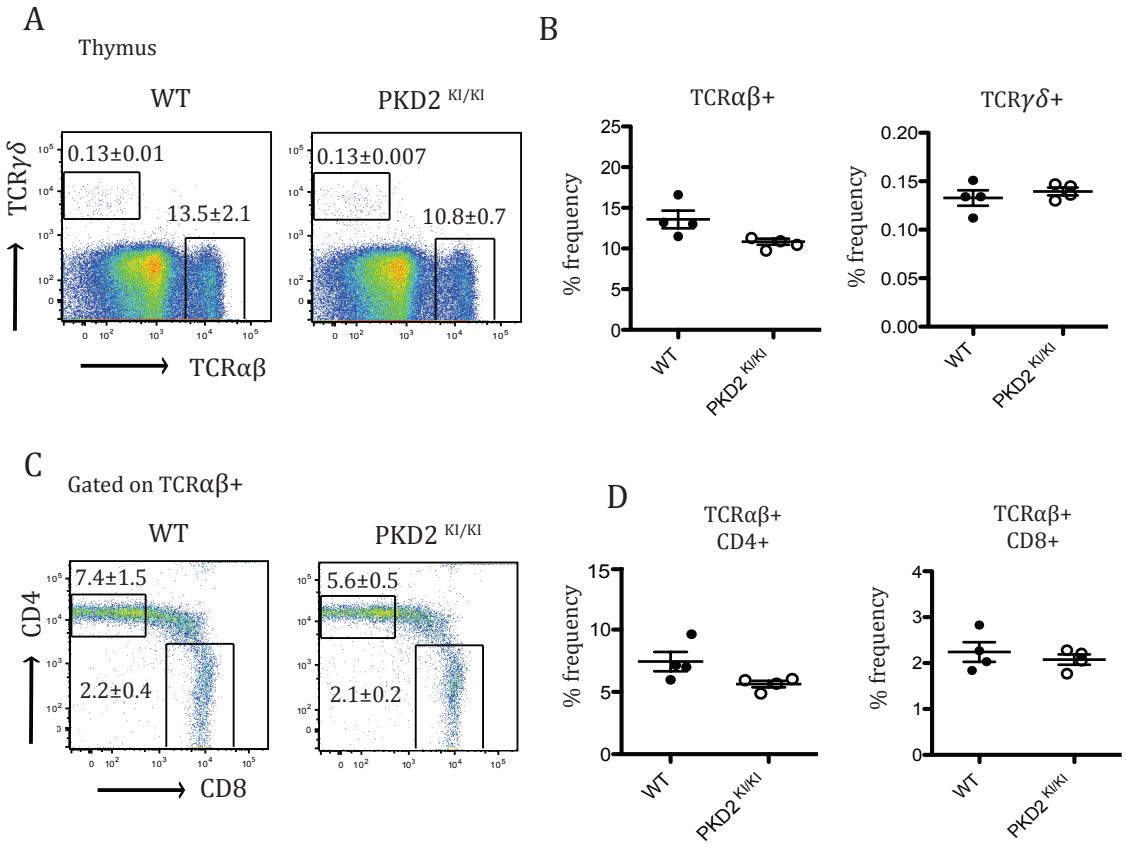

Figure 5.12 T cell subsets are normal within the thymus of PKD2 $^{KI/KI}$ mice

(A) Representative dot plots showing live T cell subsets within thymus of WT and PKD2 $^{KI/KI}$ mice by TCRαβ and TCRγδ surface expression by Flow cytometry. Numbers represent average % frequency and SD (B) Combined data showing% frequency of TCRαβ+ and TCRγδ+ cell subsets (C) Representative dot plots showing CD4+ and CD8+ populations (gated on TCRαβ+ T cells) of WT and PKD2 $^{KI/KI}$ mice. (D) Combined data showing % frequency of TCRαβ+ CD4+ and TCRαβ+ CD8+ subsets. Data obtained from two independent experiments, n=2 mice per genotype.

Collectively, these results demonstrate that although T cell development is clearly intact in PKD$^{KI/KI}$ mice within normal T lymphocyte output from the thymus, significant changes are observed when T lymphocytes populate the periphery with an obvious increase in the number of Tregs within multiple lymphoid tissues.

As discussed previously, HDAC has been implicated in governing the both the development of Tregs but also their suppressive capabilities (reviewed (L. Wang et al. 2009)) . Class IIa HDACs including HDAC7 and HDAC9 have been shown to be expressed in CD4+ FoxP3+ T cells (Dequiedt et al. 2003) (Fontenot

et al. 2005)). Furthermore, the treatment of mice with HDAC inhibitors (HDACi) has been shown to boost the number of Tregs within multiple lymphoid tissues (Tao et al. 2007). This has been shown to be due to increased stability of the FoxP3 protein HDAC9 has been shown to directly acetylate FoxP3 and promote its subsequent degradation (van Loosdregt et al. 2010) (de Zoeten et al. 2010).. In human Tregs, FoxP3 has been shown to form a complex with histone acetyltransferase (TIP60) and with HDAC7 which functions as a transcriptional repressor (B. Li et al. 2007). Importantly, PKD has been shown to regulate class IIa HDACs in multiple cells including B and T lymphocytes downstream of antigen receptor ligation via the BCR and TCR respectively (Parra et al. 2005) (Matthews et al. 2006). HDAC7 which is structurally similar to HDAC9, is highly expressed in the thymus and is essential for normal T cell development from the double negative 3 stage (DN3) in which deletion of HDAC7 using an Lck specific Cre results in a defect in the ability of thymocytes to undergo positive selection (Dequiedt et al. 2003) (Kasler et al. 2011).

As such, we hypothesised that the increase in Tregs we observe in peripheral tissues of $PKD2^{KI/KI}$ mice may be caused by dysregulated FoxP3 protein degradation, mediated via a PKD-HDAC pathway. Within the lab HDAC7 vav-cre ($HDAC7^{-/-}$) mice are available. These mice display a similar phenotype observed in Lck-Cre HDAC7 mice in which there is a developmental block at the DN3 stage within thymocyte differentiation during positive selection (unpublished data, *S.Matthews*). More recently, the exportation of HDAC7 from the nucleus as been shown to be required for the upregulation of CD25 (IL-2Rα) on CD8+ CTLs (Navarro et al. 2011). Hence the nuclear exclusion of HDAC7 by phosphorylation and exportation to the cytoplasm favours the expression of the CD25 receptor on lymphocyte cell surface. As shown throughout this chapter, CD25 is constitutively highly expressed on the surface of Tregs. We therefore sought to address the development of Tregs within the thymus and peripheral lymphoid organs such as spleen and lymph nodes of $HDAC7^{-/-}$ mice.

As can be seen in Figure 5.13A-B, % frequency of nTregs within the thymus of $HDAC7^{-/-}$ mice was significantly reduced (6-fold) when compared to WT mice. Interestingly however the % frequency of Tregs within the peripheral tissues of $HDAC7^{-/-}$ were normal (Figure 5.13E-G). Furthermore, we also

assessed level of FoxP3 expression within CD4+ CD25+ gated cells from WT and HDAC7$^{-/-}$ within the spleen and observed no difference from WT mice (Figure 5.13D-E). This was also the case for other lymphoid tissues including mLN and lymph nodes (Figure 5.13F-G).

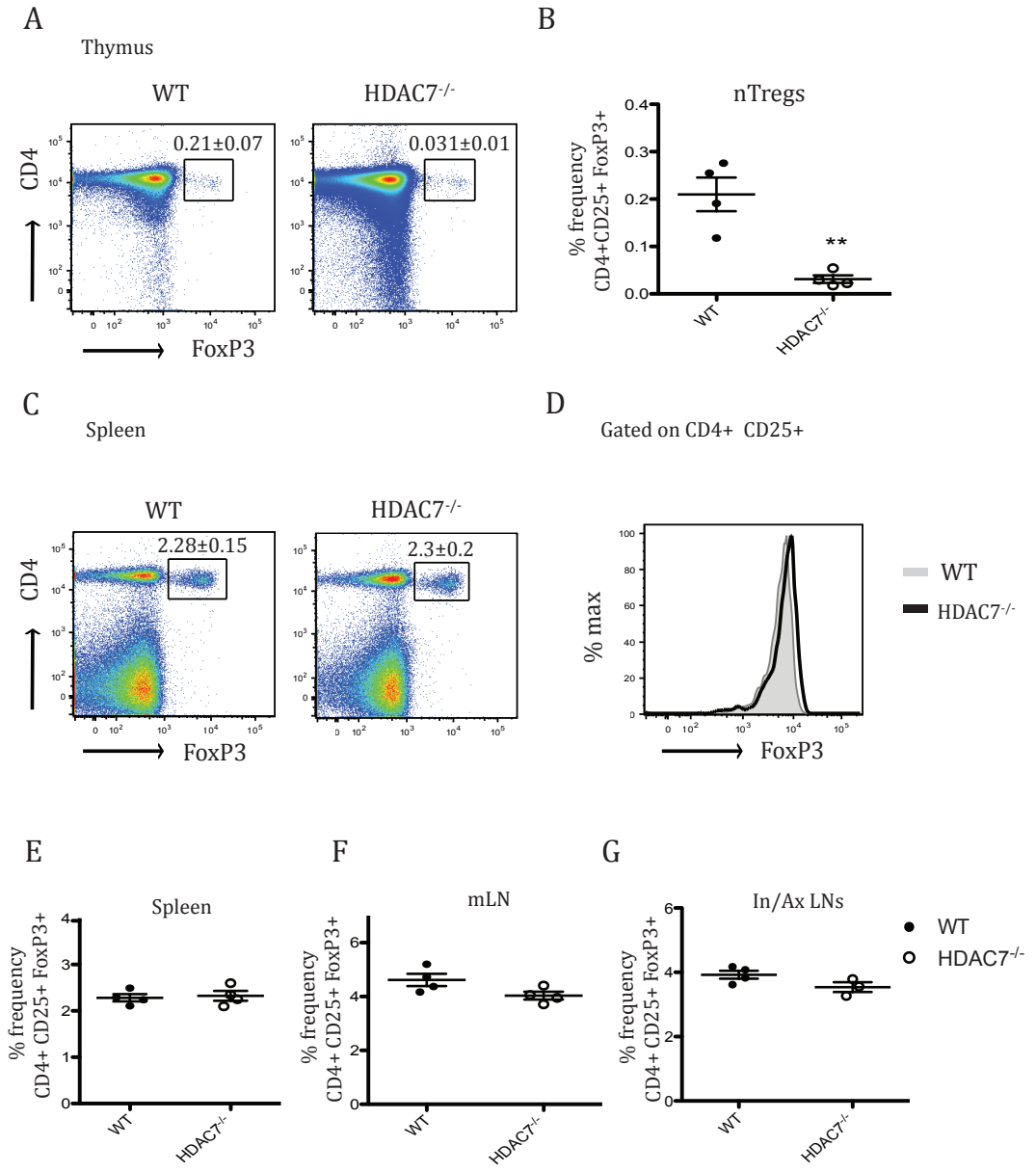

Figure 5.13 Exploring Treg populations within lymphoid tissues of HDAC7$^{-/-}$ mice

(A) Representative dot plots showing nTreg populations within thymus of WT and HDAC7$^{-/-}$ mice by CD4 surface expression and intracellular FoxP3 expression by Flow cytometry. Numbers represent average % frequency and SD. (B) Combined data showing % frequency of nTregs within the thymus. (C) Representative dot plots showing Treg populations within spleen of WT and HDAC7$^{-/-}$ mice. Numbers represent average % frequency and SD. (D) Histogram overlaying FoxP3 expression within CD4+ CD25+ gated lymphocytes in WT and HDAC7$^{-/-}$ mice. (E-G) Combined data showing % Frequency of CD4+ CD25+ FoxP3+ Tregs within spleen, mLN and inguinal/axillary (In/Ax) respectively. Data obtained from two independent experiments, n=4 mice per genotype. ** = $p \leq 0.01$ analysed by student's t tests.

Collectively these data revealed that a PKD regulated HDAC7 mechanism is unlikely to be involved in the regulation of FoxP3 protein stability and therefore does not explain the increase in Tregs observed in PKD2$^{KI/KI}$ mice.

5.3.3 CD103+ population of Tregs is increased within PKD2 $^{KI/KI}$ mice

In order to explore possible explanations to account for increased abundance of Treg populations within the periphery of PKD2$^{KI/KI}$ mice yet lack of increased output from the thymus we assessed known memory markers that indicate if Tregs are activated or indeed memory effector Tregs. CD103 (αEβ7) is an integrin highly expressed in mucosal sites that binds E-cadherin, and is widely expressed on epithelial cells (but not on the endothelium). In contrast to well-defined homing receptors, CD103 is thought to retain expressing lymphocytes at the epithelial surface rather than assist in the extravasation of T cells from tissues. In regard to expression, CD103 is expressed at high levels on IELs, tolergenic DC subsets within gastrointestinal sites, CD8+ CTLs within the lung and more recently a unique subset of functionally distinct Tregs (Schön et al. 1999) (Lehmann et al. 2002) (Huehn et al. 2004) (D. Zhao et al. 2008).

CD103 function and expression on Tregs has been studied using multiple inflammatory and infection models both *in vitro* and *in vivo*. These studies have revealed CD103 as an excellent marker for memory and activated Tregs (Lehmann et al. 2002) (Huehn et al. 2004) (Suffia et al. 2005) (Banz et al. 2003) (McHugh et al. 2002). CD103^{+} CD4^{+} CD25^{+} FoxP3^{+} Tregs have been shown to be highly proliferative when compared to CD103- Treg subsets. Furthermore, CD103+ Treg population have been shown to be more potent suppressor within an experimental arthritis model than CD103- Treg cells. For these reasons, we decided to assess expression of CD103 on the cell surface of WT and PKD2$^{KI/KI}$ Tregs ex vivo, with the hypothesis that Tregs from PKD2$^{KI/KI}$ mice would display a more activated or memory phenotype, which would explain why they are increased in abundance within these tissues if they have become activated after antigen recognition and are subsequently proliferating.

In agreement with previous experiments we observed a significant (2-fold) increase in the abundance of $CD4^+$ $CD25^+$ $FoxP3^+$ Treg populations within the spleen of $PKD2^{KI/KI}$ when compared to WT controls (Figure 5.14A-B). Upon assessing surface expression of CD103 on splenic Treg populations we observed that approximately 3% of WT splenic Tregs expressed high levels of CD103 whereas CD103+ splenic Tregs in $PKD2^{KI/KI}$ mice were significantly increased with approximately 10% of Tregs positive for CD103 (Figure 5.14C). This was also true for total cell numbers (Figure 5.14D).

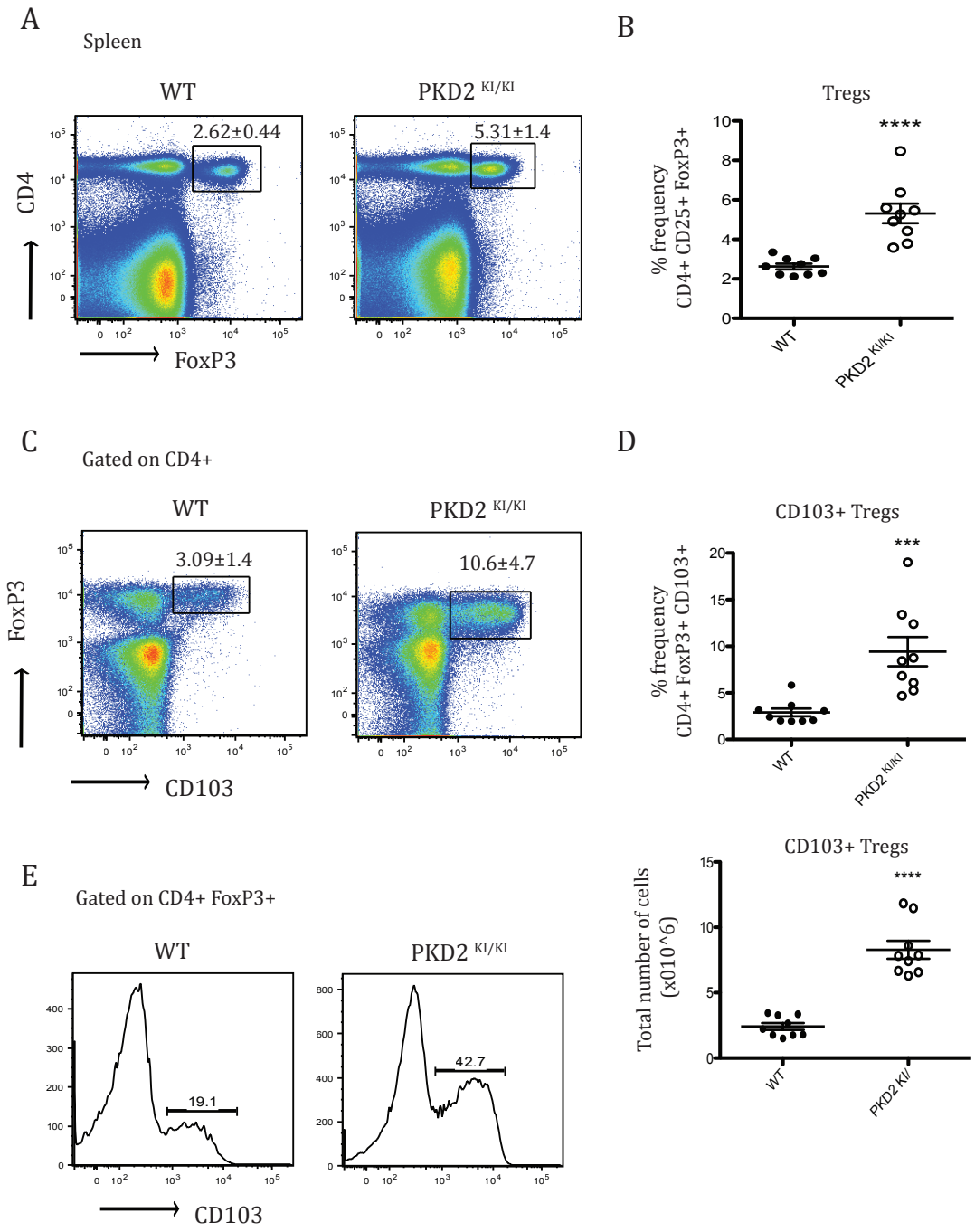

Figure 5.14 CD103+ Treg populations are increased within the spleen of PKD2$^{KI/KI}$ mice

(A) Representative dot plots showing Treg populations within spleen of WT and PKD2 $^{KI/KI}$ mice by CD4 surface expression and intracellular FoxP3 expression by Flow cytometry. Numbers represent average % frequency and SD. (B) Combined data showing % frequency of CD4+FoxP3+CD25+ Tregs within the spleen (C) Representative dot plots showing CD103 expressing populations of Treg within spleen (Gated on CD4+ population) (D) Combined data showing % frequency of CD4+ FoxP3+ CD103+ Tregs within spleen. Data obtained from 3 independent experiments, n=9 mice per genotype. *** = p≤0.001 and **** = p≤0.0001 analysed by students t test.

These data collectively suggests that the increase in Tregs we observe within peripheral lymphoid tissues of PKD2 $^{KI/KI}$ mice are either activated Tregs or memory Tregs when compared to Treg populations within WT mice.

We also assessed IL-7R (CD127) expression on the cell surface of WT and PKD2 $^{KI/KI}$ Tregs from the spleen and found no change in expression on the cell surface (data not shown).

5.3.4 Aging mice

It is known that $CD4^+$ $CD25^+$ $FoxP3^+$ Treg populations accumulate with increase in age in various tissues in mice, including spleen and lymph nodes. We next to decided to assess if Treg populations within $PKD2^{KI/KI}$ mice increased with age when compared to age matched WT mice. We also wished to address if CD103+ population of Tregs also expands with increase in age as observed in $PKD2^{KI/KI}$ mice between 4-8 weeks of age. Mice used in this study were allowed to age to 12 months.

Assessment of Tregs within spleen of $PKD2^{KI/KI}$ aged mice revealed a 2-fold increase (Figure 5.15A-B) when compared to WT mice of the same age. Although WT mice had an increase of Tregs within the spleen as expected with an increase in age, $PKD2^{KI/KI}$ mice still retained a 2 fold increase, suggesting the expanded pool observed in younger mice is retained as the difference in fold change remains constant between genotypes with age.

Furthermore, CD103 expression on Tregs displayed a 4-fold increase on $PKD2^{KI/KI}$ Tregs (Figure 5.15C-D). These data imply that not only is CD103 found to be up regulated on the cell surface of Tregs within tissues of younger mice (between 4-8 weeks), but that this up-regulation continues over time in aging $PKD2^{KI/KI}$ mice.

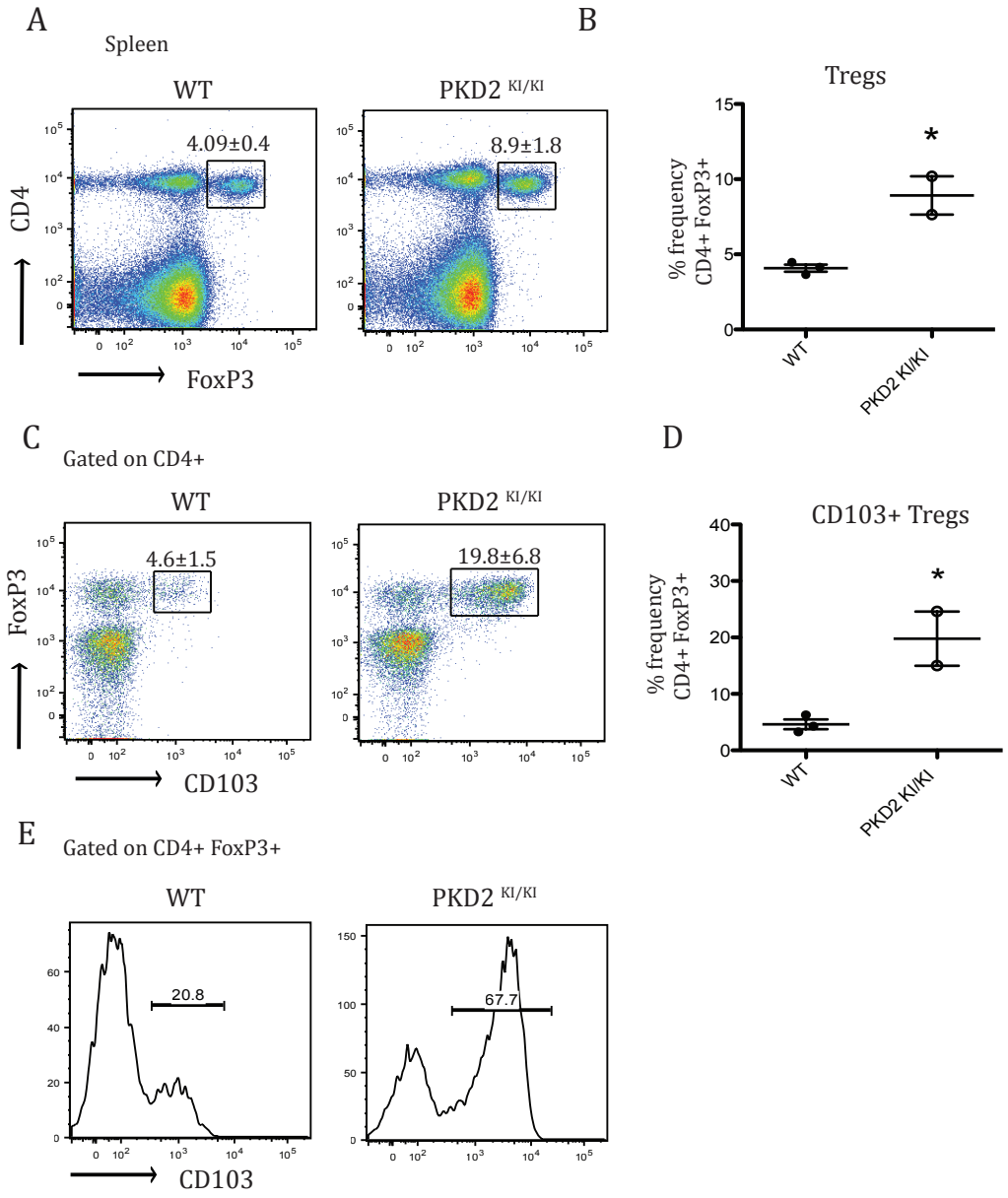

Figure 5.15 CD103+ Treg populations are increased in spleen of aged PKD2$^{KI/KI}$ mice

(A) Representative dot plots showing Treg populations within spleen of aged WT and PKD2$^{KI/KI}$ mice by CD4 surface expression and intracellular FoxP3 expression by Flow cytometry. Numbers represent average % frequency and SD. (B) % frequency of CD4+FoxP3+CD25+ Tregs within the spleen (C) Representative dot plots showing CD103 surface expression and intracellular Foxp3 expression of Treg populations within spleen (Gated on CD4+ population) (D) Combined data showing % frequency of CD4+ FoxP3+ CD103+ Tregs within spleen. (E) Histogram showing CD103 surface expression in CD4+ FoxP3+ Tregs within spleen of WT and PKD2$^{KI/KI}$ aged mice. Data obtained from 1 independent experiment, 3 WT mice and 2 PKD2$^{KI/KI}$ mice * = p≤ 0.05 analysed by students t test.

In addition to the Tregs within the spleen, we also assessed Treg populations within the inguinal and axillary lymph nodes of aged mice. As expected, aged $PKD2^{KI/KI}$ mice displayed a significant increased in % frequency of $CD4^{+}$ $CD25^{+}$ $FoxP3^{+}$ populations (Figure 5.16A-B), again this increase was approximately 2 fold in agreement with data obtained from the spleen. Furthermore, analysis of CD103 expression on $PKD2^{KI/KI}$ Tregs showed that this was also significantly increased (Figure 5.16C-D).

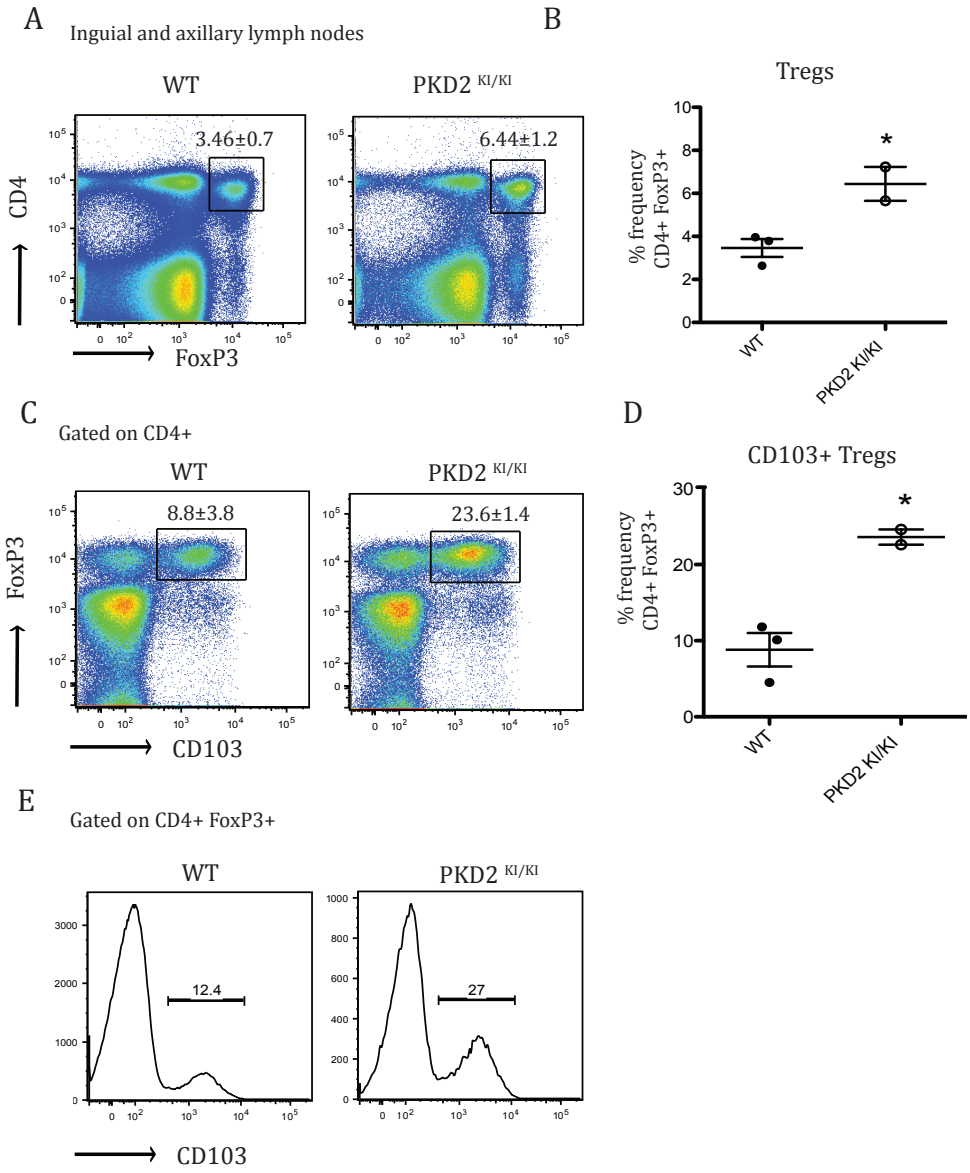

Figure 5.16 CD103+ Treg populations are increased in inguinal and axillary lymph nodes of aged PKD2$^{KI/KI}$ mice.

(A) Dot plots showing Treg populations within inguinal and axillary lymph nodes of aged WT and PKD2 $^{KI/KI}$ mice by CD4 surface expression and intracellular FoxP3 expression by Flow cytometry. Numbers represent average % frequency and SD. (B) % frequency of CD4+FoxP3+CD25+ Tregs within the lymph nodes (C) Dot plots showing CD103 surface expression and intracellular Foxp3 expression of Treg populations within lymph nodes (Gated on CD4+ population) (D) % frequency of CD4+ FoxP3+ CD103+ Tregs within spleen. (E) Histogram showing CD103 surface expression in CD4+ FoxP3+ Tregs within lymph nodes of WT and PKD2 $^{KI/KI}$ aged mice. Data obtained from 1 independent experiment, n= 3 WT mice and 2 PKD$^{KI/KI}$ mice. * = p≤ 0.05 analysed by students t test.

5.4 Analysis of lymphocyte populations in the small intestine of PKD2 $^{KI/KI}$ mice

After initially observing the increased lymphoid tissues, specifically the GALTs including the mLN and PPs, we decided to next assess lymphocyte populations within the small intestine in PKD2$^{KI/KI}$ mice. The mucosal immune system within the small intestine can be separated into two anatomically distinct layers, the lamnia propria and the intraepithelial layer, both of which are populated with distinct cell subsets. The lamina propria is characterised by a heterogeneous population of immune cells, including multiple innate immune cell subsets such as DC subsets, macrophages, eosinophils, neutrophils, and mast cells. Adaptive immune cells include IgA producing B cells and T cells (mostly CD4+), including CD4+ Foxp3+ Tregs (Extensively reviewed (Mowat & Agace 2014)) . In contrast, the intraepithelial layer contains a more homogenous population primarily consisting of T cells known as intraepithelial lymphocytes (IELs).

PKD isoform expression within GALT tissues is largely unknown, however embryonic in situ hybridisation studies have demonstrated PKD2 transcript levels within the mucosa of the intestine and the intestinal villi (Oster et al. 2006). Recently, PKD1 has been be implicated in mediating class IIa HDAC export within intestinal epithelial cells as well as promoting rapid migration of these cells (Sinnett-Smith et al. 2014) (Young et al. 2012).

As PKD2 is the dominant isoform expressed by CD4+ and CD8+ T lymphocytes from the thymus and lymph node tissue it is plausible that PKD2 will be selectively expressed within GALTs and within lymphocytes residing in the small intestine. However, the role of PKD2 within the mucosal immune system and indeed if it plays a role in mucosal associated lymphocyte populations has not been addressed.

5.4.1 Intraepithelial lymphocytes

As discussed within introduction, the intraepithelial epithelium of mammals within mucosal membranes found within the tissues such as the

gastrointestinal system and the lung, contains IELs that are found at the basement membrane between enterocytes. In the human small intestine IELs are reported to exist at a frequency between 10-15 IELs per 100 epithelial cells(A 1977). Due to the direct contact IELs have with enterocytes within the gut and their immediate proximity to luminal antigens they form the front line of immune defense from pathogens within the gut. However, IELs are also exposed to antigen from food and commensal bacteria and therefore have to maintain a delicate balance between immune response and tolerance.

We sought to characterise IEL populations within the small intestine of WT and PKD2 $^{KI/KI}$ mice to establish if loss of PKD2 catalytic activity played a role in gut lymphocyte homeostasis. It should be noted that these experiments were performed in collaboration with Mr. George Ramsay in Doreen Cantrell's lab within University of Dundee. One of the first observations within this study was a significant increase in the total number (x10^6) of IELs within PKD2$^{KI/KI}$ when compared to age matched WT mice (Figure 5.17).

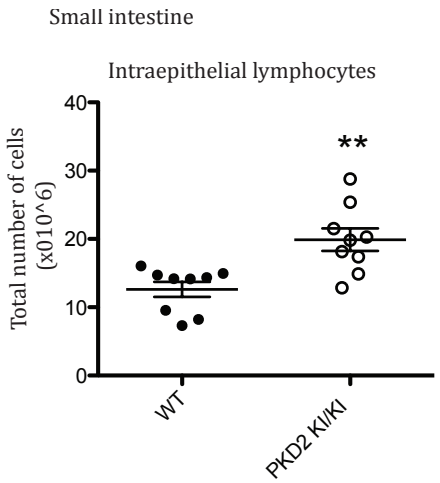

Figure 5.17 Intraepithelial lymphocytes are increased in the small intestine of PKD2$^{KI/KI}$ mice

Total live cell number (x10^6) of intraepithelial lymphocytes in WT and PKD2 $^{KI/KI}$ intraepithelial layer of the small intestine determined by Flow Cytometry. (n=3) ** = p≤0.01 analysed by students t test. Error bars represent SD. (Data obtained from from 3 independent biological experiments n=9 mice per genotype). Experiments were performed in collaboration with Mr. George Ramsay, Doreen Cantrell's lab, University of Dundee.

We next assessed IEL populations within the small intestine via flow cytometry. We observed a significant increase (1.7 fold) in the % frequency in TCRαβ+ IELs within the intraepithelial layer of the small intestine in $PKD2^{KI/KI}$ mice when compared to WT mice. Interestingly, we also observed a significant reduction (1.5 fold) in the % frequency of TCRγδ+ IEL in the small intestine (Figure 5.18A-C). These data could suggest a potential role for PKD2 catalytic activity in the maintenance of "normal" T cell subset population and homeostasis within the intraepithelial layer. These data also imply that loss of PKD2 catalytic activity has led to a converted lymphocyte profile within the gut, either due to skewed differentiation, impaired homeostasis, and lymphocyte homing multiple mechanisms.

Furthermore, these experiments revealed no difference in the % frequency of TCRαβ+ CD4+ IEL although there was a significant increase (2.6 fold) in the % frequency of TCRαβ+ CD8+ IEL within the small intestine of $PKD2^{KI/KI}$ mice when compared to WT mice (Figure 5.18D-F).

Although all IEL display an antigen experienced phenotype or activated phenotype, they can be further divided into two major subsets including natural IEL and inducible IEL, which are defined by the mechanism, in which they were activated and the unique surface markers they display. Natural IEL have been described as a regulatory subset required to maintain gut epithelium integrity. These subsets are defined as either $TCR\alpha\beta^{+}$ $CD8\alpha\alpha^{-/+}$ or $TCR\gamma\delta^{+}$ $CD8\alpha\alpha^{-/+}$ and importantly do not express CD4 or CD8αβ. Inducible IEL are either $TCR\alpha\beta^{+}$ $CD4^{+}$ $CD8\alpha\alpha^{-/+}$ or $TCR\alpha\beta^{+}$ $CD8\alpha\beta^{+}$ $CD8\alpha\alpha^{-/+}$, furthermore we were also able to analyse TCRαβ+ CD8αβ+ and $TCR\alpha\beta^{+}$ $CD8\alpha\alpha^{+}$. Interestingly, we also observed a significant increase in the % frequency of $TCR\alpha\beta^{+}$ $CD8\alpha\beta^{+}$ inducible IEL subset (Figure 5.18G-I) and a concurrent significant decrease in the % frequency of $TCR\alpha\beta^{+}$ $CD8\alpha\beta^{-}$ $CD8\alpha\alpha^{+}$ natural IEL subset.

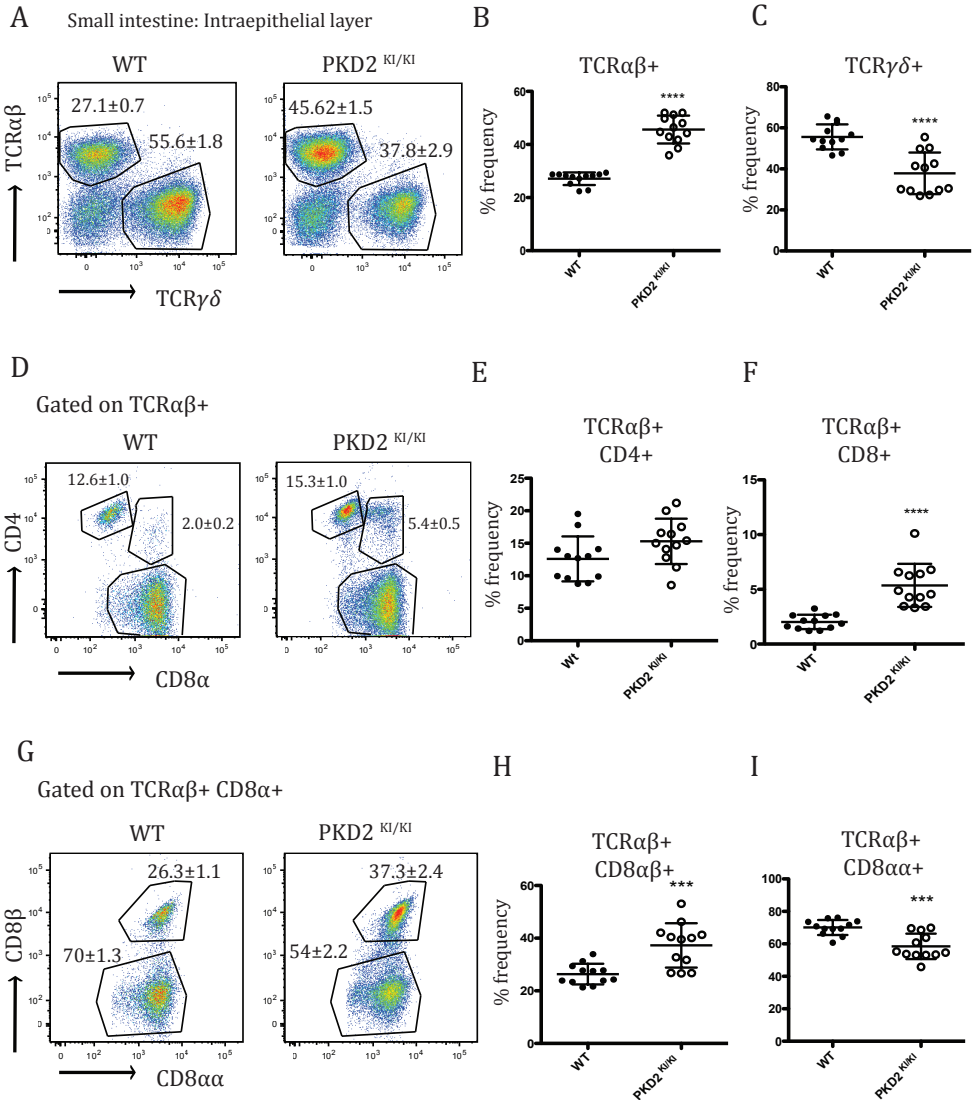

Figure 5.18 Analysis of specific T lymphocyte subsets in the intraepithelial layer of small intestine of PKD2$^{KI/KI}$

(A) Representative dot plots showing live CD45+ TCRαβ+ and TCRγδ+ populations of WT and PKD2 $^{KI/KI}$ mice within IEL layer by Flow cytometry. Numbers represent average % frequency and SD. (B) Combined data showing % frequency of TCRαβ+ subsets within IEL layer (C) % frequency of TCRγδ+ subsets within IEL layer (D) Dot plots showing live CD45+ TCRαβ+ CD4+, CD45+ TCRαβ+ CD8α+ and TCRαβ+CD4+ CD8α+ double positive populations of WT and PKD2 $^{KI/KI}$ mice. (E) % Frequency of CD45+ TCRαβ+ CD4+ populations (F) Combined data showing % frequency of CD45+ TCRαβ+ CD8α+ populations (G) Dot plots showing live CD45+ TCRαβ+ CD8αβ and CD45+ TCRαβ+ CD8αα+ T cell subsets of WT and PKD2 $^{KI/KI}$ mice within IEL. (H) % Frequency of CD45+ TCRαβ+ CD8αβ+ (I) Combined data showing % Frequency of CD45+ TCRαβ+ CD8αα+ T cell subsets. Error bars represent SD. Data obtained from 3 independent experiments, n=13 mice per genotype. *** = p≤0.001 and **** = p≤0.0001 analysed by students t test. Experiments were performed in

collaboration with Mr. George Ramsay, Doreen Cantrell's lab, University of Dundee.

5.4.2 Lamina Propria

In contrast to the intraepithelial layer, which mainly consists of T lymphocytes, the lamina propria layer (LP) layer within the small intestine is far more heterogeneous containing a variety of immune cell subsets including B cells, T cells, macrophages and dendritic cells. We next assessed if lymphocyte populations including B cells and T cell subsets were affected by loss of PKD2 catalytic activity. The % frequency of B cells ($B220^{+}$) and $TCR\alpha\beta^{+}$ within the LP layer of PKD2 $^{KI/KI}$ mice were normal when compared to age and sex matched WT mice (Figure 5.19A-C). A more detailed analysis of T cell subsets within the LP layer revealed no significant changes within PKD2 $^{KI/KI}$ mice including % frequency of TCRαβ+ CD4+, TCRαβ+ CD8α+ and TCRαβ+ CD4+ CD8α+ double positive populations (Figure 5.19D-G). These data were in contrast to dramatic differences observed within the intraepithelial layer of PKD2 $^{KI/KI}$ mice indicating that PKD2 may play a selective role in this layer of the gut and perhaps not within the LP layer.

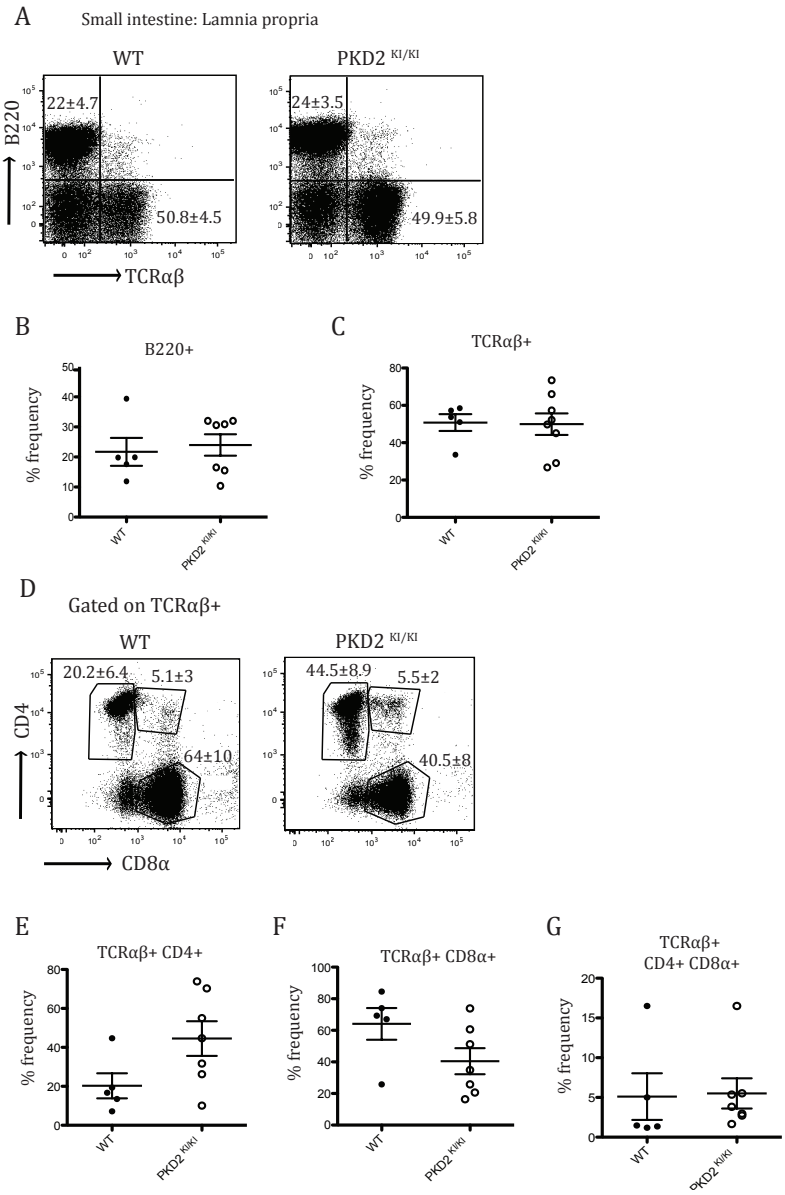

Figure 5.19 B cells and T cell subsets within lamnia propria layer are normal within the small intestine of PKD2$^{KI/KI}$ mice

(A) Representative dot plots showing live CD45+ B220+ and TCRαβ + populations of WT and PKD2 $^{KI/KI}$ mice within lamnia propria by Flow cytometry. Numbers represent average % frequency and SD. (B) Combined data showing % frequency of B220+ subsets within IEL layer (C) % frequency of TCRαβ + subsets within IEL layer (D) Dot plots showing live CD45+ TCRαβ+ CD4+, CD45+ TCRαβ+ CD8α+ and TCRαβ+CD4+ CD8α+ double positive populations of WT and PKD2 $^{KI/KI}$ mice. (E) % Frequency of CD45+ TCRαβ+ CD4+ populations (F) % frequency of CD45+ TCRαβ+ CD8α+ populations (G) Dot plots showing live CD45+ TCRαβ+ CD8αβ and CD45+ TCRαβ+ CD8αα+ T cell subsets of WT and PKD2 $^{KI/KI}$ mice within IEL. (H) % Frequency of CD45+ TCRαβ+ CD8αβ+ (I) % Frequency of CD45+ TCRαβ+ CD8αα+ T cell subsets. Data obtained from 3 independent experiments, n=5 WT mice and 6 PKD2$^{KI/KI}$ mice per genotype. Experiments were performed in collaboration with Mr. George Ramsay, Doreen Cantrell's lab, University of Dundee.

5.4.3 Analysis of Tregs within the IEL and lamina propria of PKD2$^{KI/KI}$ mice

As we had thoroughly established that peripheral Tregs were significantly increased within multiple tissues including the spleen, mLN and PPs in PKD2$^{KI/KI}$ mice *ex vivo,* we also sought to assess if Treg populations were also increased in the gastrointestinal tract. To assess this we examined Treg populations within the IEL and lamnia propria layers of WT and PKD2$^{KI/KI}$ mice *ex vivo*.

As can be seen in Figure 5.20A-B, % frequency of CD4^{+} FoxP3^{+} Tregs were increased within the IEL layer of the small intestine of PKD2$^{KI/KI}$ mice, this was also true in regard to total cell number (x10^{6}) of CD4+ FoxP3+ cells (Figure 5.20C).

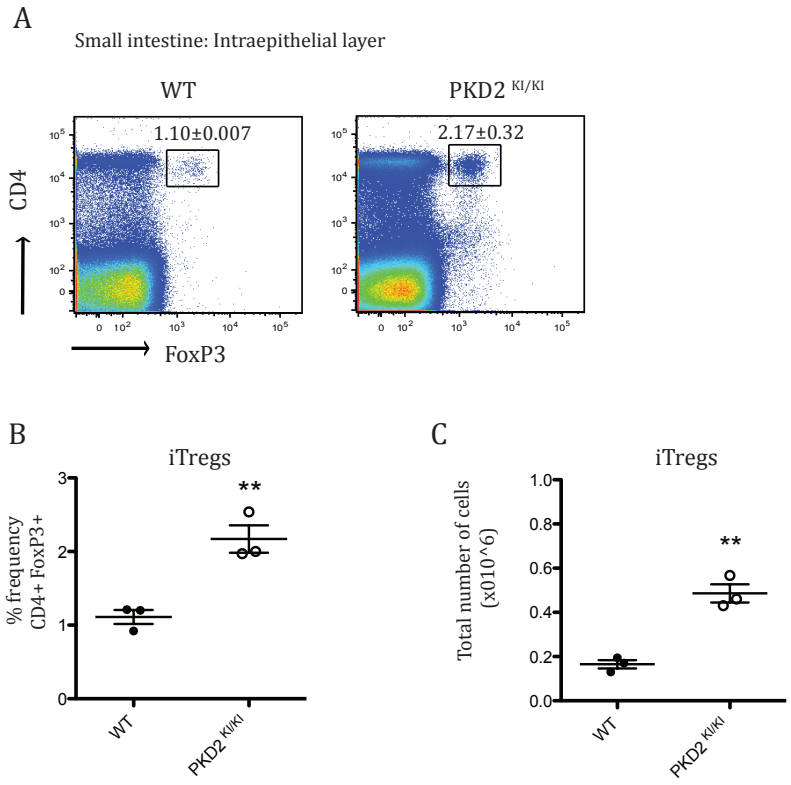

Figure 5.20 Treg populations are increased in the intraepithelial layer within the small intestine of PKD2$^{KI/KI}$ mice

(A) Representative dot plots showing Treg populations in the intraepithelial layer within small intestine of WT and PKD2 $^{KI/KI}$ mice shown by CD4 surface expression and intracellular FoxP3 expression by Flow cytometry. Numbers represent average % frequency and SD. (B) % frequency of CD4+FoxP3+ Tregs within the intraepithelial layer of the small intestine (C) Total number (x10^6) of CD4+FoxP3+ Tregs within the intraepithelial layer of the small intestine Data obtained from two independent experiments, n=3 mice per genotype. ** = p≤0.01 analysed by students t test. Experiments were performed in collaboration with Mr. George Ramsay, Doreen Cantrell's lab, University of Dundee.

We were also able to assess CD4$^+$ FoxP3$^+$ Tregs within the LP layer of the small intestine in PKD2$^{KI/KI}$ mice, although unfortunately we were unable to gather a large cohort for this due to difficulties obtaining preparations of the LP layer. In successful samples we observed a trend in the increase (3-fold) of % frequency of CD4$^+$ FoxP3$^+$ Tregs within the LP of PKD2$^{KI/KI}$ mice (Figure 5.21A-B).

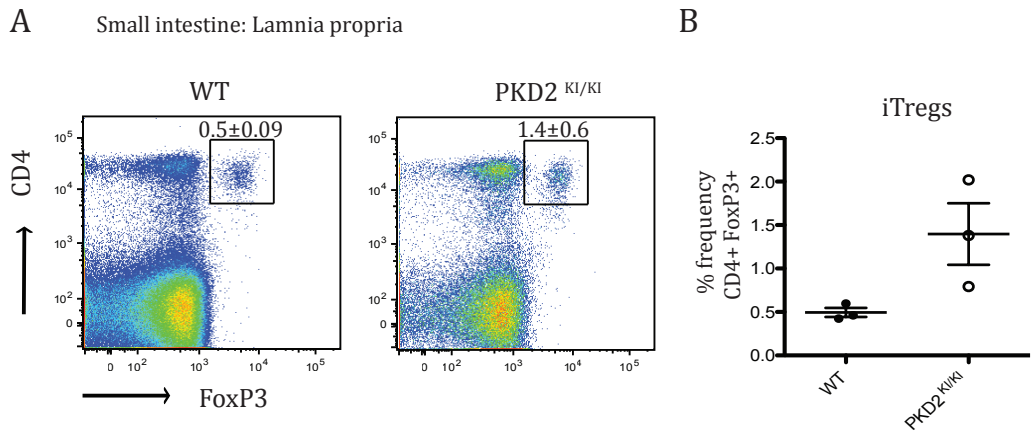

Figure 5.21 Tregs within lamnia propria layer of small intestine of PKD2$^{KI/KI}$ mice

(A) Representative dot plots showing Treg populations in the lamnia propria layer within small intestine of WT and PKD2$^{KI/KI}$ mice shown by CD4 surface expression and intracellular FoxP3 expression by Flow cytometry. Numbers represent average % frequency and SD. (B) Combined data showing % frequency of CD4+FoxP3+ Tregs within the lamnia propria. Data obtained from 2 independent experiments, n=3 mice per genotype. Experiments were performed in collaboration with Mr. George Ramsay, Doreen Cantrell's lab, University of Dundee.

5.5 *In vivo* colitis model

Inflammatory bowel diseases (IBD) can be separated into two clinically defined forms of chronic inflammatory conditions including Crohn's disease (CD) and ulcerative colitis (UC), although characteristically different both diseases involve chronic inflammation that affects the gastrointestinal tract. The etiology of IBD is thought to be multifaceted involving a genetic basis, environmental factors, microbiota within the gastrointestinal tract and a dysregulated immune system although exact mechanisms remains largely unknown (Reviewed extensively (Kaser et al. 2010)).

Studies investigating the mechanisms of IBDs have exploded in recent years due to increased availability of multiple animal models to study intestinal inflammation (Reviewed (Ostanin et al. 2008)). Data obtained from multiple studies have demonstrated chronic gut inflammation is the result of a immune dysregulation. Specifically T cells have been shown to be involved in both protective and pathogenic roles in gut inflammation (Reviewed (Powrie 1995)). As such, the T cell transfer model of chronic colitis has become widely used as an appropriate animal model to study early immune events during the development of colitis (Powrie et al. 1993) (Asseman et al. 1999) (Read et al. 2006) (Uhlig et al. 2006). This model is based upon the disruption of T cell homeostasis initiated by the transfer of naïve CD4+ CD45Rb^{hi} T cells from WT mice into a synergic host resulting in intestinal inflammation. Importantly, this model allows the study of cytokine levels within distinct sections of the small intestine involved in the pathogenesis of disease, in contrast to spontaneous models of intestinal inflammation such as IL-2$^{-/-}$ and IL-10$^{-/-}$ animal models (Powrie et al. 1996). In this study RAG2 KO mice were used as recipient synergic hosts whereby mature T and B cells are absent due to an inability to undergo VDJ rearrangement to produce a functional antigen receptor (Shinkai et al. 1992). It is important to note that RAG2$^{-/-}$ mice retain a functional and complete innate immune system including macrophages and dendritic cell subsets. Recipient hosts receiving naïve CD4+ CD45Rb^{hi} T cells go on to develop inflammation within the colon resulting in colitis typically following 5-8 weeks of T cell transfer, although this time period varies depending on mouse strain and the animal facilities animals

are housed in. During the time period following T cell transfer recipient mice progressively lose weight, this is usually accompanied by diarrhoea. Furthermore, histopathological analyses of proximal and distal colon sections from mice with active disease reveal mild to moderate inflammatory cell infiltration within the lamina propria and submucosa, epithelial cell hyperplasia and mucosal erosion. Additionally, this disease model is also frequently used to study the functionality of Tregs in their ability to actively suppress and limit the onset of intestinal inflammation. Tregs injected into recipient mice have also been shown to dynamically reverse established intestinal inflammation, demonstrating not only its potential therapeutic use within patients with established disease but indeed its usefulness as a tool to study Treg function in an intestinal inflammation model (Mottet et al. 2003). Protection by Tregs against intestinal inflammation within this model has been shown to be exerted in an IL-10 dependent fashion (Asseman et al. 1999).

We decided utilise this disease model to assess if Tregs isolated from $PKD2^{KI/KI}$ mice were suppressive in the development of colitis in $RAG2^{-/-}$ synergic hosts, as an indication of Treg functionality. This study was ultimately to address if Tregs lacking PKD2 catalytic activity are functional, but also addresses if resulting increase in Treg populations we observe in $PKD2^{KI/KI}$ mice is intrinsic or extrinsic (i.e. within cell or environment). The experimental approach for this study is described in Table 5.1. It should be noted that although this study was set up with 5 mice per group, one mouse died (Group 1) due to extenuating circumstances that were not related to development of colitis and another mouse (Group 3) was removed from the study due to failed IP injection.

Experimental group	**Phenotype of cells**		**Number of cells injected**
Group 1 WT naïve only	CD45RB ^{high} CD4+ CD25-		400,000 cells
Group 2 PKD2 $^{KI/KI}$ naïve only	CD45RB ^{high} CD4+ CD25-		400,000 cells
Group 3 WT naïve + WT Treg	WT naïve CD45RB ^{high} CD4+ CD25-	WT Treg CD45RB ^{low} CD4+ CD25+	400,000 naïve + 100,000 Tregs
Group 4 WT naïve + PKD2$^{KI/KI}$ Treg	WT naïve CD45RB ^{high} CD4+ CD25-	PKD2 $^{KI/KI}$ Treg CD45RB ^{low} CD4+ CD25+	400,000 naïve + 100,000 Tregs

Table 5.1 Experimental set up for *in vivo* colitis model to assess colitis development in naïve T cells and Treg cells lacking PKD2 catalytic activity

After injection of cells into synergic hosts the study was carried out for 3 weeks to assess the development of colitis, which was assessed by weekly weighing of the mice.

RAG2$^{-/-}$ mice injected with WT naïve CD4^{+}CD45Rb^{hi} cells (Group 1) displayed a slight weight gain after 1 week of T cell transfer, however within week 2 subsequently began to display clinical signs of colitis including loose stools and weight loss (Figure 5.22). Within this group the average % weight change from initial weight by the end of the study was 3.4%. In contrast, RAG2$^{-/-}$ mice injected with PKD2$^{KI/KI}$ naïve CD4^{+}CD45Rb^{hi} cells (Group 2) began to lose weight from week 1 and consistently lost weight over the course of the study with the average % weight change was 9.2% (Figure 5.22A). RAG2$^{-/-}$ receiving

WT naïve $CD4^+CD45Rb^{hi}$ cells co-injected with WT $CD4^+$ $CD25^+$ Tregs (Group 3) displayed weight loss from week 1 which continued throughout the study where the % average weight change was 8.6% by the end of the study (Figure 5.22B).

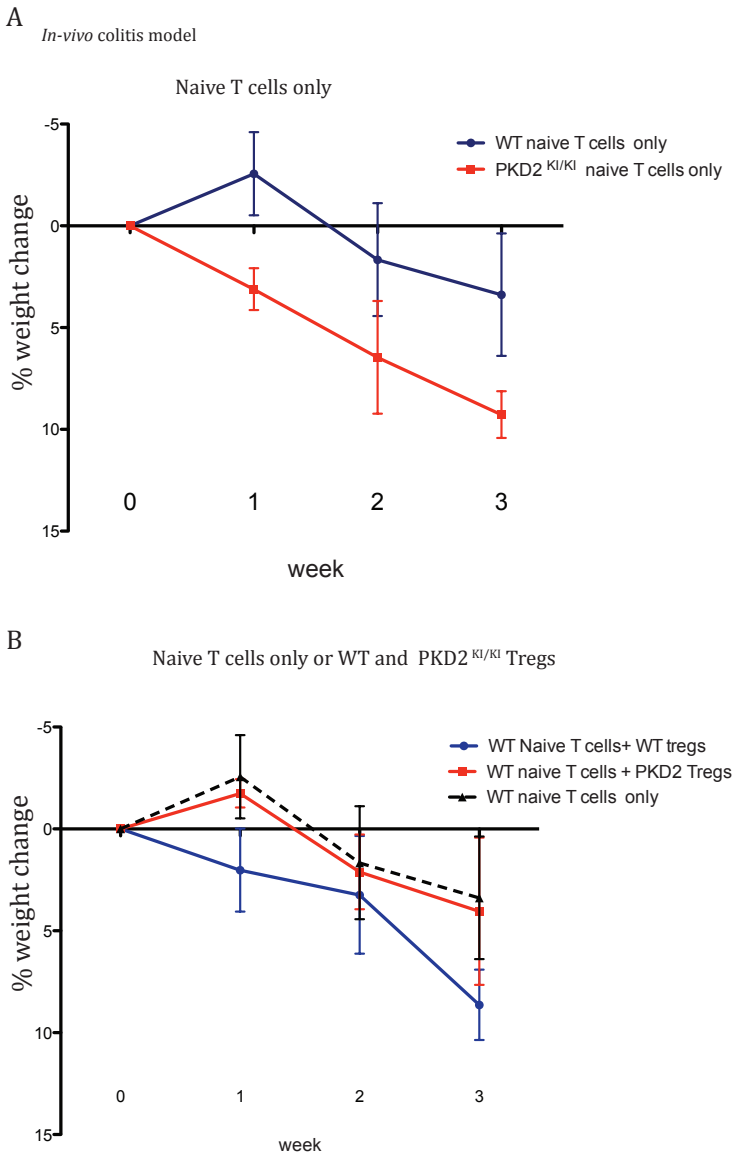

Figure 5.22 Clinical colitis score monitored by percentage weight change in RAG2$^{-/-}$ recipient mice

(A) % Body weight change from day 0 weight after adoptive transfer of either WT naïve T cells only^{-} (Group 1) or PKD2$^{KI/KI}$ naïve T cells only (Group 2). (B) % Body weight change from day 0 of RAG2$^{-/-}$ mice after injection with either WT naïve only (group 1), WT naïve T cells + WT Tregs (Group 3) or WT naïve T cells + PKD2KI/KI Tregs. Mice were monitored for total of 3 weeks. (4 mice used per group (groups 1 and 3), 5 mice per group (groups 2 and 4). Data from 1 independent experiment. Experiments were performed in collaboration with Mr. George Ramsay, Doreen Cantrell's lab, University of Dundee.

These data initially indicated to us that perhaps co-injection with WT $CD4^+CD25^+$ Tregs did not result in any protection from the development or progression of colitis. However, as weight loss is not the only clinical measurement of severity of colitis we also assessed colitis severity in each experimental group by other indicators including weight of tissues such as the spleen and colon, as well as colon length. Additionally, we assessed colitis severity by histopathological scoring.

As can be seen in Figure 5.23A, mice coinjected with WT naïve $CD4^+CD45Rb^{high}$ and WT $CD4^+$ $CD25^+$ Tregs displayed significantly lower spleen weight indicating a good degree of reduction in inflammation and therefore protection from progression of colitis. Interestingly, $RAG2^{-/-}$ mice receiving co-injection of WT naïve $CD4^+CD45Rb^{high}$ cells and $PKD2^{KI/KI}$ $CD4^+$ $CD25^+$ Tregs also displayed significantly lower spleen weight in comparison to $RAG2^{-/-}$ receiving WT naïve WT $CD4^+CD45Rb^{high}$ only cells, suggesting a slight protection but not as efficient as WT Tregs. Assessment of colon weight within each experiment group revealed no significant differences (Figure 5.23B). However, measurement of colon length can also be used as in indication of severity of colitis as the colon characteristically shorten in length upon disease progression. Analysis of colon length $RAG2^{-/-}$ mice receiving WT naïve $CD4^+CD45Rb^{high}$ and WT $CD4^+$ $CD25^+$ Tregs were significantly longer when compared with $RAG2^{-/-}$ mice receiving WT naïve $CD4^+CD45Rb^{high}$ only (Figure 5.23C).

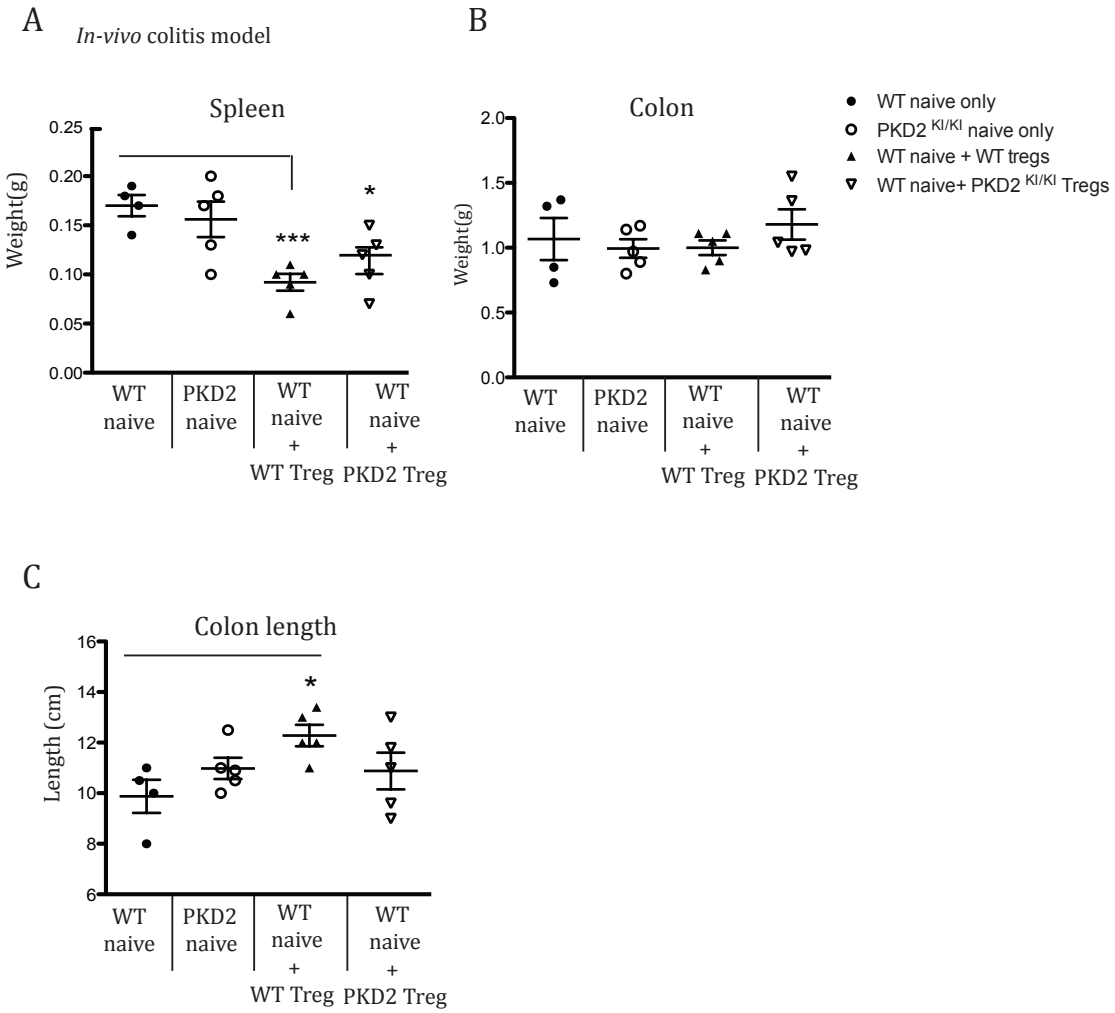

Figure 5.23 Tissue size in RAG2$^{-/-}$ mice after transfer of WT and PKD2 $^{KI/KI}$ naive and Treg subsets

Tissue weight and colon length from RAG2$^{-/-}$ recipient mice after transfer of indicated sets of cell after 3 weeks. (A) Spleen weight (g) (B) Colon weight (g) (C) Length of colon (cm) (4-5 mice per group n=1) * = p≤ 0.05 and *** = p≤0.001 analysed by students t test. Data from 1 independent experiment. Experiments were performed in collaboration with Mr. George Ramsay, Doreen Cantrell's lab, University of Dundee.

In addition to assessment of clinical markers such as % body weight change and size or length of tissues including the spleen and colon, we also received histopathological evaluation of tissue sections from the proximal and distal colon of all experimental groups. This was performed using tissue sectioning, HE staining and subsequent assessment by two independent pathologists for clinical signs and severity scoring for colitis. As can be seen in (Figure 5.24A) under normal conditions the mucosa within RAG2$^{-/-}$ mice is well preserved with regularly arranged glandular crypts, there is also the presence of well differentiated goblet cells. Importantly, there is no inflammatory cell infiltration present within the lamina propria and submucosa. In contrast to this, RAG2$^{-/-}$ mice injected with WT naïve CD4^{+}CD45Rb^{hi} cells develop moderate to marked inflammatory cell infiltration within the lamina propria and submucosa. There is also the presence of focally extension moderate mucosal erosion (Figure 5.24B indicated by blue arrows)

Assessment of histological changes within the proximal colon of RAG2$^{-/-}$ receiving WT naïve CD4^{+}CD45Rb^{hi} cells revealed the presence of moderate inflammatory cell infiltration in the lamina propria, mild inflammation in the submucosa as well as mild to moderate crypt hyperplasia (Figure 5.25A). These histopathological changes within the colonic architecture are consistent with the presence of established colitis. Assessment of histological changes within the proximal colon of RAG2$^{-/-}$ mice receiving PKD2$^{KI/KI}$ naïve CD4^{+}CD45Rb^{hi} cells displayed moderate to marked transmural inflammatory cell infiltration, which was most prominent within the lamina propria (Figure 5.25B). These data illustrate that both WT naïve CD4^{+}CD45Rb^{hi} cells and PKD2$^{KI/KI}$ naïve CD4^{+}CD45Rb^{hi} cells were able to initiate and cause established colitis within the T cell transfer model. Interestingly naïve PKD2$^{KI/KI}$ CD4^{+}CD45Rb^{hi} cells appear to cause a minor exacerbated, or quickened, development of colitis as demonstrated by histology and by increased weight loss.

Histological assessment of the proximal colon of RAG2$^{-/-}$ mice injected with WT naïve CD4^{+}CD45Rb^{hi} and WT CD4^{+} CD25^{+} Tregs displayed mild to moderate inflammation within the lamina propria and submucosa along with moderate hyperplasia of the glandular crypts (Figure 5.26A). Interestingly, histological sections assessed from RAG2$^{-/-}$ injected with WT naïve CD4^{+}CD45Rb^{hi} cells

$PKD2^{KI/KI}$ $CD4^{+}$ $CD25^{+}$ Tregs displayed more exacerbated signs of colitis including the presence of moderate inflammation within the lamina propria, submucosa as well as moderate crypt hyperplasia and goblet cell loss (Figure 5.26B).

The data combined from the assessment of histological changes within colonic architecture using clinical colitis scoring parameters demonstrated. This is also in conclusion with data obtained from calculation of percentage body weight, the size of the spleen and length of the colon that show protection some degree of protection from the development of colitis in $RAG2^{-/-}$ injected with WT naïve $CD4^{+}CD45Rb^{hi}$ in combination with WT $CD4^{+}$ $CD25^{+}$ Tregs.

A

Normal colon in RAG2 KO

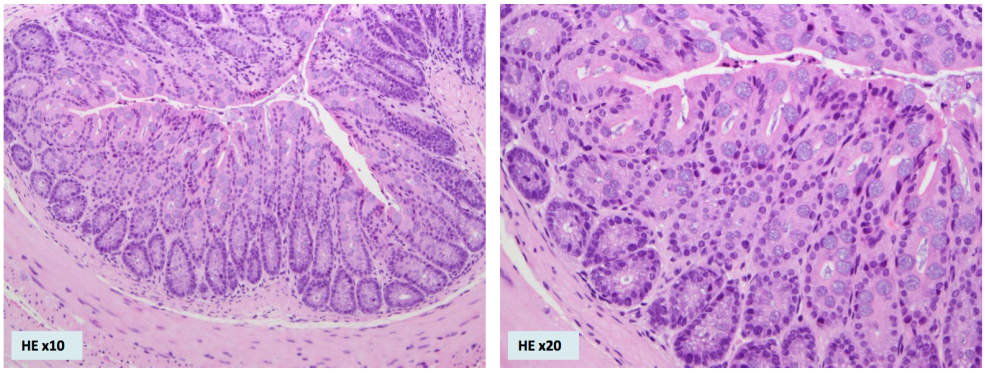

B

Inflamed colon in RAG2 KO injected with WT naïve CD4+ CD45Rb ^{hi} cells

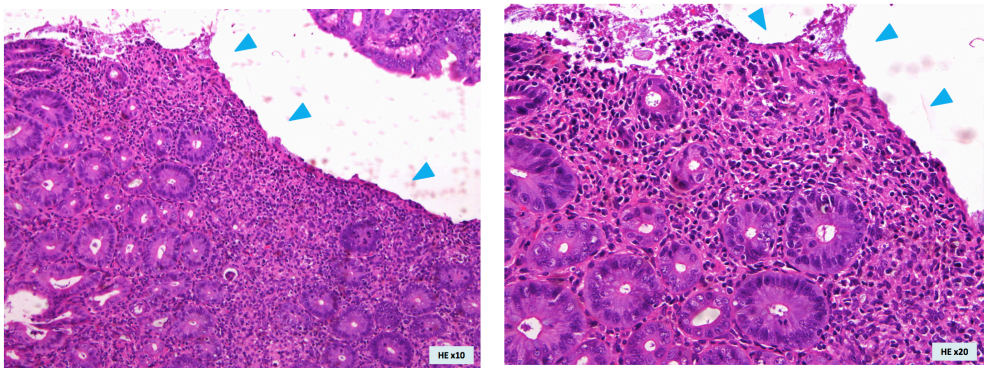

Figure 5.24 Typical histopathological sections of RAG2$^{-/-}$ recipient mice colon during in an *in vivo* colitis model

A) Normal presentation of colon in RAG2$^{-/-}$ mice untreated. (B) Moderate to marked inflammatory cell infiltration in colon of RAG2$^{-/-}$ mice injected with WT naïve CD4+ CD45Rb hi colitis inducing cells and epithelial hyperplasia indicated by blue arrows. (4x and 10x magnification as indicated).

A

Proximal colon: WT naïve CD4+ CD45Rb^{hi}

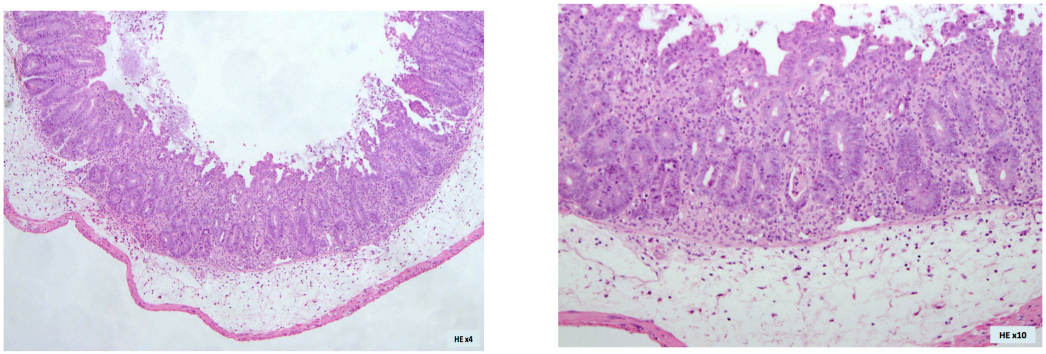

B

Proximal colon: PKD2 $^{KI/KI}$ naïve CD4+ CD45Rb^{hi}

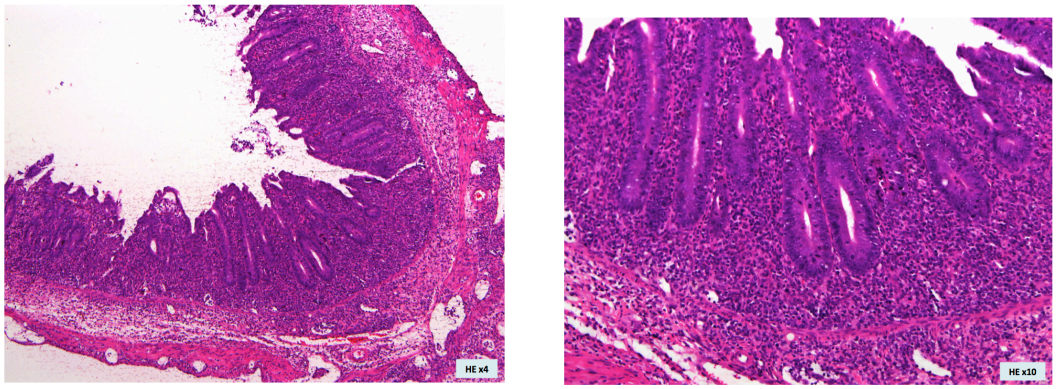

Figure 5.25 Histopathological sections in proximal colon of RAG2$^{-/-}$ hosts injected with WT naive or PKD2$^{KI/KI}$ T cells

(A) Proximal colon of RAG2$^{-/-}$ hosts receiving WT naïve CD4^{+} CD45Rb^{hi} cells (B) Proximal colon of RAG2$^{-/-}$ hosts receiving PKD2$^{KI/KI}$ naïve CD4^{+} CD45Rb^{hi} cells. (4x and 10x magnification as indicated).

A

Proximal colon: WT naïve CD4+ CD45Rb^{hi} + WT CD4+ CD25+ Tregs

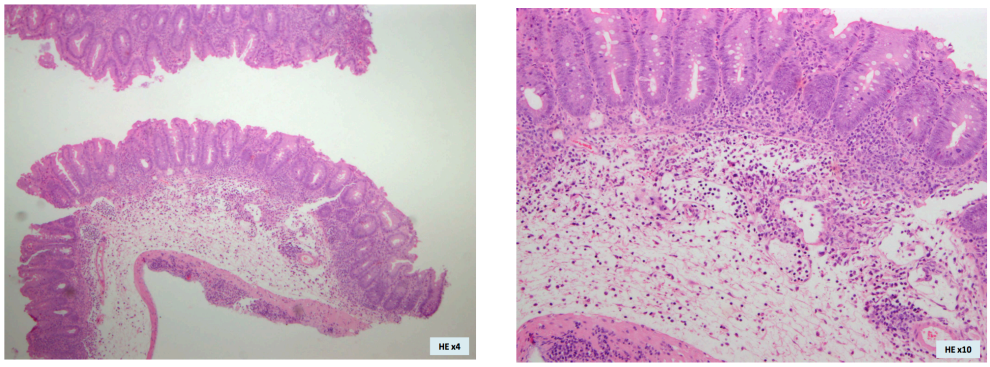

B

Proximal colon: WT naïve CD4+ CD45Rb^{hi} + PKD2 $^{KI/KI}$ CD4+ CD25+ Tregs

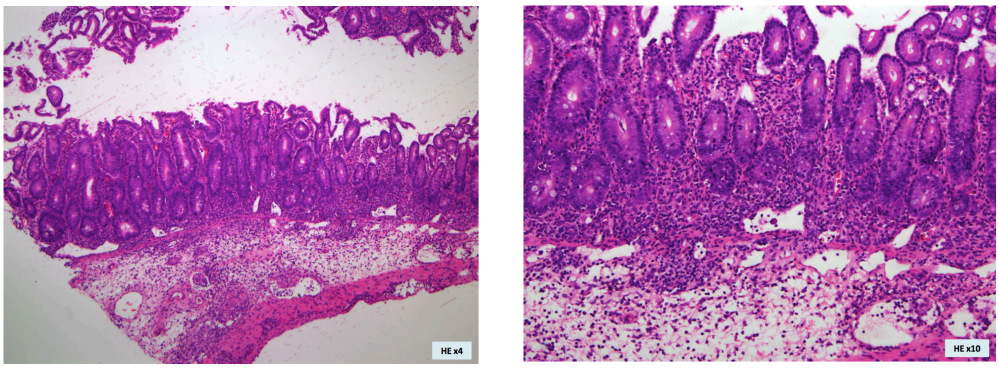

Figure 5.26 Histological sections in proximal colon of RAG2$^{-/-}$ hosts injected with WT naive + WT Tregs or WT naive + PKD2 $^{KI/KI}$ Tregs

(A) Proximal colon of RAG2$^{-/-}$ hosts receiving WT naïve CD4^{+} CD45Rb^{hi} cells (4x10^{5}) + WT CD4^{+} CD25^{+} Tregs (1x10^{5}) (B) Proximal colon of RAG2$^{-/-}$ hosts receiving PKD2 $^{KI/KI}$ naïve CD4^{+} CD45Rb^{hi} cells (4x10^{5}) + PKD2 $^{KI/KI}$ CD4^{+} CD25^{+} Tregs (1x10^{5}). (4x and 10x magnification as indicated.

Histopatholgical changes within proximal colon

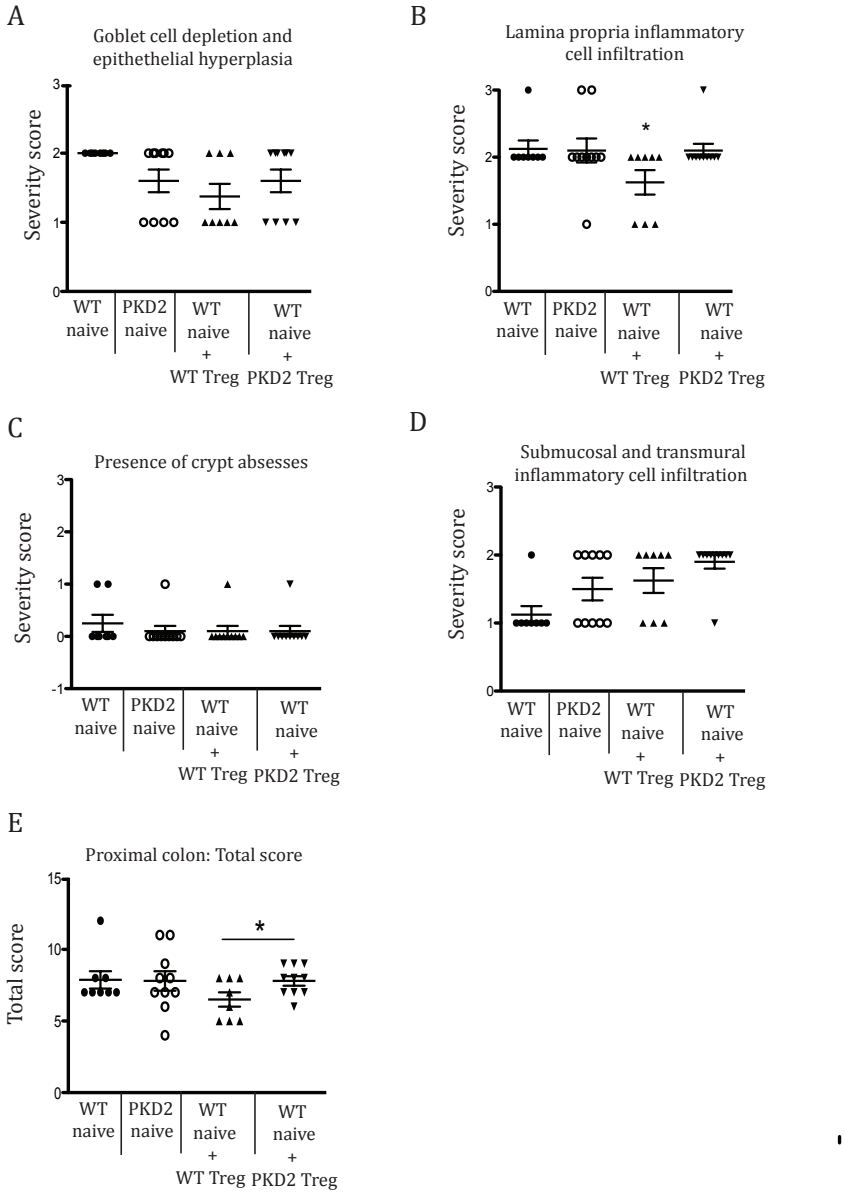

Figure 5.27 Assessment of histopathological changes within proximal colon of recipient RAG2$^{-/-}$ mice

Severity score (0-3) within proximal colon of RAG2$^{-/-}$ recipient mice for presence of; (A) goblet cell depletion and epithelial hyperplasia (B) lamina propria inflammatory cell infiltration (C) crypt abscesses (D) submucosal and transmural inflammatory cell infiltration. (E) Total colitis score of proximal colon. * = p≤ 0.05 analysed by students t test. Two scores were taken per mouse per tissue. *Scoring was performed by Dr. Francesco Marchesi, University of Glasgow.*

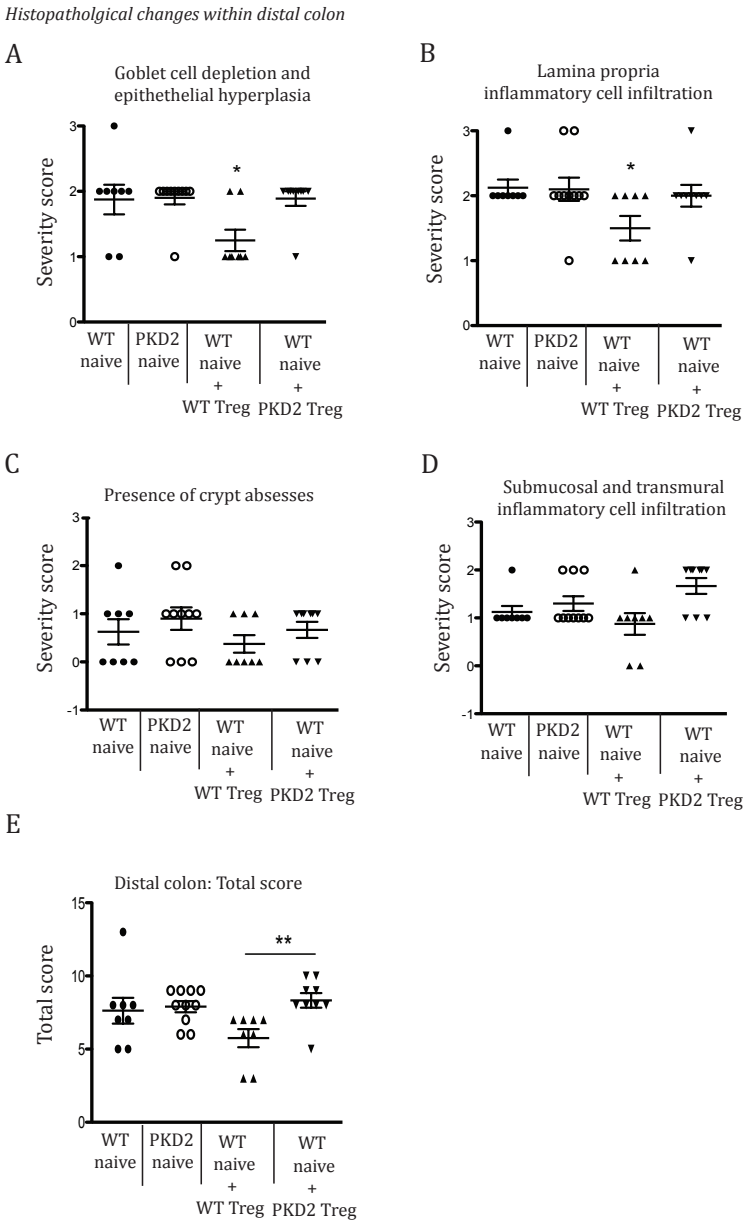

Figure 5.28 Assessment of histopathological changes within distal colon of recipient RAG2$^{-/-}$ mice

Severity score (0-3) within proximal colon of RAG2$^{-/-}$ recipient mice for presence of; (A) goblet cell depletion and epithelial hyperplasia (B) lamina propria inflammatory cell infiltration (C) crypt abscesses (D) submucosal and transmural inflammatory cell infiltration. (E) Total colitis score of distal colon. * = p≤ 0.05 and ** = p≤0.01 analysed by students t test. Two scores were taken per mouse per tissue. *Scoring was performed by Dr. Francesco Marchesi, University of Glasgow.*

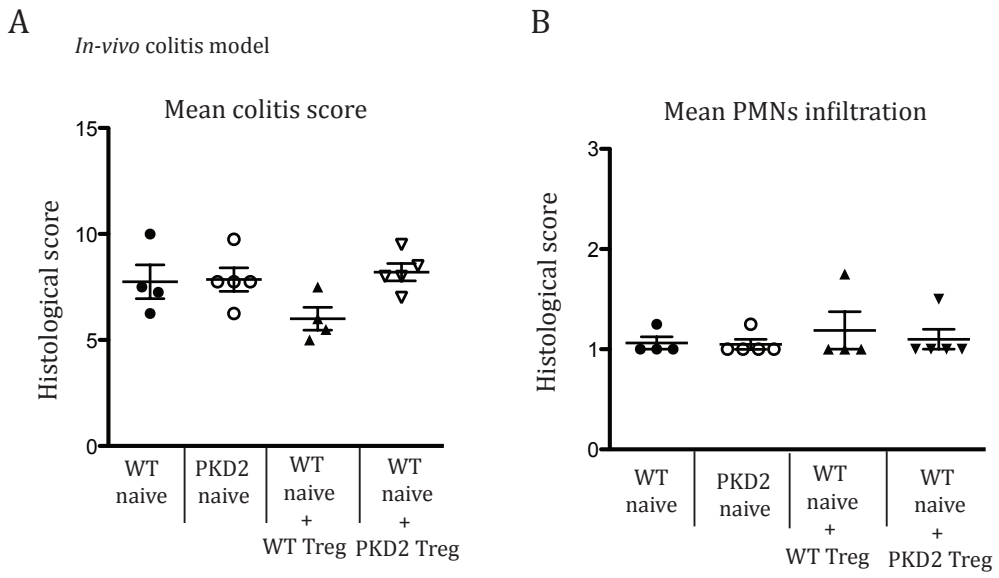

Figure 5.29 Mean clinical colitis score assessment and PMNs infiltration in RAG2$^{-/-}$ recipient mice

(A) Average colitis score from histopathological assessment for individual mice (B) Average polymorphonuclear leukocyte (PMNs) infiltration score as indication of more severe tissue damage. (4 mice used per group (groups 1 and 3), 5 mice per group (groups 2 and 4). Data from 1 independent experiment. *Scoring was performed by Dr. Francesco Marchesi, University of Glasgow.*

Collectively, these data reveal that although RAG2$^{-/-}$ hosts receiving WT naïve CD4^{+} CD45Rb^{hi} + WT Tregs did develop histopathological signs of inflammation and colitis they did have a lower mean colitis score when compared to RAG2-/- treated with WT naïve only (Figure 5.29A). Additionally the pathologists concluded that there was an overall trend of increased severity in colonic inflammation when comparing with mice co-injected with WT naïve CD4^{+} CD45Rb^{hi} + WT Tregs and WT naïve CD4^{+} CD45Rb^{hi} + PKD2$^{KI/KI}$ Tregs .

One of the possible reasons behind lack of protection by PKD2$^{KI/KI}$ Tregs is the possibility that mice injected a mixture of WT naïve T cells and PKD2$^{KI/KI}$ had lower viability than WT naïve and WT Tregs or also the possibility that PKD2$^{KI/KI}$ Tregs simply failed to expand within tissues after injection into RAG2$^{-/-}$ recipient mice. To address this issue, upon ending the colitis study at 3 weeks we harvested spleen and mLNs and assessed them for presence of Tregs within all groups, including naïve only groups 1 and group 2. Additionally, this allowed us

to check that WT and PKD2$^{KI/KI}$ naïve only mice did not differentiate into Treg subsets after transfer into mice. Upon assessment of Treg population's *ex vivo* we observed that only experimental groups 3 and 4 (WT naïve + WT Treg and WT naïve + PKD2$^{KI/KI}$ Treg) showed obvious Treg populations in both the spleen and mLN (Figure 5.30A-D). Importantly, experimental group 1 and 2 (WT naïve only and PKD2$^{KI/KI}$ naïve only) showed little development of Treg populations, although they were detectable at low levels. Indeed these data also revealed no significant changes in the expansion of PKD2$^{KI/KI}$ Tregs when compared to expansion of WT Tregs within recipient hosts.

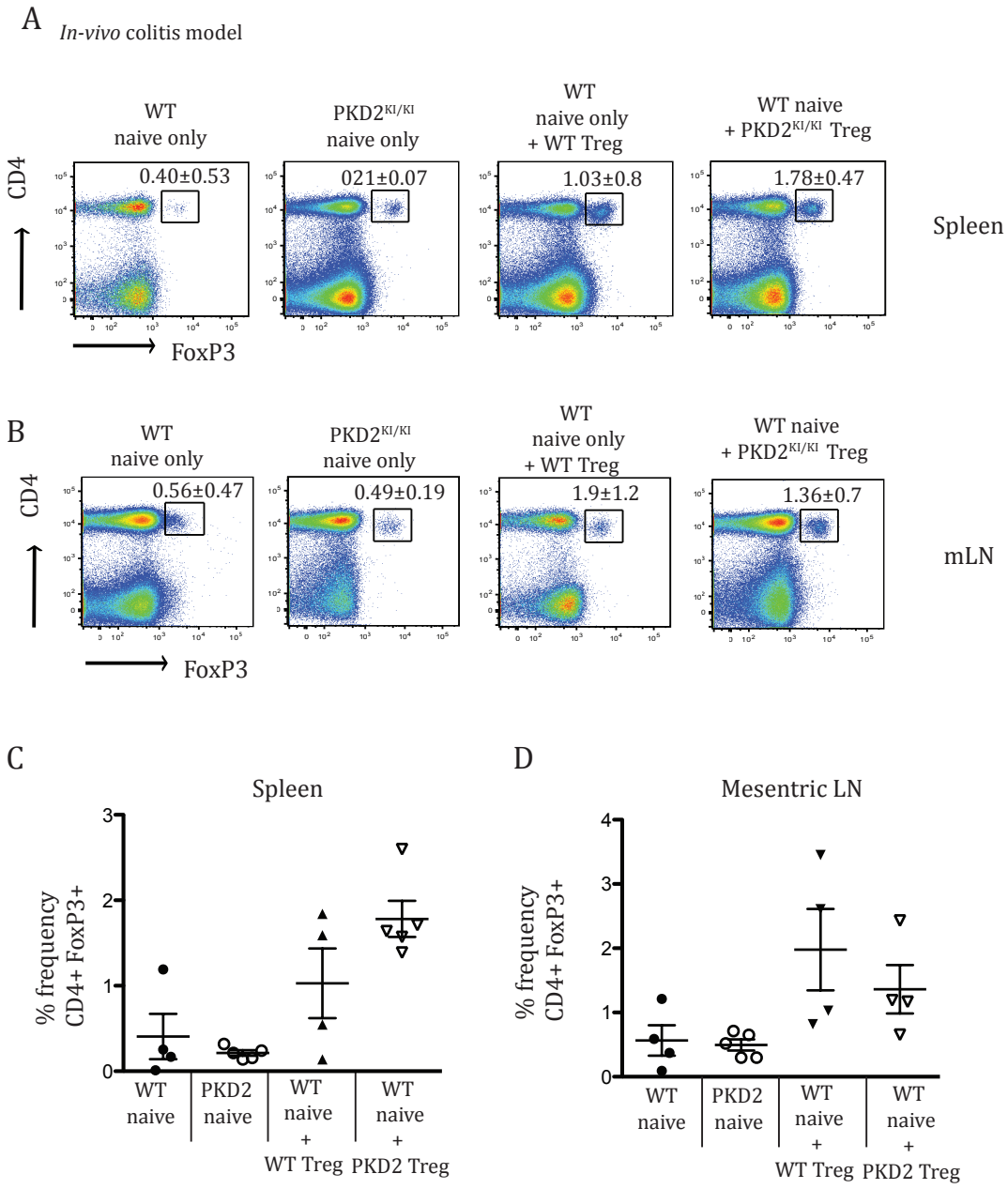

Figure 5.30 Treg populations in RAG2$^{-/-}$ recipient mice at end of colitis study

(A) Representative dot plots showing Treg populations in the spleen of RAG2$^{-/-}$ recipient mice after IP transfer of each experimental group after 3 weeks of transfer, shown by CD4 surface expression and intracellular FoxP3 expression by Flow cytometry. Numbers represent average % frequency and SD. (B) Dot plots showing Treg populations in the mLNs of RAG2$^{-/-}$ recipient mice after IP transfer of each experimental group after 3 weeks of transfer. (C) % Frequency of CD4+FoxP3+ found within the spleen (D) % Frequency of CD4+FoxP3+ found within the mLN. (4 mice used per group (groups 1 and 3), 5 mice per group (groups 2 and 4). Data from 1 independent experiment.

We next assessed cytokine production at the site of inflammation by measuring mRNA levels of IFNγ, IL-10 and IL-17 within the proximal colon of $RAG2^{-/-}$ recipient mice from each experimental group. As can be seen in Figure 5.31A, IFNγ mRNA expression in the proximal colon was similar between groups receiving WT naïve $CD4^{+}CD45Rb^{hi}$ cells only or $PKD2^{KI/KI}$ naïve $CD4^{+}CD45Rb^{hi}$ cells. However, mice receiving WT naïve $CD4^{+}CD45Rb^{hi}$ cells plus WT $CD4^{+}$ $CD25^{+}$ Tregs displayed a modest 3-fold reduction in the level of IFNγ when compared to mice receiving WT naïve T cells only. Interestingly, mice receiving WT naïve $CD4^{+}CD45Rb^{hi}$ cells plus $PKD2^{KI/KI}$ $CD4^{+}$ $CD25^{+}$ Tregs displayed a 8-fold increase in the level of IFNγ when compared to mice receiving WT naïve T cells plus WT Tregs.

Assessment of IL-10 with the proximal colon revealed dramatic differences between each experimental group, here IL-10 was only detectable in mice receiving WT naïve T cells plus WT Tregs (Figure 5.31B). Furthermore, mice receiving WT naïve T cells plus $PKD2^{KI/KI}$ Tregs displayed a 52-fold reduction in the level of IL-10 found within the proximal colon when compared to mice receiving WT Tregs. These results show that Tregs lacking PKD2 catalytic activity are unable to produce IL-10 in order to dampen inflammation ongoing within the colon during the progression of colitis *in vivo* and indicates that they may be non-functional.

Finally, assessment of IL-17 levels did not reveal any striking differences between experimental groups, however mice receiving WT and $PKD2^{KI/KI}$ Tregs displayed a notable reduction in levels of IL-17 within the proximal colon when compared to mice injected with WT naïve T cells only, again reflecting that WT Tregs within this study did carry out protective functions against colitis *in vivo* (Figure 5.31C).

Altogether, RT-PCR data showing higher levels of IFNγ levels in the proximal colon of mice within the WT naïve T cell only group and $PKD2^{KI/KI}$ naïve T cell only group correlated well with our observation of higher histopathological colon scores as compared to mice receiving WT naïve T cells and WT Tregs. Furthermore, reduced IL-10 levels within the colon of mice receiving WT naïve T cells and $PKD2^{KI/KI}$ Tregs revealed potential mechanism behind suggested lack of function when compared to groups receiving WT Tregs.

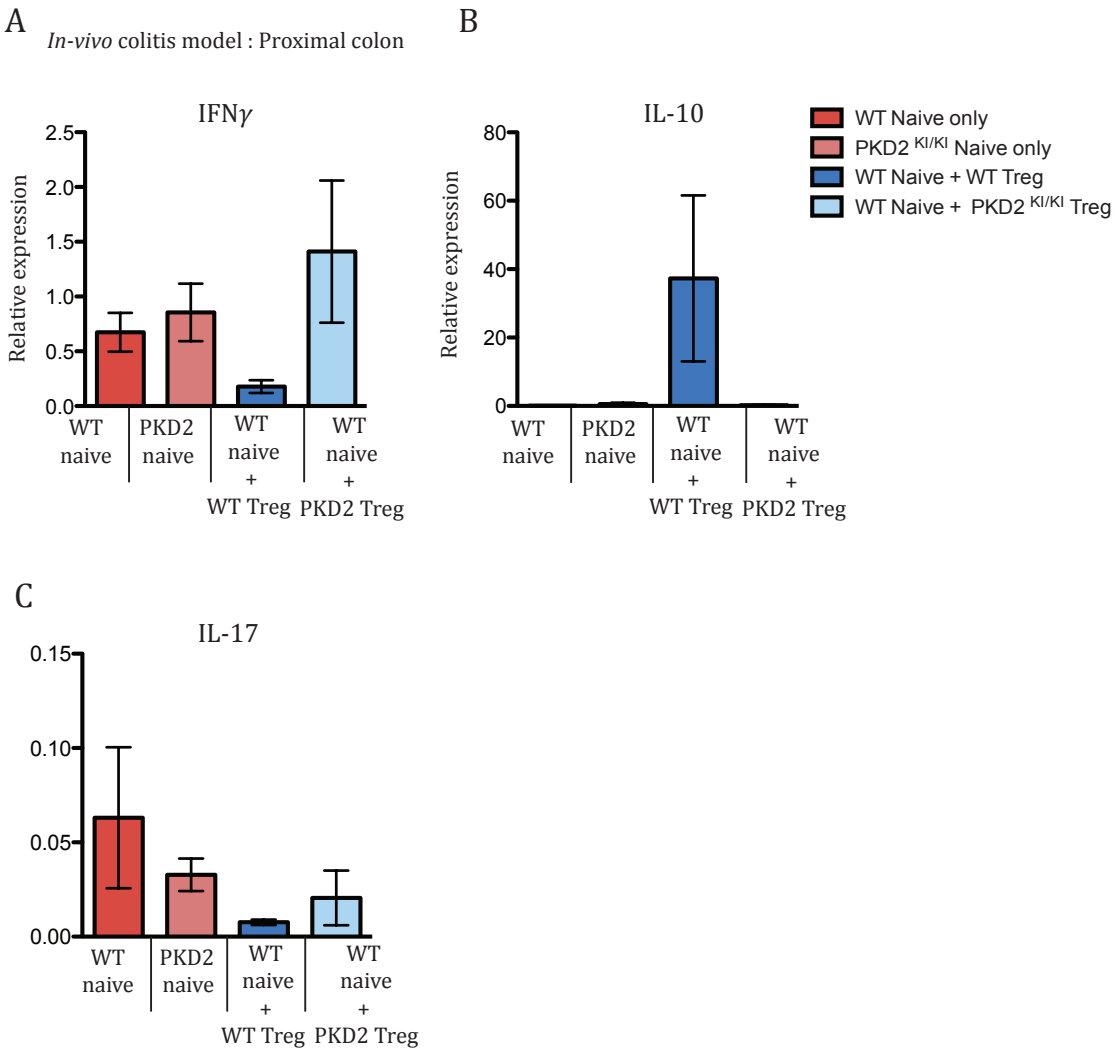

Figure 5.31 RT-PCR analysis of cytokine mRNA levels in proximal colon tissue from RAG2$^{-/-}$ mice after induction of colitis.

(A) Relative IFNγ mRNA level (B) IL-10 (C) IL-17. (Cytokine expression is relative expression to CD45) (4-5 mice per group). Data from 1 independent experiment. *Experiment was performed in collaboration with Mr. George Ramsay, Doreen Cantrell lab, University of Dundee.*

5.6 Discussion

The aim of this chapter was to explore the role of PKD2 catalytic activity in peripheral T cells specifically within the mucosal immune system, this included T lymphocyte subsets within the small intestine and within GALTs as we had observed a visible increase in the size of mLN and PPs tissue. Additionally, we sought to explore the requirement for PKD2 catalytic activity in Treg development and effector function. Although accumulating evidence demonstrates a key role of PKD2 catalytic activity within CD8+ CTLs, the requirement for PKD2 within T lymphocytes within the mucosal immune system remains or indeed within Treg development or effector function remains unaddressed.

Assessment of mLNs of $PKD2^{KI/KI}$ mice by histology revealed the presence of expanded germinal centres with irregular architecture when compared with WT mLN tissue. Subsequent analysis of T and B lymphocytes within the mLN of $PKD2^{KI/KI}$ mice revealed a significant increased in the number of B lymphocytes, however we found no difference in the expression of GL-7, which would have corresponded well with the histopathological data. Our analysis of PPs within WT and $PKD2^{KI/KI}$ was particularly difficult due to the nature of the small size of these lymphoid sites. However, histopathology analysis reciprocated the phenotype observed within mLN tissue in which PPs from $PKD2^{KI/KI}$ mice displayed expanded germinal centres. Surprisingly, although B lymphocyte numbers were normal, we observed a significant increase in the expression of GL-7 within the PPs of $PKD2^{KI/KI}$ mice, which did correlate with obtained histopathology data, demonstrates increased size in germinal centres formation. Furthermore, the presence of various expected lymphocyte populations confirmed that these tissues were indeed lymphoid PPs, rather than the presence of intestinal polyps for example. A wealth of studies comparing germ free mice and bacterial colonised mice demonstrate that the adaptive immune system, predominantly the mucosal compartment, is highly influenced by the presence of commensal microbiota within the intestine. Interestingly, this also includes direct influence on PP and germinal center size (Shroff et al. 1995)as well as shaping multiple populations of immune cells including IgA producing plasma

cells (Benveniste et al. 1971), CD4+ T cell subsets and TCRαβ+ CD8αβ+ IELs (reviewed (Macpherson & Harris 2004)). It is tempting to speculate that PKD2$^{KI/KI}$ mice may display this phenotype as a result of lack of tolerance to oral or commensal antigens. This could be assessed by future studies by assessing tolerance induction in a PKD2$^{KI/KI}$ animal crossed onto an OT II background in which supplementation of animal drinking water with OVA peptide exists as an established model to assess oral tolerance induction (X. Zhang, Izikson, et al. 2001b) (Pabst & Mowat 2012).

It was striking PKD2$^{KI/KI}$ mice had significantly increased CD4+ CD25+ FoxP3+ Tregs within multiple peripheral lymphoid tissues, including the mLN and the spleen, which was not the case within the thymus. This suggested to us that rather than a defect within thymocyte development or increased thymic output of Tregs, the loss of PKD2 instead may led to the increased conversion of CD4+ naïve T cells into Tregs within the periphery. Further analysis revealed significantly expanded population of CD103+ Tregs within PKD2$^{KI/KI}$ mice, which is well established marker for activated and memory Tregs (Lehmann et al. 2002) (Huehn et al. 2004) (Suffia et al. 2005) (Banz et al. 2003) (McHugh et al. 2002). This result suggests that increased Tregs within PKD2$^{KI/KI}$ mice are antigen experienced with a memory phenotype. Surprisingly, these results were even more pronounced when we assessed aging PKD2$^{KI/KI}$ mice. As discussed, class IIa HDACs have been shown to regulate FoxP3 stabilisation by acetylation of the N-terminal of FoxP3 protein. We therefore speculated that Treg conversion might be due to enhanced stabilisation of the FoxP3 protein via a PKD-HDAC mediated pathway. It was therefore surprising to find that loss of HDAC7 did not result in the generation of Tregs, or indeed the abundance of FoxP3, although we did note a reduction in the number of nTregs within the thymus. It is plausible that the increase in CD4+FoxP3+ Treg population is a consequence of on-going inflammation within PKD2$^{KI/KI}$ mice. This speculation correlates well with the visible increase in the size and cellularity of the mLNs and PPs including observations within the histological changes observed which include larger germinal centres within PKD2$^{KI/KI}$ mice. This speculation would also concur from studies assessing Treg frequencies in patients with on-going IBD in which increased abundance of CD4+ FoxP3+ T lymphocyte and FoxP3

mRNA transcript are found in on-going IBD lesions within the small intestine (Maul et al. 2005) (Hölttä et al. 2008) and within patients with rheumatoid arthritis (Leipe et al. 2005).

Analysis of T lymphocytes within the small intestine revealed a striking role for PKD2 in the normal generation or homeostasis of lymphocytes within the gut, which was specifically limited to the intraepithelial layer in which the total numbers of IELs were significantly increased in $PKD2^{KI/KI}$ mice. Specific IEL populations within $PKD2^{KI/KI}$ mice were strikingly different from WT mice, in which TCRγδ+ T lymphocytes normally predominant, however in contrast $PKD2^{KI/KI}$ mice had more TCRαβ+ rather than TCRγδ+ IELs. A more in depth analysis of these populations also implicated further dysregulation with these subsets including obvious differences between natural and induced populations of IEL. Specifically we observed significantly fewer TCRαβ+ CD8αα+ IEL, which was accompanied by an increase in TCRαβ+ CD8αβ+ cells. Interestingly, a similar phenotype is observed in TGF-$\beta^{-/-}$ mice (Konkel et al. 2011). Furthermore, within the same study TGF-β has also been shown to be required for the proliferation of the precursor for the TCRαβ+ CD8αα+ IEL which are CD4- CD8- double negative thymocytes that have successfully rearranged a TCR and undergone positive selection so are therefore positive for CD5 (Gangadharan et al. 2006). PKD2 has been implicated in the upregulation of the CD5 protein via the phosphorylation of C-Cbl, an ubiquitin ligase (Marklund et al. 2003) (Navarro, Goebel, et al. 2014b). Additionally, TGF-$\beta^{-/-}$ IEL also express higher levels of CD103, similarly to $PKD2^{KI/KI}$ Tregs. It would be interesting to expand these studies in the future and address precursor number within the thymus of PKD2 mice and address TGF-β production within cells from $PKD2^{KI/KI}$ mice. Importantly, we also observed increased Tregs within the IEL and the LP layers of the small intestine in $PKD2^{KI/KI}$ mice. This was significant as it is well established that normal Treg presence within the IEL is extremely low (Ostanin et al. 2010) (Denning et al. 2007). To address the biological relevance of changes within gut lymphocyte populations within the small intestine of $PKD2^{KI/KI}$ mice an infection model could be carried out in the future. Established models to investigate the immune response within the gut include infection with *L.Monocytogenes*, *toxoplasma gondii,, rotavirus* and *helicobacter pylori* (Huleatt et al. 2001) (Kullberg et al.

2006) (Liesenfeld 2002) (Schreiner & Liesenfeld 2009) (Pizarro-Cerdá et al. 2012).

Although there are multiple possible mechanisms to explain the increase in abundance of Tregs within $PKD2^{KI/KI}$ mice we could not exclude the possibility that a lack of functionality within $PKD2^{KI/KI}$ Tregs was driving their proliferation in attempt to compensate and maintain immune regulation and homeostasis. This was plausible as loss of PKD2 catalytic activity has been associated with lack of functionality in other T lymphocytes including CD4+ naïve T cells and CD8+ CTLs, in which severely reduced cytokine production by these subsets has been observed. To address Treg functionality in $PKD2^{KI/KI}$ mice we choose to use an intestinal in *vivo* model of inflammation. Analysis of Tregs lacking PKD2 catalytic activity an *in vivo* colitis model revealed noteworthy results in which $PKD2^{KI/KI}$ Tregs displayed reduced ability to prevent the development or severity of colitis which was associated with severely reduced IL-10 levels within the proximal colon which was associated with increased IFNγ levels. In this context, IL-10 has been shown to be essential in the function of Tregs within intestinal inflammation (Asseman et al. 1999) (Uhlig et al. 2006). These results collectively implicate a role for PKD2 within Treg effector function specifically the production of IL-10 and that Tregs lacking PKD2 catalytic activity are nonfunctional within an intestinal model of inflammation.

6 Final Discussion and Future Perspectives

6.1 Novel PKD inhibitors are specific for PKD but do display individual off target effects

The work within this thesis explores the role of PKD kinases in multiple cells of the mammalian immune system including cells from both the innate and adaptive lineages, as well as exploring a role for PKD within malignant myeloid cells. Accumulating evidence has implicated the PKD family in a wealth of fundamental biological processes including angiogenesis, proliferation and cell survival, cell motility and within various inflammatory pathways. It is therefore not surprising that PKD has been implicated in cancer development and progression. As a result, there have been significant advances in the development of small molecule inhibitors for PKD for their therapeutic use in cancer therapy. Previous studies have reported positive results in pancreatic and prostate cancer models (Wille et al. 2014) (Ochi et al. 2011) (Harikumar et al. 2010) (LaValle et al. 2012). Although improved bioavailability and specificity of these compounds will hopefully allow movement of these inhibitors into further studies little is known about their effect in the immune system, where PKD2 has ben shown to be predominantly expressed and play a key role in effector functions of adaptive immune cells (Matthews et al. 2000) (Matthews et al. 2010) (Navarro, Feijoo Carnero, et al. 2014a) (Spitaler, Emslie, Wood & Cantrell 2006b).

Data within this thesis provide significant insight into the specificity of novel inhibitors of PKD which was gained through the use of *in vitro* kinase screen profiling, adding to our knowledge of the off target effects displayed by these compounds. Importantly, all three novel inhibitors had no significant effect on PKC isoforms (Results, Chapter 3), which has complicated the pharmacological inhibition of PKD in previous studies. Significantly, comparative analysis revealed that the common target was the inhibition of PKD. We also explored if pharmacological inhibition of PKD by these compounds led to biological results that would be expected from previously assigned functions of PKD within the

literature. To this extent, our data yielded mixed results. Of note, the pharmacological inhibition of PKD within murine T lymphocytes severely reduced IL-2 and IFNγ production after TCR triggering, as reported in $PKD2^{KO/KO}$ and $PKD2^{KI/KI}$ CD4+ and CD8+ T lymphocytes (Matthews et al. 2010). As PKD2 as been implicated in the development and perhaps the progression of CML we also explored the use of novel small molecule inhibitors of PKD in a malignant myeloid cell line (human Bcr-Abl+ K562 CML cells) (Mihailovic et al. 2004) (Z.-F. Yang et al. 2013) (Bhattacharya et al. 2011; H. Zheng et al. 2011). One discrepancy with reports in the literature that was established in these experiments was that we could not detect any basal activity of PKD (either within the PKC mediated transphorylation site (Ser744/Ser748) or within the autophosphorylation loops (p. SER916)). Although additional reports have demonstrated that PKD2 is tyrosine phosphorylated within the PH domain (Mihailovic et al. 2004). If K562 CML cells have constitutive tyrosine phosphorylation will need to be addressed in the future. Furthermore, to address constitutive PKD activity within CML cells, patient samples could be obtained to address this within clinical samples rather than with cell lines, which would provide a more relevant approach if these inhibitors are to be used within the clinic. Despite this, we did show that all three inhibitors effectively block phorbol ester induced activation of PKD using phospho-flow cytometry. Additionally, PKD2 has been implicated in the enhanced internalisation of the IFNAR1 from the cell surface of CML cell line (KT1 cells) mediated by the phosphorylation of serine residues within the IFNAR1 degron. Within the same studies it has been shown that knockdown of PKD2 or pharmacological inhibition of PKD (CID755673 compound) led to reduced phosphorylation of the Ser535 site and an increase in total IFNAR1. We established that the K562 CML cell line displayed a similar phenotype with low surface expression of IFNAR1 yet high levels are found intracellularly. Our experiments assessing the effect of 12a, CRT101 and CRT051 compounds on IFNAR1 expression gave mixed results where only the CRT101 compound showed any significant increase of IFNAR1 receptor expression within CML cells.

As the CRT101 is orally bioavailable, studies could be performed in the future to examine the effect of oral dosing of this compound could be performed

in mice and its effects within the immune system assessed. This would be particularly interesting to look at Treg populations within the spleen and mLNs as we have shown that loss of PKD catalytic activity affects these populations *in vivo* (Results, Chapter 5). Although it is worth emphasising that although these novel compounds were highly specific for PKD, we did note individual off target effects that we believe may have affected results obtained from cell cycle analysis of and indeed our analysis on p. STAT5 levels, both within K562 CML cells. However, cancer research technologies are improving these compounds at the moment (Personal communication).

6.2 PKD2 is dispensible for myeloid cell development *in vivo* but may play a role in myeloid cell effector functions

The second part of the project focused on PKD expression and function within myeloid cells through use of isoform specific PKD transgenic animals in an attempt to ascertain the true physiological role of PKD kinases in these processes. Work carried out within this thesis reports for the first time an in depth analysis of the expression of PKD kinases and their role within the development of myeloid cell *in vivo* (Results, Chapter 4). These data is significant, as it reveals for the first time that PKD1 and PKD2 catalytic activity is dispensable for the generation of myeloid cells *in vivo.* A significant observation was the predominant expression of PKD2 in primary myeloid cells including BMDMOs and BMDCs, similar to cells of the adaptive lineages.

Importantly, we did not observe any defects within myeloid cell development (including cDCs, pDCs, neutrophils and macrophages from PKD mutant bone marrow *in vitro* or within the bone marrow in either $PKD2^{KI/KI}$ or $PKD1^{WT/KI}$ x $PKD2^{KI/KI}$ mice *in vivo.* Furthermore, these populations were normal within the spleen, suggested no obvious role for either PKD1 or PKD2 catalytic activity in the migration or homeostasis of these subsets.

Our analysis of TLR mediated activation of PKD led to unexpected results that challenges previous reports in the literature that report PKD1 is key for myeloid cell effector functions and is activated downstream of TLRs utilising the Myd88 pathway. In these experiments we could not detect strong activation of

PKD in response to TLR4 or TLR9 activation within either RAW264.7 macrophages or BMDCs. Surprisingly, our preliminary data suggests a potential role for PKD activation downstream of dectin-1: TLR2 stimulation with zymosan and therefore implicates a role for PKD within antifungal immunity. It will need to be determined in future experiments if PKD activation is a result of either a combination of both dectin-1: TLR2 or by dectin-1 or TLR2 individually. This could be achieved through use of single agonists for each receptor.

Analysis of effector function of BMDCs lacking PKD2 catalytic activity generated *in vitro* gave unexpected results in which we observed an overactive response to LPS characterised by increased costimulatory molecules when compared to WT BMDCs. Importantly, the functional relevance of this phenotype was explored, in an *in vitro* T lymphocyte activation model revealing that although loss of PKD2 catalytic activity within BMDCs did not affect their ability to present peptide and activate OVA specific T lymphocytes, as demonstrated by successful upregulation of key T lymphocyte activation markers. However, our preliminary data show that T lymphocytes stimulated with $PKD2^{KI/KI}$ BMDCs did display heightened IFNγ production which is most likely being induced by increased IL-12p40 levels observed in $PKD2^{KI/KI}$ BMDCs (Athie-Morales et al. 2004). As discussed, these data collectively implicate a regulatory role for PKD2 downstream of TLR ligation or indeed a role for limitation of the response directed by BMDCs. In this context, PKD has been implicated in the regulation of A20 within the βTC3 cell line (Liuwantara et al. 2006), which is a well known negative regulator of TLR and NFκB pathways (Boone et al. 2004). Future experiment will be required to assess if this is the case within myeloid cells as A20 has a key role within DCs specifically and their mediation of normal immune homeostasis (Kool et al. 2011).

6.3 PKD2 catalytic activity is required for normal gut associated lymphoid tissue homeostasis and Treg development and function

The final part of this project led us down an unexpected path to explore the loss of PKD2 catalytic activity within T lymphocyte homeostasis within the small intestine and indeed within the development and function Treg subsets. These

experiments provide much needed insight into a subject area where the role of PKD2 has not been assessed. Ironically, the experiments described within Chapter 5 produced more questions than they answered.

Strikingly, $PKD2^{KI/KI}$ mice displayed enlarged GALTs including mLNs and PPs. A similar phenotype was noted within $PKD2^{KI/KI}$ and $PKD2^{KO/KO}$ mice when crossed onto an OT I and OT II background, however increased tissue size within these mice was only associated with spleen and inguinal lymph nodes (Navarro et al. 2012). Assessment of these tissues with histopathology revealed expanded germinal centres within $PKD2^{KI/KI}$ mice (Chapter 5). It is tempting to speculate that this may be a result in a break in oral tolerance either to food antigen or to commensal bacteria within the gastrointestinal tracts of $PKD2^{KI/KI}$ mice (Pabst & Mowat 2012) (Macpherson & Harris 2004). although further experiments will be required to confirm this.

Furthermore, TCRγδ populations in the gut are known to be essential for normal oral tolerance and our data demonstrate that TCRγδ are significantly reduced within the intraepithelial layer of $PKD2^{KI/KI}$ mice. In this context, it would be very interesting to assess the microbiota present within $PKD2^{KI/KI}$ mice, as it is becoming increasingly accepted that intestinal microbiota play an essential role in shaping the immune system and for normal homeostasis of multiple immune cell subsets (Belkaid & Hand 2014) (H.-J. Wu & E. Wu 2014). Moreover, studies have demonstrated that the distinct bacterial species that make up the microbiota can favour or disfavour FoxP3+ Treg induction (Atarashi et al. 2014) (Atarashi et al. 2011).

Many of the experiments we sought to perform limited by the technical difficultly of successful intracellular staining for the FoxP3 protein when combining this technique with other methods, for example phospho flow. It is also not possible to sort live FoxP3+ cells without fixation and permeabilisation of these cells first thereby limiting their use for downstream applications. To overcome this difficult for future experiments to allow further charaterisation of the role of PKD2 in Treg development and effector functions it would be greatly advantageous to cross the $PKD2^{KI/KI}$ mouse onto a $FoxP3^{GFP}$ strain (Fontenot et al. 2005). Collectively, observations from the colitis model imply that Tregs from $PKD2^{KI/KI}$ mice are less protective in preventing the development or indeed

limiting the severity of disease induced in this model. This will need to be confirmed with more intricate experiments to more directly assess cytokine production by PKD2$^{KI/KI}$ Tregs. This could be achieved by sorting (in the case of mice crossed on to the FoxP3^{GFP} stain) WT and PKD2$^{KI/KI}$ CD4+ FoxP3+ Tregs and assessing cytokine production such as IL-10 and TGFβ. Additionally, a more global approach to investigate why loss of PKD2 catalytic activity led to an accumulation of Tregs that have a memory like phenotype within multiple tissues of PKD2$^{KI/KI}$ mice would be to perform phosphoproteomics on these cell subsets in future experiments.

Another important observation was the intriguing differences between T cell subsets within the IEL of WT and PKD2$^{KI/KI}$ mice. Significantly, we observed reduction of key regulatory subsets within this layer including TCRγδ+ subsets but also TCRαβ+ CD8αα+ subsets both of which have been shown to perform key regulatory properties within the gut including maintenance of gut epithelium and resolution of inflammation. Although there are multiple possibilities to begin to explain this phenotype, there are two major mechanisms that could be explored in future experiments. Firstly, CD5 is known to be required for the generation of these subsets within the thymus and PKD2 has been directly implicated in the upregulation of the CD5 via the phosphorylation of C-Cbl (Marklund et al. 2003) (Navarro, Goebel, et al. 2014b). Secondly, TGFβ$^{-/-}$ mice have a similar phenotype within the intraepithelial layer, with decreased TCRαβ+ CD8αα+ subsets (Konkel et al. 2011). As lack of PKD2 catalytic activity has been shown to result in severely reduced cytokine production by T lymphocytes it is tempting to speculate that TGFβ production may also be affected. Furthermore, data generated in collaboration with Dr. George Ramsay within Professor Doreen Cantrell's Lab (University of Dundee) has shown that PKD2$^{KI/KI}$ Th17 cells display a significant reduction in the production of IL-17 *in vitro* (Data not shown).

Collectively, our data reveal novel and surprising roles for PKD in multiple cells within the immune system. Although there is much more to be learned about the specific details of PKD function within these cells, our studies have provided substantial evidence to clarify and identify the role of PKD isoforms

within both myeloid cell and adaptive immune cell development and their effector functions.

7 Appendix A

Primer	Sense primer	Anti-sense primer
PKD1	5'-GTTCATAGAACACCGGCAGA-3'	5'GCCAAGACAAATCAACAGAAGC-3'

Table 7.1 Primer sequences for genotyping of $PKD1^{WT/KI}$ mice

PKD1: predicted WT size - 600bp predicted PKD1 heterozygous size -635bp

Primer	Sense primer	Anti-sense primer
PKD2	5'-AGTGGCACGTTCCCCTTCAATG-3'	5'-CTTTGCCCAATCCCTTACAGCCT-3'

Table 7.2 Primer sequences for genotyping of $PKD2^{KI/KI}$ mice

PKD2: predicted WT size - 236 predicted homozygous - 344bp

Primer	**Sense primer**	**Anti-sense primer**
IFNγ	5'-TTACTGCCACGGCACAGTC-3'	5'-AGATAATCTGGCTCTGCAGG-3'
IL-17	5'-AGCTCCAGAAGGCCCTCAGACTACC-3'	5'-CAGCTTTCCCTCCGCATTGACAC-3'
IL-10	5'-CCCTTTGCTATGGTGTCCTTTC-3'	5'-GATCTCCCTGGTTTCTCTTCCC-3'
CD45	5'-TGATGGTCACAGGATGTGAAG A-3'	5'-ATGCCGAGTGCCTTCCT-3'

Table 7.3 Primer sequences used for detection of cytokine mRNA

Score	Expect	Identities	Gaps	Strand
713 bits(386)	0.0	388/390(99%)	0/390(0%)	Plus/Plus

```
Query  943   CTGTCTTACTTTGTGTGGCAACGGAGAATGAATATTTTATTTTGCCACTTTCTAGAACTG  1002
             ||||||||||||||||||||||||||||||||||||||||||||||||||||| |||||||
Sbjct  102   CTGTCTTACTTTGTGTGGCAACGGAGAATGAATATTTTATTTTGCCACTTTCWAGAACTG  161

Query  1003  TTAGGGCTCTGCTGTTGTTCAGTATGAGAACATACGTATGTGTGATGATTCCTTTAGAAT  1062
             ||||||||||||||||||||||||||||||||||||||||||||||||||||||||||||
Sbjct  162   TTAGGGCTCTGCTGTTGTTCAGTATGAGAACATACGTATGTGTGATGATTCCTTTAGAAT  221

Query  1063  AGGGTACCTTGGCAGTCTTACAGTATTTAAATTTATATTCTTGTTAATCCATACTTGTCT  1122
             ||||||||||||||||||||||||||||||||||||||||||||||||||||||||||||
Sbjct  222   AGGGTACCTTGGCAGTCTTACAGTATTTAAATTTATATTCTTGTTAATCCATACTTGTCT  281

Query  1123  CCTCTTAATGGAATAGTCTTACTTTAAATGGAAGTGGCTGGTGGGCCAGAGGATATGATG  1182
             ||||||||||||||||||||||||||||||||||||||||||| ||||||||||||||
Sbjct  282   CCTCTTAATGGAATAGTCTTACTTTAAATGGAAGTGGCTGGTGGGCMAGAGGATATGATG  341

Query  1183  AGTTCAATGTTTTAAAAGTAGTTCTTCAGTCAATATCCTTTGGAGTCCATTTAATTCTCA  1242
             ||||||||||||||||||||||||||||||||||||||||||||||||||||||||||||
Sbjct  342   AGTTCAATGTTTTAAAAGTAGTTCTTCAGTCAATATCCTTTGGAGTCCATTTAATTCTCA  401

Query  1243  TTAAAATCCTATAAAGATAGGTGTTGTTTTTAAATATGTATCATAAAAACTAAGTGTAAC  1302
             ||||||||||||||||||||||||||||||||||||||||||||||||||||||||||||
Sbjct  402   TTAAAATCCTATAAAGATAGGTGTTGTTTTTAAATATGTATCATAAAAACTAAGTGTAAC  461

Query  1303  AAGTGATACCAGGCATCCAAATCACCCAAA  1332
             |||||||||||||||||||||||||||||
Sbjct  462   AAGTGATACCAGGCATCCAAATCACCCAAA  491
```

Figure 7.1 PKD1 forward primer sequence alignment

Score	Expect	Identities	Gaps	Strand
652 bits(353)	0.0	354/355(99%)	0/355(0%)	Plus/Minus

```
Query  943   CTGTCTTACTTTGTGTGGCAACGGAGAATGAATATTTTATTTTGCCACTTTCTAGAACTG  1002
             |||||||||||||||||||||||||||||||||||||||||||||||||||||||||||
Sbjct  362   CTGTCTTACTTTGTGTGGCAACGGAGAATGAATATTTTATTTTGCCACTTTCTAGAACTG  303

Query  1003  TTAGGGCTCTGCTGTTGTTCAGTATGAGAACATACGTATGTGTGATGATTCCTTTAGAAT  1062
             ||||||||||||||||||||||||||||||||||||||||||||||||||||||||||||
Sbjct  302   TTAGGGCTCTGCTGTTGTTCAGTATGAGAACATACGTATGTGTGATGATTCCTTTAGAAT  243

Query  1063  AGGGTACCTTGGCAGTCTTACAGTATTTAAATTTATATTCTTGTTAATCCATACTTGTCT  1122
             ||||||||||||||||||||||||||||||||||||||||||||||||||||||||||||
Sbjct  242   AGGGTACCTTGGCAGTCTTACAGTATTTAAATTTATATTCTTGTTAATCCATACTTGTCT  183

Query  1123  CCTCTTAATGGAATAGTCTTACTTTAAATGGAAGTGGCTGGTGGGCCAGAGGATATGATG  1182
             ||||||||||||||||||||||||||||||||||||||||||||||||||||||||||||
Sbjct  182   CCTCTTAATGGAATAGTCTTACTTTAAATGGAAGTGGCTGGTGGGCCAGAGGATATGATG  123

Query  1183  AGTTCAATGTTTTAAAAGTAGTTCTTCAGTCAATATCCTTTGGAGTCCATTTAATTCTCA  1242
             |||||||||||||||||||||||||||||||||||||||||| ||||||||||||||||
Sbjct  122   AGTTCAATGTTTTAAAAGTAGTTCTTCAGTCAATATCCTTTGGARTCCATTTAATTCTCA  63

Query  1243  TTAAAATCCTATAAAGATAGGTGTTGTTTTTAAATATGTATCATAAAAACTAAGT  1297
             |||||||||||||||||||||||||||||||||||||||||||||||||||||||
Sbjct  62    TTAAAATCCTATAAAGATAGGTGTTGTTTTTAAATATGTATCATAAAAACTAAGT  8
```

Figure 7.2 PKD1 reverse primer sequence alignment

8 Appendix B full kinase screen of Novartis 12a, CRT0066101 and CRT0066051

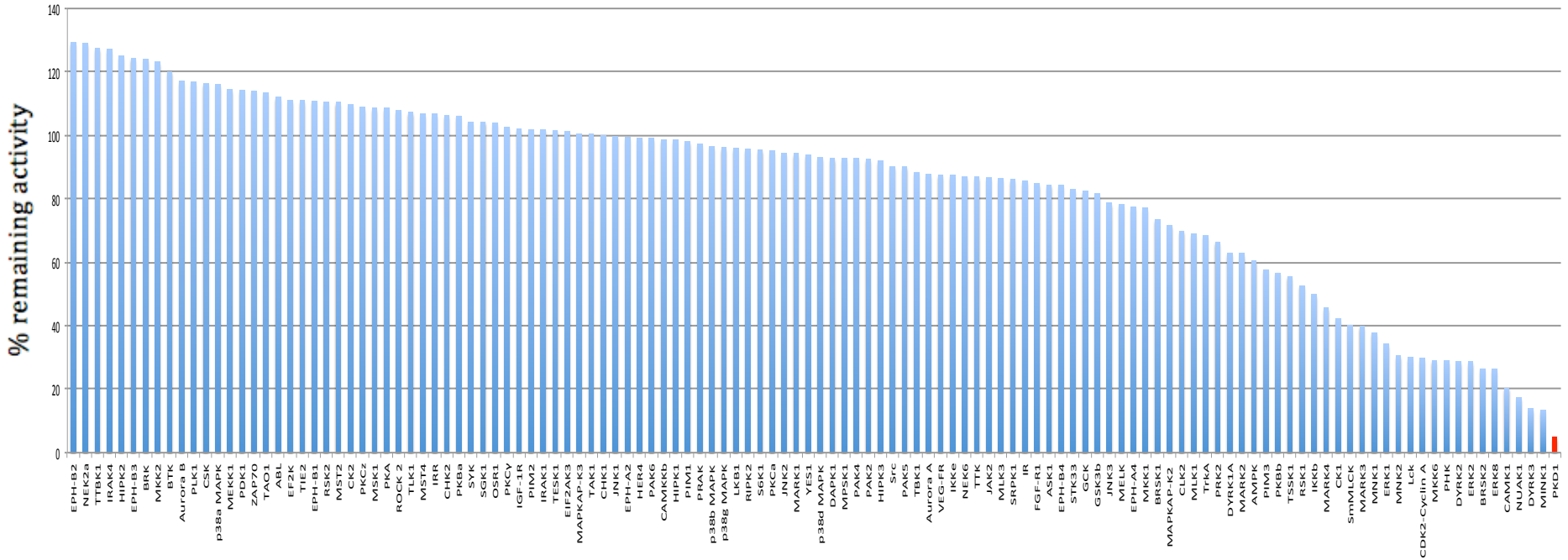

Figure 8.1 Full in vitro kinase screen Novartis 12a compound at 1μM against 124 kinases

In vitro kinase screen of 124 kinases shown in descending order of % remaining activity (PKD1 is shown in red)

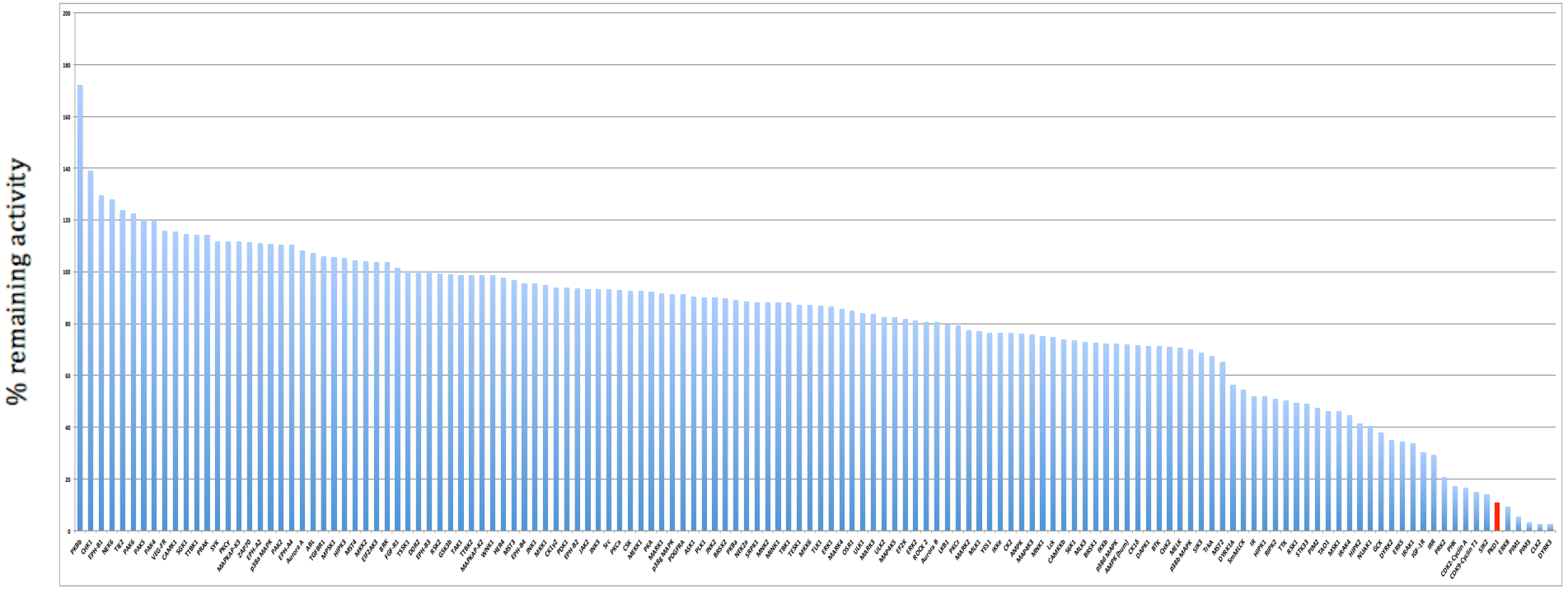

Figure 8.2 Full in vitro kinase screen for CRT101 compound at 1μM against 124 kinases

In vitro kinase screen of 124 kinases shown in descending order of % remaining activity (PKD1 is shown in red)

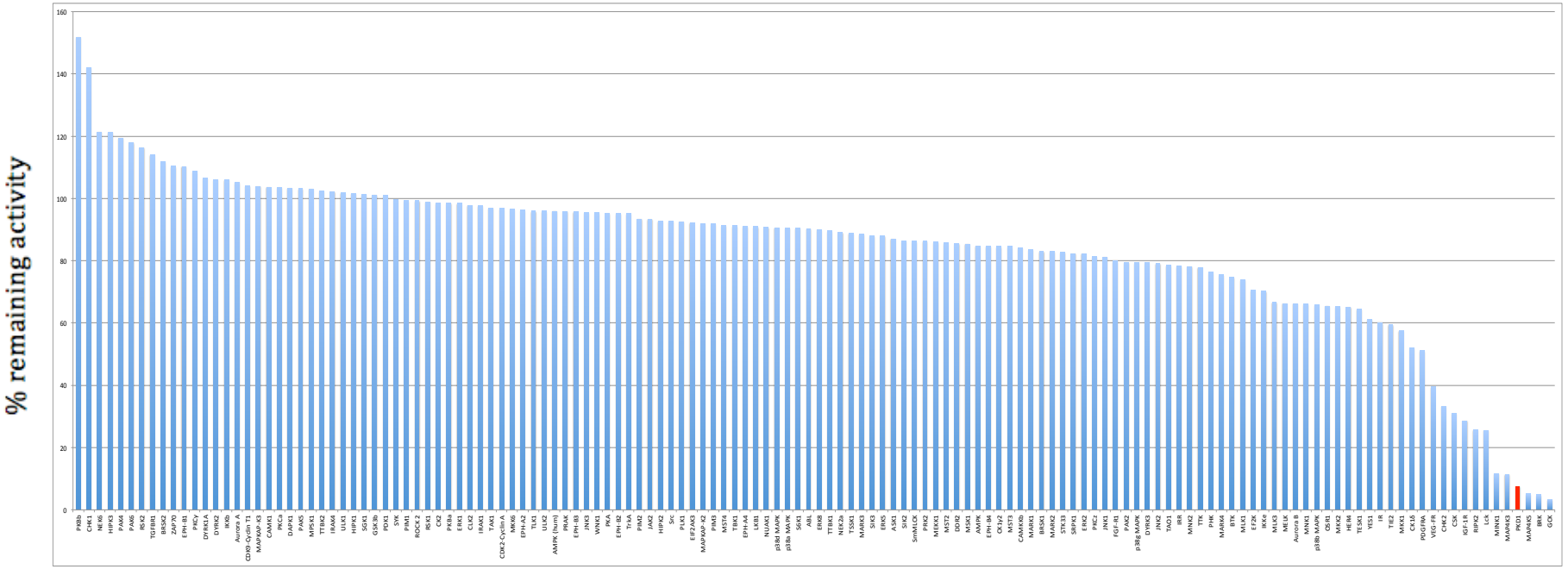

Figure 8.3 Full in vitro kinase screen for CRT051 compound at 2.5μM against 124 kinases

In vitro kinase screen of 124 kinases shown in descending order of % remaining activity (PKD1 is shown in red)

9 References

.

Abreu, M.T., 2010. Toll-like receptor signalling in the intestinal epithelium: how bacterial recognition shapes intestinal function. *Nature Publishing Group*, 10(2), pp.131–144.

Acuto, O., Bartolo, V.D. & Michel, F., 2008. Tailoring T-cell receptor signals by proximal negative feedback mechanisms. *Nature Reviews Immunology*, 8(9), pp.699–712.

Ahmed, W. & Van Etten, R.A., 2013. Signal Transduction in the Chronic Leukemias: Implications for Targeted Therapies. *Current Hematologic Malignancy Reports*, 8(1), pp.71–80.

Akashi, K. et al., 2000. A clonogenic common myeloid progenitor that gives rise to all myeloid lineages. *Nature*, 404(6774), pp.193–197.

Akira, S. & Takeda, K., 2004. Toll-like receptor signalling. *Nature Reviews Immunology*, 4(7), pp.499–511.

Akira, S., Uematsu, S. & Takeuchi, O., 2006. Pathogen Recognition and Innate Immunity. *Cell*, 124(4), pp.783–801.

Alexopoulou, L. et al., 2001. Recognition of double-stranded RNA and activation of NF-kappaB by Toll-like receptor 3. *Nature*, 413(6857), pp.732–738.

Allenspach, E.J. et al., 2008. Migratory and Lymphoid-Resident Dendritic Cells Cooperate to Efficiently Prime Naive CD4 T cells. *Immunity*, 29(5), pp.795–806.

Ananieva, O. et al., 2008. The kinases MSK1 and MSK2 act as negative regulators of Toll-like receptor signaling. *Nature Immunology*, 9(9), pp.1028–1036.

Angstreich, G.R. et al., 2005. Effects of imatinib and interferon on primitive chronic myeloid leukaemia progenitors. *British Journal of Haematology*, 130(3), pp.373–381.

Anon, 2011. The STAT5 inhibitor pimozide decreases survival of chronic myelogenous leukemia cells resistant to kinase inhibitors. pp.1–10.

Appleman, L.J. & Boussiotis, V.A., 2003. T cell anergy and costimulation. *Immunological reviews*, 192, pp.161–180.

Arthur, J.S.C. & Ley, S.C., 2013. Mitogen-activated protein kinases in innate immunity. *Nature Publishing Group*, 13(9), pp.679–692.

Arun, S.N. et al., 2010. Ultraviolet B irradiation and activation of protein kinase D in primary mouse epidermal keratinocytes. *Oncogene*, 30(13), pp.1586–

1596.

Asano, M. et al., 1996. Autoimmune disease as a consequence of developmental abnormality of a T cell subpopulation. *Journal of Experimental Medicine*, 184(2), pp.387–396.

Asseman, C. et al., 1999. An essential role for interleukin 10 in the function of regulatory T cells that inhibit intestinal inflammation. *Journal of Experimental Medicine*, 190(7), pp.995–1004.

Atarashi, K. et al., 2011. Induction of colonic regulatory T cells by indigenous Clostridium species. *Science*, 331(6015), pp.337–341.

Atarashi, K. et al., 2014. Treg induction by a rationally selected mixture of Clostridia strains from the human microbiota. *Nature*, 500(7461), pp.232–236.

Athie-Morales, V. et al., 2004. Sustained IL-12 signaling is required for Th1 development. *The Journal of Immunology*, 172(1), pp.61–69.

Auffray, C., Sieweke, M.H. & Geissmann, F., 2009. Blood Monocytes: Development, Heterogeneity, and Relationship with Dendritic Cells. *Annual Review of Immunology*, 27(1), pp.669–692.

Azoitei, N. et al., 2010. Protein kinase D2 is a crucial regulator of tumour cell-endothelial cell communication in gastrointestinal tumours. *Gut*, 59(10), pp.1316–1330.

Bain, J. et al., 2007. The selectivity of protein kinase inhibitors: a further update. *Biochemical Journal*, 408(3), p.297.

Bain, J. et al., 2003. The specificities of protein kinase inhibitors: an update. *Biochemical Journal*, 371(Pt 1), pp.199–204.

Baldwin, A.S., 1996. The NF-kappa B and I kappa B proteins: new discoveries and insights. *Annual Review of Immunology*, 14(1), pp.649–683.

Baldwin, T.A., Hogquist, K.A. & Jameson, S.C., 2004. The fourth way? Harnessing aggressive tendencies in the thymus. *The Journal of Immunology*, 173(11), pp.6515–6520.

Banchereau, J. & Steinman, R.M., 1998. Dendritic cells and the control of immunity. *Nature*, 392(6673), pp.245–252.

Banz, A. et al., 2003. A unique subpopulation of CD4+ regulatory T cells controls wasting disease, IL-10 secretion and T cell homeostasis. *European Journal of Immunology*, 33(9), pp.2419–2428.

Basset, C. et al., 2003. Innate immunity and pathogen–host interaction. *Vaccine*, 21, pp.S12–S23.

Belkaid, Y. & Hand, T.W., 2014. Role of the Microbiota in Immunity and Inflammation. *Cell*, 157(1), pp.121–141.

Belz, G.T. & Nutt, S.L., 2012. Transcriptional programming of the dendritic cell network. *Nature Reviews Immunology*, 12(2), pp.101–113.

Ben-Neriah, Y. & Karin, M., 2011. Inflammation meets cancer, with NF-κB as the matchmaker. *Nature Immunology*, 12(8), pp.715–723.

Bennett, C.L. et al., 2001. The immune dysregulation, polyendocrinopathy, enteropathy, X-linked syndrome (IPEX) is caused by mutations of FOXP3. *Nature Genetics*, 27(1), pp.20–21.

Benson, M.J. et al., 2007. All-trans retinoic acid mediates enhanced T reg cell growth, differentiation, and gut homing in the face of high levels of co-stimulation. *Journal of Experimental Medicine*, 204(8), pp.1765–1774.

Benveniste, J., Lespinats, G. & Salomon, J., 1971. Serum and secretory IgA in axenic and holoxenic mice. *The Journal of Immunology*, 107(6), pp.1656–1662.

Bernhart, E. et al., 2013. Protein kinase D2 regulates migration and invasion of U87MG glioblastoma cells in vitro. *Experimental cell research*, 319(13), pp.2037–2048.

Bettelli, E., Oukka, M. & Kuchroo, V.K., 2007. T(H)-17 cells in the circle of immunity and autoimmunity. *Nature Immunology*, 8(4), pp.345–350.

Bhattacharya, S. et al., 2011. Bcr-abl signals to desensitize chronic myeloid leukemia cells to IFN via accelerating the degradation of its receptor. *Blood*, 118(15), pp.4179–4187.

Bilate, A.M. & Lafaille, J.J., 2012. Induced CD4 +Foxp3 +Regulatory T Cells in Immune Tolerance. *Annual Review of Immunology*, 30(1), pp.733–758.

Bishop, A.C. et al., 1999. Generation of Monospecific Nanomolar Tyrosine Kinase Inhibitors via a Chemical Genetic Approach. *Journal of the American Chemical Society*, 121(4), pp.627–631.

Blair, P.J. et al., 1994. CD4+CD8- T cells are the effector cells in disease pathogenesis in the scurfy (sf) mouse. *The Journal of Immunology*, 153(8), pp.3764–3774.

Bonizzi, G. & Karin, M., 2004. The two NF-κB activation pathways and their role in innate and adaptive immunity. *Trends in Immunology*, 25(6), pp.280–288.

Boone, D.L. et al., 2004. The ubiquitin-modifying enzyme A20 is required for termination of Toll-like receptor responses. *Nature Immunology*, 5(10), pp.1052–1060.

Borges, S. et al., 2013. Pharmacologic reversion of epigenetic silencing of the

PRKD1 promoter blocks breast tumor cell invasion and metastasis. 15(2), pp.1–1.

Botos, I., Segal, D.M. & Davies, D.R., 2011. The Structural Biology of Toll-like Receptors. *Structure*, 19(4), pp.447–459.

Bouneaud, C., Kourilsky, P. & Bousso, P., 2000. Impact of negative selection on the T cell repertoire reactive to a self-peptide: a large fraction of T cell clones escapes clonal deletion. *Immunity*, 13(6), pp.829–840.

Bour-Jordan, H. & Bluestone, J.A., 2009. Regulating the regulators: costimulatory signals control the homeostasis and function of regulatory T cells. *Immunological reviews*, 229(1), pp.41–66.

Brandtzaeg, P. & Johansen, F.-E., 2005. Mucosal B cells: phenotypic characteristics, transcriptional regulation, and homing properties. *Immunological reviews*, 206(1), pp.32–63.

Breitfeld, D. et al., 2000. Follicular B helper T cells express CXC chemokine receptor 5, localize to B cell follicles, and support immunoglobulin production. *Journal of Experimental Medicine*, 192(11), pp.1545–1552.

Brown, G.D. & Gordon, S., 2001. Immune recognition. A new receptor for beta-glucans. *Nature*, 413(6851), pp.36–37.

Brown, G.D. et al., 2002. Dectin-1 is a major beta-glucan receptor on macrophages. *Journal of Experimental Medicine*, 196(3), pp.407–412.

Brownlie, R.J. & Zamoyska, R., 2013. T cell receptor signalling networks: branched, diversified and bounded. *Nature Publishing Group*, 13(4), pp.257–269.

Brunkow, M.E. et al., 2001. Disruption of a new forkhead/winged-helix protein, scurfin, results in the fatal lymphoproliferative disorder of the scurfy mouse. *Nature Genetics*, 27(1), pp.68–73.

Canton, J., Neculai, D. & Grinstein, S., 2013. Scavenger receptors in homeostasis and immunity. *Nature Publishing Group*, 13(9), pp.621–634.

Cao, X. et al., 2007. Granzyme B and Perforin Are Important for Regulatory T Cell-Mediated Suppression of Tumor Clearance. *Immunity*, 27(4), pp.635–646.

Cargnello, M. & Roux, P.P., 2011. Activation and function of the MAPKs and their substrates, the MAPK-activated protein kinases. *Microbiology and molecular biology reviews : MMBR*, 75(1), pp.50–83.

Carpenter, G. & Ji, Q.S., 1999. Phospholipase C-gamma as a signal-transducing element. *Experimental cell research*, 253(1), pp.15–24.

Carrasco, S. & Mérida, I., 2007. Diacylglycerol, when simplicity becomes complex. *Trends in Biochemical Sciences*, 32(1), pp.27–36.

Catalfamo, M. & Henkart, P.A., 2003. Perforin and the granule exocytosis cytotoxicity pathway. *Current opinion in immunology*, 15(5), pp.522–527.

Cepek, K.L. et al., 1994. Adhesion between epithelial cells and T lymphocytes mediated by E-cadherin and the alpha E beta 7 integrin. *Nature*, 372(6502), pp.190–193.

Chardès, T. et al., 1994. Toxoplasma gondii oral infection induces specific cytotoxic CD8 alpha/beta+ Thy-1+ gut intraepithelial lymphocytes, lytic for parasite-infected enterocytes. *The Journal of Immunology*, 153(10), pp.4596–4603.

Chen, F. et al., 1999. New insights into the role of nuclear factor-kappaB, a ubiquitous transcription factor in the initiation of diseases. *Clinical chemistry*, 45(1), pp.7–17.

Chen, J. et al., 2011. Protein kinase D3 sensitizes RAF inhibitor RAF265 in melanoma cells by preventing reactivation of MAPK signaling. *Cancer research*, 71(12), pp.4280–4291.

Chen, Y. & Li, S., 2013. Molecular signatures of chronic myeloid leukemia stem cells. 1(1), pp.1–1.

Chen, Z.J., Parent, L. & Maniatis, T., 1996. Site-specific phosphorylation of IkappaBalpha by a novel ubiquitination-dependent protein kinase activity. *Cell*, 84(6), pp.853–862.

Cheroutre, H., Lambolez, F. & Mucida, D., 2011. The light and dark sides of intestinal intraepithelial lymphocytes. *Nature Publishing Group*, 11(7), pp.445–456.

Chirdo, F.G. et al., 2005. Immunomodulatory dendritic cells in intestinal lamina propria. *European Journal of Immunology*, 35(6), pp.1831–1840.

Cisse, B. et al., 2008. Transcription Factor E2-2 Is an Essential and Specific Regulator of Plasmacytoid Dendritic Cell Development. *Cell*, 135(1), pp.37–48.

Coccia, M. et al., 2012. IL-1 mediates chronic intestinal inflammation by promoting the accumulation of IL-17A secreting innate lymphoid cells and CD4+ Th17 cells. *Journal of Experimental Medicine*, 209(9), pp.1595–1609.

Cohen, P., 2014. Immune diseases caused by mutations in kinases and components of the ubiquitin system. *Nature Immunology*, 15(6), pp.521–529.

Colón-González, F. & Kazanietz, M.G., 2006. C1 domains exposed: from diacylglycerol binding to protein-protein interactions. *Biochimica et biophysica acta*, 1761(8), pp.827–837.

Cooper, M.D., 2015. The early history of B cells. *Nature Publishing Group*, pp.1–7.

Copland, M., 2006. Dasatinib (BMS-354825) targets an earlier progenitor population than imatinib in primary CML but does not eliminate the quiescent fraction. *Blood*, 107(11), pp.4532–4539.

Cowell, C.F., Döppler, H., et al., 2009a. Mitochondrial diacylglycerol initiates protein-kinase D1-mediated ROS signaling. *Journal of cell science*, 122(Pt 7), pp.919–928.

Cowell, C.F., Yan, I.K., et al., 2009b. Loss of cell-cell contacts induces NF-κB via RhoA-mediated activation of protein kinase D1. *Journal of cellular biochemistry*, 106(4), pp.714–728.

Crotty, S., 2011. Follicular Helper CD4 T Cells (T FH). *Annual Review of Immunology*, 29(1), pp.621–663.

Cusson-Hermance, N. et al., 2005. Rip1 mediates the Trif-dependent toll-like receptor 3- and 4-induced NF-{kappa}B activation but does not contribute to interferon regulatory factor 3 activation. *Journal of Biological Chemistry*, 280(44), pp.36560–36566.

Dale, D.C., Boxer, L. & Liles, W.C., 2008. The phagocytes: neutrophils and monocytes. *Blood*, 112(4), pp.935–945.

Davies, L.C. et al., 2013. Tissue-resident macrophages. *Nature Immunology*, 14(10), pp.986–995.

De Silva, N.S. & Klein, U., 2015. Dynamics of B cells in germinal centres. *Nature Publishing Group*, pp.1–12.

de Zoeten, E.F. et al., 2010. Inhibition of HDAC9 Increases T Regulatory Cell Function and Prevents Colitis in Mice. *YGAST*, 138(2), pp.583–594.

Del Prete, A. et al., 2008. Role of mitochondria and reactive oxygen species in dendritic cell differentiation and functions. *Free Radical Biology Medicine*, 44(7), pp.1443–1451.

del Rio, M.-L. et al., 2010. Development and functional specialization of CD103+ dendritic cells. *Immunological reviews*, 234(1), pp.268–281.

Denning, T.L. et al., 2007. Mouse TCRalphabeta+CD8alphaalpha intraepithelial lymphocytes express genes that down-regulate their antigen reactivity and suppress immune responses. *The Journal of Immunology*, 178(7), pp.4230–4239.

Dequiedt, F. et al., 2003. HDAC7, a thymus-specific class II histone deacetylase, regulates Nur77 transcription and TCR-mediated apoptosis. *Immunity*, 18(5), pp.687–698.

Dequiedt, F. et al., 2005. Phosphorylation of histone deacetylase 7 by protein kinase D mediates T cell receptor-induced Nur77 expression and apoptosis. *Journal of Experimental Medicine*, 201(5), pp.793–804.

Di Bernardo, M.C. et al., 2008. A genome-wide association study identifies six susceptibility loci for chronic lymphocytic leukemia. *Nature Genetics*, 40(10), pp.1204–1210.

Diebold, S.S. et al., 2004. Innate antiviral responses by means of TLR7-mediated recognition of single-stranded RNA. *Science*, 303(5663), pp.1529–1531.

Dieu, M.C. et al., 1998. Selective recruitment of immature and mature dendritic cells by distinct chemokines expressed in different anatomic sites. *Journal of Experimental Medicine*, 188(2), pp.373–386.

Döppler, H. et al., 2005. A phosphorylation state-specific antibody recognizes Hsp27, a novel substrate of protein kinase D. *Journal of Biological Chemistry*, 280(15), pp.15013–15019.

Du, C. et al., 2010. Protein kinase D1 suppresses epithelial-to-mesenchymal transition through phosphorylation of snail. *Cancer research*, 70(20), pp.7810–7819.

Dziarski, R. & Gupta, D., 2000. Role of MD-2 in TLR2- and TLR4-mediated recognition of Gram-negative and Gram-positive bacteria and activation of chemokine genes. *Journal of endotoxin research*, 6(5), pp.401–405.

Eiseler, T. et al., 2010. Protein kinase D controls actin polymerization and cell motility through phosphorylation of cortactin. *The Journal of biological chemistry*, 285(24), pp.18672–18683.

Eiseler, T. et al., 2009. Protein kinase D1 regulates cofilin-mediated F-actin reorganization and cell motility through slingshot. *Nature cell biology*, 11(5), pp.545–556.

Ekambaram, R. et al., 2013. Selective Bisubstrate Inhibitors with Sub-nanomolar Affinity for Protein Kinase Pim-1. *ChemMedChem*, 8(6), pp.909–913.

Ellwanger, K. & Hausser, A., 2013. Physiological functions of protein kinase D in vivo. *IUBMB Life*, 65(2), pp.98–107.

Ermolaeva, M.A. et al., 2008. Function of TRADD in tumor necrosis factor receptor 1 signaling and in TRIF-dependent inflammatory responses. *Nature Immunology*, 9(9), pp.1037–1046.

Evans, I.M. & Zachary, I.C., 2011. Protein kinase D in vascular biology and angiogenesis. *IUBMB Life*, 63(4), pp.258–263.

Evans, I.M. et al., 2010. Characterization of the biological effects of a novel protein kinase D inhibitor in endothelial cells. *Biochemical Journal*, 429(3), pp.565–572.

Feng, H. et al., 2007. Properties, regulation, and in vivo functions of a novel protein kinase D: Caenorhabditis elegans DKF-2 links diacylglycerol second messenger to the regulation of stress responses and life span. *Journal of*

Biological Chemistry, 282(43), pp.31273–31288.

Feng, H., Ren, M. & Rubin, C.S., 2006a. Conserved domains subserve novel mechanisms and functions in DKF-1, a Caenorhabditis elegans protein kinase D. *Journal of Biological Chemistry*, 281(26), pp.17815–17826.

Feng, H., Ren, M., Wu, S.-L., et al., 2006b. Characterization of a novel protein kinase D: Caenorhabditis elegans DKF-1 is activated by translocation-phosphorylation and regulates movement and growth in vivo. *Journal of Biological Chemistry*, 281(26), pp.17801–17814.

Ferguson, A., 1977. Intraepithelial lymphocytes of the small intestine. *Gut*, 18(11), pp.921–937.

Fielitz, J. et al., 2008. Requirement of protein kinase D1 for pathological cardiac remodeling. *Proceedings of the National Academy of Sciences of the United States of America*, 105(8), pp.3059–3063.

Flynn, J.L. et al., 1993. An essential role for interferon gamma in resistance to Mycobacterium tuberculosis infection. *Journal of Experimental Medicine*, 178(6), pp.2249–2254.

Fontenot, J.D. et al., 2005. Regulatory T Cell Lineage Specification by the Forkhead Transcription Factor Foxp3. *Immunity*, 22(3), pp.329–341.

Fontenot, J.D., Gavin, M.A. & Rudensky, A.Y., 2003. Foxp3 programs the development and function of CD4+CD25+ regulatory T cells. *Nature Immunology*, 4(4), pp.330–336.

Fu, Y. & Rubin, C.S., 2011. Protein kinase D: coupling extracellular stimuli to the regulation of cell physiology. *Nature Publishing Group*, 12(8), pp.785–796.

Fugmann, T. et al., 2007. Regulation of secretory transport by protein kinase D-mediated phosphorylation of the ceramide transfer protein. *The Journal of cell biology*, 178(1), pp.15–22.

Fujihashi, K. et al., 1999. gammadelta T cells regulate mucosally induced tolerance in a dose-dependent fashion. *International Immunology*, 11(12), pp.1907–1916.

Gallegos, A.M. & Bevan, M.J., 2004. Central tolerance to tissue-specific antigens mediated by direct and indirect antigen presentation. *Journal of Experimental Medicine*, 200(8), pp.1039–1049.

Gangadharan, D. et al., 2006. Identification of Pre- and Postselection TCRαβ+ Intraepithelial Lymphocyte Precursors in the Thymus. *Immunity*, 25(4), pp.631–641.

Ganguly, D. et al., 2013. The role of dendritic cells in autoimmunity. *Nature Publishing Group*, 13(8), pp.566–577.

Gantner, B.N. et al., 2003. Collaborative induction of inflammatory responses by dectin-1 and Toll-like receptor 2. *Journal of Experimental Medicine*, 197(9), pp.1107–1117.

Geissmann, F. et al., 2010. Development of monocytes, macrophages, and dendritic cells. *Science*, 327(5966), pp.656–661.

Genot, E. & Cantrell, D.A., 2000. Ras regulation and function in lymphocytes. *Current opinion in immunology*, 12(3), pp.289–294.

Gerondakis, S. & Siebenlist, U., 2010. Roles of the NF-kappaB pathway in lymphocyte development and function. *Cold Spring Harbor Perspectives in Biology*, 2(5), pp.a000182–a000182.

Gerstein, R.M., 2009. Deciding the decider: Mef2c in hematopoiesis. *Nature Immunology*, 10(3), pp.235–236.

Gesbert, F. & Griffin, J.D., 2000. Bcr/Abl activates transcription of the Bcl-X gene through STAT5. *Blood*, 96(6), pp.2269–2276.

Gharbi, S.I. et al., 2011. Diacylglycerol kinase ζ controls diacylglycerol metabolism at the immunological synapse. *Molecular biology of the cell*, 22(22), pp.4406–4414.

Gilliet, M., Cao, W. & Liu, Y.-J., 2008. Plasmacytoid dendritic cells: sensing nucleic acids in viral infection and autoimmune diseases. *Nature Reviews Immunology*, 8(8), pp.594–606.

Ginhoux, F. & Jung, S., 2014. Monocytes and macrophages: developmental pathways and tissue homeostasis. *Nature Publishing Group*, 14(6), pp.392–404.

Girardi, M., 2006. Immunosurveillance and Immunoregulation by γδ T Cells. *Journal of Investigative Dermatology*, 126(1), pp.25–31.

Gondek, D.C. et al., 2005. Cutting edge: contact-mediated suppression by CD4+CD25+ regulatory cells involves a granzyme B-dependent, perforin-independent mechanism. *The Journal of Immunology*, 174(4), pp.1783–1786.

González-Navajas, J.M. et al., 2012. Immunomodulatory functions of type I interferons. *Nature Publishing Group*, 12(2), pp.125–135.

Goodridge, H.S., Simmons, R.M. & Underhill, D.M., 2007. Dectin-1 stimulation by Candida albicans yeast or zymosan triggers NFAT activation in macrophages and dendritic cells. *The Journal of Immunology*, 178(5), pp.3107–3115.

Gordon, S. & Martinez, F.O., 2010. Alternative Activation of Macrophages: Mechanism and Functions. *Immunity*, 32(5), pp.593–604.

Graham, S.M., 2002. Primitive, quiescent, Philadelphia-positive stem cells from patients with chronic myeloid leukemia are insensitive to STI571 in vitro.

Blood, 99(1), pp.319–325.

Grandage, V.L. et al., 2006. G$\hat{\square}$6976 is a potent inhibitor of the JAK 2 and FLT3 tyrosine kinases with significant activity in primary acute myeloid leukaemia cells. *British Journal of Haematology*, 135(3), pp.303–316.

Grant, S.K., 2009. Therapeutic protein kinase inhibitors. *Cellular and molecular life sciences : CMLS*, 66(7), pp.1163–1177.

Griner, E.M. & Kazanietz, M.G., 2007. Protein kinase C and other diacylglycerol effectors in cancer. *Nature Reviews Cancer*, 7(4), pp.281–294.

Gschwendt, M., Dieterich, S., et al., 1996a. Inhibition of protein kinase C mu by various inhibitors. Differentiation from protein kinase c isoenzymes. *FEBS Letters*, 392(2), pp.77–80.

Gschwendt, M., dieterich, S., et al., 1996b. Inhibition of protein kinase C by various inhibitors. Differentiation from protein kinase c isoenzymes. *FEBS Letters*, pp.1–4.

Guha, S., Rey, O. & Rozengurt, E., 2002. Neurotensin induces protein kinase C-dependent protein kinase D activation and DNA synthesis in human pancreatic carcinoma cell line PANC-1. *Cancer research*, 62(6), pp.1632–1640.

Guo, J. et al., 2013. In vitro cytotoxicity, pharmacokinetics, tissue distribution, and metabolism of small-molecule protein kinase D inhibitors, kb-NB142-70 and kb-NB165-09, in mice bearing human cancer xenografts. *Cancer chemotherapy and pharmacology*, 71(2), pp.331–344.

Guo, R. et al., 2008. Synergistic control of T cell development and tumor suppression by diacylglycerol kinase alpha and zeta. *Proceedings of the National Academy of Sciences of the United States of America*, 105(33), pp.11909–11914.

Haan, den, J.M., Lehar, S.M. & Bevan, M.J., 2000. CD8(+) but not CD8(-) dendritic cells cross-prime cytotoxic T cells in vivo. *Journal of Experimental Medicine*, 192(12), pp.1685–1696.

Hacker, H. & Karin, M., 2006. Regulation and function of IKK and IKK-related kinases. *Science's STKE : signal transduction knowledge environment*, 2006(357), pp.re13–re13.

Hamilton, J.A. & Tak, P.P., 2009. The dynamics of macrophage lineage populations in inflammatory and autoimmune diseases. *Arthritis & Rheumatism*, 60(5), pp.1210–1221.

Hantschel, O. et al., 2012. BCR-ABL uncouples canonical JAK2-STAT5 signaling in chronic myeloid leukemia. *Nature Chemical Biology*, 8(3), pp.285–293.

Hao, Q., Wang, L. & Tang, H., 2009. Vascular endothelial growth factor induces

protein kinase D-dependent production of proinflammatory cytokines in endothelial cells. *AJP: Cell Physiology*, 296(4), pp.C821–C827.

Harikumar, K.B. et al., 2010. A novel small-molecule inhibitor of protein kinase D blocks pancreatic cancer growth in vitro and in vivo. *Molecular Cancer Therapeutics*, 9(5), pp.1136–1146.

Hausser, A. et al., 2006. Phospho-specific binding of 14-3-3 proteins to phosphatidylinositol 4-kinase III beta protects from dephosphorylation and stabilizes lipid kinase activity. *Journal of cell science*, 119(Pt 17), pp.3613–3621.

Hausser, A. et al., 2005. Protein kinase D regulates vesicular transport by phosphorylating and activating phosphatidylinositol-4 kinase IIIbeta at the Golgi complex. *Nature cell biology*, 7(9), pp.880–886.

Hayashi, A. et al., 1999. PKCnu, a new member of the protein kinase C family, composes a fourth subfamily with PKCmu. *Biochimica et biophysica acta*, 1450(1), pp.99–106.

Hayashi, F. et al., 2001. The innate immune response to bacterial flagellin is mediated by Toll-like receptor 5. *Nature*, 410(6832), pp.1099–1103.

Hayden, M.S. & Ghosh, S., 2011. NF-κB in immunobiology. *Nature Publishing Group*, 21(2), pp.223–244.

Heil, F. et al., 2004. Species-specific recognition of single-stranded RNA via toll-like receptor 7 and 8. *Science*, 303(5663), pp.1526–1529.

Helft, J. et al., 2010. Origin and functional heterogeneity of non-lymphoid tissue dendritic cells in mice. *Immunological reviews*, 234(1), pp.55–75.

Hemmi, H. et al., 2000. A Toll-like receptor recognizes bacterial DNA. *Nature*, 408(6813), pp.740–745.

Henson, P.M. & Hume, D.A., 2006. Apoptotic cell removal in development and tissue homeostasis. *Trends in Immunology*, 27(5), pp.244–250.

Hespel, C. & Moser, M., 2012. Role of inflammatory dendritic cells in innate and adaptive immunity. *European Journal of Immunology*, 42(10), pp.2535–2543.

Hoelbl, A. et al., 2010. Stat5 is indispensable for the maintenance of bcr/abl-positive leukaemia. *EMBO Molecular Medicine*, 2(3), pp.98–110.

Holyoake, T.L. & Helgason, G.V., 2015. Do we need more drugs for chronic myeloid leukemia? *Immunological reviews*, 263(1), pp.106–123.

Honda, K. et al., 2005. IRF-7 is the master regulator of type-I interferon-dependent immune responses. *Nature*, 434(7034), pp.772–777.

Honda, K., Takaoka, A. & Taniguchi, T., 2006. Type I Inteferon Gene Induction by

the Interferon Regulatory Factor Family of Transcription Factors. *Immunity*, 25(3), pp.349–360.

Hoshino, K. et al., 1999. Cutting edge: Toll-like receptor 4 (TLR4)-deficient mice are hyporesponsive to lipopolysaccharide: evidence for TLR4 as the Lps gene product. *The Journal of Immunology*, 162(7), pp.3749–3752.

Hölttä, V. et al., 2008. IL-23/IL-17 immunity as a hallmark of Crohn's disease. *Inflammatory Bowel Diseases*, 14(9), pp.1175–1184.

Hsieh, C.-S. et al., 1997. *Pillars article: development of TH1 CD4+ T cells through IL-12 produced by Listeria-induced macrophages. 1993. Science 260(5107): 547-549*,

Hsieh, C.-S., Lee, H.-M. & Lio, C.-W.J., 2012. Selection of regulatory T cells in the thymus. *Nature Publishing Group*, 12(3), pp.157–167.

Hu, B. et al., 2001. S and G2 phase roles for Cdk2 revealed by inducible expression of a dominant-negative mutant in human cells. *Molecular and Cellular Biology*, 21(8), pp.2755–2766.

Huang, T.T. & Miyamoto, S., 2001. Postrepression activation of NF-kappaB requires the amino-terminal nuclear export signal specific to IkappaBalpha. *Molecular and Cellular Biology*, 21(14), pp.4737–4747.

Huehn, J. et al., 2004. Developmental stage, phenotype, and migration distinguish naive- and effector/memory-like CD4+ regulatory T cells. *Journal of Experimental Medicine*, 199(3), pp.303–313.

Huffnagle, G.B. et al., 1999. Cutting edge: Role of C-C chemokine receptor 5 in organ-specific and innate immunity to Cryptococcus neoformans. *The Journal of Immunology*, 163(9), pp.4642–4646.

Huleatt, J.W. et al., 2001. Intestinal and splenic T cell responses to enteric Listeria monocytogenes infection: distinct repertoires of responding CD8 T lymphocytes. *The Journal of Immunology*, 166(6), pp.4065–4073.

Husebye, H. et al., 2006. Endocytic pathways regulate Toll-like receptor 4 signaling and link innate and adaptive immunity. *The EMBO journal*, 25(4), pp.683–692.

Hutti, J.E. et al., 2004. A rapid method for determining protein kinase phosphorylation specificity. *Nature Methods*, 1(1), pp.27–29.

Iglesias, T. & Rozengurt, E., 1999. Protein kinase D activation by deletion of its cysteine-rich motifs. *FEBS Letters*, 454(1-2), pp.53–56.

Iglesias, T. & Rozengurt, E., 1998. Protein Kinase D Activation by Mutations within Its Pleckstrin Homology Domain. *Journal of Biological Chemistry*, 273(1), pp.410–416.

Iglesias, T. et al., 2000. Identification and cloning of Kidins220, a novel neuronal substrate of protein kinase D. *Journal of Biological Chemistry*, 275(51), pp.40048–40056.

Iglesias, T., Waldron, R.T. & Rozengurt, E., 1998. Identification of in vivo phosphorylation sites required for protein kinase D activation. *Journal of Biological Chemistry*, 273(42), pp.27662–27667.

Imhof, B.A. & Aurrand-Lions, M., 2004. Adhesion mechanisms regulating the migration of monocytes. *Nature Reviews Immunology*, 4(6), pp.432–444.

Inaba, K. et al., 2009. Isolation of dendritic cells. *Current protocols in immunology / edited by John E. Coligan ... [et al.]*, Chapter 3, pp.Unit 3.7–3.7.19.

Irie, A. et al., 2006. Protein kinase D2 contributes to either IL-2 promoter regulation or induction of cell death upon TCR stimulation depending on its activity in Jurkat cells. *International Immunology*, 18(12), pp.1737–1747.

Ivashkiv, L.B. & Donlin, L.T., 2014. Regulation of type I interferon responses. *Nature Publishing Group*, 14(1), pp.36–49.

Ivison, S.M. et al., 2007. Protein kinase D interaction with TLR5 is required for inflammatory signaling in response to bacterial flagellin. *The Journal of Immunology*, 178(9), pp.5735–5743.

Iwasaki, A., 2007. Mucosal Dendritic Cells. *Annual Review of Immunology*, 25(1), pp.381–418.

Iwasaki, H. & Akashi, K., 2007. Myeloid Lineage Commitment from the Hematopoietic Stem Cell. *Immunity*, 26(6), pp.726–740.

Izcue, A. et al., 2008. Interleukin-23 Restrains Regulatory T Cell Activity to Drive T Cell-Dependent Colitis. *Immunity*, 28(4), pp.559–570.

Jacamo, R. et al., 2008. Sequential protein kinase C (PKC)-dependent and PKC-independent protein kinase D catalytic activation via Gq-coupled receptors: differential regulation of activation loop Ser(744) and Ser(748) phosphorylation. *Journal of Biological Chemistry*, 283(19), pp.12877–12887.

Jakubzick, C. et al., 2008. Lymph-migrating, tissue-derived dendritic cells are minor constituents within steady-state lymph nodes. *The Journal of experimental medicine*, 205(12), pp.2839–2850.

Janeway, C.A. & Medzhitov, R., 2002. Innate immune recognition. *Annual Review of Immunology*, 20, pp.197–216.

Jensen, E.D., Gopalakrishnan, R. & Westendorf, J.J., 2009. Bone morphogenic protein 2 activates protein kinase D to regulate histone deacetylase 7 localization and repression of Runx2. *Journal of Biological Chemistry*, 284(4), pp.2225–2234.

Jeohn, G.H. et al., 2002. Gö6976 inhibits LPS-induced microglial TNFalpha release by suppressing p38 MAP kinase activation. *Neuroscience*, 114(3), pp.689–697.

Jin, M.S. et al., 2007. Crystal Structure of the TLR1-TLR2 Heterodimer Induced by Binding of a Tri-Acylated Lipopeptide. *Cell*, 130(6), pp.1071–1082.

Joffre, O.P. et al., 2012. Cross-presentation by dendritic cells. *Nature Publishing Group*, pp.1–13.

Johannes, F.J. et al., 1994. PKCu is a novel, atypical member of the protein kinase C family. *Journal of Biological Chemistry*, 269(8), pp.6140–6148.

Johansson-Lindbom, B. & Agace, W.W., 2007. Generation of gut-homing T cells and their localization to the small intestinal mucosa. *Immunological reviews*, 215(1), pp.226–242.

Johansson-Lindbom, B. et al., 2005. Functional specialization of gut CD103+ dendritic cells in the regulation of tissue-selective T cell homing. *Journal of Experimental Medicine*, 202(8), pp.1063–1073.

Josefowicz, S.Z., Lu, L.-F. & Rudensky, A.Y., 2012. Regulatory T cells: mechanisms of differentiation and function. *Annual Review of Immunology*, 30, pp.531–564.

Jung, C., Hugot, J.-P. & Barreau, F., 2010. Peyer's Patches: The Immune Sensors of the Intestine. *International Journal of Inflammation*, 2010(3), pp.823710–12.

Kaisho, T. et al., 2001. Endotoxin-induced maturation of MyD88-deficient dendritic cells. *The Journal of Immunology*, 166(9), pp.5688–5694.

Kanayama, A. et al., 2004. TAB2 and TAB3 Activate the NF-κB Pathway through Binding to Polyubiquitin Chains. *Molecular Cell*, 15(4), pp.535–548.

Kang, J.Y. et al., 2009. Recognition of Lipopeptide Patterns by Toll-like Receptor 2-Toll-like Receptor 6 Heterodimer. *Immunity*, 31(6), pp.873–884.

Kang, S.G. et al., 2007. Vitamin A metabolites induce gut-homing FoxP3+ regulatory T cells. *The Journal of Immunology*, 179(6), pp.3724–3733.

Kaser, A., Zeissig, S. & Blumberg, R.S., 2010. Inflammatory Bowel Disease. *Annual Review of Immunology*, 28(1), pp.573–621.

Kasler, H.G. et al., 2011. Histone deacetylase 7 regulates cell survival and TCR signaling in CD4/CD8 double-positive thymocytes. *Journal of immunology (Baltimore, Md. : 1950)*, 186(8), pp.4782–4793.

Kawagoe, T. et al., 2008. Sequential control of Toll-like receptor–dependent responses by IRAK1 and IRAK2. *Nature Immunology*, 9(6), pp.684–691.

Kawai, T. & Akira, S., 2010. The role of pattern-recognition receptors in innate

immunity: update on Toll-like receptors. *Nature Immunology*, 11(5), pp.373–384.

Kawai, T. et al., 2001. Lipopolysaccharide stimulates the MyD88-independent pathway and results in activation of IFN-regulatory factor 3 and the expression of a subset of lipopolysaccharide-inducible genes. *The Journal of Immunology*, 167(10), pp.5887–5894.

Kilshaw, P.J. & Baker, K.C., 1988. A unique surface antigen on intraepithelial lymphocytes in the mouse. *Immunology letters*, 18(2), pp.149–154.

Kim, H.M. et al., 2007. Crystal Structure of the TLR4-MD-2 Complex with Bound Endotoxin Antagonist Eritoran. *Cell*, 130(5), pp.906–917.

Kim, S.J. et al., 2011. Tolerogenic function of Blimp-1 in dendritic cells. *The Journal of experimental medicine*, 208(11), pp.2193–2199.

Kim, T.S. & Braciale, T.J., 2009. Respiratory Dendritic Cell Subsets Differ in Their Capacity to Support the Induction of Virus-Specific Cytotoxic CD8+ T Cell Responses D. Unutmaz, ed. *PLoS ONE*, 4(1), p.e4204.

Koboziev, I., Karlsson, F. & Grisham, M.B., 2010. Gut-associated lymphoid tissue, T cell trafficking, and chronic intestinal inflammation. *Annals of the New York Academy of Sciences*, 1207(s1), pp.E86–E93.

Koch, U. & Radtke, F., 2011. Mechanisms of T Cell Development and Transformation. *Annual Review of Cell and Developmental Biology*, 27(1), pp.539–562.

Kolaczkowska, E. & Kubes, P., 2013. Neutrophil recruitment and function in health and inflammation. *Nature Publishing Group*, 13(3), pp.159–175.

Kondo, M., Weissman, I.L. & Akashi, K., 1997. Identification of clonogenic common lymphoid progenitors in mouse bone marrow. *Cell*, 91(5), pp.661–672.

Konkel, J.E. et al., 2011. Control of the development of CD8αα+ intestinal intraepithelial lymphocytes by TGF-β. *Nature Publishing Group*, 12(4), pp.312–319.

Kool, M. et al., 2011. The Ubiquitin-Editing Protein A20 Prevents Dendritic Cell Activation, Recognition of Apoptotic Cells, and Systemic Autoimmunity. *Immunity*, 35(1), pp.82–96.

Korn, T. et al., 2009. IL-17 and Th17 Cells. *Annual Review of Immunology*, 27(1), pp.485–517.

Kotlyarov, A. et al., 1999. MAPKAP kinase 2 is essential for LPS-induced TNF-alpha biosynthesis. *Nature cell biology*, 1(2), pp.94–97.

Kujawski, L.A. & Talpaz, M., 2007. The role of interferon-alpha in the treatment of

chronic myeloid leukemia. *Cytokine & Growth Factor Reviews*, 18(5-6), pp.459–471.

Kullberg, M.C. et al., 2006. IL-23 plays a key role in Helicobacter hepaticus-induced T cell-dependent colitis. *Journal of Experimental Medicine*, 203(11), pp.2485–2494.

Kumagai, Y., Takeuchi, O. & Akira, S., 2008. TLR9 as a key receptor for the recognition of DNA. *Advanced drug delivery reviews*, 60(7), pp.795–804.

Kumar, K.G.S. et al., 2003. SCF(HOS) ubiquitin ligase mediates the ligand-induced down-regulation of the interferon-alpha receptor. *The EMBO journal*, 22(20), pp.5480–5490.

Kumar, K.G.S. et al., 2007. Site-specific ubiquitination exposes a linear motif to promote interferon-alpha receptor endocytosis. *The Journal of cell biology*, 179(5), pp.935–950.

Kunkel, M.T. et al., 2007. Calcium-dependent regulation of protein kinase D revealed by a genetically encoded kinase activity reporter. *Journal of Biological Chemistry*, 282(9), pp.6733–6742.

Langrish, C.L. et al., 2005. IL-23 drives a pathogenic T cell population that induces autoimmune inflammation. *Journal of Experimental Medicine*, 201(2), pp.233–240.

Laszlo, G. et al., 1993. Characterization of a novel cell-surface molecule expressed on subpopulations of activated T and B cells. *The Journal of Immunology*, 150(12), pp.5252–5262.

LaValle, C.R. et al., 2012. Inducible silencing of protein kinase D3 inhibits secretion of tumor-promoting factors in prostate cancer. *Molecular Cancer Therapeutics*, 11(7), pp.1389–1399.

LaValle, C.R., Bravo-Altamirano, K., et al., 2010a. Novel protein kinase D inhibitors cause potent arrest in prostate cancer cell growth and motility. *BMC Chemical Biology*, 10(1), p.5.

LaValle, C.R., George, K.M., et al., 2010b. Protein kinase D as a potential new target for cancer therapy. *Biochimica et Biophysica Acta (BBA) - Reviews on Cancer*, 1806(2), pp.183–192.

Lehmann, J. et al., 2002. Expression of the integrin alpha Ebeta 7 identifies unique subsets of CD25+ as well as CD25- regulatory T cells. *Proceedings of the National Academy of Sciences of the United States of America*, 99(20), pp.13031–13036.

Leipe, J. et al., 2005. Regulatory T cells in rheumatoid arthritis. *Arthritis research & therapy*, 7(3), p.93.

Leonard, J.N. et al., 2008. The TLR3 signaling complex forms by cooperative

receptor dimerization. *Proceedings of the National Academy of Sciences of the United States of America*, 105(1), pp.258–263.

Levine, A.G. et al., 2014. Continuous requirement for the TCR in regulatory T cell function. *Nature Immunology*, 15(11), pp.1070–1078.

Li, B. et al., 2007. FOXP3 interactions with histone acetyltransferase and class II histone deacetylases are required for repression. *Proceedings of the National Academy of Sciences of the United States of America*, 104(11), pp.4571–4576.

Li, J. et al., 2004. The role of protein kinase D in neurotensin secretion mediated by protein kinase C-alpha/-delta and Rho/Rho kinase. *Journal of Biological Chemistry*, 279(27), pp.28466–28474.

Liesenfeld, O., 2002. Oral infection of C57BL/6 mice with Toxoplasma gondii: a new model of inflammatory bowel disease? *The Journal of infectious diseases*, 185 Suppl 1(s1), pp.S96–101.

Liew, F.Y. et al., 2005. Negative regulation of Toll-like receptor-mediated immune responses. *Nature Reviews Immunology*, 5(6), pp.446–458.

Liljedahl, M. et al., 2001. Protein kinase D regulates the fission of cell surface destined transport carriers from the trans-Golgi network. *Cell*, 104(3), pp.409–420.

Lin, S.-C., Lo, Y.-C. & Wu, H., 2011. Helical assembly in the MyD88-IRAK4-IRAK2 complex in TLR/IL-1R signalling. *Nature*, 465(7300), pp.885–890.

Liopeta, K. et al., 2009. cAMP regulates IL-10 production by normal human T lymphocytes at multiple levels: A potential role for MEF2. *Molecular Immunology*, 46(3), pp.345–354.

Liu, S. & Chen, Z.J., 2010. Expanding role of ubiquitination in NF-κB signaling. *Nature Publishing Group*, 21(1), pp.6–21.

Liuwantara, D. et al., 2006. Nuclear factor-kappaB regulates beta-cell death: a critical role for A20 in beta-cell protection. *Diabetes*, 55(9), pp.2491–2501.

Loke, P. et al., 2007. Alternative activation is an innate response to injury that requires CD4+ T cells to be sustained during chronic infection. *The Journal of Immunology*, 179(6), pp.3926–3936.

Lund, J.M. et al., 2004. Recognition of single-stranded RNA viruses by Toll-like receptor 7. *Proceedings of the National Academy of Sciences of the United States of America*, 101(15), pp.5598–5603.

MacKenzie, K.F. et al., 2013. MSK1 and MSK2 inhibit lipopolysaccharide-induced prostaglandin production via an interleukin-10 feedback loop. *Molecular and Cellular Biology*, 33(7), pp.1456–1467.

Macpherson, A.J. & Harris, N.L., 2004. Interactions between commensal intestinal

bacteria and the immune system. *Nature Reviews Immunology*, 4(6), pp.478–485.

Macpherson, A.J. & Uhr, T., 2004. Induction of protective IgA by intestinal dendritic cells carrying commensal bacteria. *Science*, 303(5664), pp.1662–1665.

Maier, D. et al., 2006. Drosophila protein kinase D is broadly expressed and a fraction localizes to the Golgi compartment. *Gene expression patterns : GEP*, 6(8), pp.849–856.

Malhotra, V. & Campelo, F., 2011. PKD Regulates Membrane Fission to Generate TGN to Cell Surface Transport Carriers. *Cold Spring Harbor Perspectives in Biology*, 3(2), pp.a005280–a005280.

Mancuso, G. et al., 2009. Bacterial recognition by TLR7 in the lysosomes of conventional dendritic cells. *Nature Immunology*, 10(6), pp.587–594.

Manzanero, S., 2011. Generation of Mouse Bone Marrow-Derived Macrophages. In *Suppression and Regulation of Immune Responses*. Methods in Molecular Biology. Totowa, NJ: Humana Press, pp. 177–181.

Marklund, U., Lightfoot, K. & Cantrell, D., 2003. Intracellular location and cell context-dependent function of protein kinase D. *Immunity*, 19(4), pp.491–501.

Martin, M., Kettmann, R. & Dequiedt, F., 2007. Class IIa histone deacetylases: regulating the regulators. *Oncogene*, 26(37), pp.5450–5467.

Martinez, F.O. & Gordon, S., 2014. The M1 and M2 paradigm of macrophage activation: time for reassessment. *F1000prime reports*, 6(13), p.13.

Martiny-Baron, G. et al., 1993. Selective inhibition of protein kinase C isozymes by the indolocarbazole Gö 6976. *Journal of Biological Chemistry*, 268(13), pp.9194–9197.

Masahata, K. et al., 2014. Generation of colonic IgA-secreting cells in the caecal patch. *Nature communications*, 5, p.3704.

Mathis, D. & Benoist, C., 2004. Back to central tolerance. *Immunity*, 20(5), pp.509–516.

Matsue, H. et al., 2003. Generation and function of reactive oxygen species in dendritic cells during antigen presentation. *The Journal of Immunology*, 171(6), pp.3010–3018.

Matsuura, M. et al., 2003. A pathway through interferon-gamma is the main pathway for induction of nitric oxide upon stimulation with bacterial lipopolysaccharide in mouse peritoneal cells. *European journal of biochemistry / FEBS*, 270(19), pp.4016–4025.

Matthews, S.A. et al., 2006. Essential role for protein kinase D family kinases in the regulation of class II histone deacetylases in B lymphocytes. *Molecular and Cellular Biology*, 26(4), pp.1569–1577.

Matthews, S.A. et al., 2012. Protein kinase D isoforms are dispensable for integrin-mediated lymphocyte adhesion and homing to lymphoid tissues. *European Journal of Immunology*, 42(5), pp.1316–1326.

Matthews, S.A. et al., 2010. Unique functions for protein kinase D1 and protein kinase D2 in mammalian cells. *Biochemical Journal*, 432(1), pp.153–163.

Matthews, S.A., Pettit, G.R. & Rozengurt, E., 1997. Bryostatin 1 induces biphasic activation of protein kinase D in intact cells. *Journal of Biological Chemistry*, 272(32), pp.20245–20250.

Matthews, S.A., Rozengurt, E. & Cantrell, D., 1999. Characterization of serine 916 as an in vivo autophosphorylation site for protein kinase D/Protein kinase Cmu. *Journal of Biological Chemistry*, 274(37), pp.26543–26549.

Matthews, S.A., Rozengurt, E. & Cantrell, D., 2000. Protein kinase D. A selective target for antigen receptors and a downstream target for protein kinase C in lymphocytes. *Journal of Experimental Medicine*, 191(12), pp.2075–2082.

Maul, J. et al., 2005. Peripheral and Intestinal Regulatory CD4+CD25high T Cells in Inflammatory Bowel Disease. *Gastroenterology*, 128(7), pp.1868–1878.

McDonald, D., 2005. Cdk1: the dominant sibling of Cdk2. pp.1–3.

McHugh, R.S. et al., 2002. CD4(+)CD25(+) immunoregulatory T cells: gene expression analysis reveals a functional role for the glucocorticoid-induced TNF receptor. *Immunity*, 16(2), pp.311–323.

McKinsey, T.A., Zhang, C.L. & Olson, E.N., 2001. Identification of a signal-responsive nuclear export sequence in class II histone deacetylases. *Molecular and Cellular Biology*, 21(18), pp.6312–6321.

McKinsey, T.A., Zhang, C.L. & Olson, E.N., 2002. MEF2: a calcium-dependent regulator of cell division, differentiation and death. *Trends in Biochemical Sciences*, 27(1), pp.40–47.

Medeiros, R.B. et al., 2005. Protein Kinase D1 and the β1 Integrin Cytoplasmic Domain Control β1 Integrin Function via Regulation of Rap1 Activation. *Immunity*, 23(2), pp.213–226.

Melillo, J.A. et al., 2010. Dendritic cell (DC)-specific targeting reveals Stat3 as a negative regulator of DC function. *Journal of immunology (Baltimore, Md. : 1950)*, 184(5), pp.2638–2645.

Mendoza, H. et al., 2008. Roles for TAB1 in regulating the IL-1-dependent phosphorylation of the TAB3 regulatory subunit and activity of the TAK1 complex. *Biochemical Journal*, 409(3), p.711.

Merad, M. et al., 2013. The Dendritic Cell Lineage: Ontogeny and Function of Dendritic Cells and Their Subsets in the Steady State and the Inflamed Setting. *Annual Review of Immunology*, 31(1), pp.563–604.

Meredith, E.L., Ardayfio, O., et al., 2010a. Identification of Orally Available Naphthyridine Protein Kinase D Inhibitors. *Journal of Medicinal Chemistry*, 53(15), pp.5400–5421.

Meredith, E.L., Beattie, K., et al., 2010b. Identification of potent and selective amidobipyridyl inhibitors of protein kinase D. *Journal of Medicinal Chemistry*, 53(15), pp.5422–5438.

Mihailovic, T. et al., 2004. Protein kinase D2 mediates activation of nuclear factor kappaB by Bcr-Abl in Bcr-Abl+ human myeloid leukemia cells. *Cancer research*, 64(24), pp.8939–8944.

Mildner, A. & Jung, S., 2014. Development and Function of Dendritic Cell Subsets. *Immunity*, 40(5), pp.642–656.

Mody, N. et al., 2001. Effects of MAP kinase cascade inhibitors on the MKK5/ERK5 pathway. *FEBS Letters*, 502(1-2), pp.21–24.

Molina, T.J. et al., 1992. Profound block in thymocyte development in mice lacking p56lck. *Nature*, 357(6374), pp.161–164.

Monovich, L. et al., 2010. A novel kinase inhibitor establishes a predominant role for protein kinase D as a cardiac class IIa histone deacetylase kinase. *FEBS Letters*, 584(3), pp.631–637.

Mosser, D.M., 2003. The many faces of macrophage activation. *Journal of Leukocyte Biology*, 73(2), pp.209–212.

Mosser, D.M. & Edwards, J.P., 2008. Exploring the full spectrum of macrophage activation. *Nature Reviews Immunology*, 8(12), pp.958–969.

Mottet, C., Uhlig, H.H. & Powrie, F., 2003. Cutting edge: cure of colitis by CD4+CD25+ regulatory T cells. *The Journal of Immunology*, 170(8), pp.3939–3943.

Mount, A.M. et al., 2008. Multiple Dendritic Cell Populations Activate CD4+ T Cells after Viral Stimulation M. M. Rodrigues, ed. *PLoS ONE*, 3(2), p.e1691.

Mowat, A.M., 2003. Anatomical basis of tolerance and immunity to intestinal antigens. *Nature Reviews Immunology*, 3(4), pp.331–341.

Mowat, A.M. & Agace, W.W., 2014. Regional specialization within the intestinal immune system. *Nature Publishing Group*, 14(10), pp.667–685.

Muñoz, L.E. et al., 2010. The role of defective clearance of apoptotic cells in systemic autoimmunity. *Nature Publishing Group*, 6(5), pp.280–289.

Murai, M. et al., 1999. Active participation of CCR5(+)CD8(+) T lymphocytes in the pathogenesis of liver injury in graft-versus-host disease. *Journal of Clinical Investigation*, 104(1), pp.49–57.

Murphy, T.R., Legere, H.J. & Katz, H.R., 2007. Activation of protein kinase D1 in mast cells in response to innate, adaptive, and growth factor signals. *The Journal of Immunology*, 179(11), pp.7876–7882.

Müller, S., Bühler-Jungo, M. & Mueller, C., 2000. Intestinal intraepithelial lymphocytes exert potent protective cytotoxic activity during an acute virus infection. *The Journal of Immunology*, 164(4), pp.1986–1994.

Nakamura, K. et al., 2007. Dectin-1 is not required for the host defense to Cryptococcus neoformans. *Microbiology and immunology*, 51(11), pp.1115–1119.

Navarro, M.N. et al., 2011. Phosphoproteomic analysis reveals an intrinsic pathway for the regulation of histone deacetylase 7 that controls the function of cytotoxic T lymphocytes. *Nature Immunology*, 12(4), pp.352–361.

Navarro, M.N. et al., 2012. Protein kinase D2 has a restricted but critical role in T-cell antigen receptor signalling in mature T-cells. *Biochemical Journal*, 442(3), pp.649–659.

Navarro, M.N., Feijoo Carnero, C., et al., 2014a. Protein kinase D2 is a digital amplifier of T cell receptor-stimulated diacylglycerol signaling in naïve CD8+ T cells. *Science signaling*, 7(348), pp.ra99–ra99.

Navarro, M.N., Goebel, J., et al., 2014b. Quantitative phosphoproteomics of cytotoxic T cells to reveal Protein Kinase D 2 regulated networks. *Molecular & cellular proteomics : MCP*, p.mcp.M113.037242.

Nelson, E.A. et al., 2011. The STAT5 inhibitor pimozide decreases survival of chronic myelogenous leukemia cells resistant to kinase inhibitors. *Blood*, 117(12), pp.3421–3429.

Neutra, M.R., Mantis, N.J. & Kraehenbuhl, J.P., 2001. Collaboration of epithelial cells with organized mucosal lymphoid tissues. *Nature Immunology*, 2(11), pp.1004–1009.

Nhek, S. et al., 2010. Regulation of oxysterol-binding protein Golgi localization through protein kinase D-mediated phosphorylation. *Molecular biology of the cell*, 21(13), pp.2327–2337.

Nishikawa, K. et al., 1997. Determination of the specific substrate sequence motifs of protein kinase C isozymes. *Journal of Biological Chemistry*, 272(2), pp.952–960.

Nomura, T. & Sakaguchi, S., 2007. Foxp3 and Aire in thymus-generated Treg cells: a link in self-tolerance. *Nature Immunology*, 8(4), pp.333–334.

O'Hare, T. et al., 2011. Targeting the BCR-ABL signaling pathway in therapy-resistant Philadelphia chromosome-positive leukemia. *Clinical Cancer Research*, 17(2), pp.212–221.

O'Neill, L.A.J. & Bowie, A.G., 2007. The family of five: TIR-domain-containing adaptors in Toll-like receptor signalling. *Nature Reviews Immunology*, 7(5), pp.353–364.

O'Neill, L.A.J., Golenbock, D. & Bowie, A.G., 2013. The history of Toll-like receptors — redefining innate immunity. *Nature Publishing Group*, 13(6), pp.453–460.

Ochi, N. et al., 2011. Protein kinase D1 promotes anchorage-independent growth, invasion, and angiogenesis by human pancreatic cancer cells. *Journal of Cellular Physiology*, 226(4), pp.1074–1085.

Oganesyan, G. et al., 2005. Critical role of TRAF3 in the Toll-like receptor-dependent and -independent antiviral response. *Nature*, 439(7073), pp.208–211.

Ohnmacht, C. et al., 2009. Constitutive ablation of dendritic cells breaks self-tolerance of CD4 T cells and results in spontaneous fatal autoimmunity. *The Journal of experimental medicine*, 206(3), pp.549–559.

Olenchock, B.A. et al., 2006. Disruption of diacylglycerol metabolism impairs the induction of T cell anergy. *Nature Immunology*, 7(11), pp.1174–1181.

Ostanin, D.V. et al., 2010. Evaluation of the immunoregulatory activity of intraepithelial lymphocytes in a mouse model of chronic intestinal inflammation. *International Immunology*, 22(12), pp.927–939.

Ostanin, D.V. et al., 2008. T cell transfer model of chronic colitis: concepts, considerations, and tricks of the trade. *AJP: Gastrointestinal and Liver Physiology*, 296(2), pp.G135–G146.

Oster, H., Abraham, D. & Leitges, M., 2006. Expression of the protein kinase D (PKD) family during mouse embryogenesis. *Gene Expression Patterns*, 6(4), pp.400–408.

P Matheu, M. et al., 2008. Generation of Bone Marrow Derived Murine Dendritic Cells for Use in 2-photon Imaging. *Journal of Visualized Experiments*, (17), pp.e773–e773.

Pabst, O. & Mowat, A.M., 2012. Oral tolerance to food protein. 5(3), pp.232–239.

Palacios, E.H. & Weiss, A., 2004. Function of the Src-family kinases, Lck and Fyn, in T-cell development and activation. *Oncogene*, 23(48), pp.7990–8000.

Palucka, K. & Banchereau, J., 2012. Cancer immunotherapy via dendritic cells. *Nature Reviews Cancer*, 12(4), pp.265–277.

Pandiyan, P. et al., 2007. CD4+CD25+Foxp3+ regulatory T cells induce cytokine deprivation–mediated apoptosis of effector CD4+ T cells. *Nature Immunology*, 8(12), pp.1353–1362.

Park, B.S. et al., 2009a. The structural basis of lipopolysaccharide recognition by the TLR4-MD-2 complex. *Nature*, 458(7242), pp.1191–1195.

Park, J.-E., Kim, Y.-I. & Yi, A.-K., 2009b. Protein kinase D1 is essential for MyD88-dependent TLR signaling pathway. *Journal of immunology (Baltimore, Md. : 1950)*, 182(10), pp.6316–6327.

Park, J.-E., Kim, Y.-I. & Yi, A.-K., 2008. Protein kinase D1: a new component in TLR9 signaling. *Journal of immunology (Baltimore, Md. : 1950)*, 181(3), pp.2044–2055.

Parra, M. et al., 2005. Protein kinase D1 phosphorylates HDAC7 and induces its nuclear export after T-cell receptor activation. *Journal of Biological Chemistry*, 280(14), pp.13762–13770.

Pizarro-Cerdá, J., Kühbacher, A. & Cossart, P., 2012. Entry of Listeria monocytogenes in mammalian epithelial cells: an updated view. *Cold Spring Harbor Perspectives in Medicine*, 2(11), pp.a010009–a010009.

Pobezinskaya, Y.L. et al., 2008. The function of TRADD in signaling through tumor necrosis factor receptor 1 and TRIF-dependent Toll-like receptors. *Nature Immunology*, 9(9), pp.1047–1054.

Powrie, F., 1995. T Cells in Inflammatory Bowel Disease: Minireview Protective and Pathogenic Roles. *Immunity*, pp.1–4.

Powrie, F. et al., 1996. A critical role for transforming growth factor-beta but not interleukin 4 in the suppression of T helper type 1-mediated colitis by CD45RB(low) CD4+ T cells. *Journal of Experimental Medicine*, 183(6), pp.2669–2674.

Powrie, F. et al., 1993. Phenotypically distinct subsets of CD4+ T cells induce or protect from chronic intestinal inflammation in C. B-17 scid mice. *International Immunology*, 5(11), pp.1461–1471.

Qureshi, O.S. et al., 2011. Trans-endocytosis of CD80 and CD86: a molecular basis for the cell-extrinsic function of CTLA-4. *Science*, 332(6029), pp.600–603.

Raman, M., Chen, W. & Cobb, M.H., 2007. Differential regulation and properties of MAPKs. *Oncogene*, 26(22), pp.3100–3112.

Randolph, G.J., Ochando, J. & Partida-Sánchez, S., 2008. Migration of Dendritic Cell Subsets and their Precursors. *Annual Review of Immunology*, 26(1), pp.293–316.

Rashel, M., Alston, N. & Ghazizadeh, S., 2014. Protein Kinase D1 Has a Key Role in Wound Healing and Skin Carcinogenesis. 134(4), pp.902–909.

Read, S. et al., 2006. Blockade of CTLA-4 on CD4+CD25+ regulatory T cells abrogates their function in vivo. *The Journal of Immunology*, 177(7), pp.4376–4383.

Reizis, B., 2010. Regulation of plasmacytoid dendritic cell development. *Current opinion in immunology*, 22(2), pp.206–211.

Reizis, B. et al., 2011. Plasmacytoid Dendritic Cells: Recent Progress and Open Questions. *Annual Review of Immunology*, 29(1), pp.163–183.

Ren, M. et al., 2009. Protein Kinase D Is an Essential Regulator of C. elegans Innate Immunity. *Immunity*, 30(4), pp.521–532.

Rey, O. et al., 2006. The nuclear import of protein kinase D3 requires its catalytic activity. *Journal of Biological Chemistry*, 281(8), pp.5149–5157.

Rey, O., Sinnett-Smith, J., et al., 2001a. Regulated nucleocytoplasmic transport of protein kinase D in response to G protein-coupled receptor activation. *Journal of Biological Chemistry*, 276(52), pp.49228–49235.

Rey, O., Young, S.H., et al., 2001b. Rapid protein kinase D translocation in response to G protein-coupled receptor activation. Dependence on protein kinase C. *Journal of Biological Chemistry*, 276(35), pp.32616–32626.

Riese, M.J. et al., 2011. Decreased diacylglycerol metabolism enhances ERK activation and augments CD8+ T cell functional responses. *The Journal of biological chemistry*, 286(7), pp.5254–5265.

Rincón, M. & Davis, R.J., 2009. Regulation of the immune response by stress-activated protein kinases. *Immunological reviews*, 228(1), pp.212–224.

Roberts, S.J. et al., 1996. T-cell alpha beta + and gamma delta + deficient mice display abnormal but distinct phenotypes toward a natural, widespread infection of the intestinal epithelium. *Proceedings of the National Academy of Sciences of the United States of America*, 93(21), pp.11774–11779.

Rozengurt, E., 2011. Protein Kinase D Signaling: Multiple Biological Functions in Health and Disease. *Physiology*, 26(1), pp.23–33.

Rozengurt, E., Rey, O. & Waldron, R.T., 2005. Protein kinase D signaling. *Journal of Biological Chemistry*, 280(14), pp.13205–13208.

Rozengurt, E., Sinnett-Smith, J. & Zugaza, J.L., 1997. Protein kinase D: a novel target for diacylglycerol and phorbol esters. *Biochemical Society transactions*, 25(2), pp.565–571.

Rubtsov, Y.P. et al., 2008. Regulatory T Cell-Derived Interleukin-10 Limits Inflammation at Environmental Interfaces. *Immunity*, 28(4), pp.546–558.

Rudensky, A.Y., 2011. Regulatory T cells and Foxp3. *Immunological reviews*, 241(1), pp.260–268.

Russell, J.H. & Ley, T.J., 2002. Lymphocyte-Mediated Cytoxicity. *Annual Review of Immunology*, 20(1), pp.323–370.

Rybin, V.O., Guo, J. & Steinberg, S.F., 2009. Protein kinase D1 autophosphorylation via distinct mechanisms at Ser744/Ser748 and Ser916. *Journal of Biological Chemistry*, 284(4), pp.2332–2343.

Sallusto, F. et al., 1999. Distinct patterns and kinetics of chemokine production regulate dendritic cell function. *European Journal of Immunology*, 29(5), pp.1617–1625.

Salmond, R.J. et al., 2009. T-cell receptor proximal signaling via the Src-family kinases, Lck and Fyn, influences T-cell activation, differentiation, and tolerance. *Immunological reviews*, 228(1), pp.9–22.

Salmond, R.J. et al., 2014. The tyrosine phosphatase PTPN22 discriminates weak self peptides from strong agonist TCR signals. *Nature Publishing Group*, 15(9), pp.875–883.

Sato, S. et al., 2005. Essential function for the kinase TAK1 in innate and adaptive immune responses. *Nature Immunology*, 6(11), pp.1087–1095.

Satpathy, A.T. et al., 2012. Re(de)fining the dendritic cell lineage. *Nature Immunology*, 13(12), pp.1145–1154.

Savignac, M., Mellström, B. & Naranjo, J.R., 2007. Calcium-dependent transcription of cytokine genes in T lymphocytes. *Pflügers Archiv - European Journal of Physiology*, 454(4), pp.523–533.

Savina, A. & Amigorena, S., 2007. Phagocytosis and antigen presentation in dendritic cells. *Immunological reviews*, 219(1), pp.143–156.

Schliehe, C. et al., 2011. CD8- dendritic cells and macrophages cross-present poly(D,L-lactate-co-glycolate) acid microsphere-encapsulated antigen in vivo. *Journal of immunology (Baltimore, Md. : 1950)*, 187(5), pp.2112–2121.

Schön, M.P. et al., 1999. Mucosal T lymphocyte numbers are selectively reduced in integrin alpha E (CD103)-deficient mice. *The Journal of Immunology*, 162(11), pp.6641–6649.

Schreiner, M. & Liesenfeld, O., 2009. Small intestinal inflammation following oral infection with Toxoplasma gondii does not occur exclusively in C57BL/6 mice: review of 70 reports from the literature. *Memórias do Instituto Oswaldo Cruz*, 104(2), pp.221–233.

Schwartz, R.H., 2003. T cell anergy. *Annual Review of Immunology*, 21, pp.305–334.

Scott, C.L., Aumeunier, A.M. & Mowat, A.M., 2011. Intestinal CD103+ dendritic cells: master regulators of tolerance? *Trends in Immunology*, 32(9), pp.412–419.

Segura, E. & Villadangos, J.A., 2009. Antigen presentation by dendritic cells in vivo. *Current opinion in immunology*, 21(1), pp.105–110.

Serbina, N.V. et al., 2008. Monocyte-Mediated Defense Against Microbial Pathogens. *Annual Review of Immunology*, 26(1), pp.421–452.

Seternes, O.-M. et al., 2004. Activation of MK5/PRAK by the atypical MAP kinase ERK3 defines a novel signal transduction pathway. *The EMBO journal*, 23(24), pp.4780–4791.

Sharlow, E.R. et al., 2008. Potent and selective disruption of protein kinase D functionality by a benzoxoloazepinolone. *Journal of Biological Chemistry*, 283(48), pp.33516–33526.

Shaw, A., Amrein, K. & Hammond, C., 1989. The Ick Tyrosine Protein Kinase Interacts with the Cytoplasmic Tail of the CD4 Glycoprotein through Its Unique Amino-Terminal Domain. *Cell*, pp.1–10.

Shelburne, C.P. & Ryan, J.J., 2001. The role of Th2 cytokines in mast cell homeostasis. *Immunological reviews*, 179, pp.82–93.

Sheng, K.-C. et al., 2008. Delivery of antigen using a novel mannosylated dendrimer potentiates immunogenicityin vitro andin vivo. *European Journal of Immunology*, 38(2), pp.424–436.

Sheng, K.-C. et al., 2010. Reactive oxygen species level defines two functionally distinctive stages of inflammatory dendritic cell development from mouse bone marrow. *Journal of immunology (Baltimore, Md. : 1950)*, 184(6), pp.2863–2872.

Shinkai, Y. et al., 1992. RAG-2-deficient mice lack mature lymphocytes owing to inability to initiate V(D)J rearrangement. *Cell*, 68(5), pp.855–867.

Shipkova, M. & Wieland, E., 2012. Surface markers of lymphocyte activation and markers of cell proliferation. *Clinica Chimica Acta*, 413(17-18), pp.1338–1349.

Shires, J., Theodoridis, E. & Hayday, A.C., 2001. Biological insights into TCRgammadelta+ and TCRalphabeta+ intraepithelial lymphocytes provided by serial analysis of gene expression (SAGE). *Immunity*, 15(3), pp.419–434.

Shlomchik, M.J. & Weisel, F., 2012. Germinal center selection and the development of memory B and plasma cells. *Immunological reviews*, 247(1), pp.52–63.

Shroff, K.E., Meslin, K. & Cebra, J.J., 1995. Commensal enteric bacteria engender a self-limiting humoral mucosal immune response while permanently colonizing the gut. *Infection and Immunity*, 63(10), pp.3904–3913.

Shuai, K., 2006. Regulation of cytokine signaling pathways by PIAS proteins. *Cell Research*, 16(2), pp.196–202.

Siegal, F.P. et al., 1999. The nature of the principal type 1 interferon-producing cells in human blood. *Science*, 284(5421), pp.1835–1837.

Sinnett-Smith, J. et al., 2009. Protein kinase D mediates mitogenic signaling by Gq-coupled receptors through protein kinase C-independent regulation of activation loop Ser744 and Ser748 phosphorylation. *Journal of Biological Chemistry*, 284(20), pp.13434–13445.

Sinnett-Smith, J. et al., 2014. Protein kinase D1 mediates class IIa histone deacetylase phosphorylation and nuclear extrusion in intestinal epithelial cells: role in mitogenic signaling. *AJP: Cell Physiology*, 306(10), pp.C961–C971.

Smith, C.M. et al., 2003. Cutting edge: conventional CD8 alpha+ dendritic cells are preferentially involved in CTL priming after footpad infection with herpes simplex virus-1. *The Journal of Immunology*, 170(9), pp.4437–4440.

Smith-Garvin, J.E., Koretzky, G.A. & Jordan, M.S., 2009. T Cell Activation. *Annual Review of Immunology*, 27(1), pp.591–619.

Song, J. et al., 2009. PKD prevents H2O2-induced apoptosis via NF-κB and p38 MAPK in RIE-1 cells. *Biochemical and Biophysical Research Communications*, 378(3), pp.610–614.

Song, J. et al., 2006a. Protein kinase D protects against oxidative stress-induced intestinal epithelial cell injury via Rho/ROK/PKC-delta pathway activation. *AJP: Cell Physiology*, 290(6), pp.C1469–76.

Song, K. et al., 2006b. The Transcriptional Coactivator CAMTA2 Stimulates Cardiac Growth by Opposing Class II Histone Deacetylases. *Cell*, 125(3), pp.453–466.

Sozzani, S. et al., 1998. Differential regulation of chemokine receptors during dendritic cell maturation: a model for their trafficking properties. *The Journal of Immunology*, 161(3), pp.1083–1086.

Sozzani, S. et al., 2010. Trafficking properties of plasmacytoid dendritic cells in health and disease. *Trends in Immunology*, 31(7), pp.270–277.

Sparwasser, T. et al., 1997. Bacterial DNA causes septic shock. *scientific correspondence*, pp.1–2.

Spitaler, M., Emslie, E., Wood, C.D. & Cantrell, D., 2006a. Diacylglycerol and Protein Kinase D Localization during T Lymphocyte Activation. *Immunity*, 24(5), pp.535–546.

Spitaler, M., Emslie, E., Wood, C.D. & Cantrell, D., 2006b. Diacylglycerol and Protein Kinase D Localization during T Lymphocyte Activation. *Immunity*, 24(5), pp.535–546.

Steinberg, S.F., 2008. Structural basis of protein kinase C isoform function.

Physiological reviews, 88(4), pp.1341–1378.

Steiner, T.S. et al., 2010. Protein kinase D1 and D2 are involved in chemokine release induced by toll-like receptors 2, 4, and 5. *Cellular Immunology*, 264(2), pp.135–142.

Steinman, R.M., 2012. Decisions About Dendritic Cells: Past, Present, and Future. *Annual Review of Immunology*, 30(1), pp.1–22.

Steinman, R.M. & Cohn, Z.A., 1973. Identification of a novel cell type in peripheral lymphoid organs of mice. I. Morphology, quantitation, tissue distribution. *Journal of Experimental Medicine*, 137(5), pp.1142–1162.

Steinman, R.M. & Witmer, M.D., 1978. Lymphoid dendritic cells are potent stimulators of the primary mixed leukocyte reaction in mice. *Proceedings of the National Academy of Sciences of the United States of America*, 75(10), pp.5132–5136.

Storz, P. & Toker, A., 2003. Protein kinase D mediates a stress-induced NF-kappaB activation and survival pathway. *The EMBO journal*, 22(1), pp.109–120.

Storz, P., Döppler, H. & Toker, A., 2004. Protein kinase Cdelta selectively regulates protein kinase D-dependent activation of NF-kappaB in oxidative stress signaling. *Molecular and Cellular Biology*, 24(7), pp.2614–2626.

Storz, P., Döppler, H. & Toker, A., 2005. Protein kinase D mediates mitochondrion-to-nucleus signaling and detoxification from mitochondrial reactive oxygen species. *Molecular and Cellular Biology*, 25(19), pp.8520–8530.

Sturany, S. et al., 2001. Molecular cloning and characterization of the human protein kinase D2. A novel member of the protein kinase D family of serine threonine kinases. *Journal of Biological Chemistry*, 276(5), pp.3310–3318.

Suffia, I. et al., 2005. A role for CD103 in the retention of CD4+CD25+ Treg and control of Leishmania major infection. *The Journal of Immunology*, 174(9), pp.5444–5455.

Suzuki, K. et al., 2004. Aberrant expansion of segmented filamentous bacteria in IgA-deficient gut. *Proceedings of the National Academy of Sciences of the United States of America*, 101(7), pp.1981–1986.

Suzuki, R. et al., 2002. Localization of intestinal intraepithelial T lymphocytes involves regulation of alphaEbeta7 expression by transforming growth factor-beta. *International Immunology*, 14(4), pp.339–345.

Swain, S.L. et al., 1990. IL-4 directs the development of Th2-like helper effectors. *The Journal of Immunology*, 145(11), pp.3796–3806.

Swirski, F.K. et al., 2009. Identification of splenic reservoir monocytes and their

deployment to inflammatory sites. *Science*, 325(5940), pp.612–616.

Szabo, S.J. et al., 2000. A novel transcription factor, T-bet, directs Th1 lineage commitment. *Cell*, 100(6), pp.655–669.

Tak, P.P. & Firestein, G.S., 2001. NF-kappaB: a key role in inflammatory diseases. *Journal of Clinical Investigation*, 107(1), pp.7–11.

Takeda, K., Kaisho, T. & Akira, S., 2003. Toll-like receptors. *Annual Review of Immunology*, 21, pp.335–376.

Takeuchi, O. & Akira, S., 2009. Innate immunity to virus infection. *Immunological reviews*, 227(1), pp.75–86.

Tan, J.K.H. & O'Neill, H.C., 2005. Maturation requirements for dendritic cells in T cell stimulation leading to tolerance versus immunity. *Journal of Leukocyte Biology*, 78(2), pp.319–324.

Tandon, M. et al., 2013. New Pyrazolopyrimidine Inhibitors of Protein Kinase D as Potent Anticancer Agents for Prostate Cancer Cells M. Kanzaki, ed. *PLoS ONE*, 8(9), p.e75601.

Taniuchi, I. & Littman, D.R., 2004. Epigenetic gene silencing by Runx proteins. *Oncogene*, 23(24), pp.4341–4345.

Tao, R. et al., 2007. Deacetylase inhibition promotes the generation and function of regulatory T cells. *Nature Medicine*, 13(11), pp.1299–1307.

Tarlinton, D. & Good-Jacobson, K., 2013. Diversity among memory B cells: origin, consequences, and utility. *Science*, 341(6151), pp.1205–1211.

Taylor, P.R. et al., 2006. Dectin-1 is required for β-glucan recognition and control of fungal infection. *Nature Immunology*, 8(1), pp.31–38.

Travis, M.A. et al., 2007. Loss of integrin αvβ8 on dendritic cells causes autoimmunity and colitis in mice. *Nature*, 449(7160), pp.361–365.

Ubersax, J.A. & Ferrell, J.E., Jr, 2007. Mechanisms of specificity in protein phosphorylation. *Nature Reviews Molecular Cell Biology*, 8(7), pp.530–541.

Uematsu, S. & Akira, S., 2009. Immune responses of TLR5+ lamina propria dendritic cells in enterobacterial infection. *Journal of Gastroenterology*, 44(8), pp.803–811.

Uematsu, S. & Akira, S., 2007. Toll-like receptors and Type I interferons. *Journal of Biological Chemistry*, 282(21), pp.15319–15323.

Uhlig, H.H. et al., 2006. Characterization of Foxp3+CD4+CD25+ and IL-10-secreting CD4+CD25+ T cells during cure of colitis. *The Journal of Immunology*, 177(9), pp.5852–5860.

Vallabhapurapu, S. et al., 2008. Nonredundant and complementary functions of TRAF2 and TRAF3 in a ubiquitination cascade that activates NIK-dependent alternative NF-κB signaling. *Nature Immunology*, 9(12), pp.1364–1370.

Valverde, A.M., Sinnett-Smith, J., et al., 1994a. Molecular cloning and characterization of protein kinase D: a target for diacylglycerol and phorbol esters with a distinctive catalytic domain. *Proceedings of the National Academy of Sciences of the United States of America*, 91(18), pp.8572–8576.

Valverde, A.M., Sinnette-Smith, J., et al., 1994b. Molecular cloning and characterisation of protein kinase D: A target for diacylgylcerol and phorbol esters with a distinctive catalytic domain. *Proceedings of the National Academy of Sciences of the United States of America*, pp.1–5.

Van Lint, J.V., Sinnett-Smith, J. & Rozengurt, E., 1995. Expression and characterization of PKD, a phorbol ester and diacylglycerol-stimulated serine protein kinase. *Journal of Biological Chemistry*, 270(3), pp.1455–1461.

van Loosdregt, J. et al., 2010. Regulation of Treg functionality by acetylation-mediated Foxp3 protein stabilization. *Blood*, 115(5), pp.965–974.

Vega, R.B. et al., 2004. Protein kinases C and D mediate agonist-dependent cardiac hypertrophy through nuclear export of histone deacetylase 5. *Molecular and Cellular Biology*, 24(19), pp.8374–8385.

Veillette, A. et al., 1988. The CD4 and CD8 T cell surface antigens are associated with the internal membrane tyrosine-protein kinase p56lck. *Cell*, 55(2), pp.301–308.

Vivier, E. et al., 2008. Functions of natural killer cells. *Nature Immunology*, 9(5), pp.503–510.

Vogelzang, A. et al., 2008. A Fundamental Role for Interleukin-21 in the Generation of T Follicular Helper Cells. *Immunity*, 29(1), pp.127–137.

Vremec, D. et al., 2000. CD4 and CD8 expression by dendritic cell subtypes in mouse thymus and spleen. *The Journal of Immunology*, 164(6), pp.2978–2986.

Vremec, D. et al., 1992. The surface phenotype of dendritic cells purified from mouse thymus and spleen: investigation of the CD8 expression by a subpopulation of dendritic cells. *Journal of Experimental Medicine*, 176(1), pp.47–58.

Waldron, R.T. et al., 2004. Oxidative stress induces protein kinase C-mediated activation loop phosphorylation and nuclear redistribution of protein kinase D. *Journal of Biological Chemistry*, 279(26), pp.27482–27493.

Waldron, R.T., Iglesias, T. & Rozengurt, E., 1999. The pleckstrin homology domain of protein kinase D interacts preferentially with the eta isoform of protein kinase C. *Journal of Biological Chemistry*, 274(14), pp.9224–9230.

Wan, Y.Y., 2010. Multi-tasking of helper T cells. *Immunology*, 130(2), pp.166–171.

Wang, H. et al., 2010. ZAP-70: an essential kinase in T-cell signaling. *Cold Spring Harbor Perspectives in Biology*, 2(5), pp.a002279–a002279.

Wang, L. et al., 2009. Immunomodulatory effects of deacetylase inhibitors: therapeutic targeting of FOXP3+ regulatory T cells. *Nature Reviews Drug Discovery*, 8(12), pp.969–981.

Wang, Q.J., 2006. PKD at the crossroads of DAG and PKC signaling. *Trends in Pharmacological Sciences*, 27(6), pp.317–323.

Warner, N. & Nuñez, G., 2013. MyD88: a critical adaptor protein in innate immunity signal transduction. *Journal of immunology (Baltimore, Md. : 1950)*, 190(1), pp.3–4.

Weber, F. et al., 2006. Double-stranded RNA is produced by positive-strand RNA viruses and DNA viruses but not in detectable amounts by negative-strand RNA viruses. *Journal of Virology*, 80(10), pp.5059–5064.

Wei, N., Chu, E., Wipf, P., et al., 2014a. Protein kinase d as a potential chemotherapeutic target for colorectal cancer. *Molecular Cancer Therapeutics*, 13(5), pp.1130–1141.

Wei, N., Chu, E., Wu, S.-Y., et al., 2014b. The cytotoxic effects of regorafenib in combination with protein kinase D inhibition in human colorectal cancer cells. *Oncotarget*.

Weinstein, S.L. et al., 1992. Bacterial lipopolysaccharide induces tyrosine phosphorylation and activation of mitogen-activated protein kinases in macrophages. *Journal of Biological Chemistry*, 267(21), pp.14955–14962.

Weiss, A., 2010. The right team at the right time to go for a home run: tyrosine kinase activation by the TCR. *Nature Immunology*, 11(2), pp.101–104.

Weiss, A. & Littman, D.R., 1994. Signal transduction by lymphocyte antigen receptors. *Cell*, 76(2), pp.263–274.

Wenner, C.A. et al., 1996. Roles of IFN-gamma and IFN-alpha in IL-12-induced T helper cell-1 development. *The Journal of Immunology*, 156(4), pp.1442–1447.

Wernersson, S. & Pejler, G., 2014. Mast cell secretory granules: armed for battle. pp.1–17.

Weston, C.R. & Davis, R.J., 2007. The JNK signal transduction pathway. *Current opinion in cell biology*, 19(2), pp.142–149.

Wildin, R.S. et al., 2001. X-linked neonatal diabetes mellitus, enteropathy and endocrinopathy syndrome is the human equivalent of mouse scurfy. *Nature Genetics*, 27(1), pp.18–20.

Wille, C. et al., 2014. Protein kinase D2 induces invasion of pancreatic cancer cells by regulating matrix metalloproteinases. *Molecular biology of the cell*, 25(3), pp.324–336.

Wilson, N.S., 2003. Most lymphoid organ dendritic cell types are phenotypically and functionally immature. *Blood*, 102(6), pp.2187–2194.

Wong, C. & Jin, Z.-G., 2005. Protein kinase C-dependent protein kinase D activation modulates ERK signal pathway and endothelial cell proliferation by vascular endothelial growth factor. *Journal of Biological Chemistry*, 280(39), pp.33262–33269.

Worbs, T. et al., 2006. Oral tolerance originates in the intestinal immune system and relies on antigen carriage by dendritic cells. *Journal of Experimental Medicine*, 203(3), pp.519–527.

Wu, H.-J. & Wu, E., 2014. The role of gut microbiota in immune homeostasis and autoimmunity. *Gut Microbes*, 3(1), pp.4–14.

Wynn, T.A., Chawla, A. & Pollard, J.W., 2013. Macrophage biology in development, homeostasis and disease. *Nature*, 496(7446), pp.445–455.

Xiong, N. & Raulet, D.H., 2007. Development and selection of gammadelta T cells. *Immunological reviews*, 215(1), pp.15–31.

Xu, S. et al., 2009. Phospholipase Cgamma2 is critical for Dectin-1-mediated Ca2+ flux and cytokine production in dendritic cells. *Journal of Biological Chemistry*, 284(11), pp.7038–7046.

Yamamoto, M. et al., 2002. Cutting edge: a novel Toll/IL-1 receptor domain-containing adapter that preferentially activates the IFN-beta promoter in the Toll-like receptor signaling. *The Journal of Immunology*, 169(12), pp.6668–6672.

Yamamoto, M. et al., 2003. Role of adaptor TRIF in the MyD88-independent toll-like receptor signaling pathway. *Science*, 301(5633), pp.640–643.

Yamashita, K. et al., 2010. High affinity receptor for IgE stimulation activates protein kinase D augmenting activator protein-1 activity for cytokine producing in mast cells. *International Immunopharmacology*, 10(3), pp.277–283.

Yanagihara, S. et al., 1998. EBI1/CCR7 is a new member of dendritic cell chemokine receptor that is up-regulated upon maturation. *The Journal of Immunology*, 161(6), pp.3096–3102.

Yang, X.-J. & Seto, E., 2008. The Rpd3/Hda1 family of lysine deacetylases: from bacteria and yeast to mice and men. *Nature Reviews Molecular Cell Biology*, 9(3), pp.206–218.

Yang, Z.-F. et al., 2013. GABP transcription factor is required for developmentof

chronic myelogenous leukemia via its controlof PRKD2. *Proceedings of the National Academy of Sciences of the United States of America*, pp.1–6.

Yeaman, C. et al., 2004. Protein kinase D regulates basolateral membrane protein exit from trans-Golgi network. *Nature cell biology*, 6(2), pp.106–112.

Yoshimura, A., 2012. SOCS, inflammation, and autoimmunity. pp.1–9.

Young, S.H. et al., 2012. Rapid protein kinase D1 signaling promotes migration of intestinal epithelial cells. *American journal of physiology. Gastrointestinal and liver physiology*, 303(3), pp.G356–66.

Zanoni, I. et al., 2011. CD14 Controls the LPS-Induced Endocytosis of Toll-like Receptor 4. *Cell*, 147(4), pp.868–880.

Zaru, R. et al., 2007. The MAPK-activated kinase Rsk controls an acute Toll-like receptor signaling response in dendritic cells and is activated through two distinct pathways. *Nature Immunology*, 8(11), pp.1227–1235.

Zhang, N. & Bevan, M.J., 2011. CD8+ T Cells: Foot Soldiers of the Immune System. *Immunity*, 35(2), pp.161–168.

Zhang, X., Goncalves, R. & Mosser, D.M., 2001a. *The Isolation and Characterization of Murine Macrophages*, Hoboken, NJ, USA: John Wiley & Sons, Inc.

Zhang, X., Izikson, L., et al., 2001b. Activation of CD25(+)CD4(+) regulatory T cells by oral antigen administration. *The Journal of Immunology*, 167(8), pp.4245–4253.

Zhang, Y. et al., 2013. ROS play a critical role in the differentiation of alternatively activated macrophages and the occurrence of tumor-associated macrophages. *Nature Publishing Group*, 23(7), pp.898–914.

Zhao, D. et al., 2008. In vivo-activated CD103+CD4+ regulatory T cells ameliorate ongoing chronic graft-versus-host disease. *Blood*, 112(5), pp.2129–2138.

Zhao, M. et al., 1999. Regulation of the MEF2 family of transcription factors by p38. *Molecular and Cellular Biology*, 19(1), pp.21–30.

Zheng, H. et al., 2011. Ligand-stimulated downregulation of the alpha interferon receptor: role of protein kinase D2. *Molecular and Cellular Biology*, 31(4), pp.710–720.

Zheng, W. & Flavell, R.A., 1997. The transcription factor GATA-3 is necessary and sufficient for Th2 cytokine gene expression in CD4 T cells. *Cell*, 89(4), pp.587–596.

Zhong, X.-P. et al., 2008. Diacylglycerol kinases in immune cell function and self-tolerance. *Immunological reviews*, 224(1), pp.249–264.

Zhong, X.-P. et al., 2003. Enhanced T cell responses due to diacylglycerol kinase

zeta deficiency. *Nature Immunology*, 4(9), pp.882–890.

Zhu, J., Yamane, H. & Paul, W.E., 2010. Differentiation of Effector CD4 T Cell Populations *. *Annual Review of Immunology*, 28(1), pp.445–489.

Ziegler, S. et al., 2011. A novel protein kinase D phosphorylation site in the tumor suppressor Rab interactor 1 is critical for coordination of cell migration. *Molecular biology of the cell*, 22(5), pp.570–580.

Zugaza, J.L. et al., 1997. Bombesin, Vasopressin, Endothelin, Bradykinin, and Platelet-derived Growth Factor Rapidly Activate Protein Kinase D through a Protein Kinase C-dependent Signal Transduction Pathway. *Journal of Biological Chemistry*, 272(38), pp.23952–23960.

Zugaza, J.L. et al., 1996. Protein kinase D (PKD) activation in intact cells through a protein kinase C-dependent signal transduction pathway. *The EMBO journal*, 15(22), pp.6220–6230.